VOLCANIC FEATURES OF HAWAII

A Basis for Comparison with Mars

218 p.

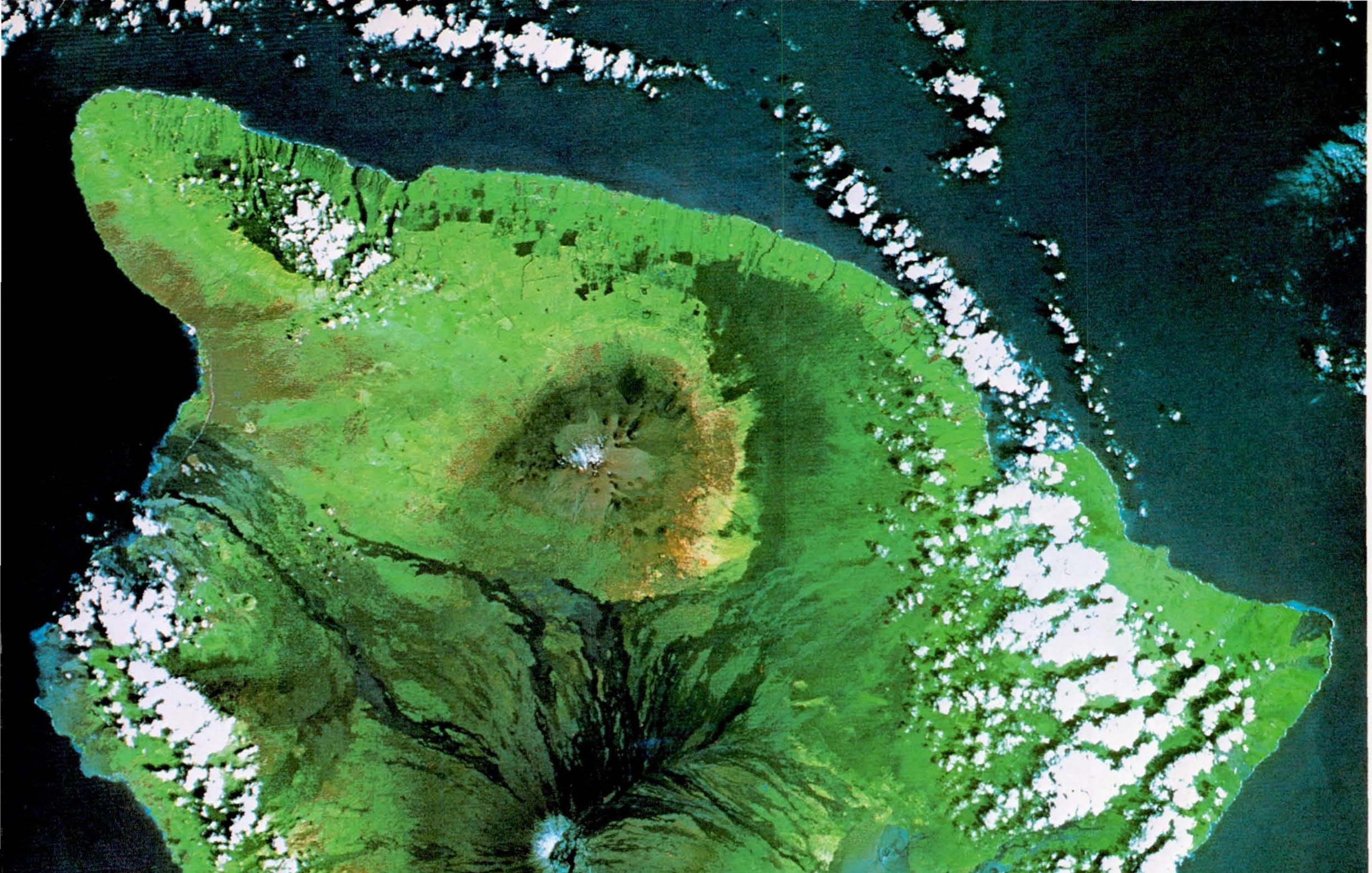

NASA SP-403

VOLCANIC FEATURES OF HAWAII

A Basis for Comparison with Mars

M. H. Carr U.S. Geological Survey, Menlo Park, California

and

R. Greeley Arizona State University and
Ames Research Center, Space Sciences Division,
Moffett Field, California

NASA Scientific and Technical Information Branch 1980
National Aeronautics and Space Administration
Washington, DC

Library of Congress Card Catalog No. 80–600024

For sale by the Superintendent of Documents, U.S. Government Printing Office
Washington, D.C. 20402

Stock Number 033-000-00788-4

CONTENTS

We wish to especially recognize Gordon Macdonald and Agatin Abbott without whose pioneering work and syntheses of Hawaiian geology this book would not have been possible.

I. INTRODUCTION

The intent of this book is to facilitate the comparison of Hawaiian and martian volcanic features. Between 1976 and 1979, the Viking mission to Mars acquired numerous remarkably clear pictures of the martian surface. The pictures are full of bizarre and exotic features but some of the more comprehensible are those of the large volcanoes. The martian volcanoes are enormous by terrestrial standards. Olympus Mons is 27 km high and over 600 km across. In comparison, the Hawaiian volcanoes, which are the largest on Earth, have a maximum height of 9 km above the sea floor and a maximum width of 120 km. Despite the difference in size, the martian and Hawaiian volcanoes have numerous characteristics in common. Specific features such as lava channels, collapsed lava tubes, levees and flow fronts, all very common in Hawaii, are also abundant on the flanks of some of the martian volcanoes. Striking differences also exist, such as the apparent lack of radial rift zones on some martian volcanoes and the paucity of cinder and spatter cones. As we acquired higher resolution photography of the martian features during the Viking mission, the similarities and contrasts became more apparent and we recognized the need for more detailed comparison of the martian volcanoes and one of their closest analogs on Earth, the Hawaiian volcanoes. The intent of this book is to help meet that need by bringing together some of the best photographs of martian and Hawaiian volcanic features so that the reader can make his own comparison and draw his own conclusions. We have deliberately avoided interpretation and kept the Hawaiian and Mars sections separate to avoid imposing an interpretation that might be implicit in the association of the pictures.

The fact that Hawaii has been chosen as the basis for comparison with Mars does not imply that all martian volcanism is of Hawaiian style or that Hawaii is necessarily the best terrestrial analog. Hawaii is representative of one style of terrestrial volcanism, that which results in formation of a shield volcano. The term 'shield' is applied to volcanoes with the profile of an inverted shield and formed largely by sustained accumulation of very fluid lava. They generally have a summit crater and flanks that slope away at angles less than 6°. Explosive eruptions of ash and cinders do occur but are relatively infrequent so that tephra constitutes only a small fraction of the edifice volume. Shield volcanoes thus contrast sharply with most stratovolcanoes in which eruptions of lava commonly alternate with explosive activity involving the production of large amounts of tephra. On the other hand, they also contrast with flood basalt eruptions, in which the lava is so fluid that large edifices do not form, only sheets of lava. Both stratovolcanoes and flood basalts are probably also represented on Mars.

Other terrestrial volcanoes may provide better analogs for specific martian features than those in Hawaii. The terraces on the flanks of the large volcanoes, for example, have no obvious Hawaiian parallels, but are similar to features on some shield volcanoes of the Galapagos Islands. Nevertheless, the Hawaiian volcanoes are probably the most intensely studied, the best documented, and consequently the ones with which comparisons can most readily be made.

The first part of the book deals exclusively with Hawaii. A short overview of Hawaiian volcanism is followed by several chapters illustrating different features of Hawaiian volcanoes. The overview section is appropriately referenced but the short texts at the start of each subsequent section largely lack citations despite our heavy reliance on previously published work. The second part of the book concerns Mars and includes a general summary of the geology of the planet in addition to a discussion of the volcanic features.

The book is not intended as a scholarly or definitive work but more as a guide. The emphasis is on the pictures; the text is kept deliberately short with the expectation that the reader will turn to more definitive works for fuller explanation of the features illustrated. Neither author claims to be an expert on Hawaiian volcanism. What familiarity we have with the subject has been gained largely in order to support our main interests which are the Moon and other planets. M. Carr spent several weeks at the Hawaiian Volcano Observatory during the summer of 1977 going through their files of photographs and seeing many of the features from the air and on the ground. Since 1969, R. Greeley has worked in the field in Hawaii largely engaged in research in support of lunar and planetary studies.

We would like to thank the staff of the Hawaiian Volcano Observatory who generously allowed us access to their files and allowed us to use numerous photographs that had not been previously published. They also provided logistical support and much needed advice. Deserving special mention is R. T. Holcomb who took many of the pictures in the book and aided in the location and interpretation of many others. The manuscript was reviewed by D. W. Peterson, D. A. Swanson, and R. T. Holcomb. Additional encouragement and support was provided by G. P. Eaton, J. Lockwood, and P. W. Lipman. The work was supported by a grant from the Planetary Geology Program Office, NASA Headquarters.

II. HAWAIIAN VOLCANISM

The Hawaiian Islands lie at the southeast end of a line of atolls, reefs, seamounts, and submerged volcanoes that stretch for 6,500 km across the Pacific. The chain, known as the *Hawaiian Archipelago*, extends from Hawaii in an approximately northwest direction for about 3,500 km. At approximately 32°N, 174°E, the chain abruptly changes direction to form a north-south chain of seamounts, the *Emperor Seamounts*. These can be traced for approximately 3,000 km to the north, where they disappear into the Aleutian Trench (Figure 2–1). Several lines of evidence suggest that the volcanoes that constitute the combined Hawaiian-Emperor chain were formed successively. The oldest volcanoes are at the extreme northern end of the chain and have ages probably in excess of 65 million years (Dalrymple and others, in press); the youngest are at the southeast extremity of the chain and form the Hawaiian Islands.

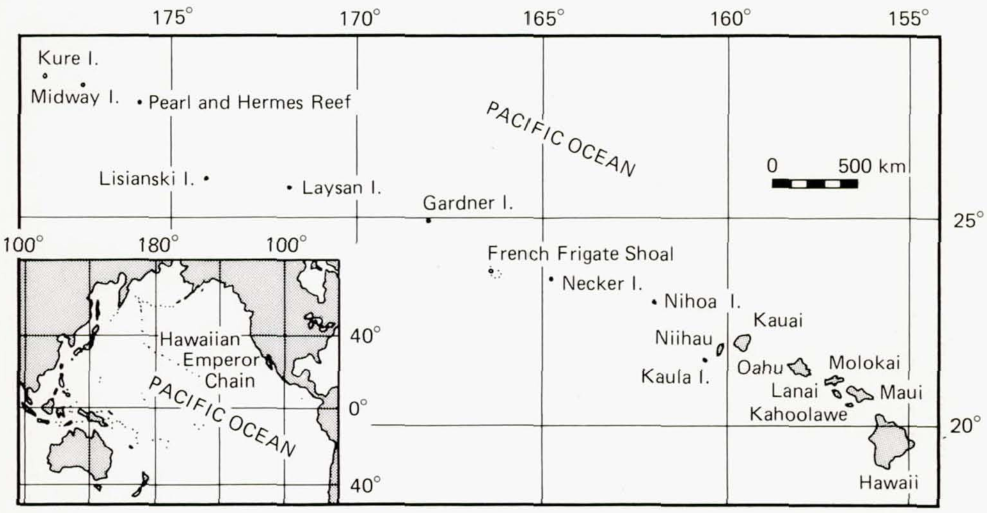

FIGURE 2–1. Map of the Hawaiian Archipelago. The small inset shows the location of the islands in the Pacific Ocean. (From Macdonald and Abbott, 1970.)

The volcanoes within the chain do not form a simple single line but appear instead to have an *echelon* arrangement, occurring along parallel lines oriented at an angle to the main axis of the chain (Jackson and others, 1972). Individual volcanic centers are spaced at an average of approximately 75 km apart along these lines. Associated with each is a positive gravity anomaly which suggests the presence of a core of relatively dense material.

Most of the Hawaiian Islands are composed of two or more volcanoes. The Island of Hawaii, for example, is composed of five – *Kilauea, Mauna Loa, Mauna Kea, Hualalai,* and *Kohala.* Each volcano is considered to have its own individual conduit to a magma source within the mantle. The volcanoes are, however, composite having numerous vents fed from the same central conduit. The bulk of each volcanic edifice is below sea level. The Hawaiian ridge rises about 5,000 m from the ocean floor to sea level, and on the Island of Hawaii extends another 4,000 m above sea level. Primary slopes in the subaerial portion of the volcanoes are relatively shallow and average about 6°. The submerged portions have significantly steeper slopes, averaging approximately 10° down to the base of the edifice.

The age of the Hawaiian volcanoes follows the pattern of the entire Hawaiian-Emperor chain. The youngest are at the extreme southeast end of the chain where the two presently active volcanoes, Mauna Loa and Kilauea, are located. The other volcanoes became progressively older to the northwest such that Kauai, 520 km northwest of Kilauea, is approximately 5.8 million years old (Dalrymple and others, in press). These data suggest that the center of volcanism has moved southeast at an average rate of 8 cm/yr while the Hawaiian Islands have been building. Age data on lavas from other islands and submerged volcanoes of the Hawaiian Archipelago to the northwest of Hawaii indicate that this rate has been maintained for at least 65 million years (Dalrymple and others, in press). The change in direction as recorded by the bend in the Hawaiian-Emperor chain appears to have occurred approximately 43 million years ago.

Origin of the Hawaiian-Emperor Chain

Wilson (1963) proposed that the Hawaiian volcanoes formed as the crust and the rigid part of the upper mantle (now together termed the *lithosphere)* moved northwestward over a fixed hot spot in the mantle. He suggested that a 'hot spot,' now under the active volcanoes Kilauea and Mauna Loa, has been an almost continuous source of magma for several million years and that volcanoes which form over the hot spot are carried to the northwest and ultimately become extinct as they are cut off from the magma source. As old volcanoes die new ones form to their southeast so that the 'hot spot' has given rise to the long line of volcanoes that we observe.

This proposal has gained wide acceptance and accords well with the current theories of plate tectonics, in which the Hawaiian Islands are part of the northwest-moving Pacific plate. Jackson and others (1972) proposed that the 'hot spot' is approximately 300 km across and currently centered about 50 km to the northeast of Kilauea to account for the width of the Hawaiian chain and the location of its axis. The distribution and nature of xenoliths in the Hawaiian magmas (Jackson and Wright, 1970) suggest that the magmas originate at depths of 50-100 km. Such depths are consistent with early seismic data (Eaton and Murata, 1960), although there have been few recent earthquakes from these depths despite much volcanism. Grommé and Vine (1972) determined the remanent magnetic pole orientation – and hence latitude at the time of formation – of some 17 million year old lavas from Midway Island, showing that, within the measurement errors, the apparent latitude of Midway Island 17 million years ago was the same as Hawaii today, indicating that the 'hot spot' has not shifted appreciably, at least in latitude, in the recent geologic past.

While there is a concensus that the Hawaiian Archipelago formed as the lithosphere moved over an essentially fixed hot spot beneath, considerable uncertainty remains as to the precise mechanism. Wilson (1963) envisaged that the lithosphere melted as it moved over an anomalously hot region in the mantle but did not elaborate on the precise mechanism. Morgan (1971, 1972a, 1972b) suggested that thermal instabilities within the mantle could cause plumes or columns of upward-moving mantle rocks at various locations around the world. As a plume impinges on the base of the lithosphere, a low density fraction of the mantle rocks is plastered on the underside and becomes a source of molten materials for surface volcanism. He postulated that such a plume is presently under Hawaii and has been responsible for the Hawaiian chain. Alternatively, McDougall (1971) proposed that the Hawaiian chain formed as a result of easy access of magma to the surface through tensional fractures in the lithosphere. He suggested that the fractures propagate themselves to the southeast as the lithosphere moves to the northwest because the lithosphere rides over a high in the mantle caused either by heating or upwelling. In yet another hypothesis, Shaw and Jackson (1973) proposed that melting at the base of the lithosphere is caused by shear as the Pacific Plate moves northwestward. The reader is referred to Jackson and others (1972) and Dalrymple and others (1975) for amplification of the above discussion.

Structure of individual volcanoes

Each volcano is a complex structure comprising a volcanic center often with a caldera, from which typically radiate two to three rift zones, identifiable by lines of collapse pits, satellitic vents, fissures, and diverging flows. Several lines of evidence suggest that swarms of near vertical dikes underlie the rift zones. The dikes can be seen directly in old dissected volcanoes and inferred indirectly from gravity and magnetic data, and from the sequence of events during eruptions. It appears that the dikes form as magma is transported laterally from the center of the volcano to the flanks. Flank eruptions along the rift zones may or may not accompany such lateral transfer. The orientation of the rift zones is controlled largely by local stress fields caused by the weight of the volcano itself and by the buttressing effect of adjacent volcanoes (Fiske and Jackson, 1972). They are generally oriented in such a way as to permit accommodation to intrusions of the dikes by the outward movement of the edifice on its unsupported flank. Intrusions into the east rift zone of Kilauea, for example, cause outward displacement of the unsupported southeast flank toward the ocean (Swanson and others, 1976a). Displacement of the northwest flank is prevented by the buttressing of Mauna Loa. The orientation of rift zones on isolated volcanoes such as Kauai, where there is no local buttressing effect, may be affected by regional stresses but the data are not conclusive.

The active volcanoes appear to incorporate or overlie a relatively shallow magma reservoir which is supplied by magma from a source region at much greater depths (Eaton, 1962). Swarms of low magnitude earthquakes near the summit of Kilauea occur in association with inflation of the volcano and movement of magma within the edifice. Plots of the foci of the earthquakes reveal an aseismic zone approximately 2 km across and extending from depths of 3 to 7 km beneath the summit caldera. Koyanagi and others (1976) suggested that this zone outlines a magma reservoir, a suggestion consistent with results of studies of ground deformation during episodes of inflation and deflation. Earthquake foci beneath the inferred magma reservoir trace a possible conduit for the magma from the upper mantle. An aseismic zone also occurs beneath the summit of Mauna Loa (Koyanagi and others, 1975). It is as yet poorly defined, but appears to be significantly larger than that for Kilauea, being approximately 10 km across and 15 to 30 km deep.

Evolutionary sequence of Hawaiian volcanoes

The Hawaiian volcanoes are each thought to be built by a similar sequence of events. Early volcanism is believed to form a thick series of pillow lavas which accumulate until the pile reaches sea level. As the edifice continues to grow further, wave action around the periphery of the volcano forms a crosscutting sequence of beach deposits buried by later lavas. Continued growth forms the characteristic domical shield with its central caldera and rift zones. Eruption rates are fairly high and the lavas are almost entirely of a type of basalt called tholeiite, which is the dominant basalt of the ocean floor, midoceanic ridges, and oceanic volcanic islands. It is relatively rich in silica and poor in alkalis compared with many continental basalts. Mauna Loa and Kilauea are in the shield-building phase. According to Moore, the combined eruption rate for the volcanoes on Hawaii is 0.05 $km^3\ yr^{-1}$, and Swanson (1972) estimates that the supply rate of magma to Kilauea in the last 20 years has been approximately 0.1 km^3 yr^{-1}. The main shield building phase may last as long as one million years. It is followed, within a few hundred thousand years, by a capping of more silicic rocks and alkalic basalt, which is poorer in SiO_2 and richer in K_2O and Na_2O than the tholeiite (Jackson and others, 1972). Flows and cinder cones of this phase fill the caldera – if one were present – and generally alter the summit profile that was built earlier. Hualalai, Mauna Kea, and Kohala have reached this stage. Toward the end of this second phase, the rate of eruption decreases significantly so that the erosion rate exceeds the accumulation rate and the volcano becomes deeply dissected. Intermittent eruptions may, however, continue at a low rate of several million years, after termination of the second phase, before the volcano becomes completely extinct.

Sequence of events during an eruption

Although every eruption is unique, observations of eruptions on Kilauea have revealed some recurring patterns. Eruption is generally preceded by a period of inflation centered on the magma reservoir below the summit caldera. Eruptions may occur at the summit or on the flanks, mainly along the rift zones. Although there are exceptions, flank eruptions commonly result in deflation of the summit region, whereas summit eruptions may cause a net expansion. In both cases inflation generally occurs locally at the eruption site. Swarms of small earthquakes in the general area of the vent accompany nearly all eruptions and are presumably caused by the magma as it works its way to the surface. In the case of flank eruptions, there may be an increase in seismic activity along the rift zone between the volcano center and the eruption site. The increase may be substantial or so small as to be undetectable. The very small increases in seismicity in some eruptions suggest that in these cases movement of magma along the rift zone is relatively unobstructed (Swanson and others, 1976b). Intrusion of magma into the rift zone also causes dilation which manifests itself by cracks and fissures at the surface. Although common, such intrusions are not necessarily accompanied by flank eruptions.

Between 1832 and 1950 Mauna Loa averaged an eruption every 3.6 years and was active 6.2 percent of the time (Stearns and Macdonald, 1946). The longest lull in historic times was between 1950 and 1975. Activity since 1832 has been almost equally divided between summit and flank eruptions. Eruptions on Mauna Loa usually start with lava fountains at the summit. The first fountains generally emerge along cracks on the floor of Mokuaweoweo, the summit caldera. The cracks may intersect the caldera wall, causing eruptions inside and outside the caldera or on the caldera wall.

As eruption progresses, activity becomes restricted to a small number of vents, perhaps just one, and cinder and spatter cones form around the remaining vents. Eruptions that are restricted to the summit are generally followed a few years later by summit-flank eruptions. These doublets generally start with fountains at the summit. Activity may then shift continuously down one of the rift zones to a new center or, alternatively, may cease and be followed a few days later by a new eruption lower down one of the rift zones. As for summit eruptions, activity soon becomes limited to one or a small number of vents around which spatter ramparts and cones may be built. Most Mauna Loa eruptions last less than a month; only two historic eruptions (1856, 1974) have lasted longer than a year.

Eruptions of Kilauea can be divided into four types: 1) lava lakes in the caldera, 2) paroxysmal explosions, 3) flank flows, and 4) flows within the caldera that resemble flank flows (Stearns and Macdonald, 1946). In historic times Kilauea has been far more active than Mauna Loa. From 1800 to 1924 Kilauea caldera was almost continuously occupied by one or more active lava lakes. From 1907 to 1924 the surface of the lake in Halemaumau periodically rose and fell, sometimes spilling over onto the floor of the caldera. Two kinds of magma were distinguished; a semisolid lava and more fluid lava. The fluid lava rose and fell faster than the semisolid lava, sometimes leaving island-like masses poking up through the lava-lake surface. The lake was constantly circulating, commonly with small fountains measuring from a few centimenters to a few meters high playing at the surface. Flank eruptions also occurred during this period, with prominent ones in 1823, 1840, 1868, and 1919-1920

In 1924 the style of activity changed dramatically. In February of that year lava drained completely from Halemaumau to leave a fuming empty pit. In late April the floor of the pit began to drop, accompanied by avalanches from the walls. By the first week in May the pit was more than 200 meters deep. Explosive activity then started and continued with extreme violence for most of the month, resulting in the effusion of vast amounts of steam and dust which formed clouds several kilometers high over the volcano. Eruptions of this type, known as *phreatomagmatic eruptions*, are caused by entry of ground water or sea water into the heated rocks below the caldera. Between 1924 and 1934 Halemaumau erupted seven times, but between 1934 and 1952 it was completely quiet. Since resumption of activity in 1952, the volcano has averaged one eruption every two years, except for the period from 1969 to 1974 when there was almost continuous activity at Mauna Ulu in the east rift zone.

III. EDIFICES

The island of Hawaii is built by lava flows from five volcanoes – Kohala, Hualalai, Mauna Kea, Mauna Loa, and Kilauea. Few of the lava flows have been dated radiometrically, but there is general agreement about the relative age of the five volcanoes. Kohala is the most eroded, yields the oldest K-Ar dates (McDougall and Swanson, 1972), and hence is the oldest. Mauna Loa and Kilauea are still active and in the tholeiitic shield-building stage, so are almost certainly the youngest of the group. The relative ages of the main tholeiitic shields of Hualalai and Mauna Kea have not been determined. Although Hualalai erupted in 1801, Fiske and Jackson (1972) assumed it was the older and reconstructed the growth of Hawaii as shown in Figure 3–1.

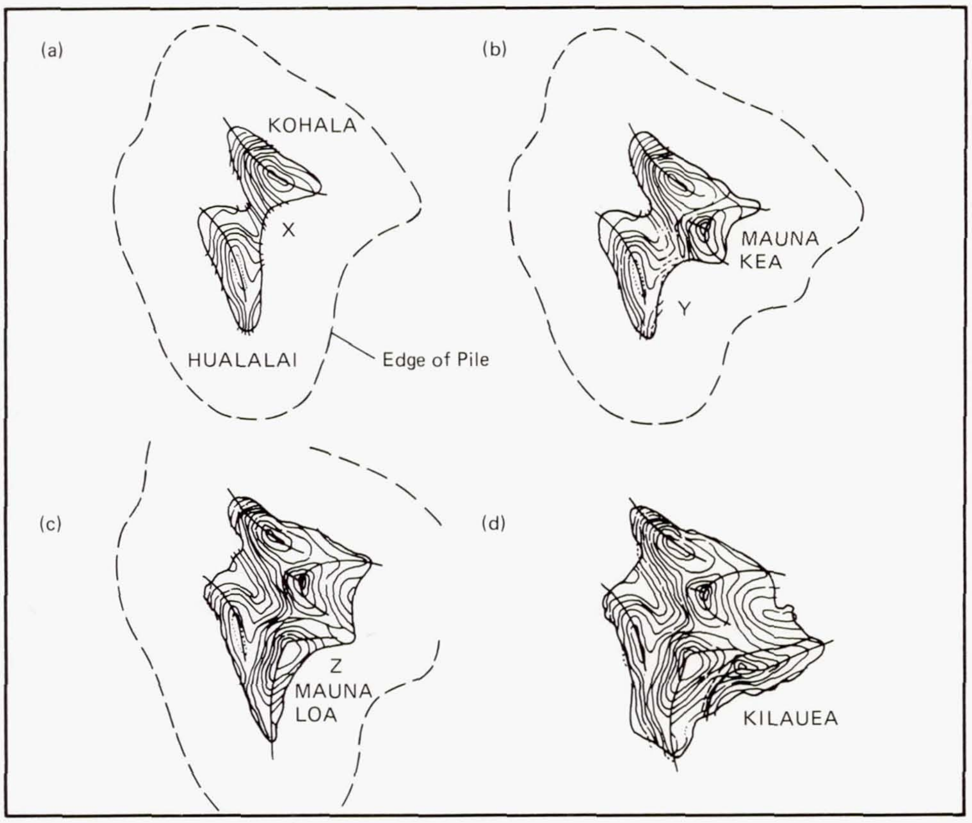

FIGURE 3–1. Stylized reconstruction of the growth of the Island of Hawaii. Contours are of positive Bouguer gravity with 10 m Gal interval (Kinoshita and others, 1963). (A) Early formed Kohala-Hualalai edifice; X marks the site of the future Mauna Kea. (B) Later stage; Y marks the site of future Mauna Loa. (C) Still later stage; Z marks the site of future Kilauea. (D) Present configuration. (From Fiske and Jackson, 1972.)

The main masses of the volcanoes are below sea level. Little is known of the early shield-building phases but long accumulation of pillow lavas must have taken place before the edifice reached sea level. Upon reaching sea level, erosion, and possibly enhanced phreatic activity, may produce a zone rich in tephra and erosional debris between the submarine and subaerial sections. As the volcano grows, its shape is controlled by the rift zones. Only if the volcano is isolated, such as west Maui, is the edifice circular. More commonly broad ridges form along the line of the rifts.

During the growth phase, collapse at the summit forms a caldera. When a caldera first forms is unclear, but collapse and refilling is repetitive and may continue throughout the shield-building stage. Kilauea and Mauna Loa are in this stage. It is not clear whether all the shield volcanoes develop a summit caldera. No evidence of a summit caldera has been found at Hualalai, for example, but this may be due to burial by later deposits.

After the main shield-building period, a cap of lava flows and pyroclastic material is built over the top of the shield and completely buries any existing caldera. The cap is generally steeper and less extensive than the previously built edifice and substantially changes the summit profile. In the shield-building phase, the edifice has a smooth profile with a relatively flat summit. After the capping stage, the profile is jagged at the summit and the slopes steeper. The change in style of volcanism is caused partly by a change in the composition of the lavas. Instead of tholeiites, the late stage lavas are mostly alkalic basalts or various non-basaltic rocks and result in more explosive activity. After termination of this phase, the volcano may become completely extinct. Activity may, however, continue very sporadically for an extended period of time to build new volcanic landforms on the erosional remnants of the main shield.

During the main tholeiitic stage, the flanks of a shield may become unstable and fail along faults approximately parallel to the edge of the shield. Traces of huge landslides have been found on the ocean floor around Hawaii. These probably form mainly by failure on the steeply sloping underwater part of the edifice. Failure also occurs on the subaerial parts. The *Hilina Pali* and *Holei Pali* on the southeast flank of Kilauea are fault scarps with the outer portion of edifice moving down and out toward the ocean. A large earthquake in 1975 was the result of such a seaward movement of the volcano flank.

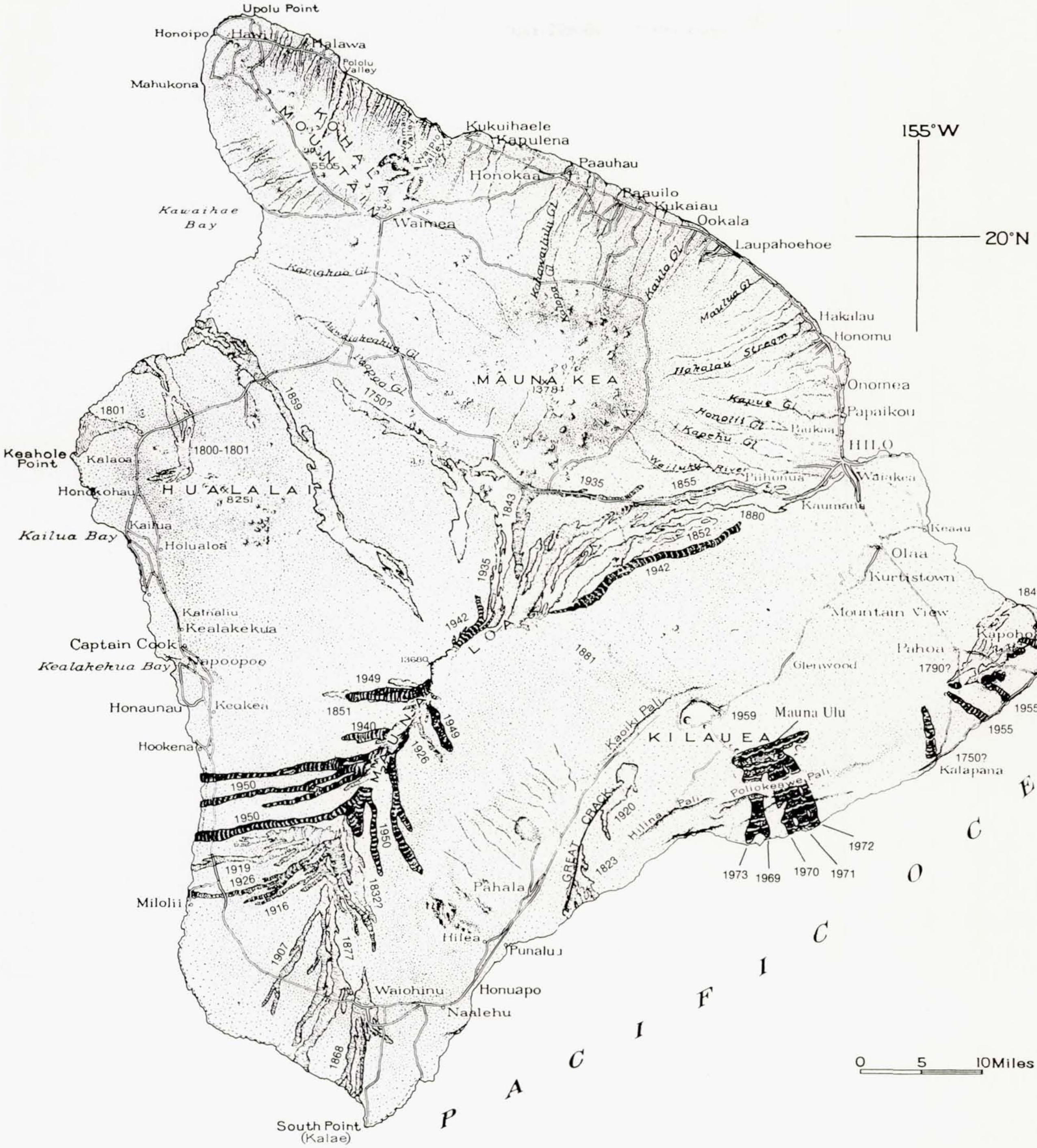

FIGURE 3–2. Map of Hawaii showing the five major volcanoes that make up the island and historic lava flows to 1969. (After Macdonald and Abbott, 1970.)

FIGURE 3–3. Profile of Mauna Loa as seen from the southeast. The profile is smooth and relatively flat toward the summit. Two ridges extend from the summit to the northeast and southwest along the rift zones. (Photograph by R. T. Holcomb, 1972.)

FIGURE 3–4. Looking west toward the Mauna Loa summit on the left and the Mauna Kea summit on the right; between the two peaks is the Humuula Saddle. Hilo Bay is to the right. The more jagged summit of Mauna Kea is due to capping by later stage lava flows and pyroclastic deposits. (U. S. Navy photograph 0066, 1954.)

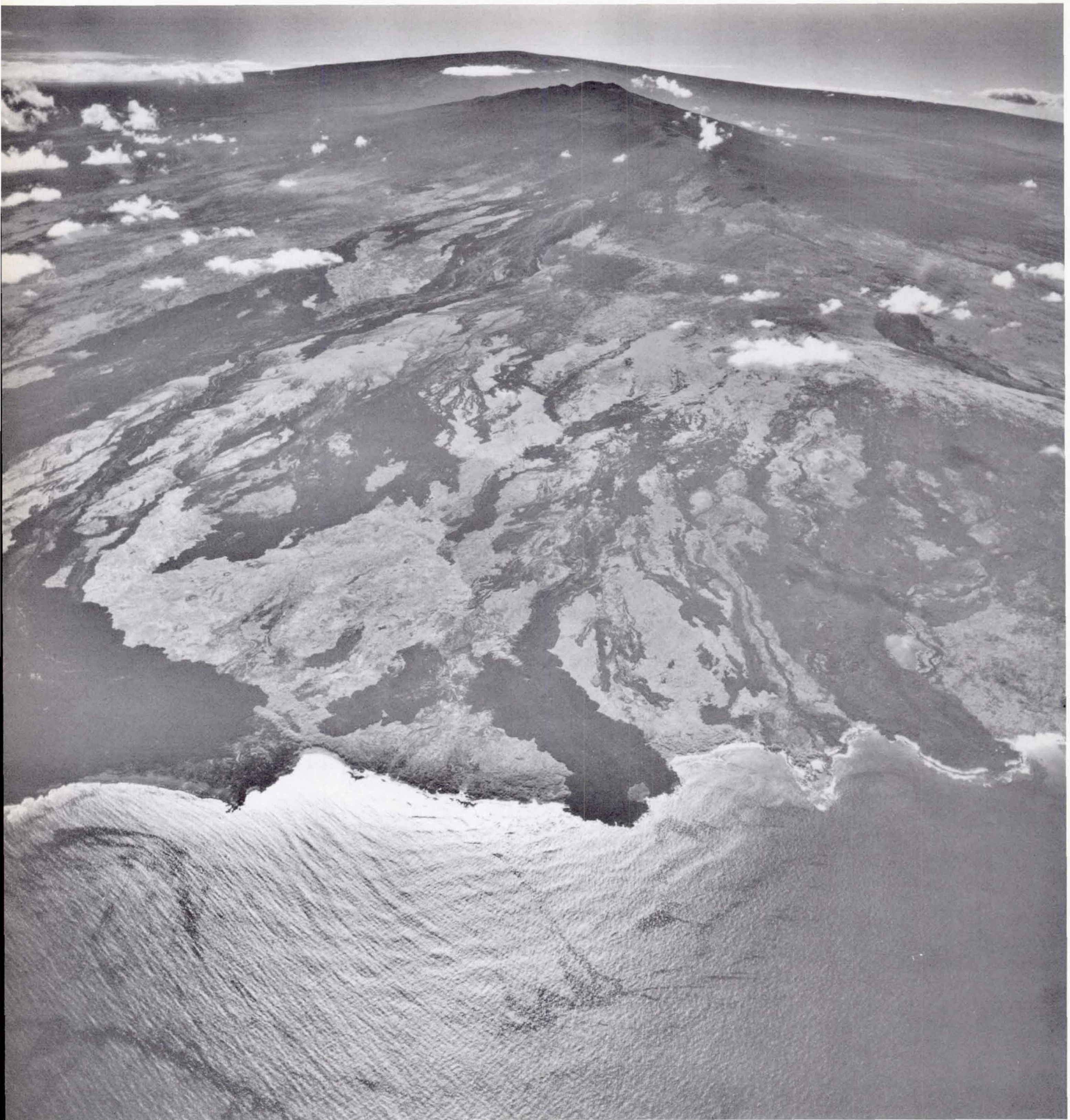

FIGURE 3–5. View to the southeast across Hualalai toward Mauna Loa. The steep profile and jagged summit of Hualalai contrasts with the smooth profile of Mauna Loa. The flows in the foreground are from Hualalai, the youngest of which was erupted in 1801. (U. S. Navy photograph 0070, 1954.)

FIGURE 3–6. View of the east across Hualalai with the summit of Mauna Kea to the left and the northeast flank of Mauna Loa to the right. (U. S. Navy photograph 0058, 1954.)

FIGURE 3–7. Panorama of Mauna Iki, in the Kau Desert on the southwest rift zone of Kilauea, as viewed from Footprint Trail. Mauna Iki is a low shield (Greeley, 1977), 1.5 km across with slopes less than one degree. It formed in late 1919 and 1920. Most of the flows are pahoehoe. (Photograph by R. Greeley, July 1978.)

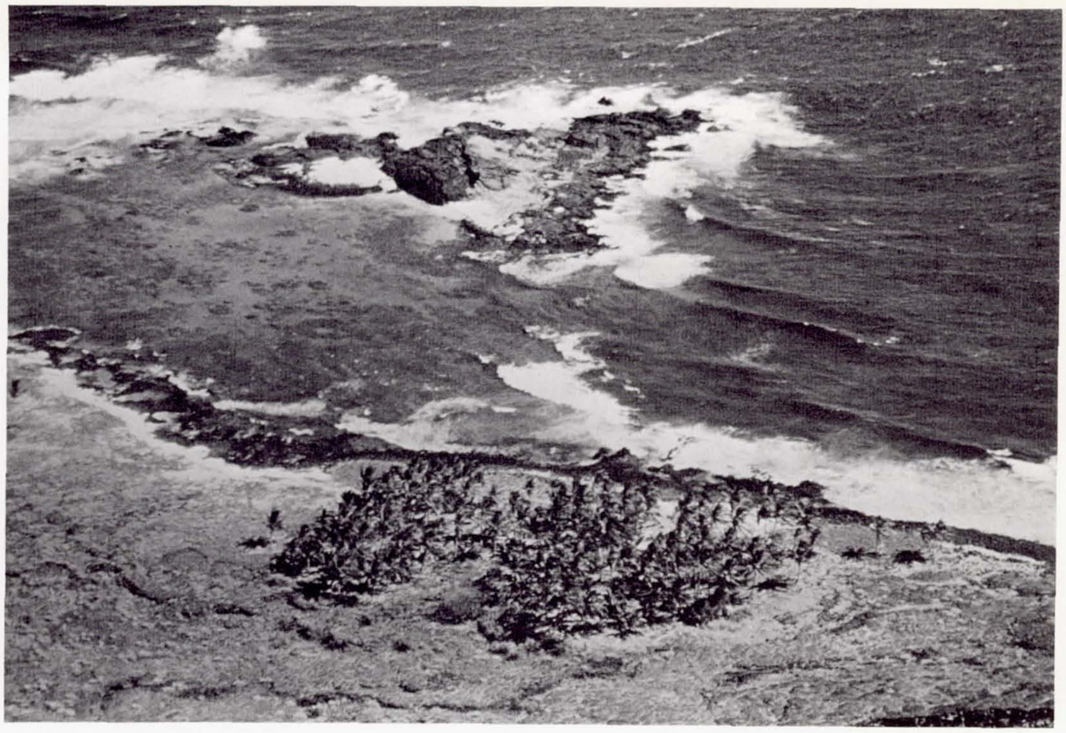

(A)

(B)

FIGURE 3–8. A 7.2 magnitude (Richter scale) earthquake struck Hawaii on November 29, 1975, centered in the Kalapana area on the southeastern coast of the island. The south flank of Kilauea Volcano moved along old and possibly new faults, with downward and seaward displacements as much as 3.5 m and more than 6 m, respectively. This subsidence is dramatically illustrated here: (A) shows the Halape area from Puu Kapukapu prior to the earthquake; (B) shows the same area after the earthquake; note palm grove that is now submerged and the offshore island that is nearly completely inundated. (From Tilling and others, 1976.)

Page intentionally left blank

IV. SUMMIT AREAS

The appearance of the summits of the Hawaiian volcanoes differs dramatically according to their stage of evolution. The younger volcanoes, represented by Kilauea and Mauna Loa, have a summit pit, or caldera, in contrast to the summits of the older volcanoes, such as Mauna Kea, Hualalai, and Kohala, where numerous cinder and spatter cones and younger flows cover all traces of any calderas that may have been present formerly. Eroded shields on older islands reveal evidence of calderas, so Kilauea and Mauna Loa are not thought to be unique. Calderas in Hawaii form primarily by collapse, probably as a result of withdrawal of magma from below. It is not known how early the caldera starts to develop but it is believed to occur when a magma reservoir is contained within the edifice. The calderas are generally roughly elliptical in outline, with flat floors and steep walls. They have a complex history of filling, upwelling, and collapse, sometimes around different centers. The walls are fault scarps along which collapse has occurred. Exposed as layers in the walls and apparently cut by the wall faults are numerous flows which must have originated from vents at elevations above the present caldera floor. Collapse may stop before onset of the late alkalic stage, when the caldera becomes filled with flows and pyroclastic deposits and numerous cinder cones dot the summit regions.

Kilauea caldera is approximately 4 km long and 3 km wide and ranges in depth from 120 m in the northwest to a few meters at its southern edge. Its rim stands close to 1,130 m above the ocean floor. In the southwest part of the caldera is an 800 m diameter pit, Halemaumau, which is at the summit of a small shield built within the caldera of recent lava flows. Just east of the main caldera is a similar but smaller feature, Kilauea Iki, a little over a kilometer in length and approximately 400 m wide. During its recorded history, Kilauea Caldera has undergone numerous collapses and refillings. Knowledge of activity in the Nineteenth Century is sketchy. In 1823 most of the caldera was occupied by a pit, the floor of which was about 200 m below the present rim. Around the pit, at a level of about 60 m below the present floor, was a black ledge believed to have formed by a then-recent collapse of the floor. A succession of eruptions followed such that by 1832 lava had once again reached the level of the black ledge. The central part of the caldera then collapsed again only to be refilled by 1840 when there was yet another collapse. During the next 25 years, the whole caldera rose *en masse* until the level of the floor was above the level of the former black ledge.

Further collapses took place in 1865, 1886, and 1891. In 1894 subsidence occurred in the Halemaumau area and the lava level withdrew and ultimately disappeared altogether. There followed a 13 year period of relative quiescence. Eruptions resumed in 1907 and the period 1907 to 1924 was one of almost continuous activity. In 1919 and 1921 Halemaumau was filled to the brim with lava and was the source of several flows which partially covered the caldera floor. In 1924 extremely violent phreatomagmatic eruptions and collapse of the walls of Halemaumau followed withdrawal of magma into the east rift zone. After the eruptions had subsided, the pit was found to be over 400 m deep with the bottom consisting of fragmental debris from the walls. Lava soon returned to Halemaumau and minor activity continued until 1934, after which there followed an 18 year quiet period. Activity resumed in 1952 and has continued episodically since that time. Thus, the history of the Kilauea Caldera is a complex succession of lava lake activity, relatively quiet eruptions onto the caldera floor, risings of the floor, violent phreatomagmatic eruptions, collapses, and quiescent periods. The causes of the constantly changing eruptive and tectonic activity are not known.

The summit caldera of Mauna Loa, known as *Mokuaweoweo*, stands at 4,000 m above sea level. It is elongate in a northeast-southwest direction, along the line of the two main rift zones. To the southwest, the main caldera is connected to a smaller pit crater known as *South Pit*. Further southwest are two near circular, 400 m diameter pit craters, *Lua Hohunu* and *Lua Hou*. To the north the remnants of a 2.5 km diameter pit crater, *North Pit*, forms a shelf slightly above the level of the floor of the main caldera. Within North Pit is a smaller pit crater *Lua Poholo*. In the southern part of Mokuaweoweo, close to the west wall, is a 75 m high spatter cone that formed during the 1949 eruption.

Although it is poorly known, Mokuaweoweo appears to have had as complex an eruption history as Kilauea caldera. In 1840 Mokuaweoweo could be divided into three pits: a central pit approximately 3 km in diameter, and two crescentic benches to the north and south which stood about 60 m above the floor of the central pit. Numerous eruptions during the last century gradually filled the central pit, and in 1914 lava flooded onto the north bench. The north bench was covered completely in 1940, and the southern bench in 1949. At that time lava which erupted within the caldera flowed into South Pit, partly filled it, overflowed its southern rim, and flowed down the side of the mountain. Of the 38 eruptions of Mauna Loa since 1832, listed by Macdonald and Abbott (1970), and including the 1975 eruption, 22 were at the summit.

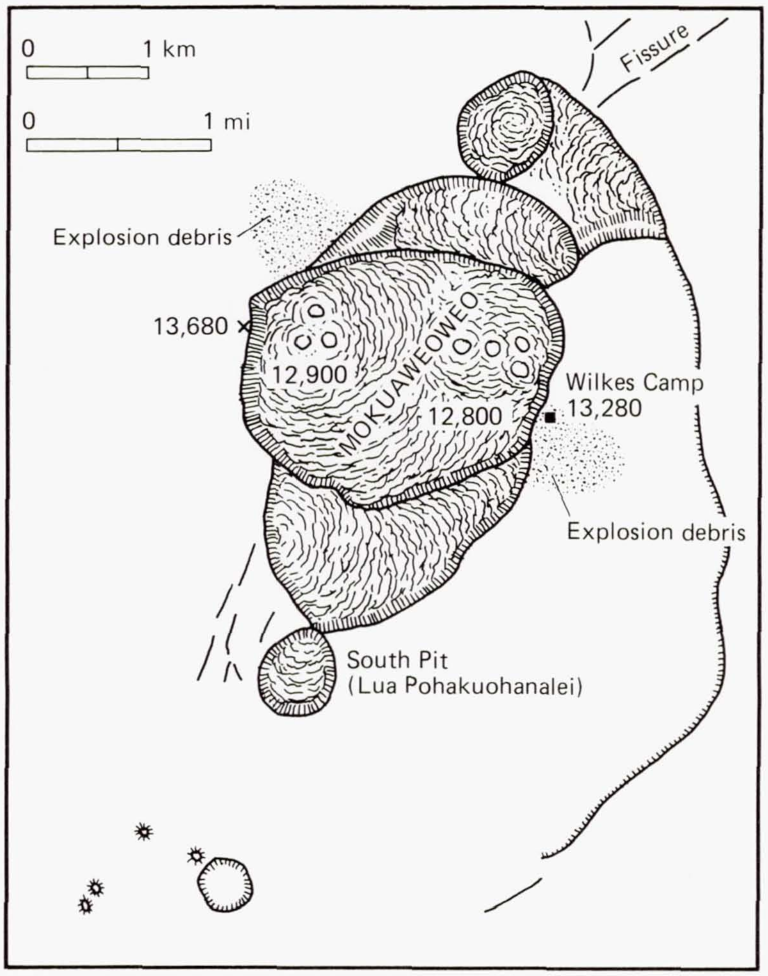

FIGURE 4–1. Map of Mokuaweoweo Caldera, Mauna Loa, in 1841 (after Wilkes, 1845). The caldera consisted of a central, nearly circular pit with benches to the north and south and two additional pits, North Pit and South Pit. Flows now fill the central pit and benches to a similar level. (After Stearns and Macdonald, 1946.)

Hualalai is the only other volcano on Hawaii that has erupted in historic times (1800–1801). It appears to have just entered the late stage in the eruptive cycle. No tholeiite flows have been found on the subaerial part of the volcano; most are alkalic basalts with some hawaiites. More than a hundred cinder and spatter cones occur at the summit and along northwest-southeast trending rift zones, so its appearance is dramatically different from Mauna Loa and Kilauea. A summit caldera, if one ever existed, has been completely buried by later deposits. The eruptions appear to have been less explosive than on Mauna Kea and Kohala, as evidenced by the smaller cones and larger proportion of spatter. There have been no historic eruptions at the summit; the 1800–1801 eruption was at a 1,800 m elevation on the northwest rift zone.

On Mauna Kea tholeiitic flows of the main shield-building phase have been almost completely buried by subsequent flow and tephra. Little trace of a former summit caldera has been found, almost certainly because of the thick cover of late stage alkali basalt and other rocks. The cinder cones and flows of the summit give Mauna Kea a significantly steeper and more jagged profile than Mauna Loa.

Traces of a former caldera occur close to the summit of Kohala, but it also has been buried by late stage lavas and pyroclastic deposits. Volcanoes on islands other than Hawaii are all too old to preserve their primary volcanic morphology.

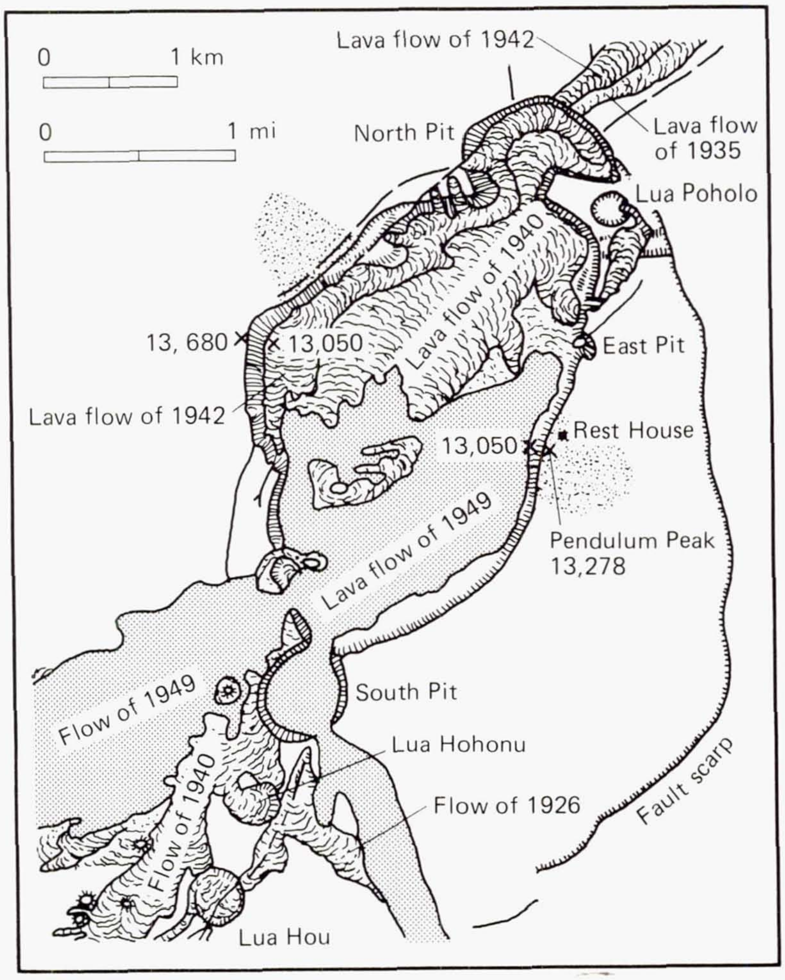

FIGURE 4–2. Map of Mokuaweoweo Caldera after the 1949 eruption. Lua Poholo, East Pit, and Lua Hohonu are pit craters that formed since 1841. (After Stearns and Macdonald, 1946, and Stearns, 1966.)

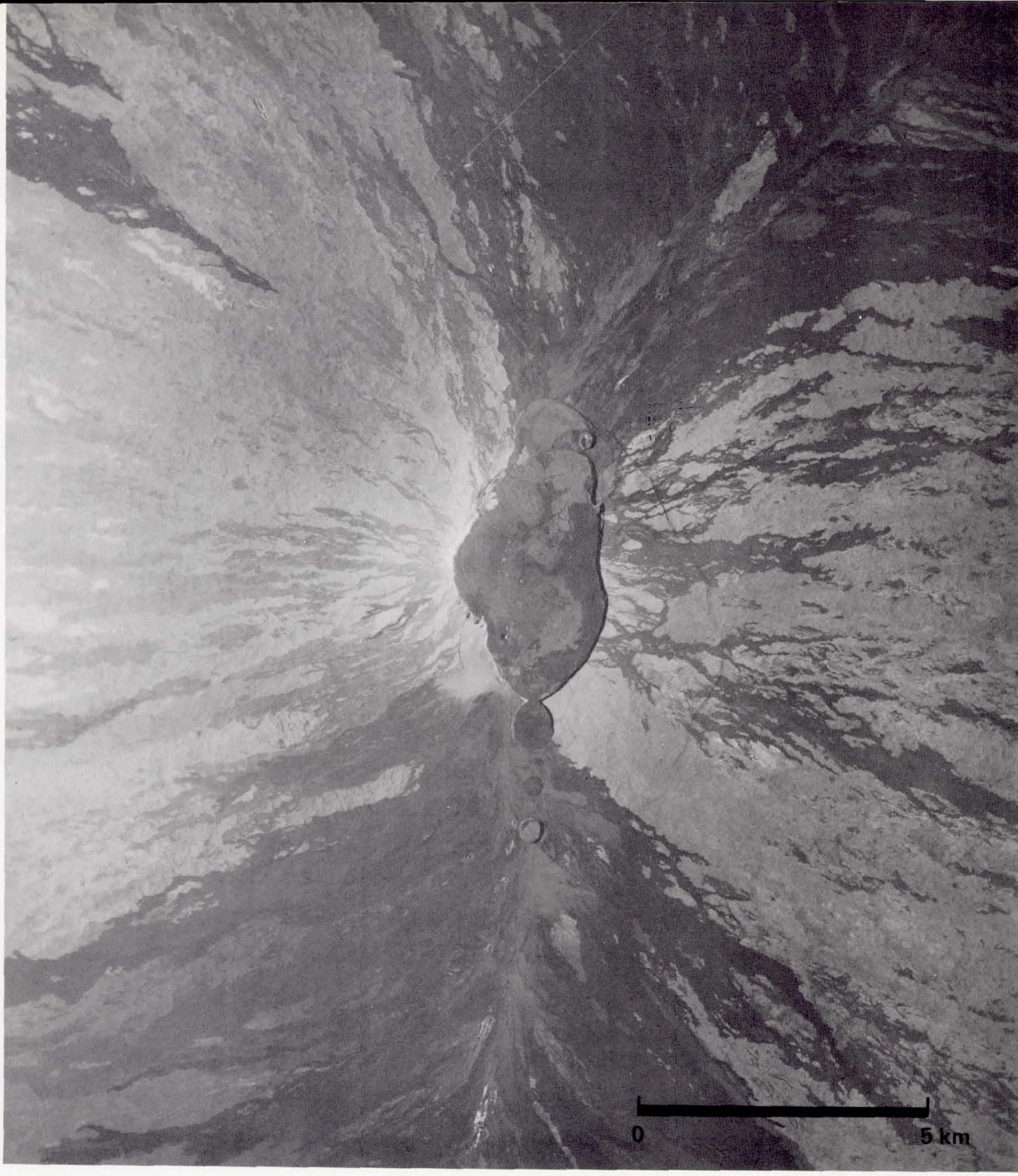

FIGURE 4–3. Summit of Mauna Loa. North Pit with its smaller pit crater, Lua Paholo, stands at a slightly higher level than the main caldera, Mokuaweoweo. To the south, the main caldera intersects South Pit, which was filled to overflowing by the 1949 eruption. One dark 1949 flow is visible, extending from the south rim down the mountain to the southeast. Two other pit craters, Lua Hohonu and Lua Hou, and numerous spatter cones occur on the rift zone southwest of the main caldera. At its widest, the caldera is 2.7 km across. (NASA-Ames, U-2 high-altitude photograph, October, 1974.)

FIGURE 4–4. Oblique aerial view to the north, across South Pit and Mokuaweoweo. The 1949 flow with its central channel is visible in the foreground. Just beyond South Pit, within the main caldera, is the 1940 cone. The gentle profile of the summit is broken only by a few low spatter cones. (U. S. Air Force photograph, 1966.)

FIGURE 4–5. Looking northwest across the center of Mokuaweoweo. Hualalai is in the middle background, Haleakala is in the far background. Part of the west wall of Mokuaweoweo at the intersection of the former central pit and northern bench has collapsed along arcuate faults. (U. S. Navy, photograph 0071, 1954.)

FIGURE 4–6. View of the west wall of Mokuaweoweo, similar to Figure 4–5, but more detailed. Layering caused by truncated flows is clearly visible in the wall. Note also slump blocks of the wall to the right. (Photograph by R. Greeley, 1969.)

FIGURE 4–7. Mokuaweoweo, North Pit, and the smaller 350 m diameter pit crater, Lua Poholo; North Pit is irregularly shaped and only incompletely encircled by fault scarps. It has been partly buried to the west by 1940 lavas. (Photograph by Towill Corp., Honolulu, frame 6682-11, 1975.)

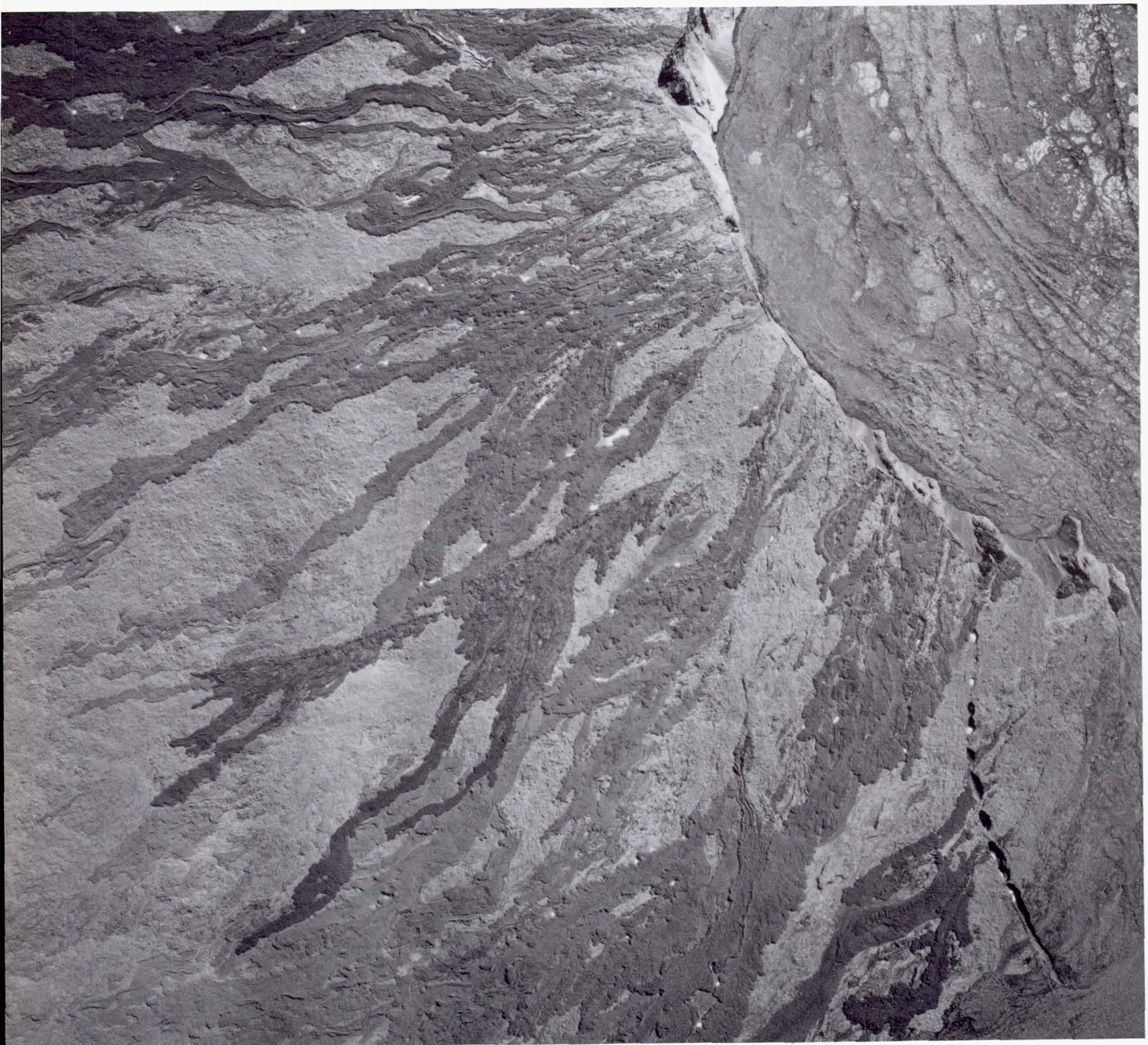

FIGURE 4–8. West wall of Mokuaweoweo, showing truncation of lava flows by the caldera walls. Many flows originate from vents at elevations above the present caldera floor. Others, at the center and bottom right, originate from fissures on the rim. (Photograph by Towill Corp., Honolulu, frame 6679-5, 1975.)

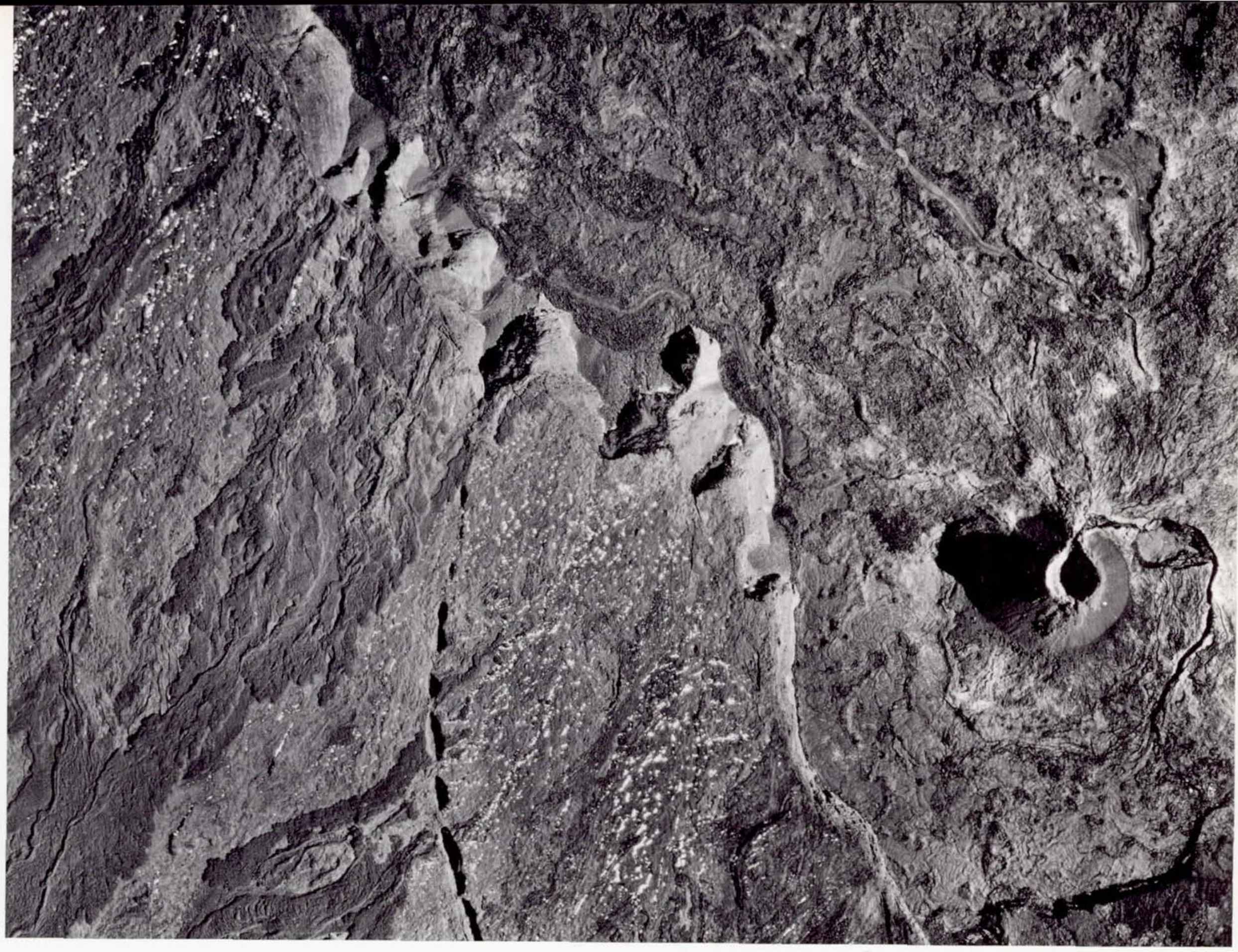

FIGURE 4–9. View of the west wall and floor of Mokuaweoweo, just to the south of the previous figure. An arcuate fissure which intersects the wall is visible on both figures. The cinder and spatter cone on the floor is from the 1940 eruption. (Department of Defense photograph, frame M-65, 1942.)

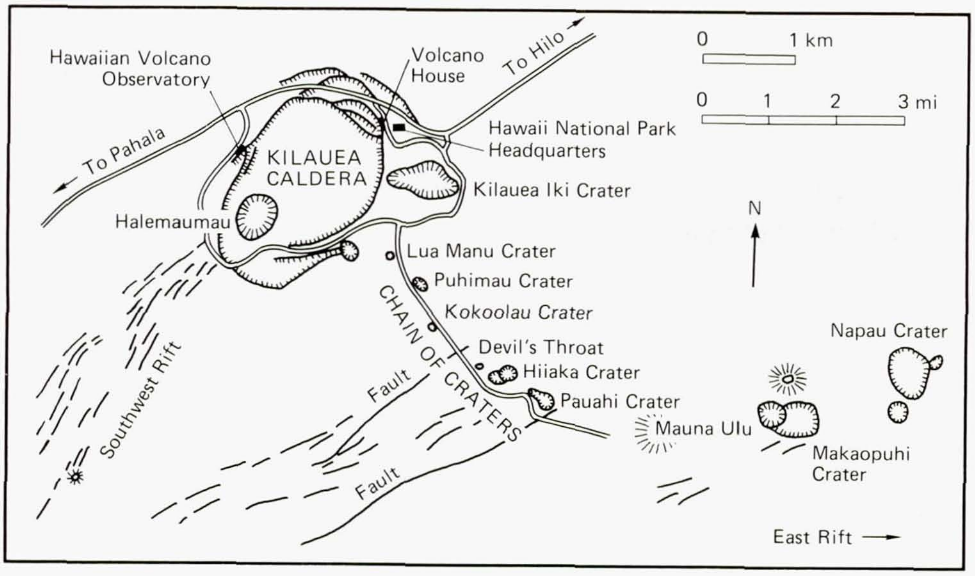

FIGURE 4–10. Sketch map of Kilauea caldera and its immediate environs. (After Stearns and Macdonald, 1946.)

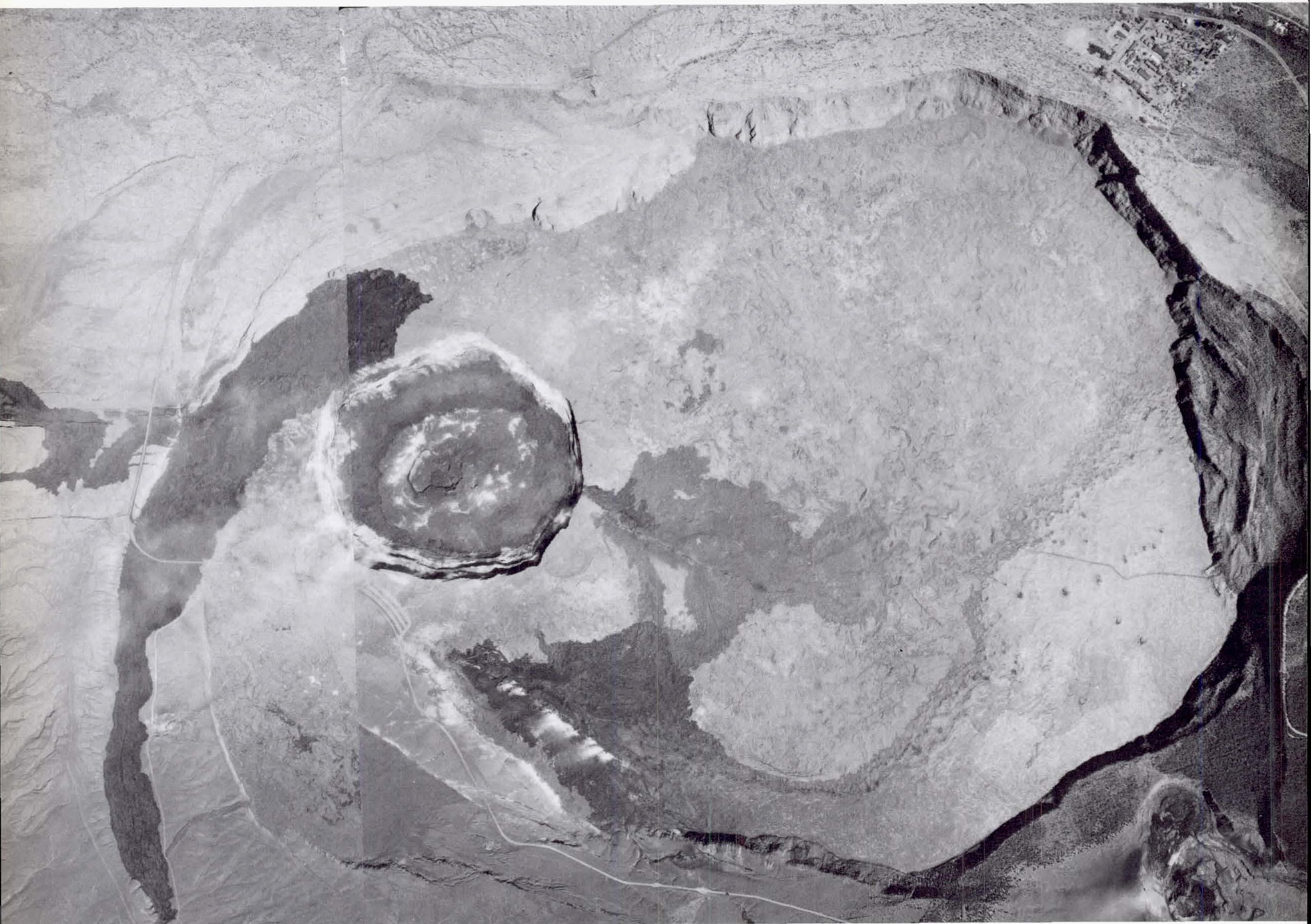

FIGURE 4–11. Aerial view of Kilauea caldera. The 1 km diameter pit, Halemaumau, in the southwest part of the caldera is approximately 120 m deep. The dark flows to the northwest were erupted in 1954. The dark flows to the southwest are from 1971, as are some in the southeast part of the caldera. (Photograph by Towill Corp., Honolulu, frames 5720-3, 5720-4, 1974.)

FIGURE 4–12. Oblique view of Kilaeua Caldera from the south with Mauna Kea in the background. The 1954 flows are clearly visible on the caldera floor. (U. S. Navy, photograph 0011, 1954.)

FIGURE 4–13. Oblique view of Halemaumau pit crater. Steam is continually emitted from vents within the crater, resulting in the formation of solfataric deposits. The fissures in the foreground are part of the southwest rift zone, which subsequently gave rise to the 1971 flows visible in Figure 4–11. (U. S. Air Force photograph, 1966.)

FIGURE 4–14. Aerial view of the summit of Hualalai. The summit is marked by numerous cinder and spatter cones and presents a marked contrast to the summits of Mauna Loa and Kilauea. The central cone is approximately 500 meters across and stands at 2,500 meters above sea level. The cinder cones extend to the northwest and southeast along rift zones and tend to be smaller and have larger proportions of spatter than those on Mauna Kea, suggesting less explosive activity. (Department of Agriculture, photograph EKL-5CC-99, 1964.)

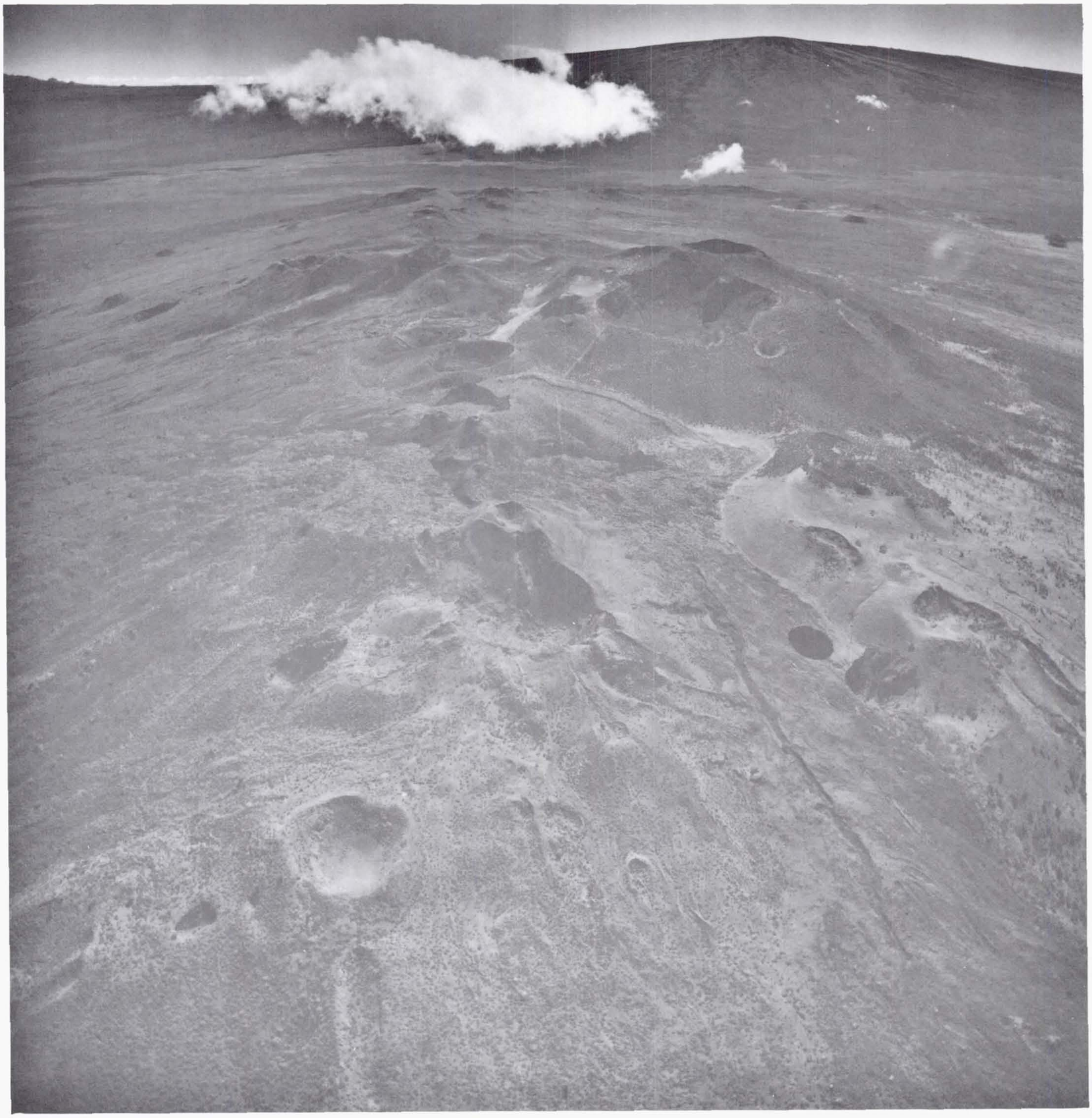

FIGURE 4–15. Oblique aerial view of the summit of Hualalai from the northwest, showing cinder cones at the summit and the upper part of the northwest rift zone. Mauna Loa is in the right background. Compare with Figures 5–20 and 5–21. (U. S. Navy, photograph 0155, 1954.)

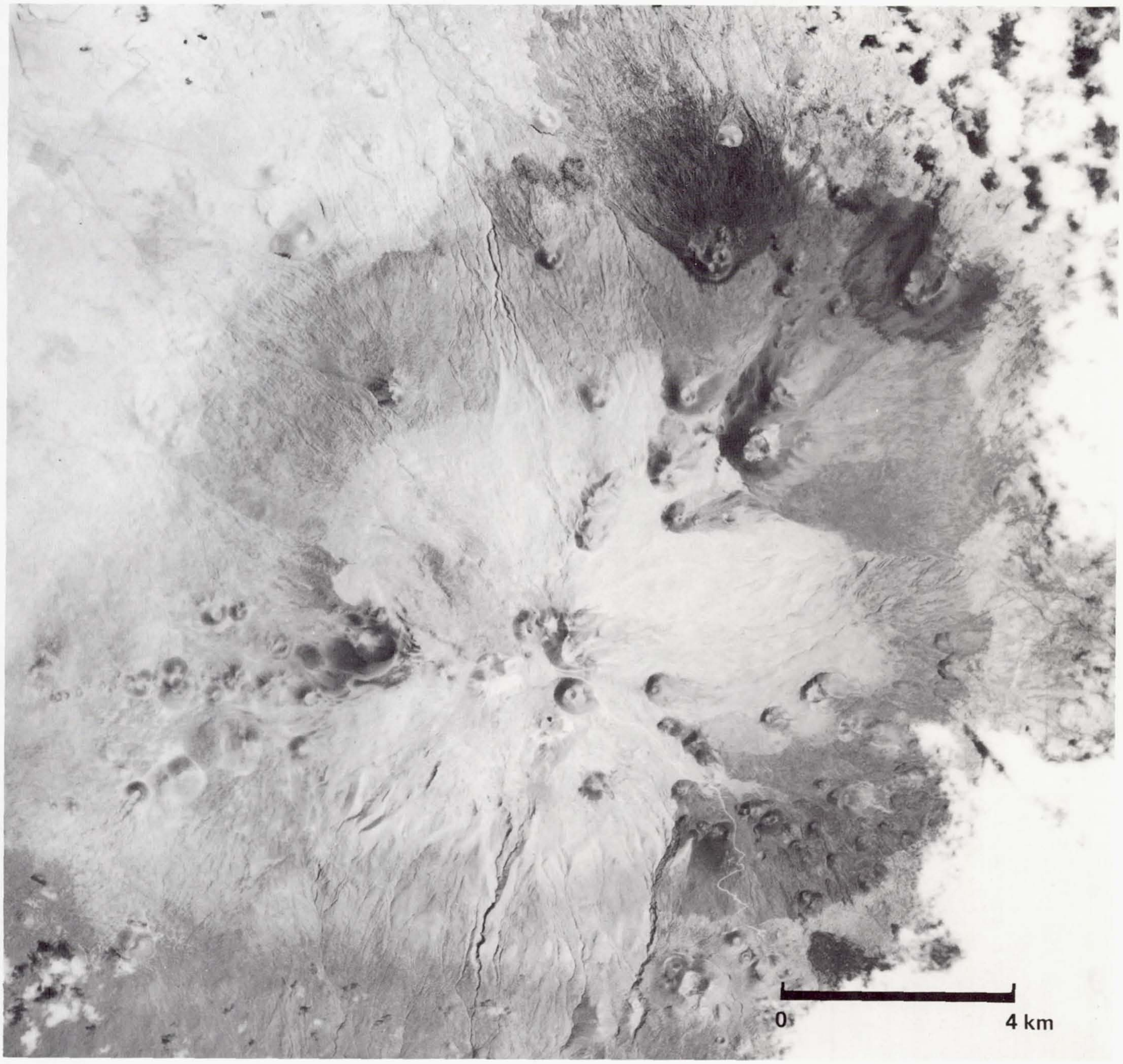

FIGURE 4–16. High altitude vertical view of the summit of Mauna Kea, showing numerous cinder cones typical of late stage Hawaiian shield volcanoes, which generally produce more viscous lava (contrast with Figure 4–3, showing summit of Mauna Loa). (NASA-Ames, U-2 photograph, 1974.)

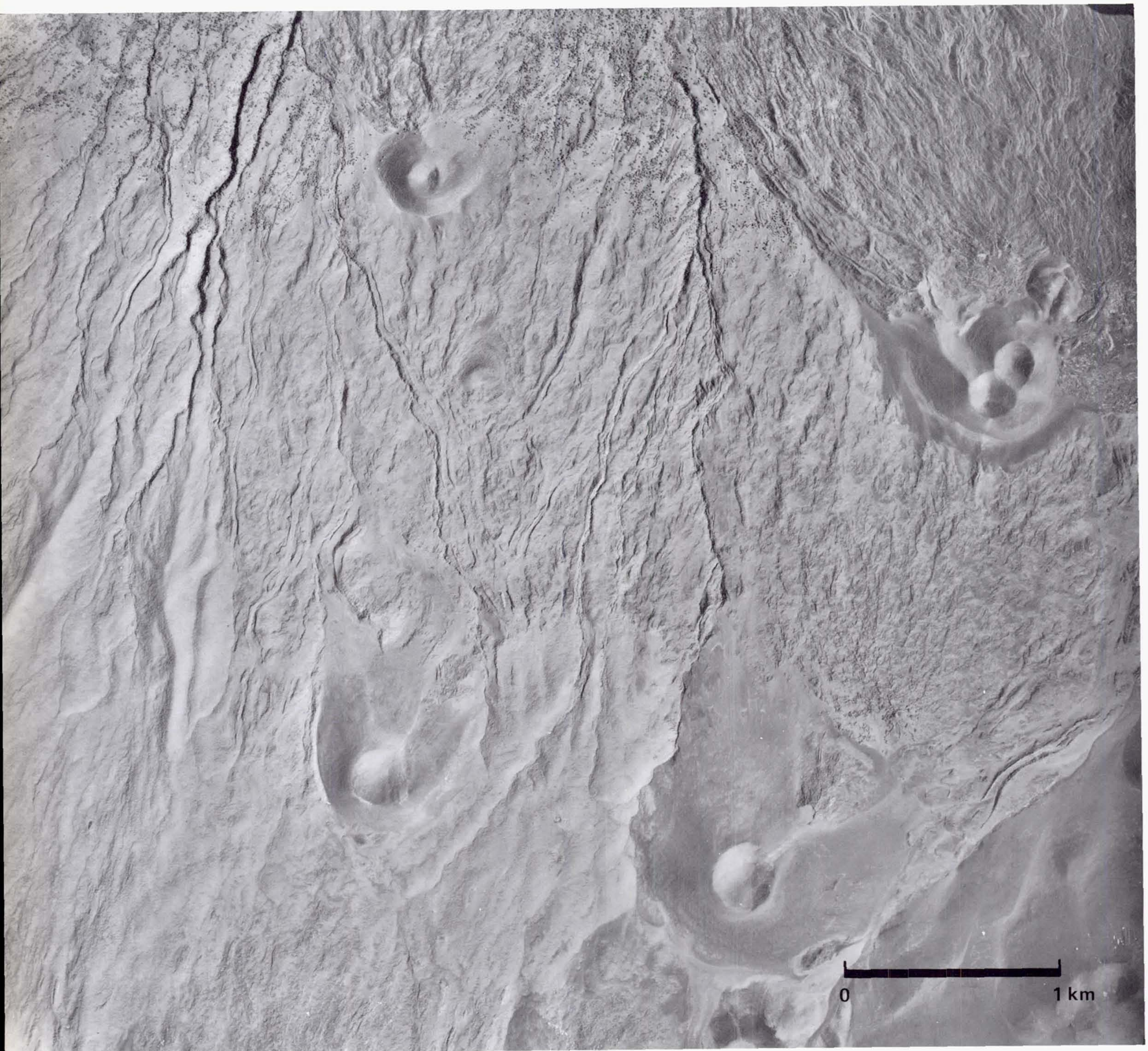

FIGURE 4–17. Vertical view of northeast flank of Mauna Kea. The summit is off the picture to the bottom left. Flows characteristically fan downslope from the cinder cones, which themselves tend to be elongate in the downslope direction. (Department of Agriculture, photograph EKL-14CC-105, 1965.)

FIGURE 4–18. View northeastward across the cinder cones at the summit of Mauna Kea. Goodrich Cone is in the middle of the picture. Summit Cone, with the astronomical observatories of the University of Hawaii, is in the background. The lake in the foreground is within Puu Waiau, a cone which is predominantly hyaloclastite, formed from a subglacial eruption. (Photograph by Agatin T. Abbott.)

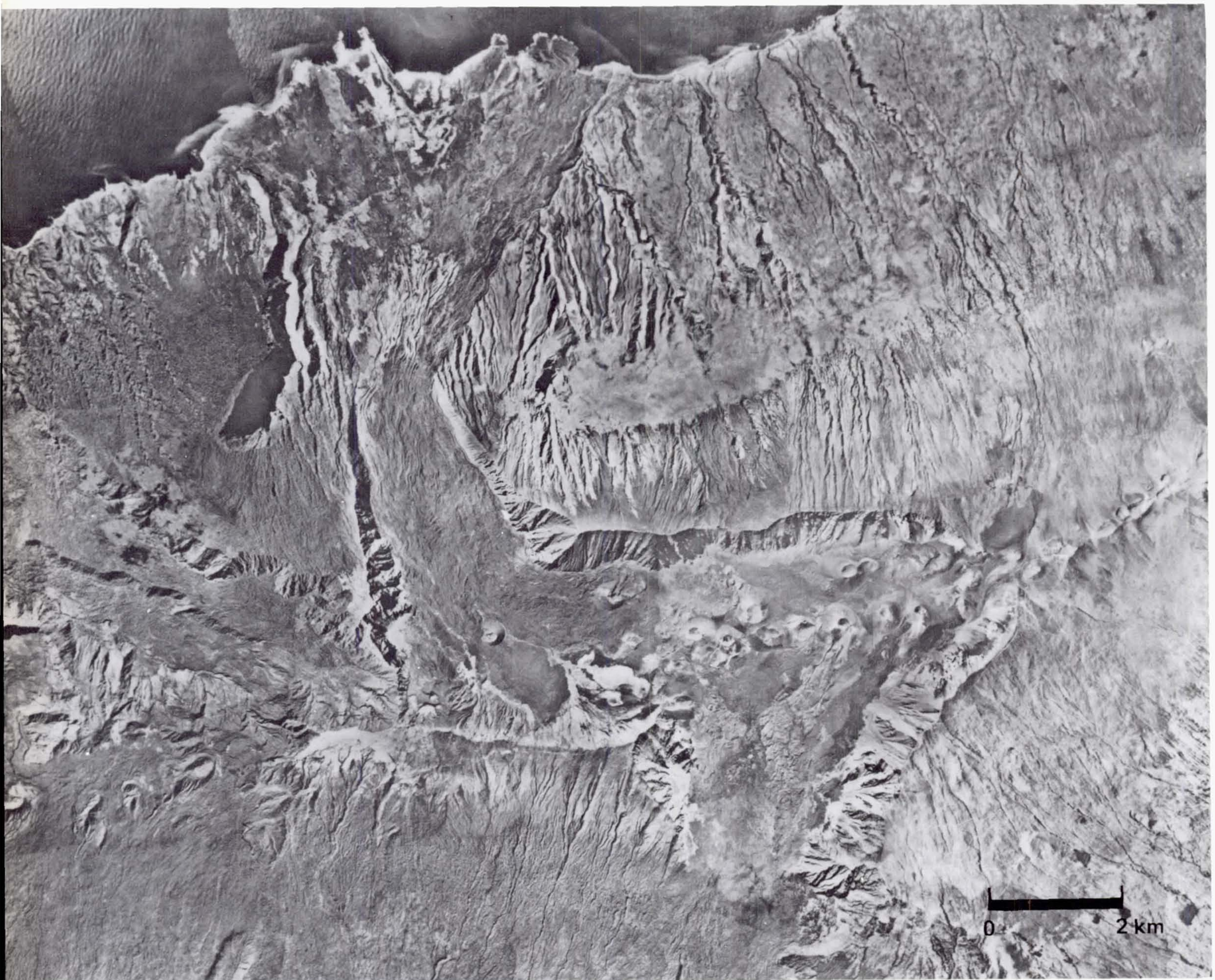

FIGURE 4–19. Mosaic of the summit of Haleakala, Maui. The summit depression is generally considered to be not a true volcanic crater but water-eroded. Deep valleys, cut into the volcano to the north and south, were later filled with lava. They now form the Koolau gap to the north and the Kaupo gap to the south. A line of cinder cone traces the rift zones across the crater. (U. S. Department of Agriculture, Soil Conservation Service Mosaic.)

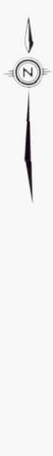

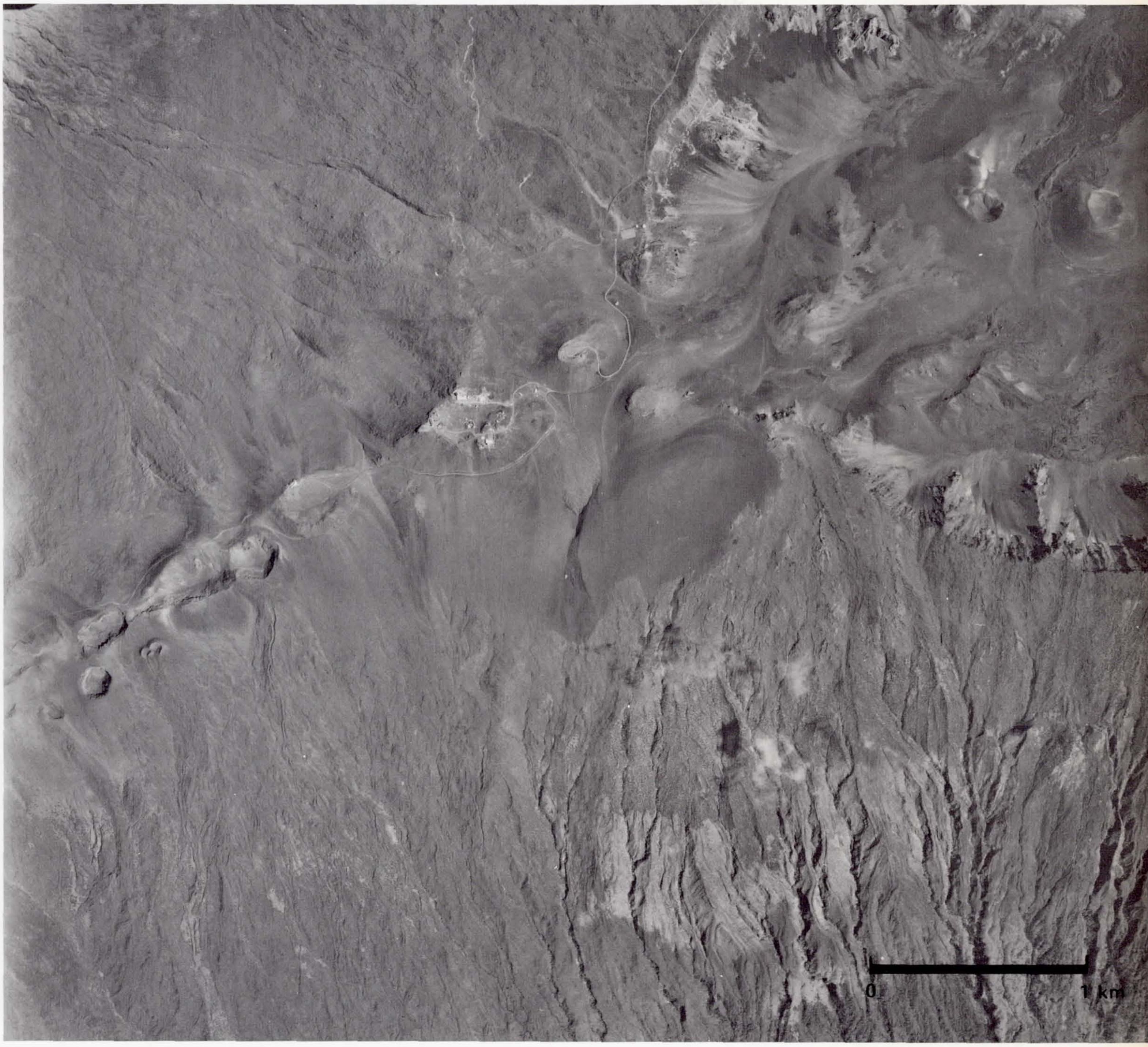

FIGURE 4–20. *Detail of the intersection of the southwest rift zone of Haleakala, Maui, with the summit crater. Although the south flank of the volcano is eroded by numerous gullies, several lava channels are still visible on top of ridges. Cinder cones occur along the rift zone and thick beds of vitric ash are common. Flows on the lower slopes are primarily hawaiites with lesser amounts of olivine basalt and ankaramites. (U. S. Department of Agriculture, photograph EKN-3CC-21, 1965.)*

FIGURE 4–21. View of the caldera wall at Haleakala Volcano, showing near vertical dikes (arrows) exposed by differential erosion. (Photograph by R. Greeley, 1977.)

V. RIFT ZONES

Most of an Hawaiian shield volcano is built during the early, very active, tholeiitic stage. The shape of the shields and the history of recent activity on Kilauea and Mauna Loa suggests that most of the flows that comprise the shields are erupted from radial rifts rather than central vents. The rift zones of Kilauea and Mauna Loa lie along the crests of massive, gently sloping ridges. Along the length of the rift zones are numerous spatter cones, spatter ramparts, fissures, and collapse pits; flows from the vents along a rift zone diverge downslope to form a feather-like configuration. Successive rift eruptions have built the ridges and result in the markedly elongate shape of each volcano. Volcanic activity may also be concentrated along rift zones even after the main shield-building phase. Although this is not obvious on Mauna Kea, the linear arrangement of cinder cones on Hualalai, Kohala, and Haleakala is very striking.

Exposed sections through rift zones on older dissected volcanoes on Oahu and Lanai suggest that dense swarms of nearly vertical dikes occupy the rift zones. This interpretation is reinforced by geophysical observations. Anomalously high seismic velocities have been observed beneath the rift zones of Mauna Loa and Kilauea and gravity highs radiate outward from each of the five volcanoes of the island of Hawaii in positions that approximate the rift zones as defined by the surface geology.

The orientation of the rift zones appears to be controlled largely by local gravitational stresses within the volcanic edifice rather than by regional stresses (Fiske and Jackson, 1972). In the case where a volcano grows immediately adjacent to an older volcano, one flank is buttressed by the preexisting volcano while the other flank faces the ocean and is unsupported. The orientation of the rift zones is generally in such a direction as to permit accommodation to magma injected into the edifice by outward movement of the unsupported seaward-facing flank. As discussed above, injection of magma into the east and southwest rift zones of Kilauea causes an outward movement of the south flank toward the ocean. In the case of a free-standing volcano, one which does not abut against another, such as Kauai, growth appears to be nearly symmetrical with no strongly preferred rift zones.

Geodetic, geologic, and geophysical data indicate that in Kilauea and Mauna Loa magma rises from the mantle through a nearly vertical conduit to a holding reservoir beneath the summit caldera. The reservoir is probably an intricate array of interconnected dikes, sills, and irregular chambers that swell as they fill, causing measurable tumescence at the surface. With continued magma supply, the strength of the reservoir rock is exceeded and magma is 'leaked' from the system, resulting in a shallow intrusion or an eruption.

Nearly all intrusions and eruptions occur either in the summit area or along the rift zones. Summit eruptions are accompanied by shallow earthquakes as magma works its way to the surface, and the overall summit area may undergo net expansion. During rift eruptions, the summit area subsides, apparently because magma migrates outward from the central reservoir into a rift zone. The pattern of seismic activity along the rift zones is very irregular. During some Kilauea east rift eruptions, few earthquakes occur between the reservoir and the eruption area, suggesting a relatively unobstructed interconnecting conduit, whereas in other eruptions, there is a sizeable increase in seismic activity. In nearly all cases, however, numerous earthquakes occur in the immediate vicinity of the eruption as magma works its way to the surface. Forceful intrusion of magma into the rift zone produces considerable dilation which results in cracks and fissures at the surface. The net effect of repeated intrusions into the rift zones of Kilauea has been a southward movement of the south flank of the volcano. The edifice thus grows not only by accumulation of surface flows but also by ground deformation that results from intrusions.

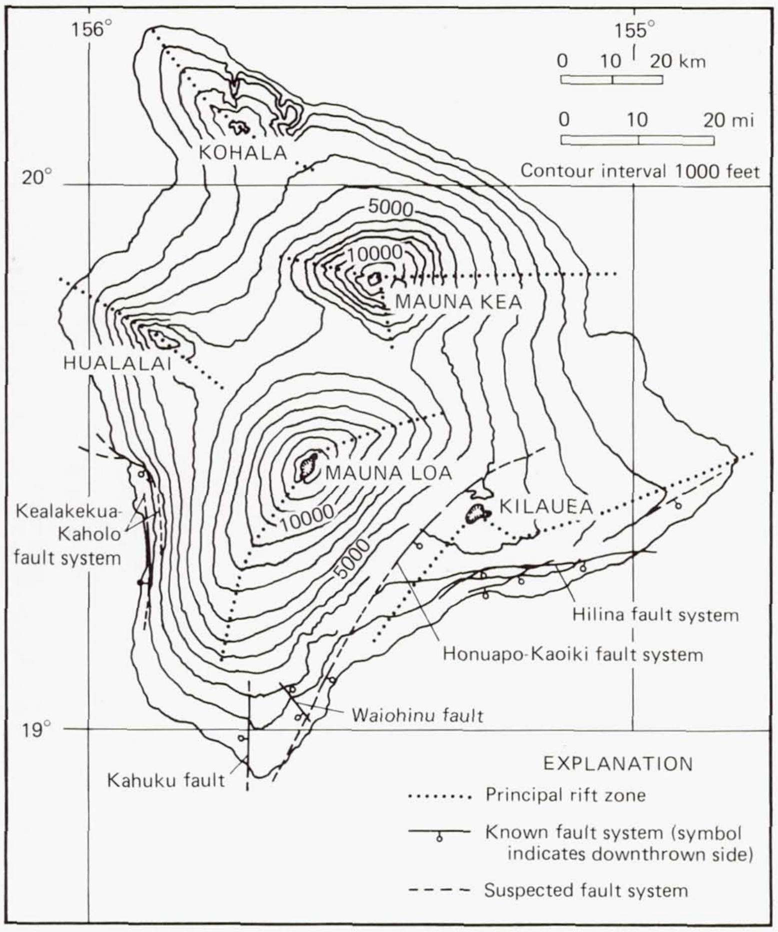

FIGURE 5–1. Map showing rift zones and major faults in the Island of Hawaii. (From Macdonald and Abbott, 1970.)

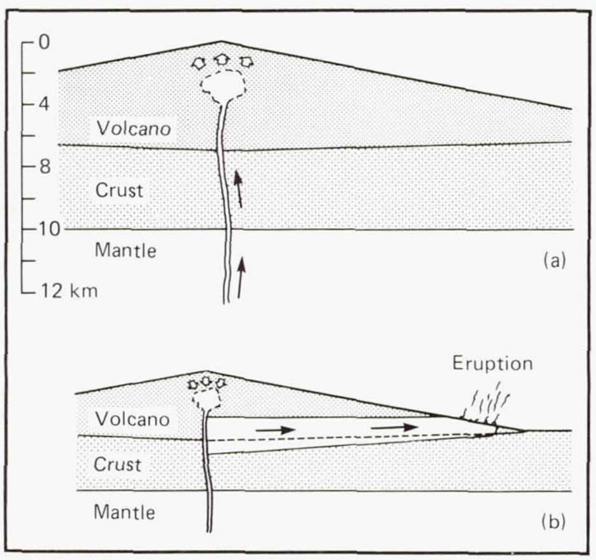

FIGURE 5–2. Schematic cross section through Kilauea Volcano. (a) Summit area during a period of inflation. Lava is transported from deep within the mantle to a holding reservoir 2-5 km below the summit. (b) Summit and rift during a period of injection and eruption. Lava removed from the rift zone during a flank eruption is replaced by new magma from beneath the summit. Magma may be stored in the rift zone for months or years before being erupted. (After Fiske and Jackson, 1972.)

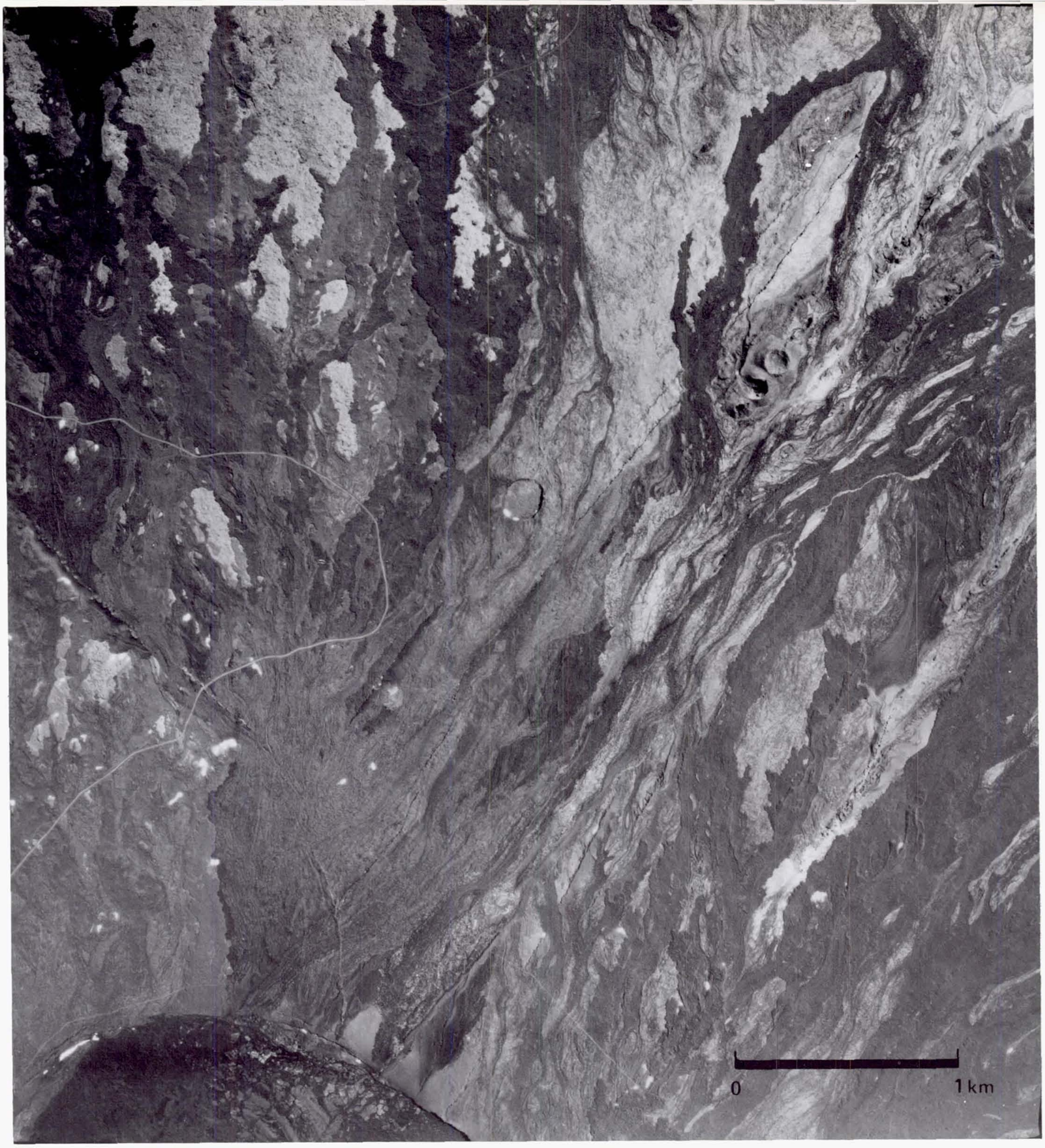

FIGURE 5–3. Intersection of the northwest rift zone of Mauna Loa with the north pit of Mokuaweoweo at the volcano summit. Several cracks trend northeast-southwest along the rift zone. At right angles is another crack which has been the source of many of the flows in the upper left of the picture. The small pit crater at the center is Lua Ioana; the large cinder cone on the right is Pohaku Hanalei. (Photography by Towill Corp., Honolulu, frame 6682-9, 1975.)

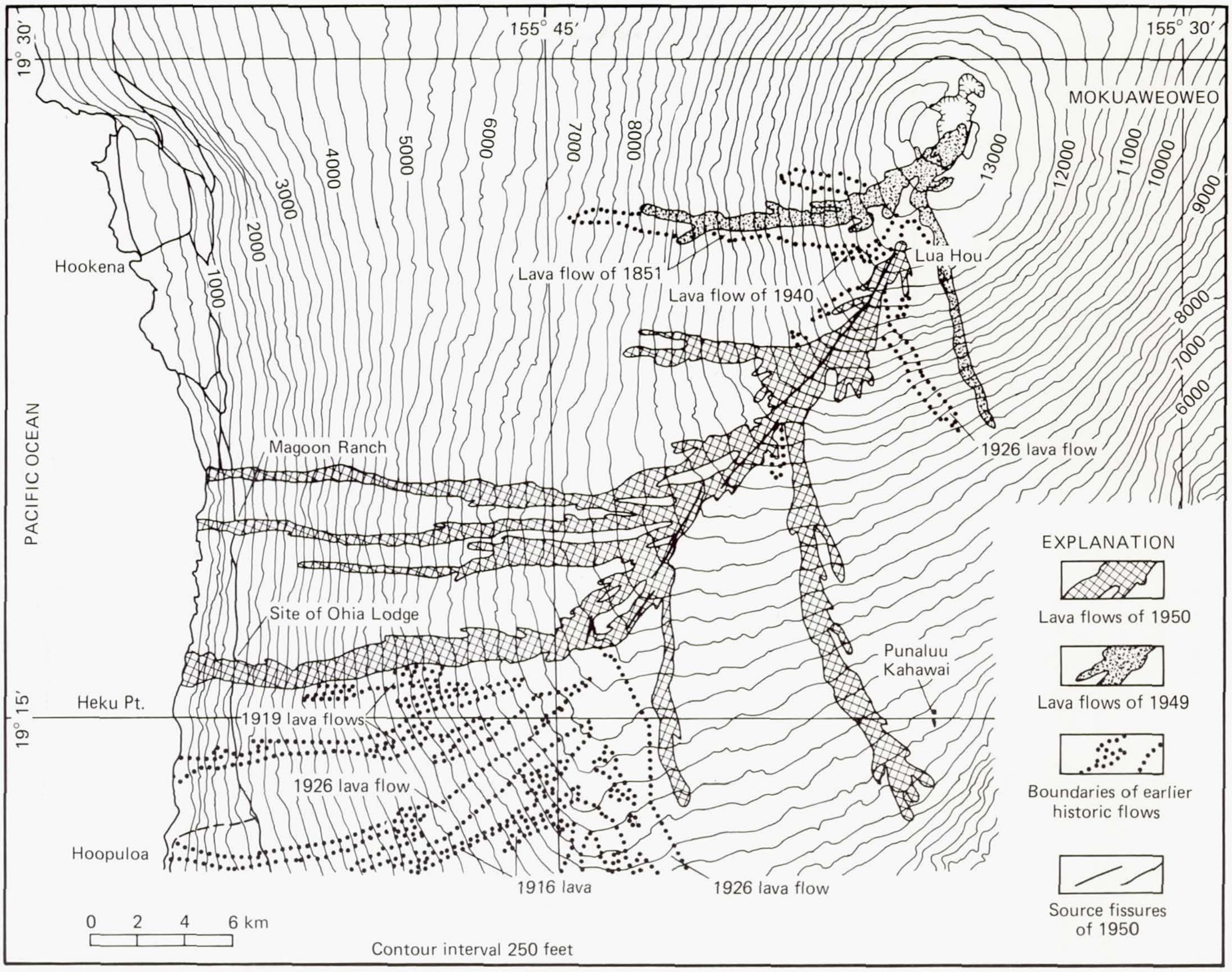

FIGURE 5–4. Map of the summit and southwest rift zone of Mauna Loa, showing the location of the rift zone and some of the historic flows. (From Macdonald and Abbott, 1970.)

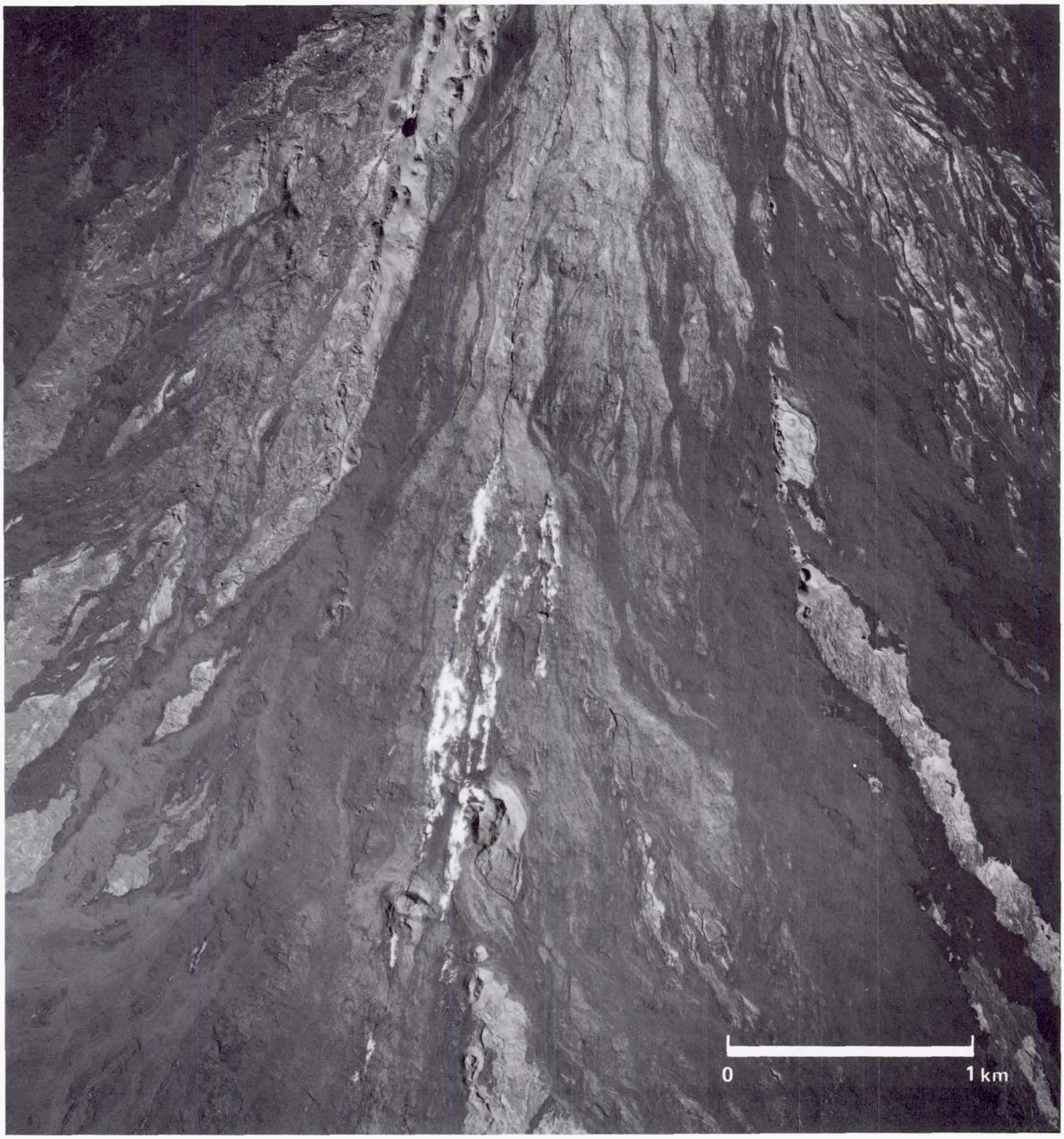

FIGURE 5–5. The southwest rift zone of Mauna Loa at the 11,000 ft level. The spatter cone at the bottom of the picture is Sulfur Cone. Just west of Sulfur Cone is a northeast-southwest trending crack that extends across the entire scene. Farther to the northwest are spatter ramparts aligned along the rift. Many of the flows are from the 1950 eruptions. (Photograph by Towill Corp., Honolulu, frame 6681-1, 1975.)

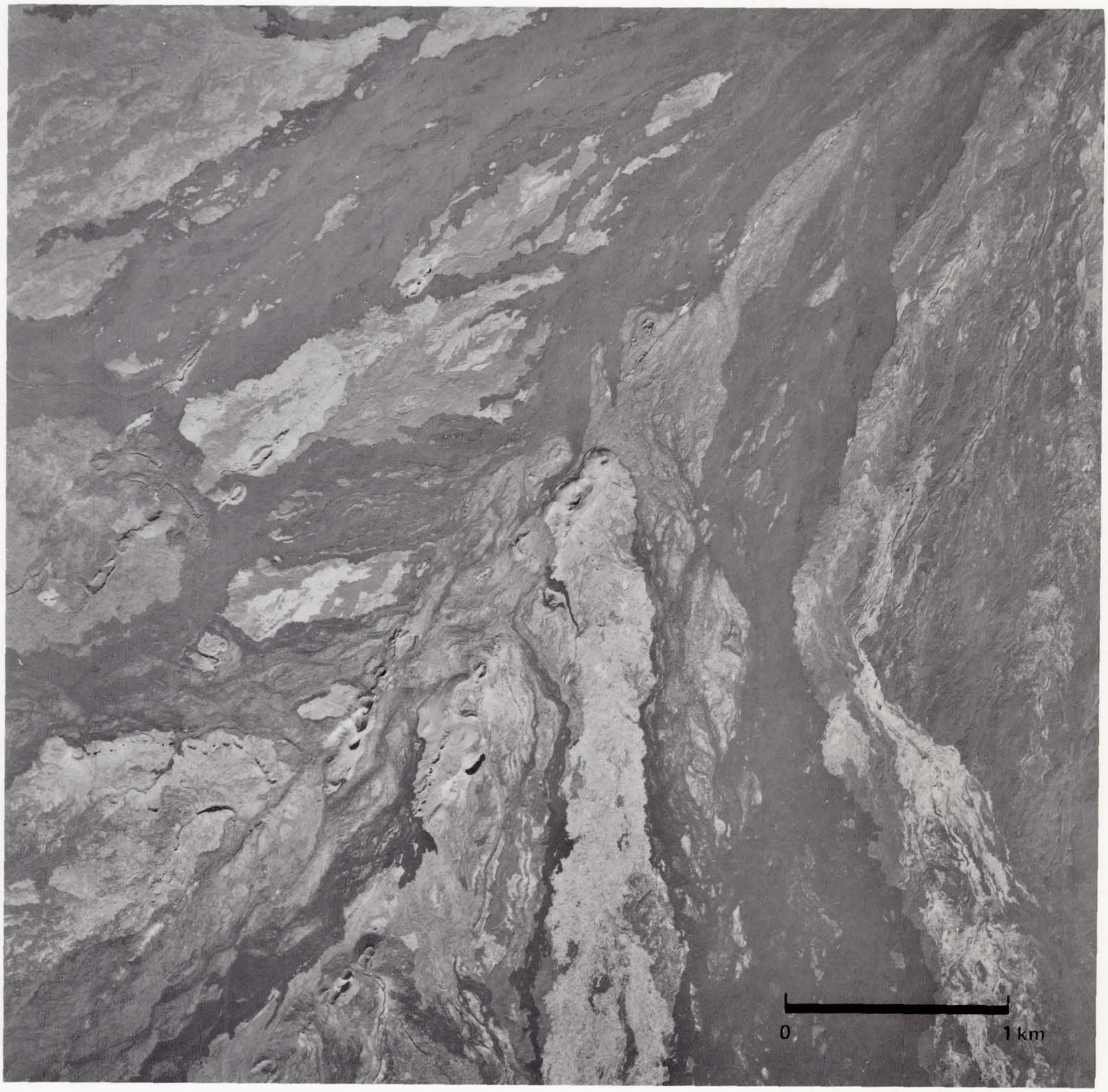

FIGURE 5–6. The southwest rift zone of Mauna Loa just below the area shown in the previous figure. The dark flows which diverge to the southwest on either side of the rift zone are 1950 flows. Several lava channels appear to start at spatter cones along the rift. A sinuous line of pits in the lower left quadrant is probably a partly collapsed lava tube. (U. S. Department of Agriculture, photograph EKL-7CC-223, 1965.)

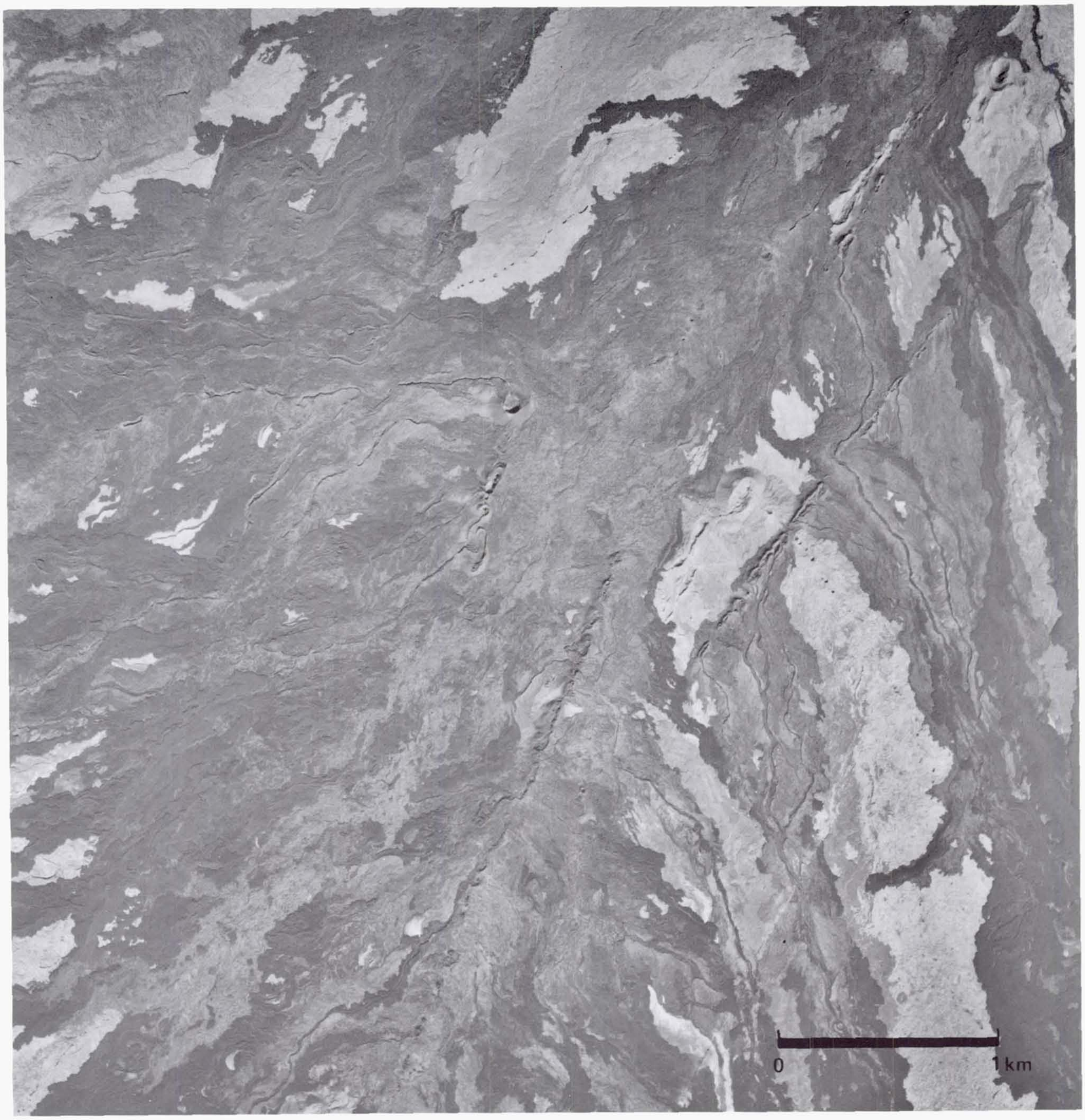

FIGURE 5–7. Southwest rift zone of Mauna Loa at the 8,000 ft level. The circular cone and lava channel, just above the center of the picture, is the Alika Cone. Northwest of the cone, a line of depressions marks the course of the lava tube, which forms the Umi Caverns. The dark flow with prominent lava channel in the right of the picture is from the 1950 eruption. The darker flow and line of spatter cones in the bottom of the picture are mostly from 1926. The flows and line of spatter cones in the left side of the picture are mostly from eruptions in 1919 and 1950. (U. S. Department of Agriculture, photograph EKL-2CC-189, 1964.)

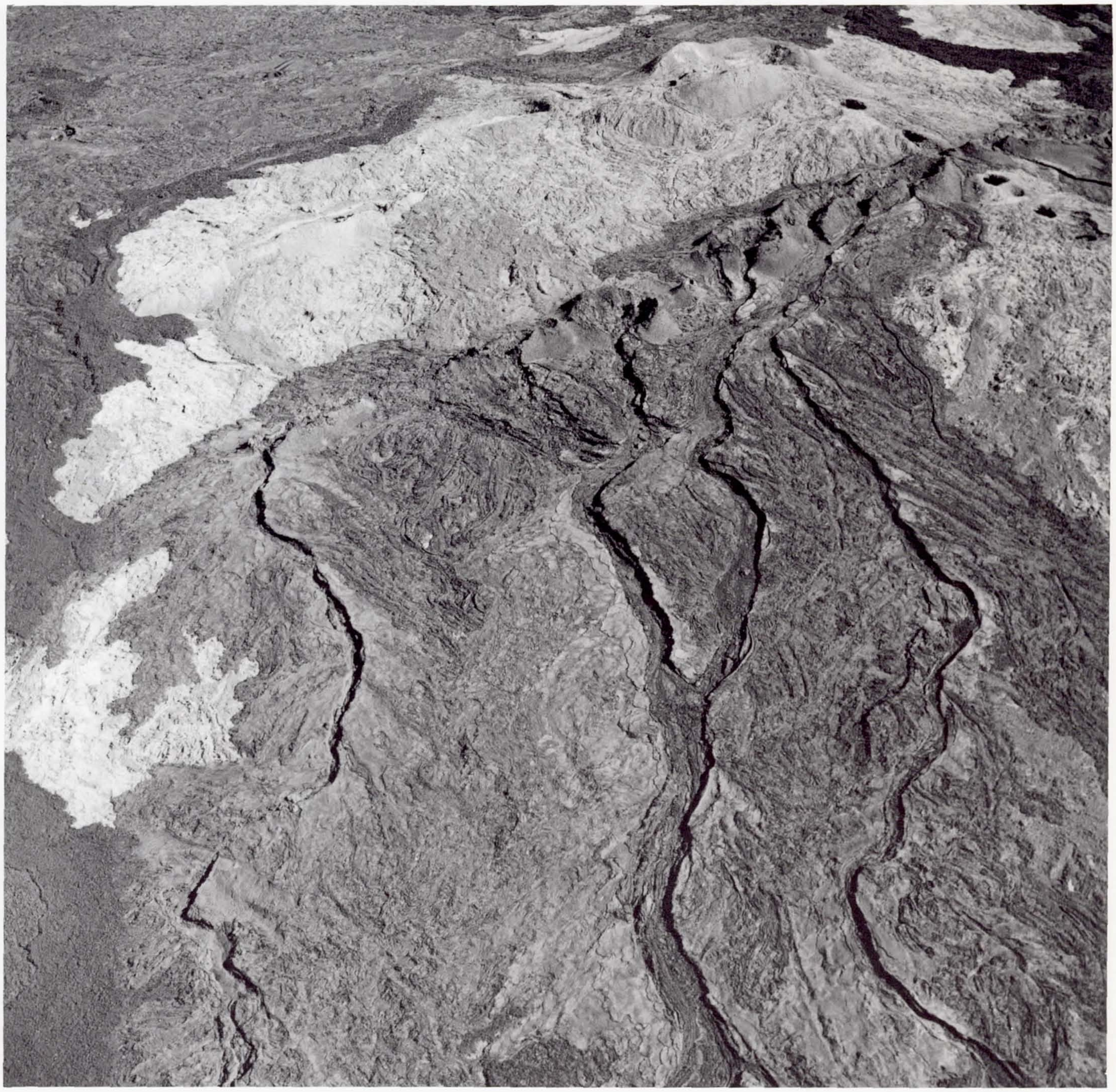

FIGURE 5–8. Oblique view of part of the area shown in previous figure, looking up the rift zone. In the foreground braided channels in pahoehoe originate at a series of spatter cones along the rift zone. At the upper right a partly collapsed lava tube extends southeast from a large cinder-spatter cone. (Photograph by R. Greeley, 1969.)

FIGURE 5–9. Oblique view of area in the previous picture, showing more clearly the collapsed lava tube. (Photograph by R. Greeley, 1969.)

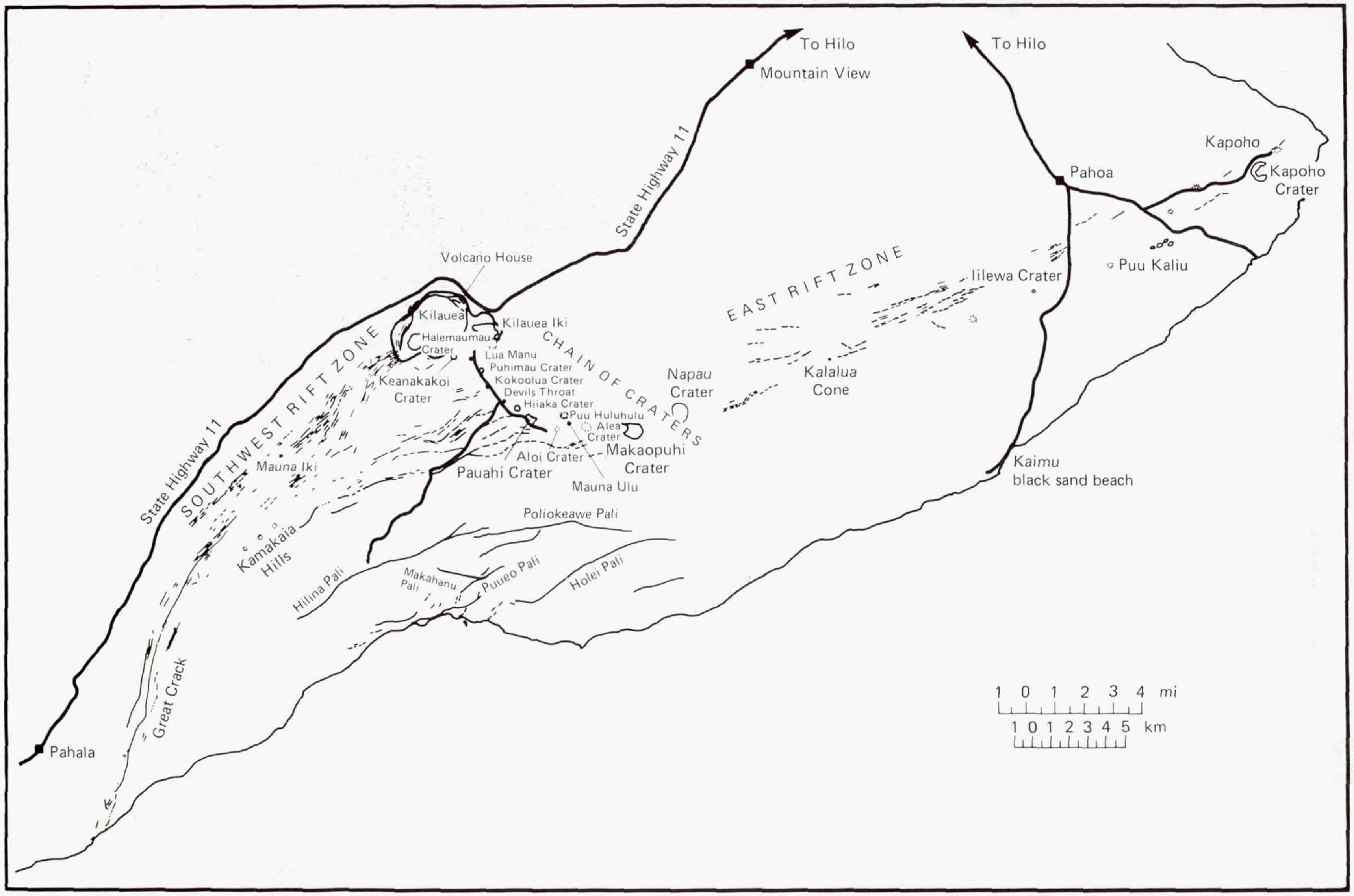

FIGURE 5–10. Sketch map of Kilauea volcano, showing the location of prominent pit craters, cones and fault. (From Hawaiian Volcano Observatory Staff, 1974.)

FIGURE 5–11. Faults in the Koae fault system south of Kilauea Caldera, along the west extension of the east rift zone. The rift zone in this area turns northwest and is marked by a line of pit craters. The irregularly shaped pit crater is Pauahi.

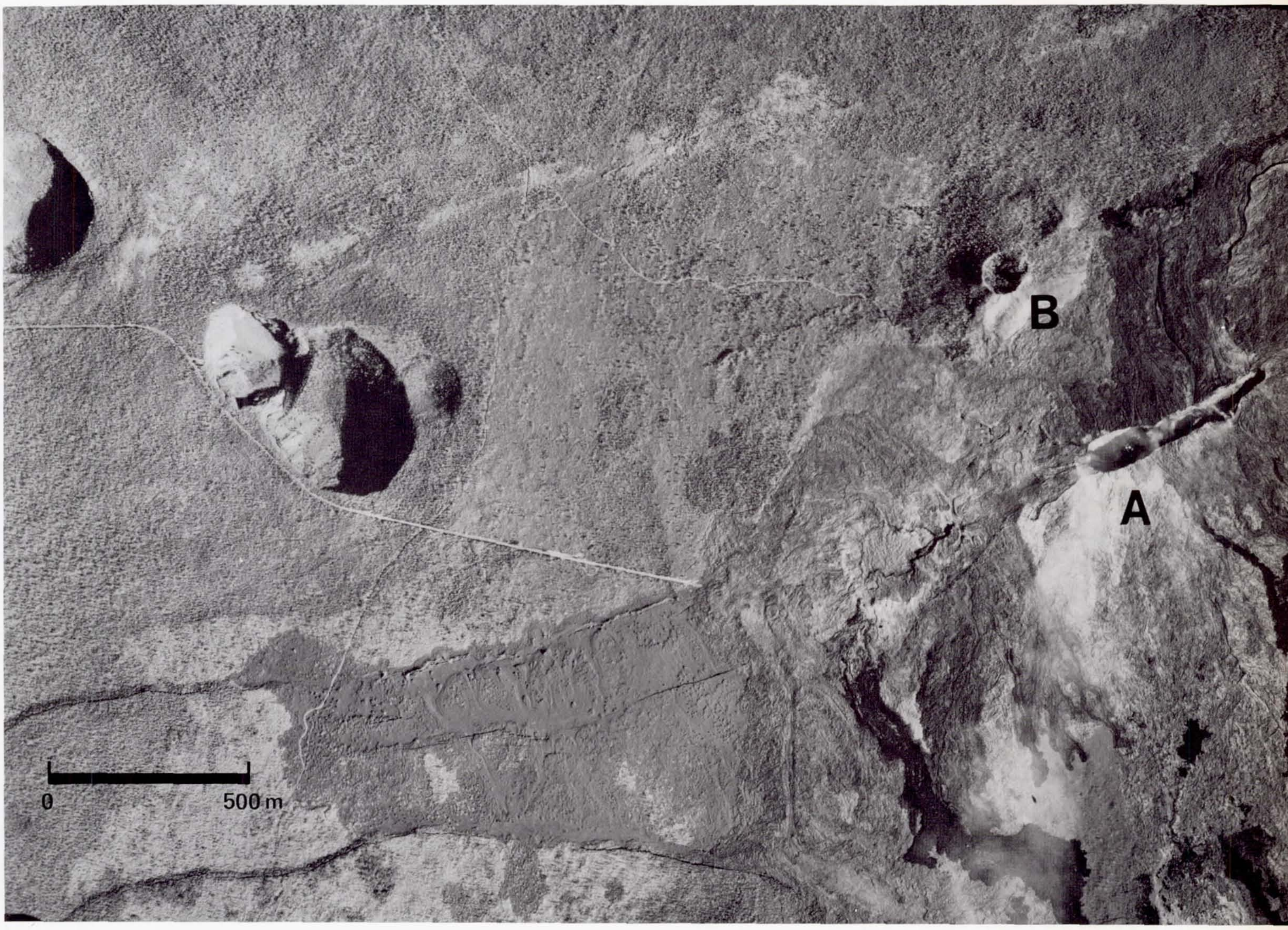

FIGURE 5–12. Scene just east of the previous figure, showing Mauna Ulu eruptions along fissures similar to those in the previous figure. The main Mauna Ulu vent (A), with its northeast trench, is at the right margin, just south of the cone Puu Huluhulu (B). Prominent flows in lower center were formed on May 24, 1969. Compare with the figures of Chapter 12. (Photograph by Towill Corp., Honolulu, frame 5812-11, 1972.)

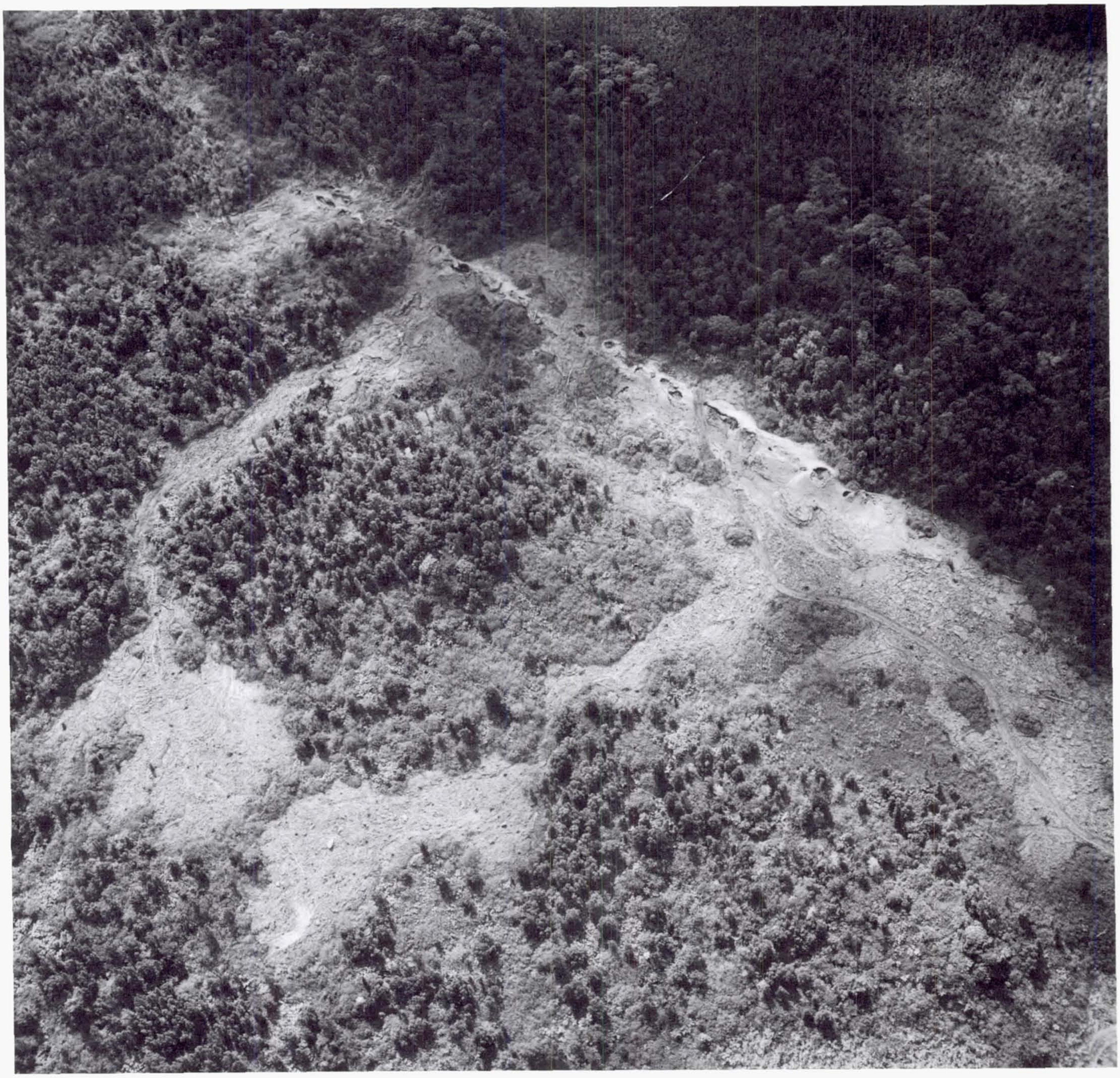

FIGURE 5–13. Line of spatter cones along fissure for 1955 eruption, Kilauea lower east rift zone. The forest downslope has been partially destroyed by the flows. (U. S. Air Force photograph, 1966.)

FIGURE 5–14. Spatter and cinder cones at some of the 1955 vents on Kilauea lower east rift zone. The area covered by previous figure is in the background. (U. S. Air Force photograph, 1966.)

FIGURE 5–15. Intersection of the Kilauea southwest rift zone with Kilauea Caldera. The caldera margin is on the right. Subparallel fissures, small cracks, and graben extend southwest along the rift zone. (U. S. Department of Agriculture, photograph EKL-SCC-9, 1965.)

FIGURE 5–16. Same field of view as previous picture, showing lava flows erupted September 24, 1971. Some new cracks developed and some pre-existing cracks widened during the eruption and were partly filled with lava. (Photograph by Towill Corp., Honolulu, frame 5816-8, 1972.)

FIGURE 5–17. Flows in the region of Mauna Iki on the Kilauea southwest rift zone. The summit pit of Mauna Iki is in the lower left. Dark 1971 flows are superimposed on somewhat lighter 1919-1920 flows. (Photograph by Towill Corp., Honolulu, frame 5720-11.)

FIGURE 5–18. Looking up the Kilauea southwest rift. The flows in the background are 1919-1920 flows from Mauna Iki. Scene is the upper half of Figure 5–17. (Photograph by R. Greeley, 1970.)

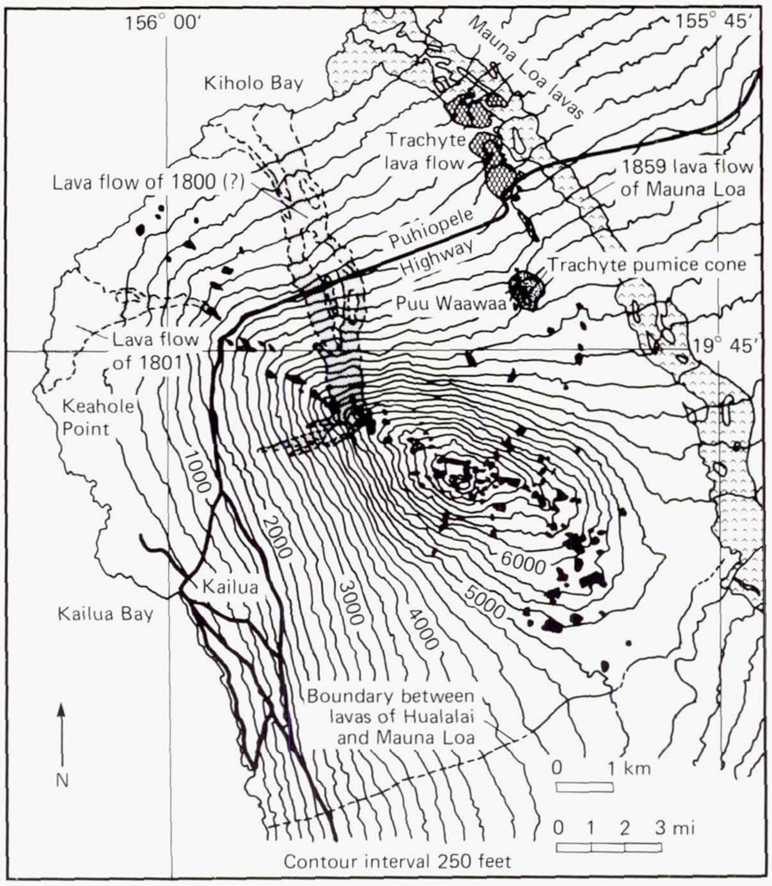

FIGURE 5–19. Map of Hualalai, showing the flows of 1800-1801, the trachyte pumice cone of Puu Waawaa, and the trachyte flow from the cone. (From Macdonald and Abbott, 1970.)

FIGURE 5–20. Aerial view of Hualalai, showing the numerous small cinder and spatter cones aligned along the southeast and northwest rift zones. Compare with the previous figure for scale. (U. S. Department of Agriculture, Soil Conservation Service, Mosaic.)

VI. PIT CRATERS

Pit craters are similar in shape and perhaps in origin to calderas. They are generally subcircular in outline, but may be multiple, formed by the intersection of two or more near circular pits. The larger ones commonly have a level floor of younger lava flows or a ponded lava. The craters have no rim deposits indicative of throw-out of material during crater formation; rather the depressions appear to form completely by collapse. Pit craters are particularly common along the upper sections of the east rift zone of Kilauea. Two prominent pit craters in this area, Aloi and Alae, were buried by flows from the Mauna Ulu eruption between 1969 and 1971.

The origin of pit craters is not clearly understood, but they are believed to form by a combination of magma stoping and withdrawal. Magma in the rift zone probably works its way toward the surface as blocks of the country rock sink into a shallow magma reservoir. Magma is then drained away, possibly as a result of an eruption lower down the rift zone, to leave an unsupported chamber which collapses, forming a depression at the surface. The depression may later, or simultaneously, be partly filled with lava to form a flat floor. Macdonald (1972) gives an account of the formation of an 8 m diameter crater during the 1955 eruptions on the Kilauea east rift zone. A sharp explosion was heard from the area of a vent. The explosion was followed by the appearance of a black cloud and several smaller explosions. Within a few minutes, the new pit, which had appeared almost instantaneously, was observed from the air. It appeared to be 20–30 meters deep with an incandescent floor. Observers on the ground found no rocks on the rim, only a thin layer of black glassy ash. The rocks that formerly occupied the site of the crater clearly had not been thrown out but had collapsed into the hole.

FIGURE 6–1. Kilauea Iki. This crater is 1.4 km long, 0.6 km across, and approximately 80 m deep. At the left of the picture is the east wall of the main depression of Kilauea Caldera. On the south wall of Kilauea Iki is the cinder cone Puu Puai. To the southwest of Puu Puai, the forest was largely destroyed by a thick blanket of tephra during the 1959 eruption. This eruption, which lasted from mid-November to mid-December, produced the highest fountains (580 m) recorded at Kilauea. (Photograph by Towill Corp., Honolulu, frame 5722-4, 1972.)

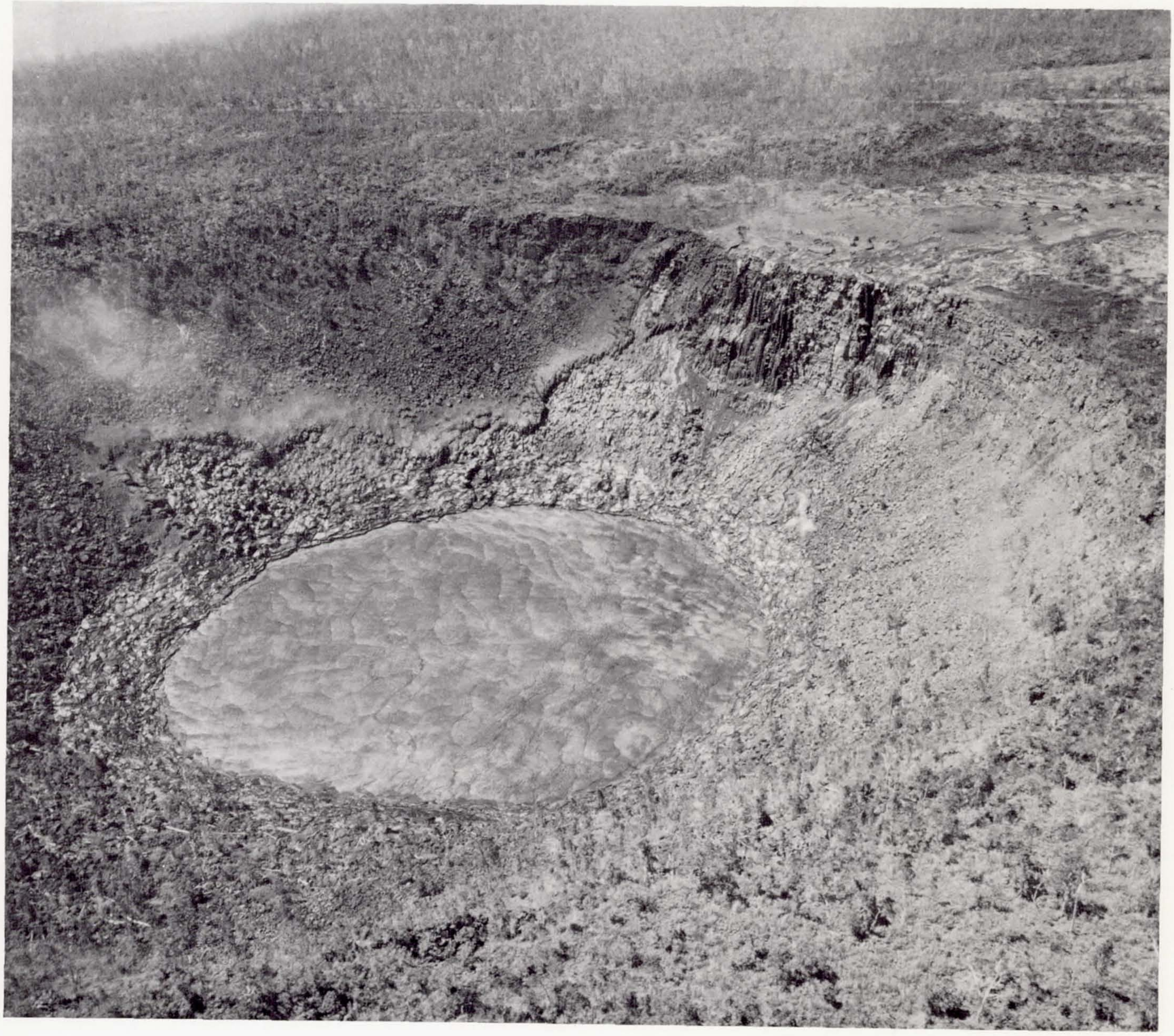

FIGURE 6–2. Hiiaka Crater. This 350 m diameter, 90 m deep crater is situated 5 km southeast of Kilauea Caldera on the east rift zone. The picture was taken after the eruption of May 1973 and shows a flat-surfaced lava pond, ringed by a lava-subsidence terrace. The top of the terrace marks the highest stand of the lava during the eruption. For the location of pit craters along the upper rift zone of Kilauea, see Figure 4–10. (Photograph by R. T. Holcomb, May 6, 1973.)

FIGURE 6–3. Aerial photograph of Pauahi, taken during the May 5, 1973 eruption. Pauahi is a multiple pit 600 m long and 350 m wide, situated 6 km southeast of Kilauea Crater. The May 5, 1973 eruption filled the deep east pit almost to the top of the septum, then subsided to leave a lava terrace which is just visible through the steam over the pit. (Photograph by R. T. Holcomb, May 1973.)

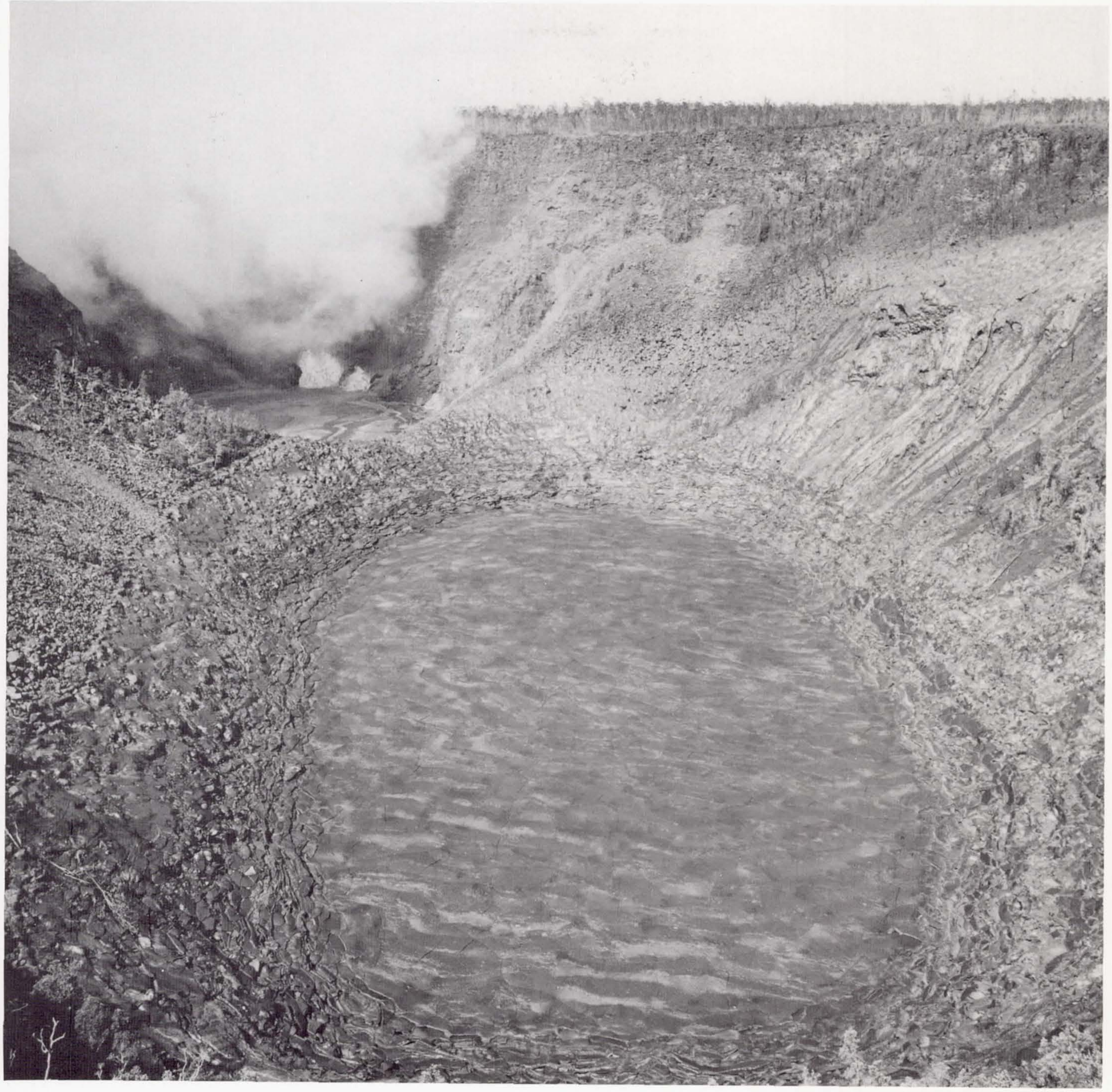

FIGURE 6–4. View westward across Pauahi during the November 1973 eruption. New lava now stands in the east pit (foreground) with ring indicating the maximum height of the lava. (Photograph by R. T. Holcomb, November 12, 1973.)

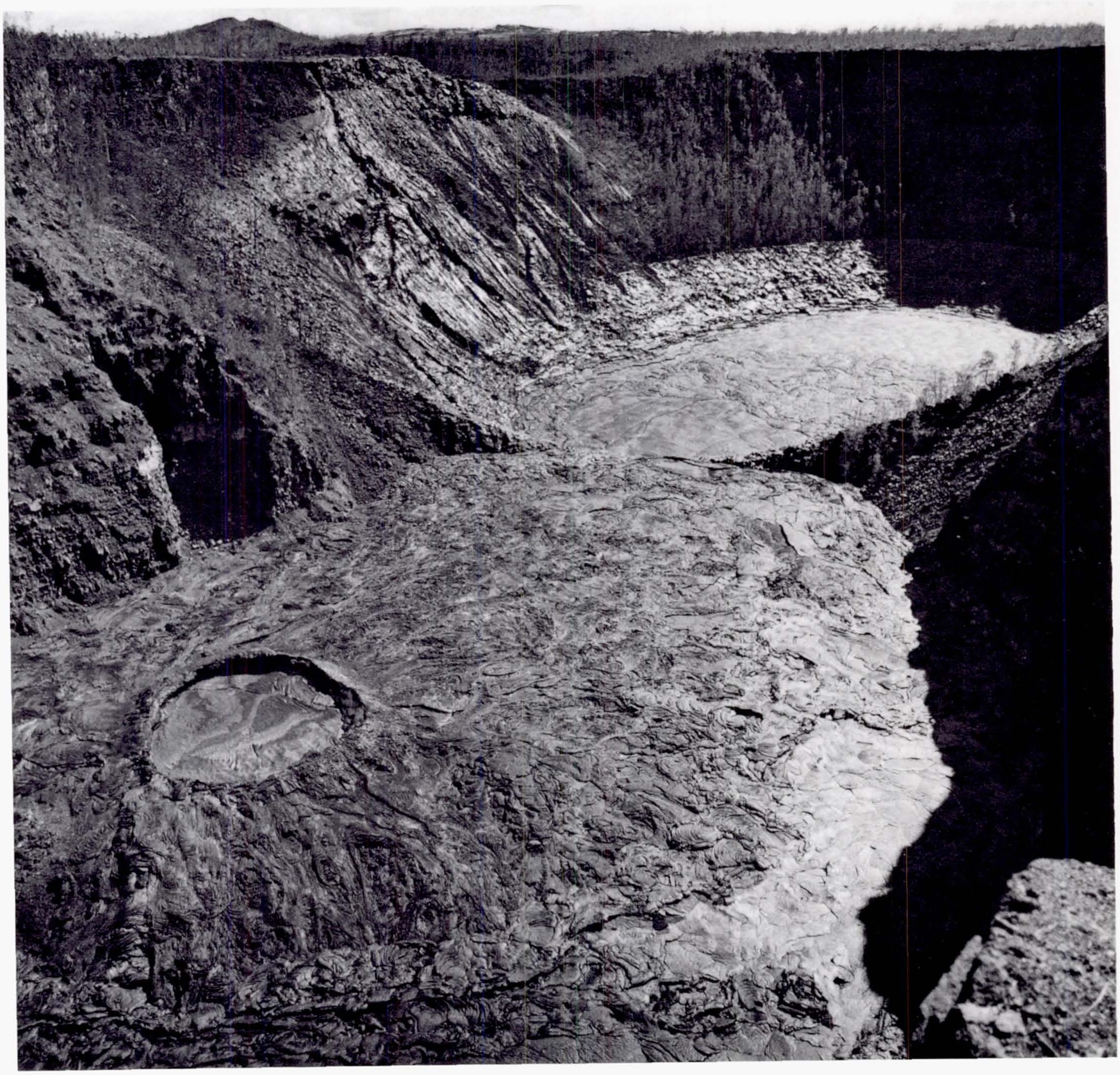

FIGURE 6–5. View eastward across Pauahi. Continued eruption in the west half has built a low lava shield. A small crater at the summit of the shield contains a pond of molten lava. A small amount of lava has flowed across the septum into the eastern pit. (Photograph by R. T. Holcomb, December 5, 1973.)

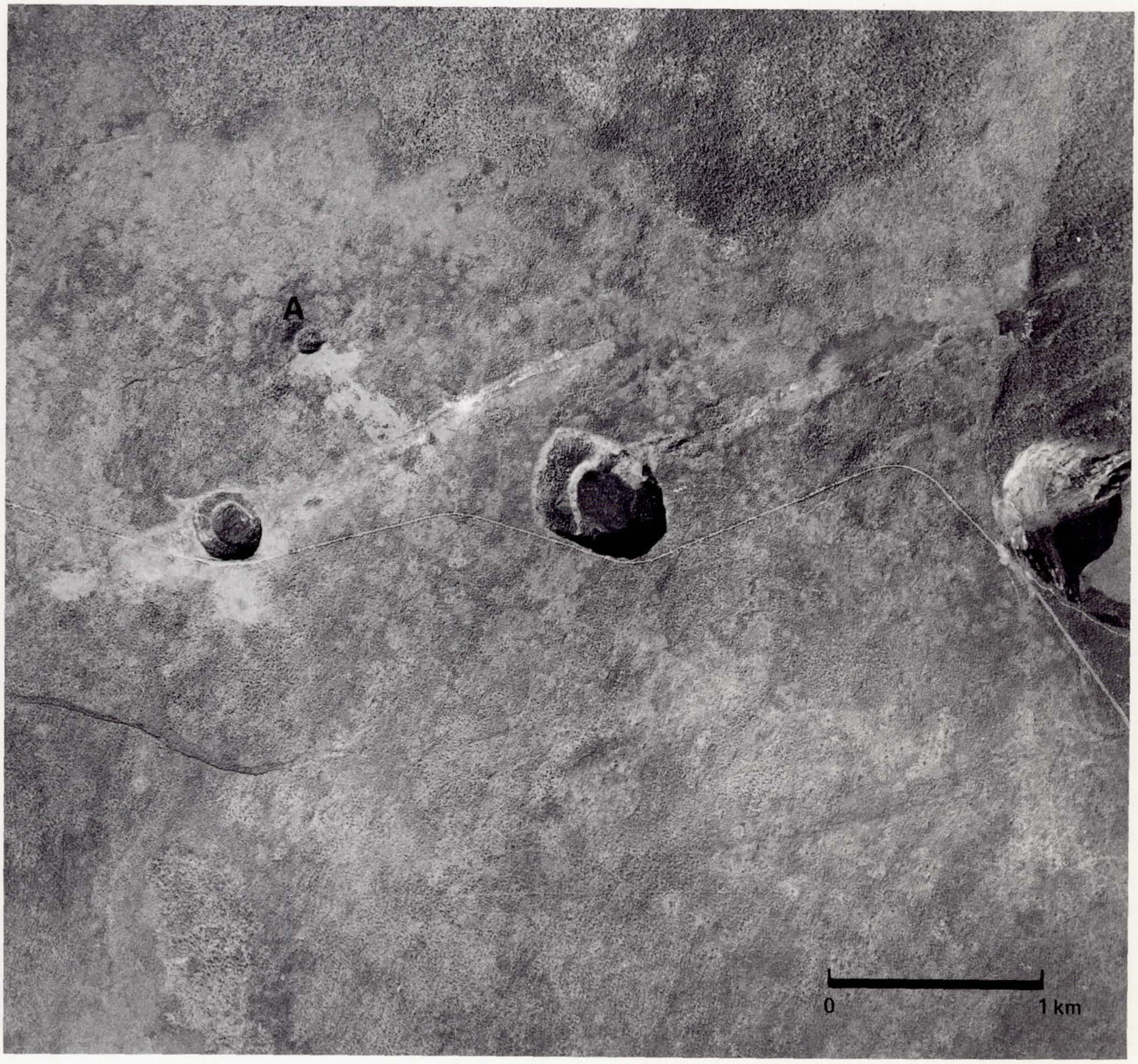

FIGURE 6–6. Pit craters along Chain of Craters Road in the Kilauea east rift zone prior to the eruption of Mauna Ulu. From the left the three craters are Aloi, Alae, and Makaopuhi. Just north of Aloi is a prehistoric spatter and lava cone with summit crater, Puu Huluhulu (A). The lava pond in the east pit of Alae Crater was formed in 1963. The general appearance of this region has changed drastically as a result of the Mauna Ulu eruption between 1969 and 1974. The summit of the Mauna Ulu shield is now halfway between Aloi and Alae, both of which have been filled by Mauna Ulu lavas. The west pit of Makaopuhi has also been filled. (U. S. Department of Agriculture, photograph EK6-12CC-174, 1965.)

N

FIGURE 6–7. View from above the east end of Makaopuhi Crater (foreground), westward across the site of the subsequent Mauna Ulu eruptions. Alae Crater is in the near background and Aloi Crater is in the far background. The western pit of Makaopuhi Crater is partly filled with lava from the March 1965 eruption. A dark ring indicates the highest level of the 1965 lavas. Thin flows from the same eruption also cover part of a prehistoric lava lake in the east pit. At this time the interior of the prehistoric lava lake was exposed in sections in the cliff separating the two pits. Subsequent Mauna Ulu eruptions between 1969 and 1974 flowed into the Makaopuhi west pit, filling it to the level of the east pit. Aloi and Alae Craters in the background were completely buried. (U. S. Air Force photograph, 1966.)

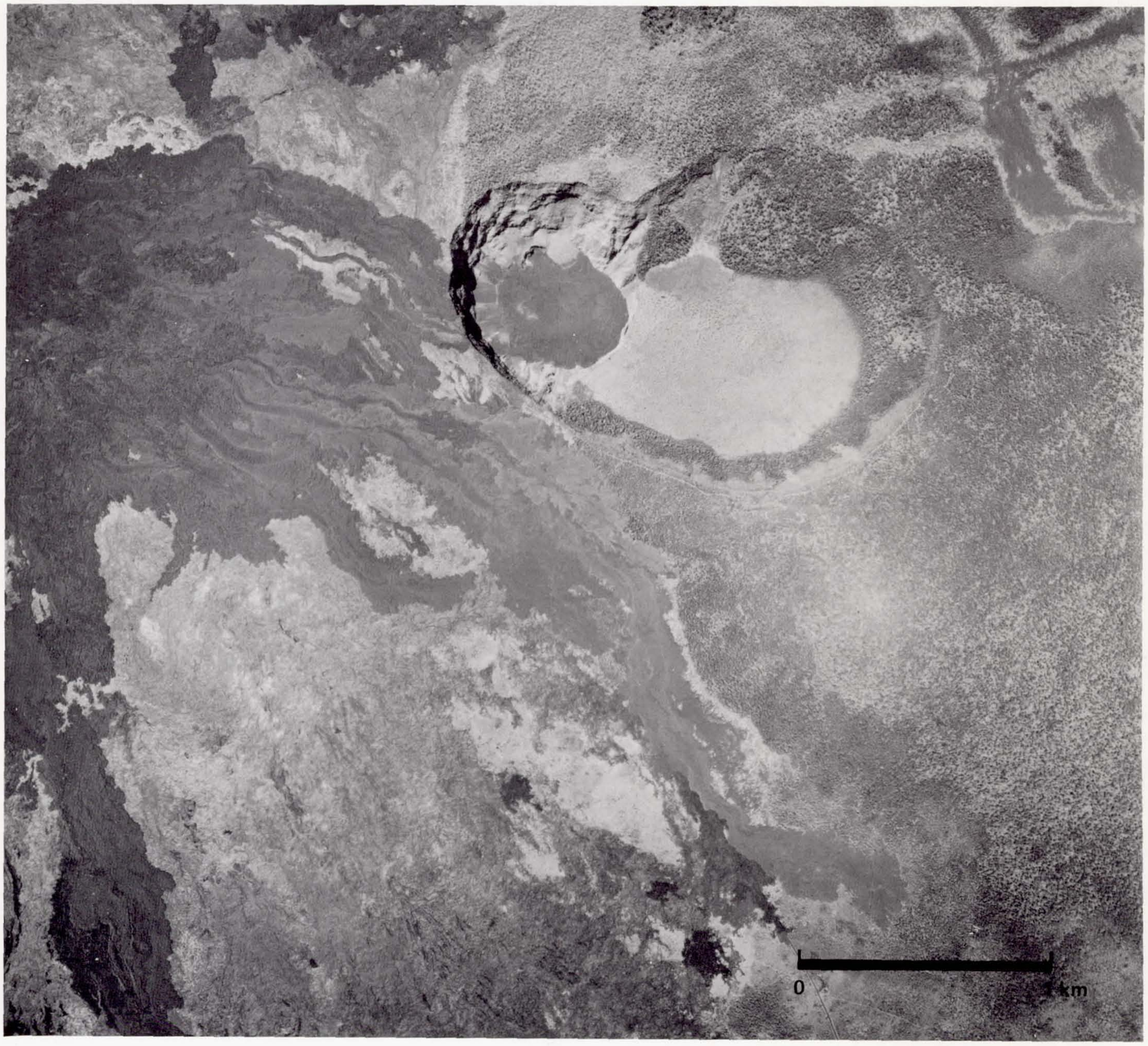

FIGURE 6–8. Makaopuhi Crater. Flows from Mauna Ulu have flowed into the west pit of Makaopuhi. The west pit was not completely filled until 1973. Chain of Crater Road (lower right), south and west of Makaopuhi, has been almost completely buried. (Photograph by Towill Corp., Honolulu, frame 5740-3, 1972.)

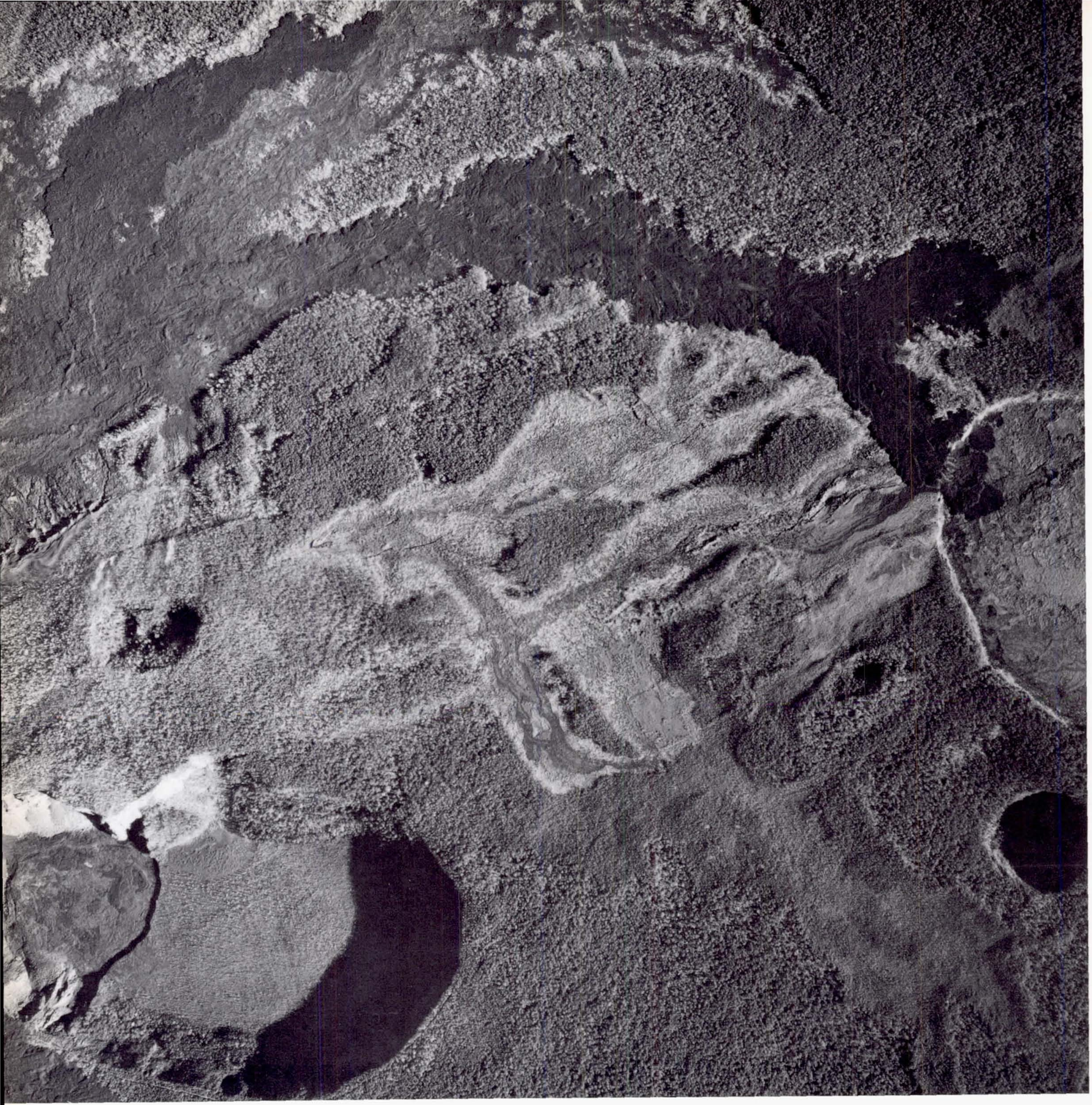

FIGURE 6–9. Makaopuhi Crater is seen here at the bottom left and the west edge of Napau Crater on the right margin. Flows from Mauna Ulu (to the left, off the picture) have reached as far as Napau and flowed onto the crater floor but most of the floor is covered by an October 1968 flow. (Photograph by Towill Corp., Honolulu, frame 5810-10, 1972.)

FIGURE 6–10. Napau Crater, 3 km east of Makaopuhi on the Kilauea east rift zone. The crater is 800 m across and approximately 60 m deep. It is transected by faults and fissures of the rift zone, along which are numerous elongate spatter cones. The deforested areas east of the crater are mainly March 1965 and October 1968 flows; those west of the crater are mainly October 1968 and February 1969 flows, except for the darkest flow (aa), which is a later flow from Mauna Ulu. (Photograph by Towill Corp., Honolulu, frame 5811-10, 1972.)

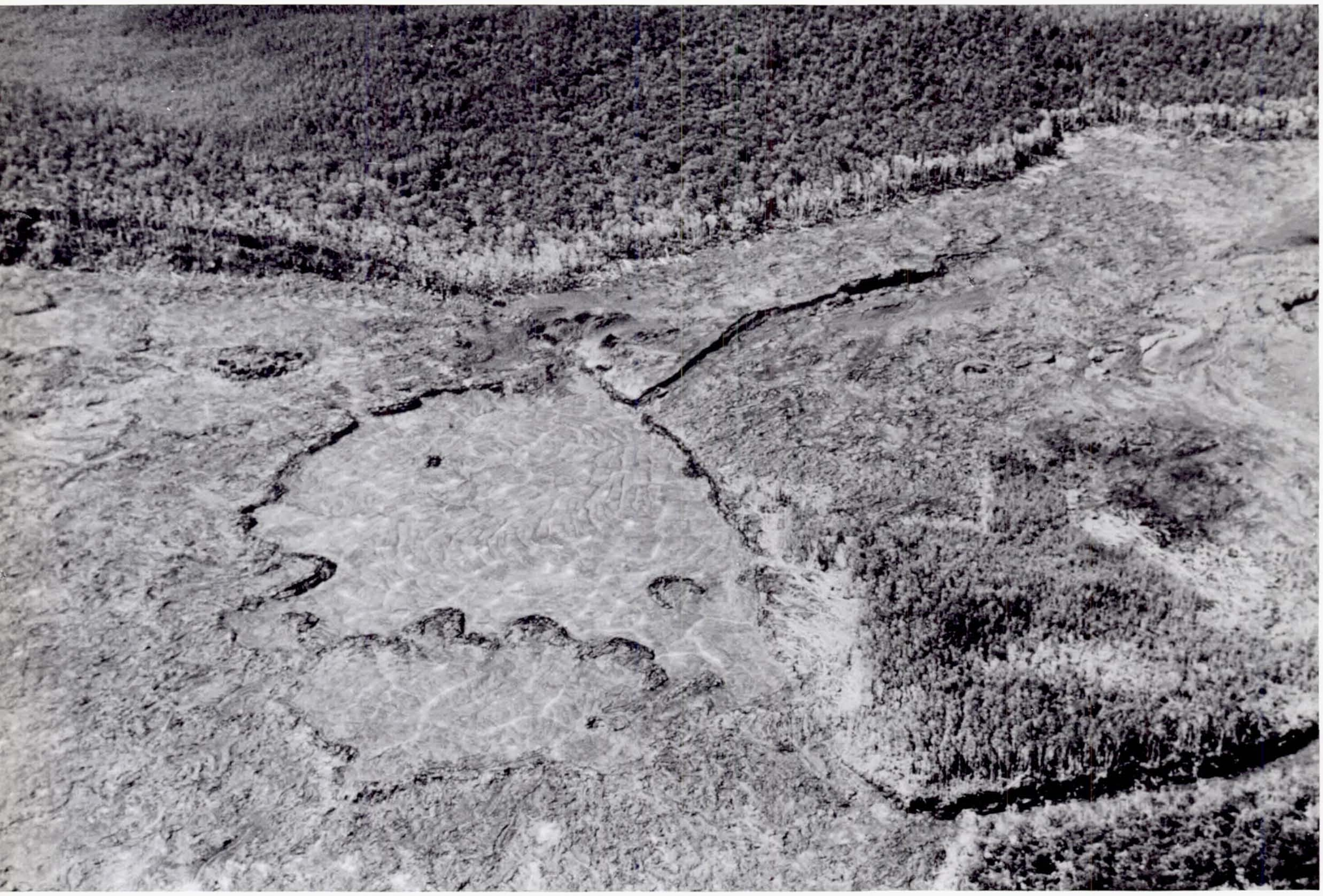

FIGURE 6–11. Low altitude oblique aerial photograph of the northeast part of Napau Crater, showing a perched lava pond formed in October 1968, surrounded by other flows of the same eruption. (Photograph by Mike Lovas, 1970.)

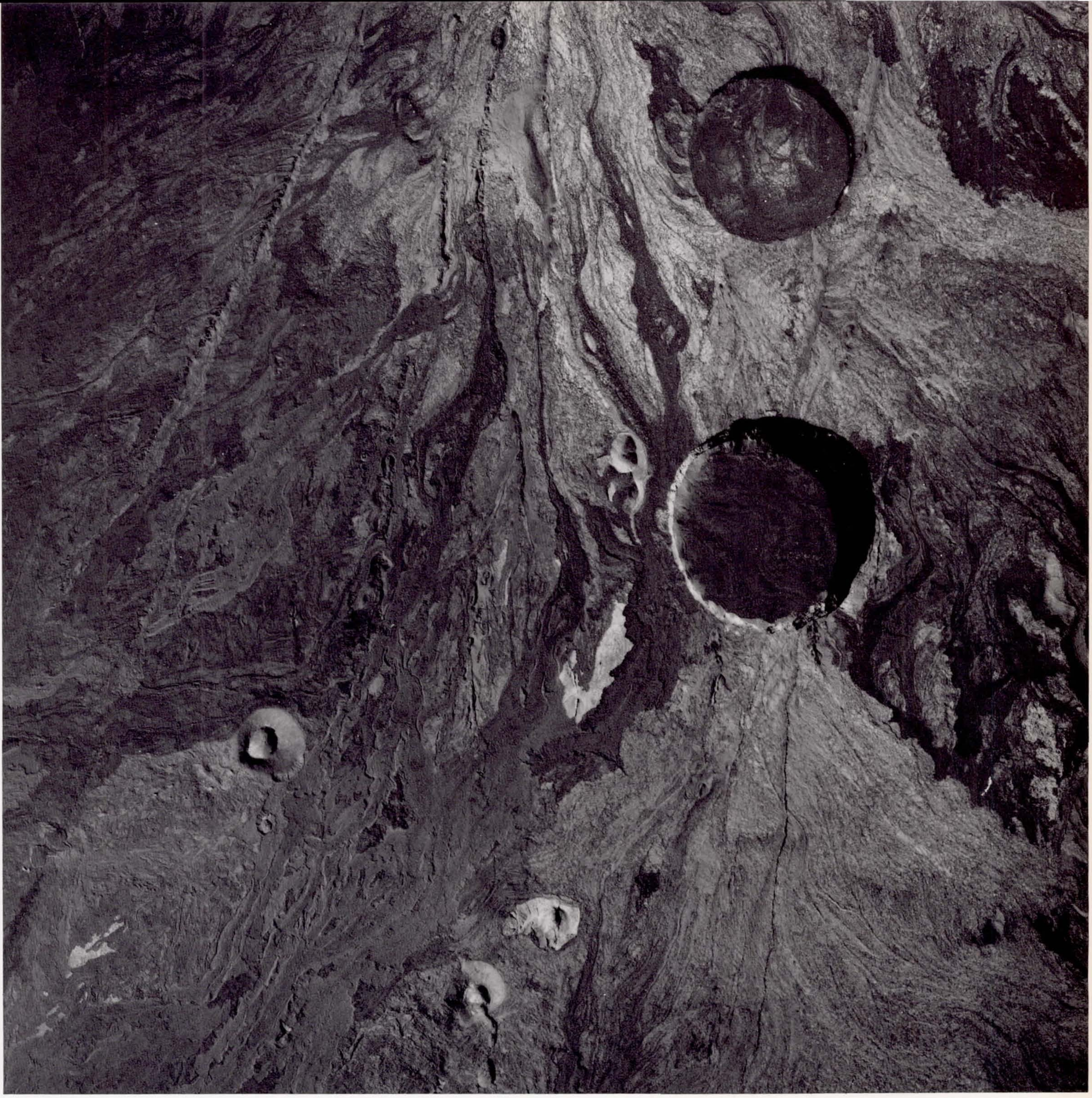

FIGURE 6–12. Pit craters at the summit of Mauna Loa. The 400 m pit crater Lua Hou is to the south, Lua Hohonu to the north. The South Pit of Mokuaweoweo is just off the picture to the top (see Figures 4–1 and 4–3). Mokuaweoweo was first mapped in 1841 by Lt. Charles Wilkes, but Lua Hohonu does not appear on his map and may have formed since that time. Numerous spatter cones and ramparts can be seen north of the two craters. (Photograph by Towill Corp., Honolulu, frame 6681-5, 1972.)

FIGURE 6–13. Vertical view of three pit craters near the Kakuku fault (see Figure 5–1). From bottom to top, the craters are Lua Pauli, Lua Poai, and Lua Palalauhala. The craters are on the lower flanks of Mauna Loa, 15 km north of South Point. The fresh flow at the base of the scarp is the 1858 flow from Mauna Loa. (U. S. Department of Agriculture, photograph EKL-14CC-25, 1965.)

VII. CINDER, SPATTER, AND LITTORAL CONES

Although the general form of Hawaiian volcanoes is a gently sloping shield, comprised mostly of lava flows, small cones are common around vents both at the summit and on the flanks of a shield. The type of cone depends on the viscosity of the lava, its volatile content, the eruption rate, the prevailing wind, and probably several other factors. When activity is explosive, generally as a result of the high volatile content and high viscosity of the lava, large amounts of tephra – ash and cinders – are produced and a cinder cone forms around the vent. During other eruptions magma may quietly upwell in the vent region and be distributed to the lower flanks of the volcano by lava tubes or as fluid flows and no cone forms at the vent. If fountaining occurs, then spatter cones or spatter ramparts, consisting of partly welded clots of lava, usually form. Cinder cones and spatter cones grade into one another as the proportion of the two constituents, spatter and scoria, changes.

Most cinder cones are near circular in plan, although an asymmetry may be imposed by the slope of the ground, as is the case for many of the cinder cones on Mauna Kea, by the prevailing wind, by the inclination of the explosive jets, or by the eruption of lava flows during cone construction. Most cones have a fairly uniform size of fragments and generally are in the 0.5 to 10 cm size range, although occasional large bombs may be found. The debris is usually close to the angle of repose. Lava flows may emerge from the base of the cone and partially undermine one side. During voluminous eruptions, a flank flow may carry away substantial fractions of the cone and breach one side. Most breached cones form, however, when lava, erupted while the cone is being built, prevents accumulation of tephra on one side.

On the island of Hawaii, cinder cones are particularly common on the three older volcanoes of Hualalai, Mauna Kea, and Kohala. Those on Hualalai tend to be smaller than those on Kohala and Mauna Kea, possibly indicating eruptions of shorter duration. They also include more spatter, suggesting that activity was less explosive. This may result from compositional differences. The Hualalai cones are predominantly alkalic olivine basalt, whereas those on Mauna Kea and Kohala are mainly hawaiite and mugearite. Cinder cones are much less common on Mauna Loa and Kilauea. Where present, such as in the Kau Desert, along the southwest rift zone of Kilauea, they are quite small and contain significant proportions of spatter.

Fountaining, such as commonly occurs during eruptions on Mauna Loa and Kilauea, generally results in formation of spatter cones and ramparts around the vents. The spatter cones may be built up rapidly as large clots of lava fall on one another around the vent. Accumulation may be so rapid that the clots merge to form rootless flows that dribble down the side of the rapidly growing cone. In fact, during periods of vigorous fountaining, such as during 1969 at Mauna Ulu, all lava flows were initially fed by fallback from fountains and hence are rootless flows in the strictest sense. As the spatter congeals, it welds to adjacent clots to form a solid structure quite unlike the loosely aggregated cinder cone. As a consequence, slopes may be substantially steeper than the angle of repose. Usually, however, the history of a larger cone is quite complex. Scoria and spatter may be complexly interbedded and frequently parts of the cone may collapse into the vent and be rebuilt repeatedly. Spatter and cinder cone may thus form a continuous sequence.

Spatter cones and ramparts are particularly common on the rift zones of Mauna Loa and on the lower east rift of Kilauea. Chapter 5 includes several pictures of the southwest rift of Mauna Loa which show numerous spatter ramparts, elongate along the direction of the rift. Many are breached by lava channels. Circular cones are common but less numerous. Most are relatively small in size, with rims no more than a few tens of meters across, as compared with the Mauna Kea cinder cones which are mostly several hundred meters across.

Cones may also form where a lava flow enters the ocean, or any other body of water. The fragmental debris formed by the explosive interaction of lava and water builds a "littoral cone" which, unlike the other discussed, is rootless.

FIGURE 7–1. Cinder cones at the 2,400 m (8,000 ft) level on the southern flank of Mauna Kea. The well-formed cone in the middle right of the picture is 500 m across at its base. The Mauna Kea-Humuula trail cuts across the cone Puu Kaleapeamoa in the top right. (U. S. Department of Agriculture, photograph EKL-10CC-67, 1965.)

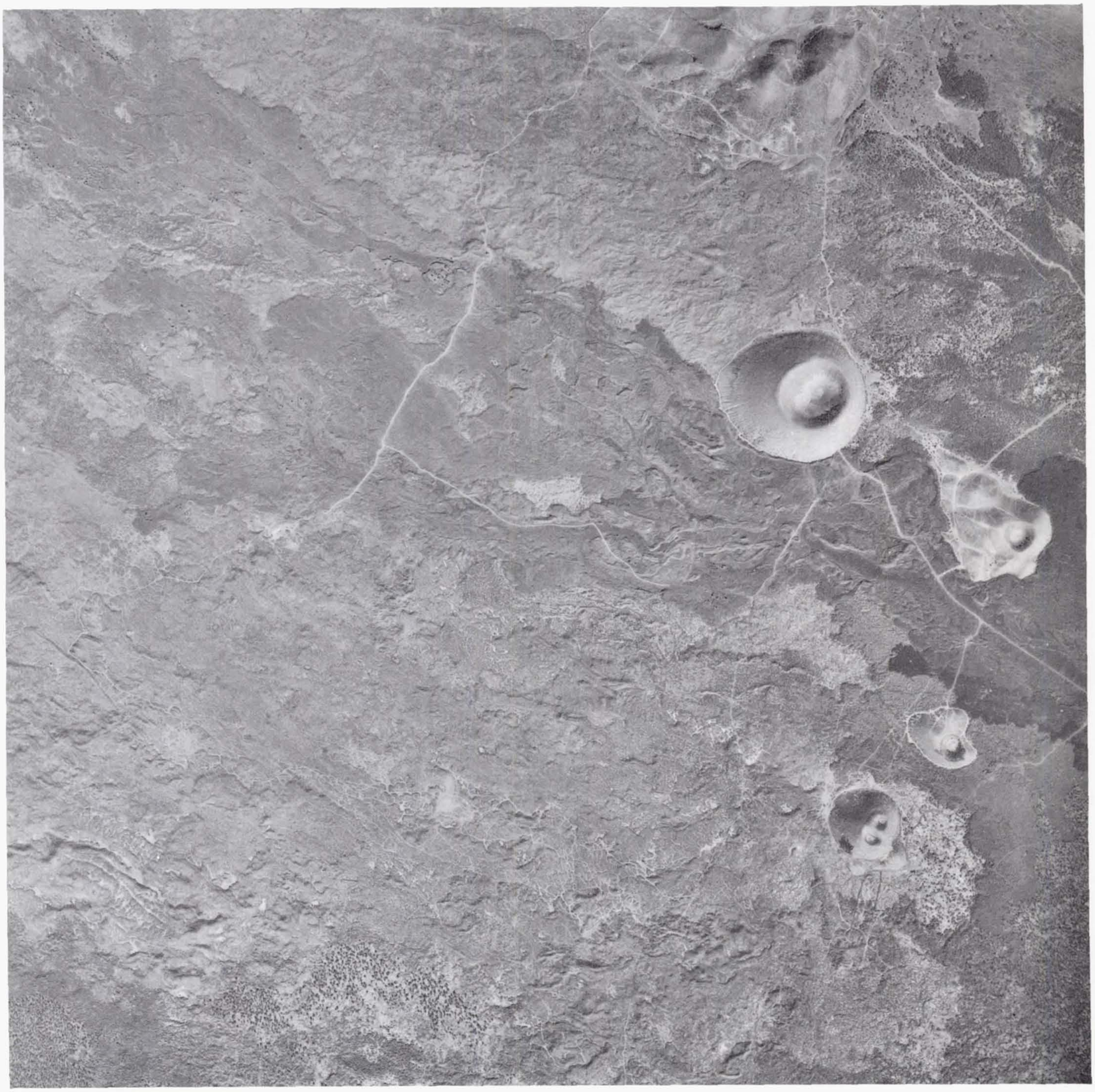

FIGURE 7–2. Cinder cones just south of the Humuula Saddle Road. The main cone, Puu Ka Pele, is approximately 550 m across and 100 m high. The cinder cones, which formed during late stage activity of Mauna Kea, have been partly buried by Mauna Loa flows. (U. S. Department of Agriculture, photograph EKL-7CC-245, 1965.)

FIGURE 7–3. Oblique aerial view westward across the summit of Mauna Kea. The cinder cone in the foreground, Puu Makanaka, is approximately 200 m high and has a central crater 400 m across. Lava flows emerge from the base of the cone in the left middle ground and form a fan below the cone. Similar flow fans occur below the other cones but are not visible in this picture. (Photograph by A. T. Abbott, University of Hawaii.)

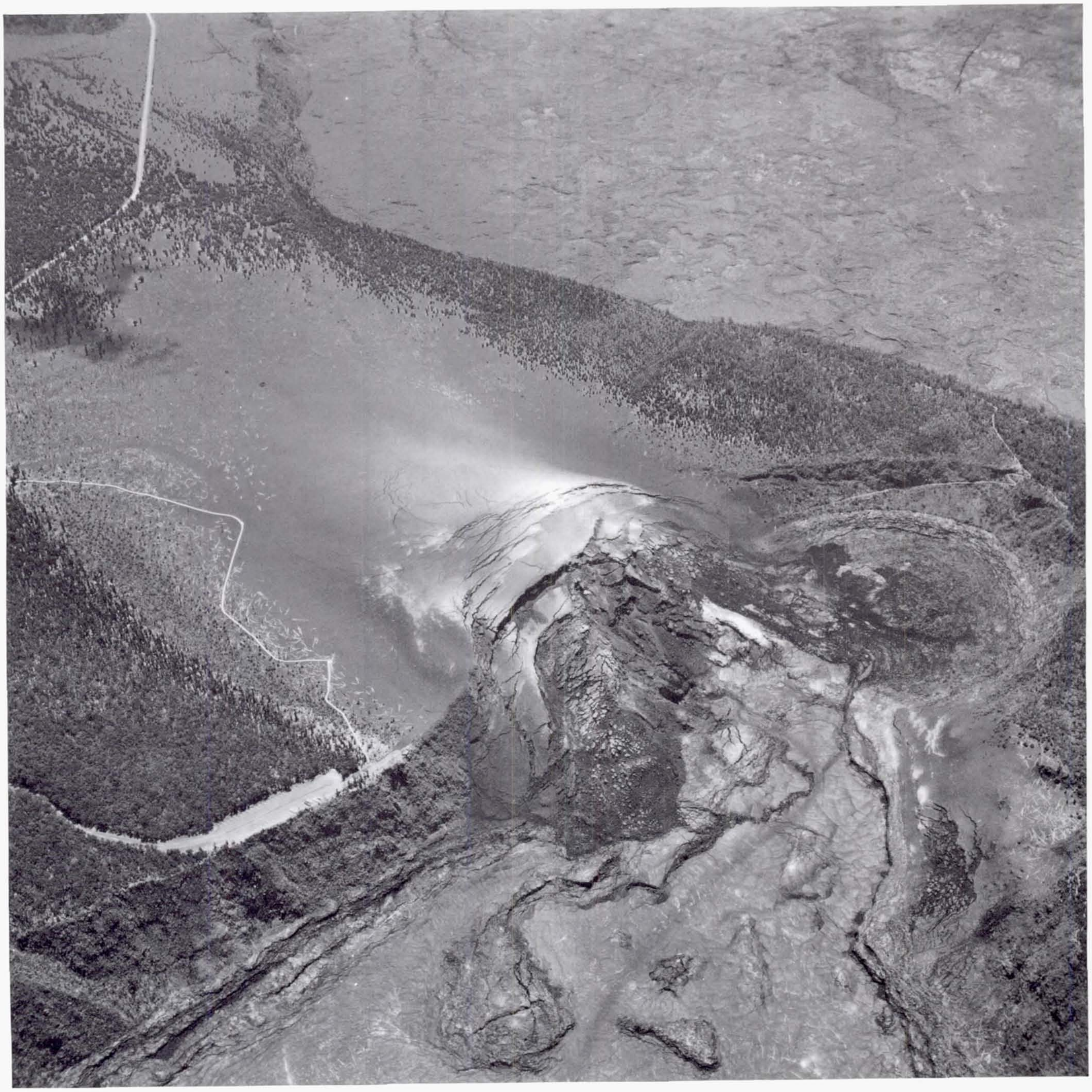

FIGURE 7–4. View looking southwest of the spatter cone Puu Puai at the west end of Kilauea Iki. The cone was formed during the 1959 eruption which produced fountains up to 580 m high. The fountains generated large volumes of ash, pumice, and reticulite, most of which was carried southwest by the tradewinds, destroying the adjacent forest and forming the asymmetric cone. The white line on the east side of the destroyed area is the Devastation Trail. The floor of Kilauea Caldera is in the upper part of the picture. (U. S. Air Force photograph, 1966.)

FIGURE 7–5. Spatter and cinder cones at the vents of some of the 1955 lava flows on the lower east rift zone of Kilauea. See Figure 5–15 for another view. (U. S. Air Force photograph, 1966.)

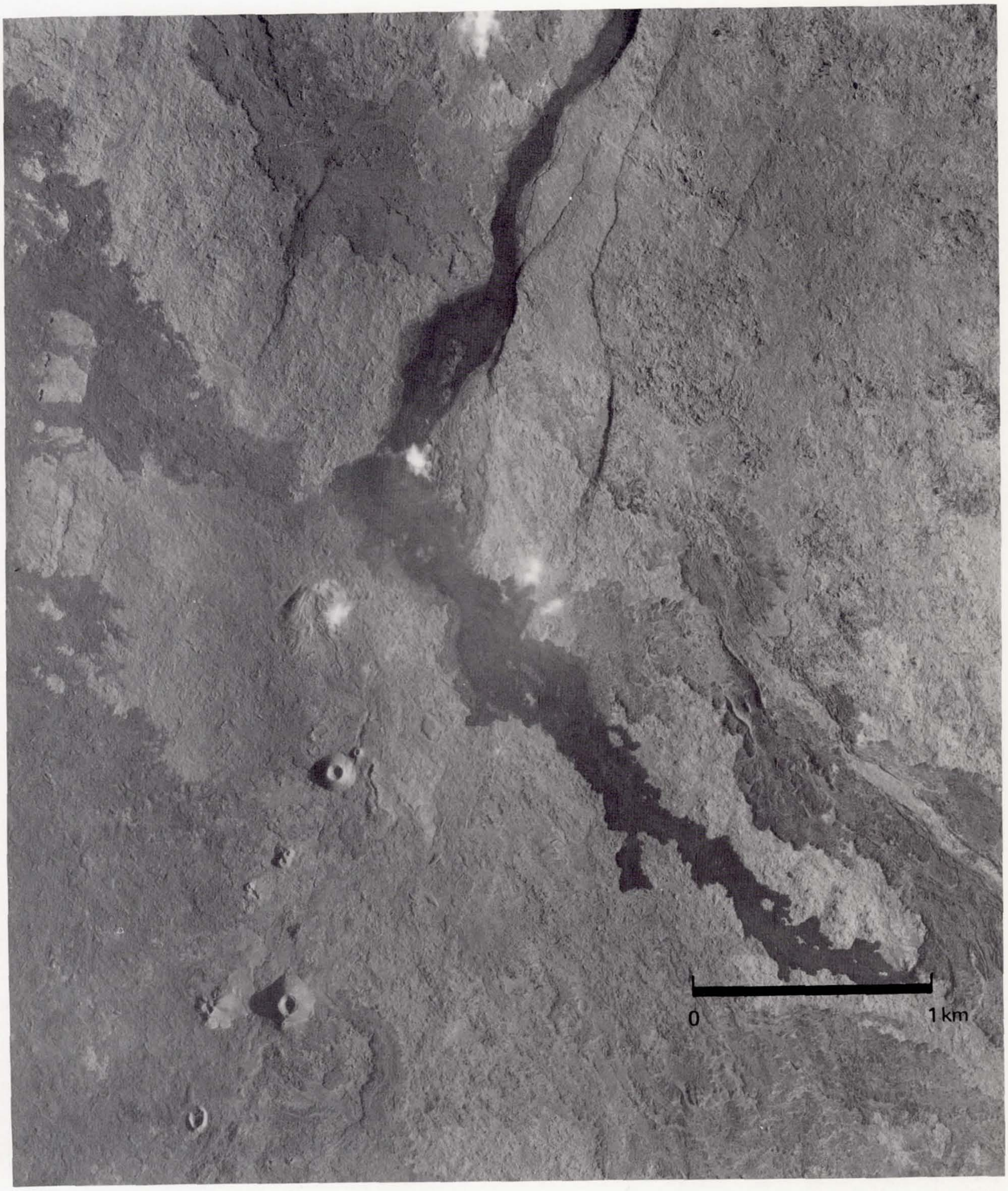

FIGURE 7–6. The Kamakaia Hills on the southwest rift zone of Kilauea. The two prominent circular cones are Kamakaiawaena to the southwest and Kamakaiauka to the northeast. Each is approximately 50 m high. The dark flow in the northwest was erupted in December, 1974. (Photograph by Towill Corp., Honolulu, frame 6536-2, 1975.)

FIGURE 7–7. Oblique aerial view of Kamakaiauka cinder cone and lava flows in the Kau Desert. Compare with previous figure. (Photograph by R. Greeley, 1970.)

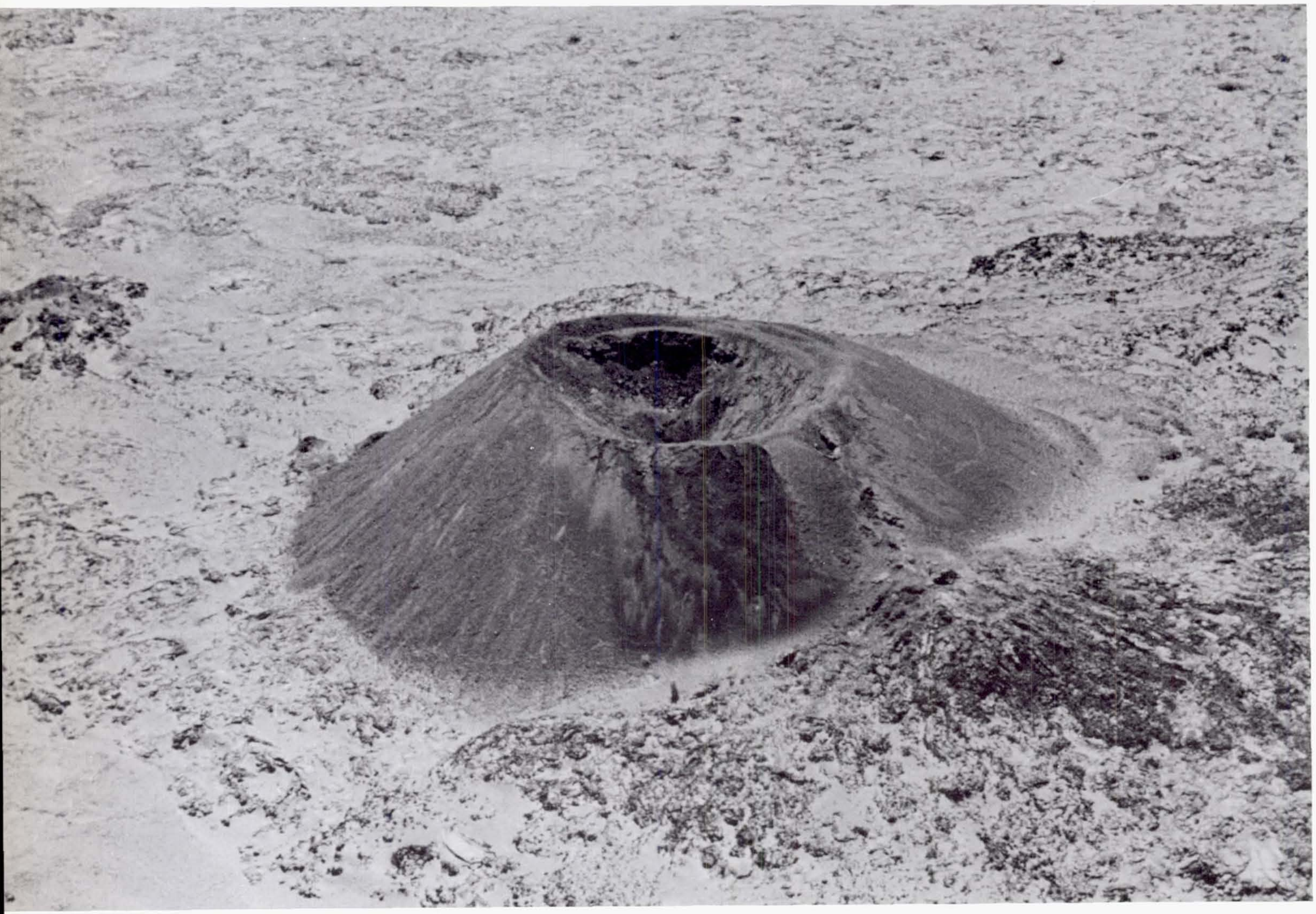

FIGURE 7–8. Low altitude aerial view of cinder cone in Kau Desert, showing small lava flow that issued from fissure on the flank (right side) of cone. (Photograph by R. Greeley, 1969.)

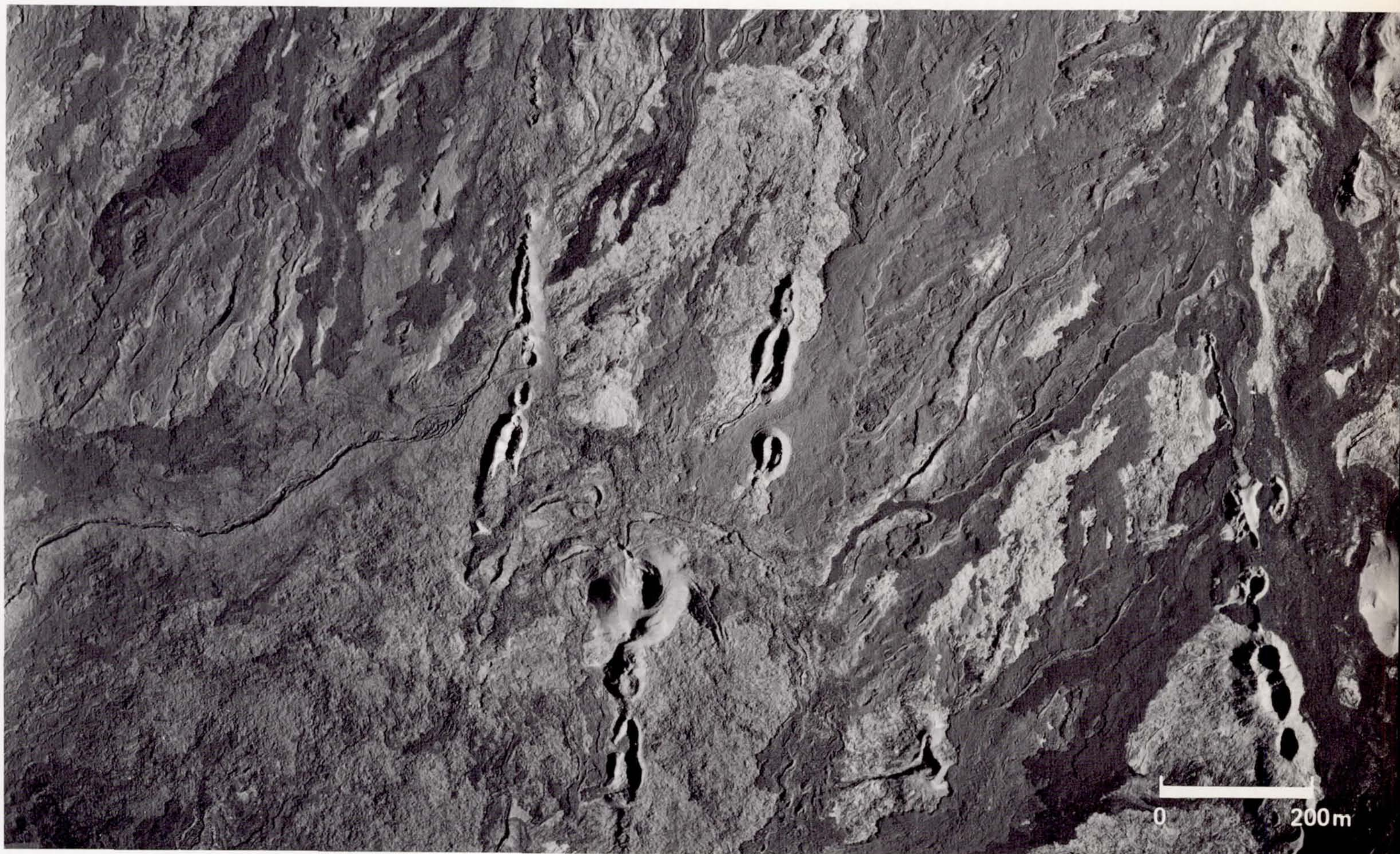

FIGURE 7–9. *Detail from the northwest quadrant of Figure 5–6. Cinder and spatter ramparts at the 3,200 m (10,500 ft) elevation on the southwest rift zone of Mauna Loa. The elongate cones and ramparts are typical of the Mauna Loa rift zones. Commonly the downslope flank is breached by flows, some of which have prominent channels. (U. S. Department of Defense, photograph 19VV, M-165, November, 1947.)*

FIGURE 7–10. Oblique view to the northeast of cinder and spatter cones at the 2,400 m (8,000 ft) level on the Mauna Loa southwest rift zone. The most distant cone is Alika Cone, which can also be seen in the center of Figure 5–7. Most of the cones are breached and probably accumulated for the most part while the lava channels in the foreground were active. (Photograph by R. Greeley, 1970.)

FIGURE 7–11. View southward of Puu WaaWaa, a trachyte pumice cone on the north flank of Hualalai volcano (see map, Figure 5–19). (Photograph by R. Greeley, 1974.)

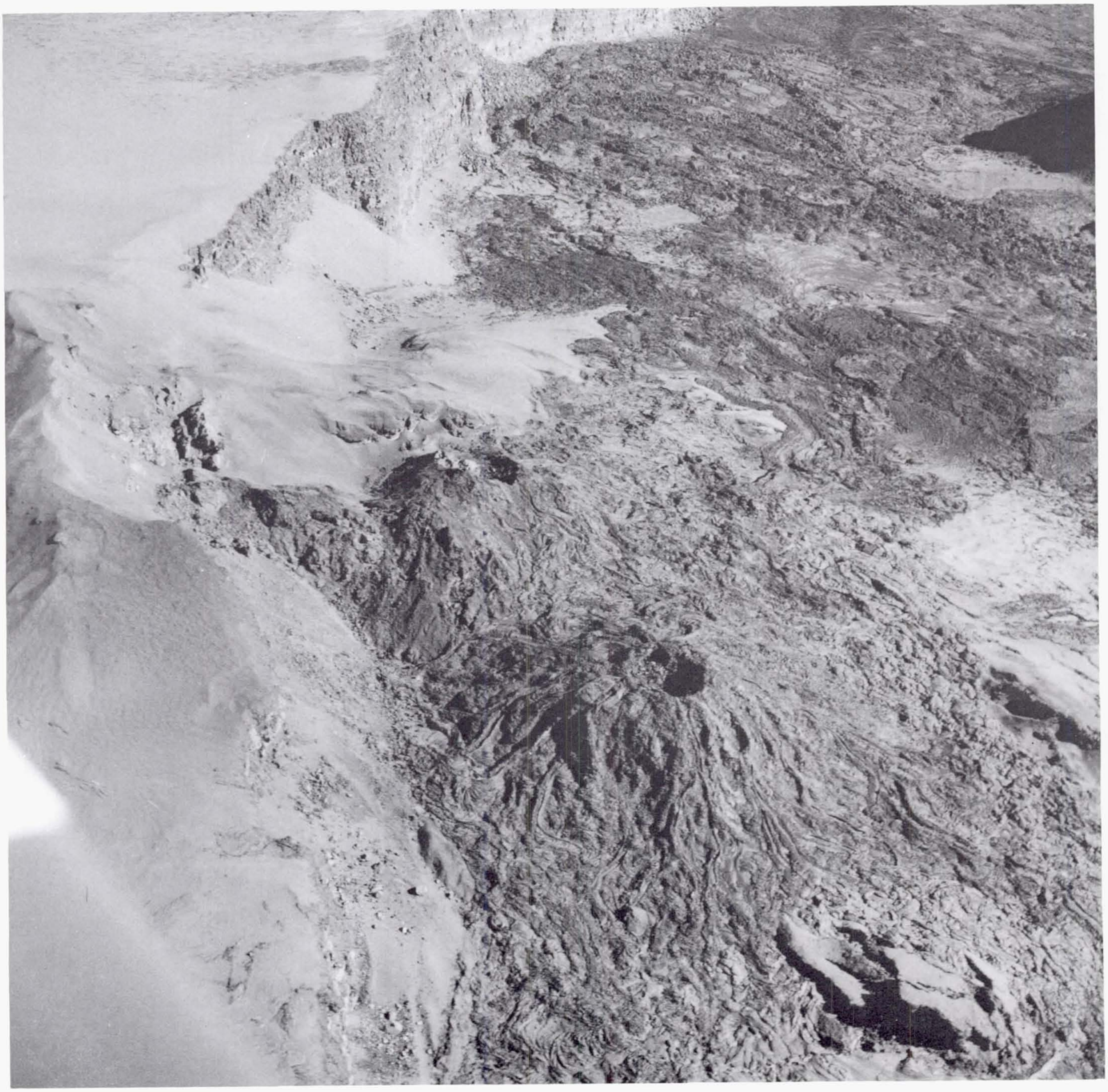

FIGURE 7–12. Low altitude oblique aerial view, looking north of two small cones formed in 1950 on the floor of Mokuaweoweo Caldera. These cones are built of both spatter and lava flows. (Photograph by R. Greeley, 1970.)

FIGURE 7–13. Low altitude oblique aerial photograph of cinder and spatter cones formed in 1960 on the east rift zone of Kilauea. Note that the far end of the cone has been breached, giving rise to a channel fed aa flow. (Photograph by R. Greeley, 1969.)

FIGURE 7–14. The littoral cone, Puu Hou, which formed when the 1868 lava flows from Mauna Loa entered the ocean. The flow forms the dark surface within and around the cone. (Photograph by R. Greeley, 1974.)

VIII. LAVA FLOW FIELDS

Hawaiian shield volcanoes result from the accumulation of thousands of individual flows. To a large extent the morphology of the shields results from that of the individual flows. Thus, it is important to understand the variety of lava flows and the factors that control their form. Hawaiian lava flows are treated in this and the next two chapters; this chapter deals with lava flow fields on a scale that can be observed from aerial views; Chapter 9 deals with the individual components of lava flows and includes features such as lava tubes, flow channels, and pressure ridges. Chapter 10 deals with fine scale features, primarily related to flow features.

The general morphology and properties of basaltic lava flows depend on many factors, including the fluidity of the lava, the characteristics of the vent, the rate and duration of effusion, and the preflow topography. Because lava is a mixture of liquid, crystals, and gas, its viscous behavior is extremely complicated (Shaw and others, 1968). In general the higher the temperature, the more fluid is the lava. A high volatile content increases the fluidity so long as the volatiles remain in solution in the magma. As soon as the volatiles begin to exsolve, a frothy vesicular mass tends to form, making the fluid more viscous. Crystals make the lava more viscous. Composition is another factor that can affect the lava fluidity. The fluidity, for example, is generally greater when the silica content is low. However, during the rapid shield building phase, the lavas have a narrow compositional range, so compositional effects tend to be secondary. Temperature is clearly the most important factor affecting fluidity since it controls the viscosity of the liquid, the degree of outgassing, and the proportion of crystals present. Although the relation between temperature and the fluidity of basaltic lavas is poorly understood, most tholeiitic lavas are fluid at temperatures above about 1075°C and become very viscous below that temperature.

Lava appears to behave as a *Bingham body*; it is essentially rigid until a critical yield stress is reached, beyond which it flows. This property has been used to estimate the yield strength of a lava from the height of a flow front, since the higher the flow front, the higher the effective yield strength. Unfortunately, yield strength cannot be simply related to other factors, such as composition or volatile content. Indeed, because of a partial dependence on the applied stress, the yield strength probably changes with the slope of the ground. This may also be true of the effective viscosity. The flow properties of lava are thus extremely complex.

Other parameters that affect lava flows are the size, shape, and arrangement of vents from which the lava is erupted. As shown in Chapter 5, vents in Hawaii are typically associated with rift-zone fissures from which lava may be erupted as a continuous stream. Eruptions may also be erupted from point-source vents which either may or may not be related to rift zones. Fissure vents can produce vast sheets of lava that spread out laterally as essentially a continuous and relatively homogeneous unit; fissure eruptions are usually of short duration. Lava flows erupted from point sources are typically more prolonged in duration and commonly lead to more complex types of lava flows, fed through networks of lava tubes and lava channels. Theoretical studies by Shaw and Swanson (1970) and an observational study by Walker (1973) have shown that the rate of effusion is important in governing the morphology of lava flows, particularly their length. High rates of effusion generally produce long lava flows. However, slow but prolonged eruptions also can produce long flows, especially if lava tubes form.

The topography of the surface over which the lava flows is obviously important in controlling the planimetric shape of lava-flow fields. Lava flows frequently accumulate in low-lying areas, with the resultant formation of structures such as lava ponds – stagnant pools of lava that behave much as lava lakes, but which are not related to vents. Flow down steep slopes increases in velocity, which in turn often increases the turbulence of the flow. This causes more rapid degassing and cooling of the lava, and consequently decreases the fluidity. Thus, pahoehoe lava flows that pour over steep slopes will often transform into aa lavas.

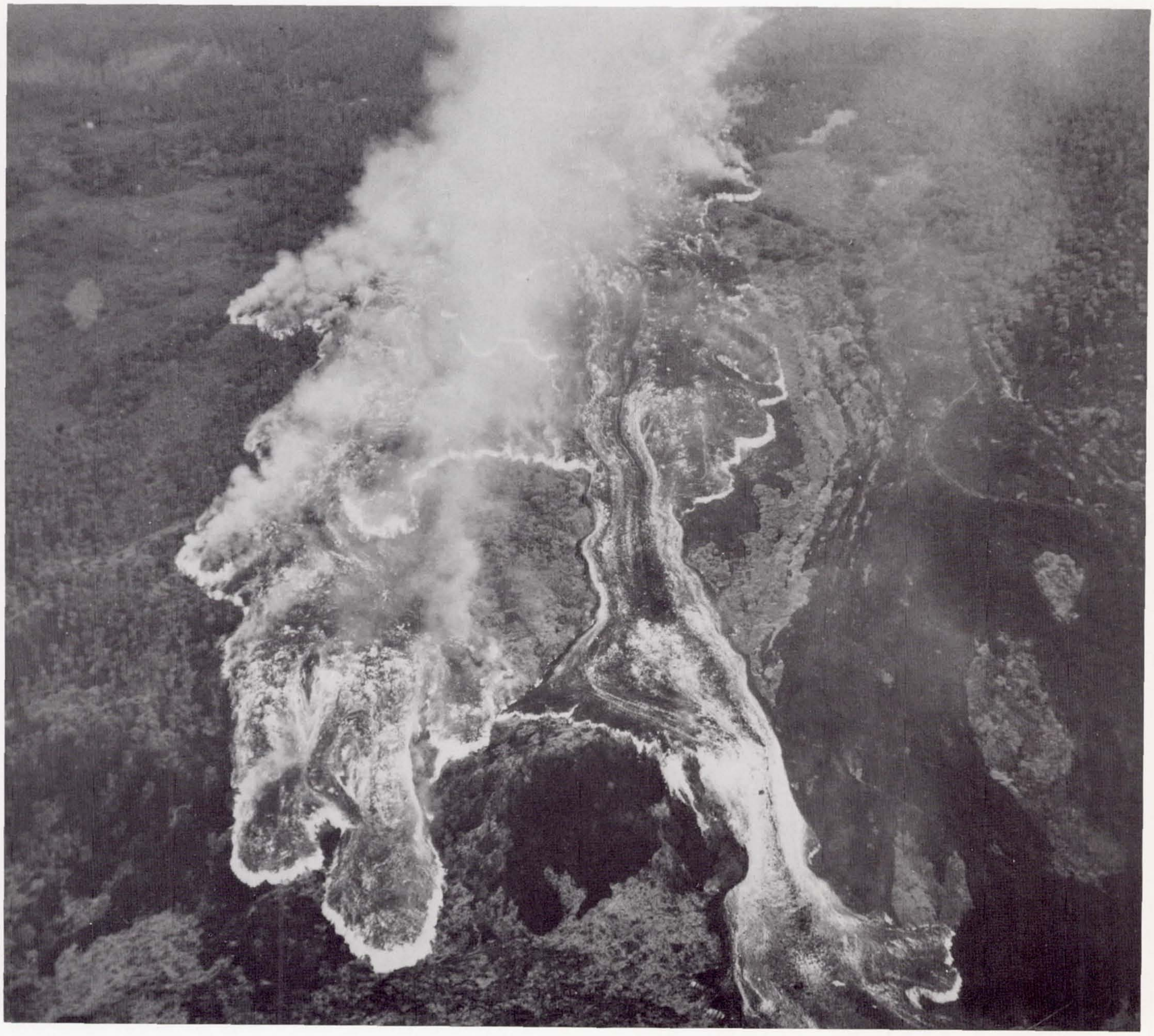

FIGURE 8–1. Active aa flows of the 1950 eruption of Mauna Loa, originating from the southwest rift zone. Stark white zones at the flow fronts and margins are areas where the interior of the flow is constantly exposed by the cooled clinkers sloughing off the steep flow edge. (Photograph by 199th Fighter Squadron, Air National Guard, Hawaii, 1950.)

FIGURE 8–2. Vertical aerial photograph of the Apua Point area on Kilauea, showing typical aa flows (dark), erupted from Mauna Ulu in 1969; area was subsequently partly covered by pahoehoe flows, also erupted from Mauna Ulu. (From Holcomb and others, 1974; photograph by Towill Corp., Honolulu, 1972.)

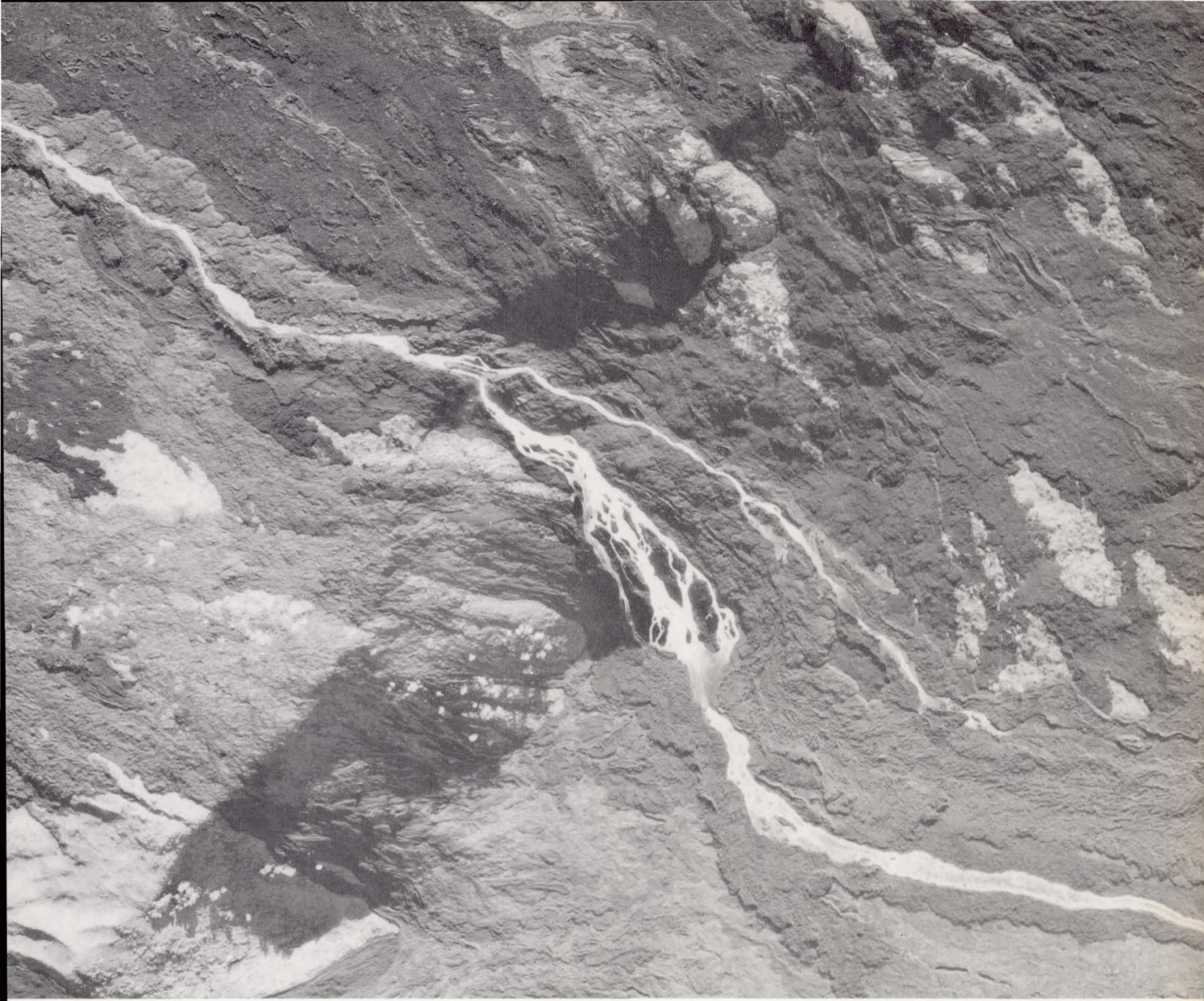

FIGURE 8–3. Braiding of lava stream on a steep slope. This active lava stream, flowing southward over Poliokeawe Pali, a 165 m high fault scarp, divides into a braided pattern on the steep slope. The stream flows over earlier very irregular aa flow from the same eruptive episode. The flow is braided on the pali because the slope prevents the ponding necessary to overtop local topographic irregularities before coalescence into a single channel. On the relatively gentle slopes above and below the scarp the stream flows with fewer channels. Above the scarp, the active lava is pahoehoe, but it changes to aa as it descends the scarp. Below the scarp, the active lava is entirely aa. North is to the left. (From Holcomb and others, 1974; photograph by Towill Corp., Honolulu, 1974.)

FIGURE 8–4. Aa flows on the flank of Mauna Kea, reflecting more viscous lava than on Mauna Loa. The furrowed textures represent primarily flow features in the form of narrow aa flow lobes, most of which were fed through steep-leveed channels. Similar textures are observed on Haleakala Volcano, Maui, and to a lesser degree, on Hualalai. (U. S. Department of Agriculture, photograph EKL-14CC-103, 1965.)

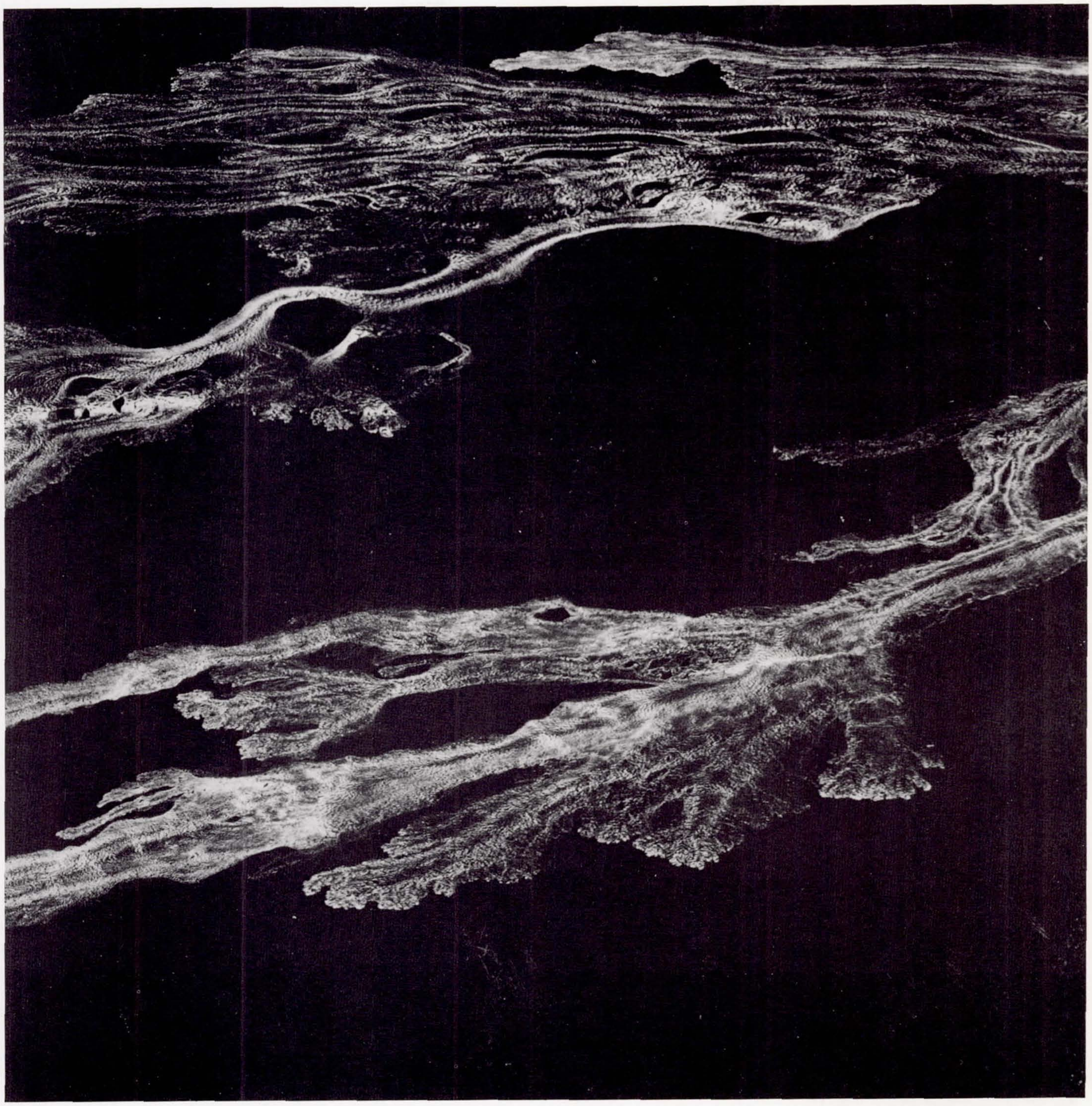

FIGURE 8–5. Night time oblique aerial view of active flows during the July 1975, eruption in Mokuaweoweo Caldera on Mauna Loa, showing multiple active flow lobes; note the patterns of crust formation on the surface of the flow. (Photograph by U. S. Geological Survey, Hawaiian Volcano Observatory, July 7, 1975.)

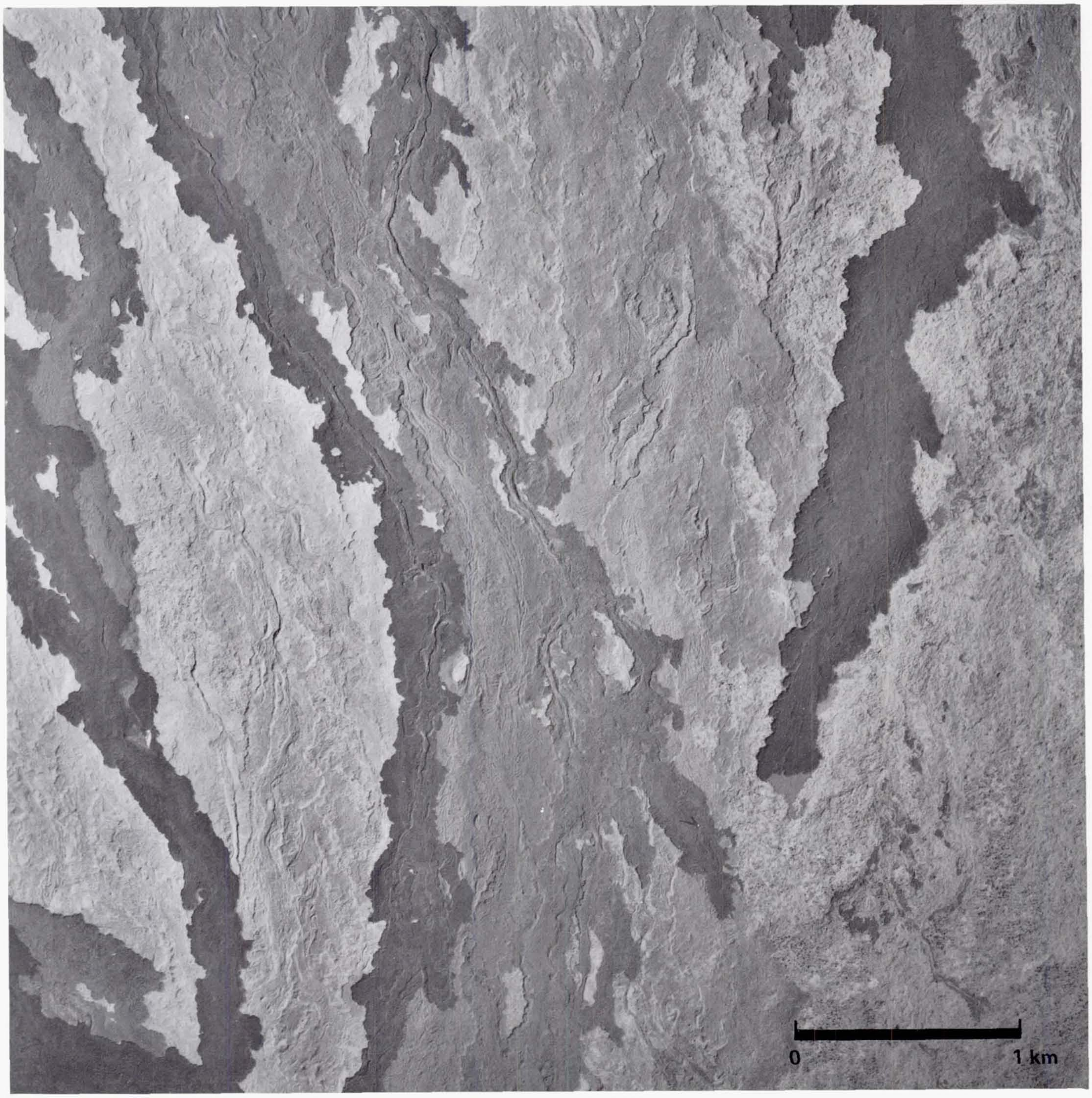

FIGURE 8–6. Vertical aerial photograph of multiple flows on the flanks of Mauna Loa; flows include both tube-fed and sheet flows. (Photograph by U. S. Department of Agriculture, photograph EKL-14CC-35, 1965.)

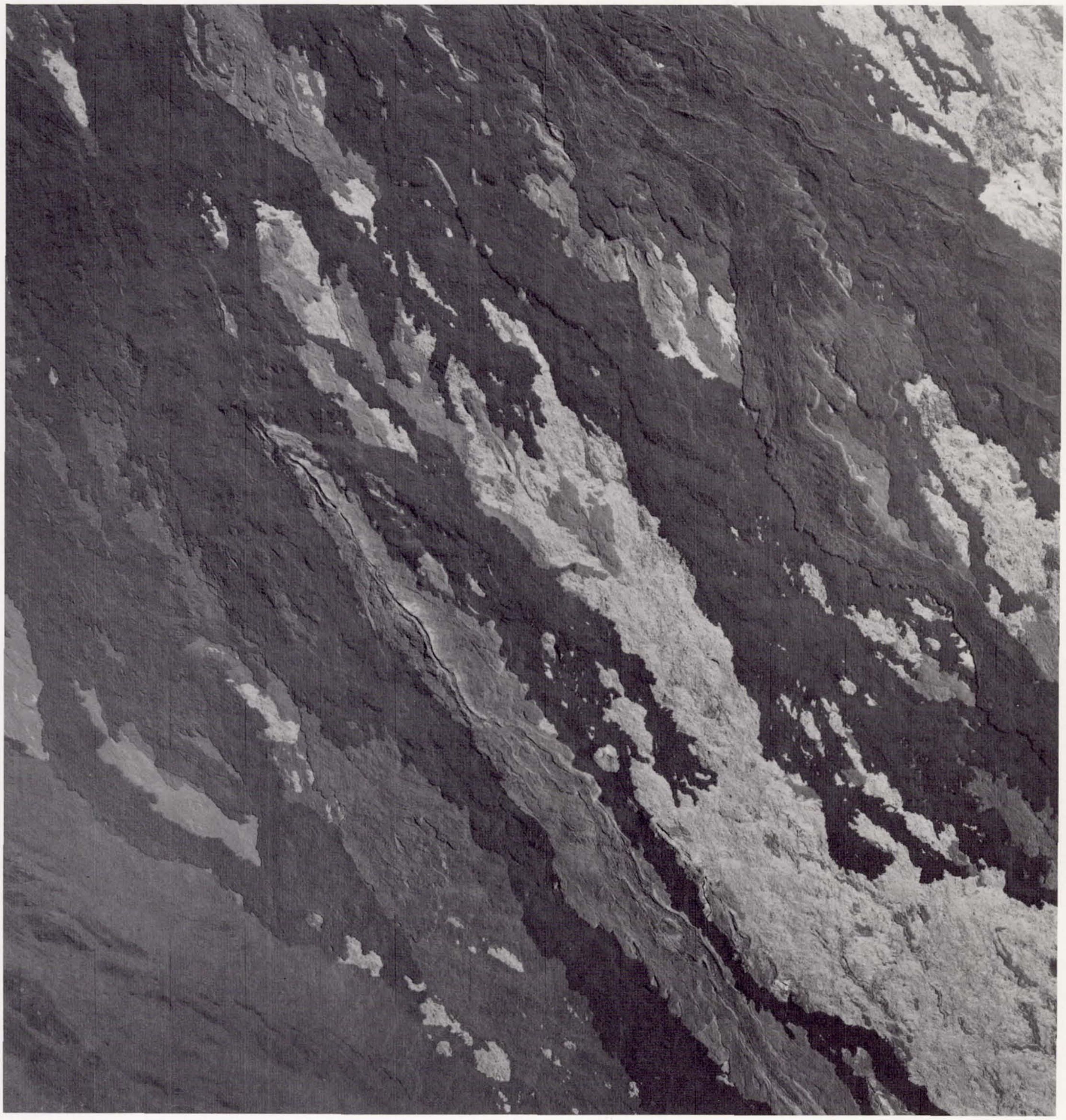

FIGURE 8–7. Vertical aerial photograph of complex anastomosing flows on Mauna Loa. Most flows are less than 5 m thick. (Photograph by Towill Corp., Honolulu, frame 6683-1, June, 1975.)

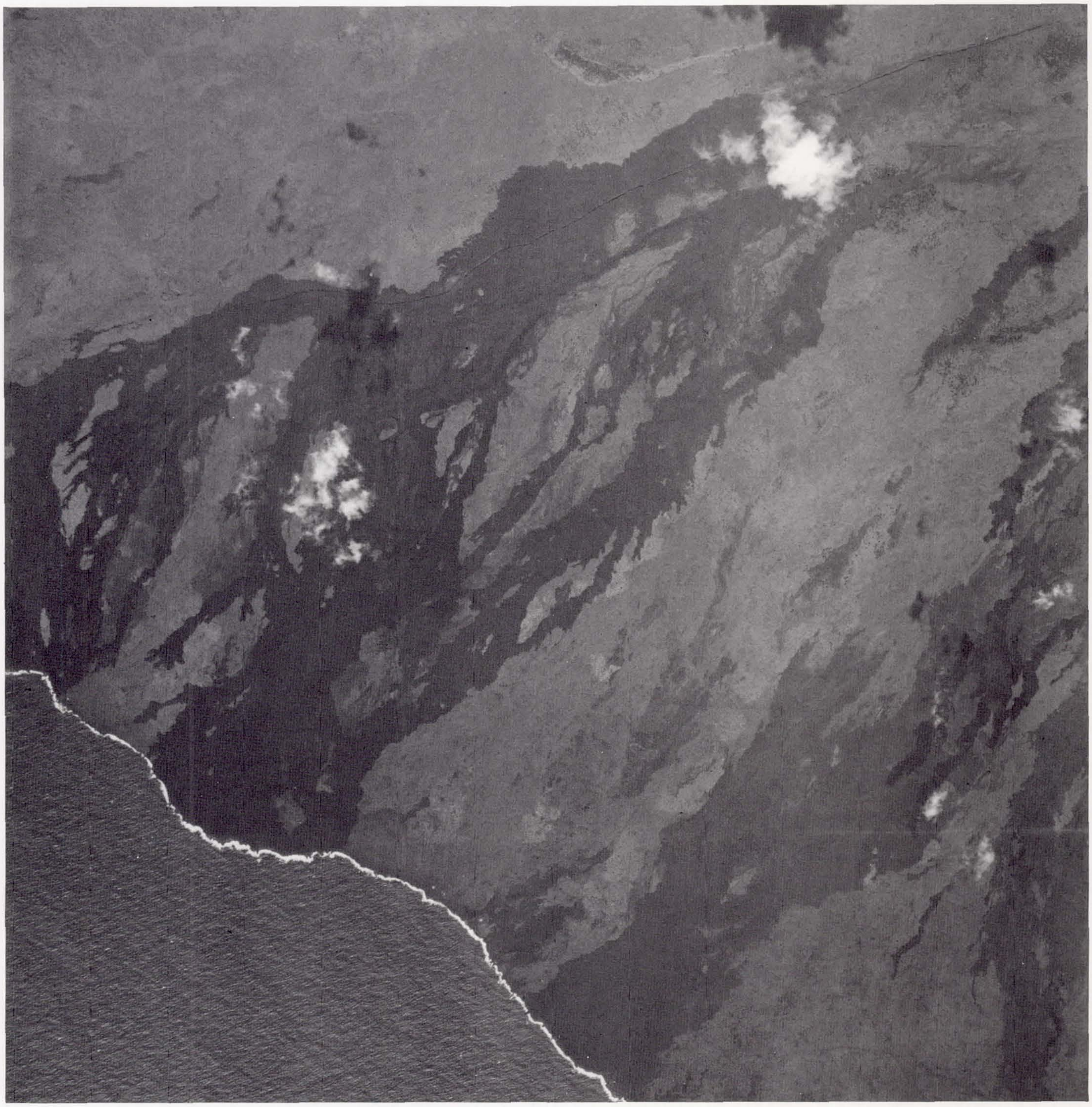

FIGURE 8–8. High altitude vertical view of the Great Crack and the 1823 lava flow, southwest rift zone, Kilauea Volcano. The fissure flow was extremely fluid and fast-moving, and drained rapidly toward the coast. Along some parts of the fissure, the flow left only a thin "scum" on the surface (see next figure). (NASA–Ames, U–2 photograph, October 1974.)

FIGURE 8–9. View southwestward down the Great Crack and the 1823 lava flow. (Photograph by R. Greeley, 1974.)

FIGURE 8–10. "Lava plastered cones" of the southwest rift zone of Kilauea Volcano. Lava from the 1823 eruption (dark flows in this view) from the Great Crack was extremely fluid and faster moving; here, the lava breached an older cinder and spatter cone (1) and had sufficient momentum to override the cone at (2), leaving a thin veneer. (Photograph by R. Greeley.)

FIGURE 8–11. View of the "Great Crack," southwest rift zone of Kilauea, and the very thin 1823 lava flow on the surface. The flow in this region was so fluid that it left only a thin "scum" less than 10 cm thick on the surface (arrow). (Photograph by R. Greeley, 1975.)

FIGURE 8–12. View of the east wall of the Great Crack fissure (compare with Figure 8–8), showing "lava balls" that were tumbled along in the flow, like snowballs. These features developed during the 1823 eruption on the southwest rift zone of Kilauea Volcano and are rather rare. (Photograph by R. Greeley, 1975.)

FIGURE 8–13. Broken "lava ball" of the 1823 flow (see previous figure), showing a core consisting of a basalt block that was caught in the flow and the layered lava that accreted to the block as it was tumbled along by the molten lava. (Photograph by R. Greeley, 1975.)

FIGURE 8–14. View westward across the southwest rift zone of Kilauea, showing the 1971 fissure flows (left of arrow) on the 1919-1920 flows of Mauna Iki. Arrow points to an area about 400 m across that represents part of the flow that foundered, apparently as a result of outflow from beneath a crust, producing a jumbled topography of several meters relief. Jumbled outflow area fed the aa flow visible in the background. (Photograph by R. Greeley, 1974.)

FIGURE 8–15. Low altitude oblique aerial view of lava flow "fans" that formed in 1969 when flows spilled over the rim of Napau Crater. (Photograph by R. Greeley, 1970.)

Page intentionally left blank

IX. FLOW COMPONENTS

In this chapter the individual structures and features of lava flows are discussed, including lava tubes, lava channels, and pressure ridges. Many of these features are indicative of basaltic volcanism and thus are important in the photointerpretation of basaltic lava flows on planetary surfaces.

Perhaps the most important flow components of Hawaiian basalt flows are tubes and lava channels, both of which play a critical role in conducting lava from the vent to the flow front. Observations of the Mauna Ulu eruptions over several years showed that most of the lava erupted was emplaced via tubes. Similarly, the morphology of flows on the flanks of Mauna Loa suggests that tubes and channels have been involved in the emplacement of most Mauna Loa lavas.

Lava tubes are tunnel-like structures that have free-standing roofs after molten lava drains from beneath the crust. *Lava channels* are open structures without a roof. Observations of active lava flows show that channels often develop thin crusts; however, when the molten lava drains from beneath the crust, large segments of the crust will collapse, leaving no, or only small sections of, free-standing roof; consequently, channels and tubes commonly alternate along a single flow conduit. Thus, distinction between tubes and channels is probably not very important. Of more significance is the observation that they typically develop as a result of relatively prolonged flow activity. In Hawaii, brief fissure eruptions produce sheet-like lava flows; emplacement is so rapid that lava tubes and channels do not have time to develop. Tubes and channels develop more commonly during longer lasting eruptions in which lava is derived from a small number of discrete vents, even though the vents may be aligned along fissures and the associated thin flows pile up in the complex assemblage.

Lava tubes are known to develop only in fluid flows such as basalt. Thus, their identification is some indication of the composition of the flows in which they are found, at least to a first approximation. This is particularly important in interpreting lava flows on Mars, as discussed in Chapter 13. Lava flowing through enclosed lava tubes cools much slower than in open flow, and thus can travel much greater distances.

The surfaces of lava flows, whether fed through lava tubes and channels or spread as sheet-like bodies, develop a crust rapidly upon exposure to air. The crust thickens with time but beneath the crust molten lava may continue to flow. This can result in the development of shear planes within the flow and deformation of the crust to form *pressure ridges* and *tumuli*. These structures may also form by surges of molten lava which rupture the overlying crust to form squeeze-outs. Tumuli may also form over lava tubes as a result of rupture of the roof by a surge of lava within the tube. *Pressure plateaus* are large elevated regions that appear to have been injected and uplifted by lava fed under a pressure, perhaps again through lava tubes.

Smaller ruptures in the crust of lava flows may produce rootless vents termed *hornitos*, which can be several meters high. A variation of the hornito is the so-called *driblet spire*, a structure which may be two or three meters high and which appears to form by lava squeezing out of a hole in the crust of a lava flow, much like toothpaste being squeezed from a tube.

Lava flows passing through forests and over marshy ground often produce bizarre structures. Fluid pahoehoe flows often form a veneer around the trunks and branches of trees, forming *lava trees*. When the wood burns, a lava structure remains as a *tree mold*. Subsidence of lava flows often leaves *high lava marks*, indicating the former level of the lava flow. Subsidence can be caused by drainage of lava to lower elevations, degassing, or a combination of the two.

FIGURE 9–1. This "skylight" (window in collapsed roof of a lava tube) shows a multiple lava tube (upper and lower levels), in which the upper level (A) has drained of lava and the lower level (B) still has flowing molten lava; note the slight arch in the roof of the upper tube. Width of the upper tube is about 5 meters. This is part of the complex series of lava tubes formed in flows erupted from Mauna Ulu. (U. S. Geological Survey, Hawaiian Volcano Observatory photograph.)

FIGURE 9–2. View through a "skylight" into active lava tube formed during eruption of Mauna Ulu; light gray area in center of picture is molten lava; note the thick (0.75 m) arch of the lava tube roof. (Photograph by R. T. Holcomb, 1973.)

FIGURE 9–3. View through a 1-m-wide "skylight" of a lava tube developed in flows erupted from Mauna Ulu, showing actively flowing lava (gray area) and the thin pahoehoe crust that forms the tube roof. (Photograph by D. W. Peterson, September 1972.)

FIGURE 9–4. Active flow in a lava channel during eruption of Mauna Ulu, showing plate-like crust in middle of channel and projections of crust from the channel banks. Width of channel is about 5 m. (Photograph by R. T. Holcomb, October 1972.)

FIGURE 9–5. View toward the summit of Mauna Ulu, showing fountaining of lava into a summit lava lake; levee of lake has been breached, permitting lava to flow down the flank of the shield where it is accumulating in a "perched lava pond" (foreground); compare with Figure 9–6. Note spatter cone that has been constructed at the summit. (Photograph by R. T. Holcomb, January 1974.)

FIGURE 9–6. Small, active lava channel associated with Mauna Ulu eruptions, showing prominent levee (left side) about 1 m high that has been built by accretion of lava that has spilled from the channel. Note the thick, wrinkled crust and flowing lava in the center of the channel, and the "lavacicles" on the channel levees. (Photograph by R. T. Holcomb, March 1974.)

FIGURE 9–7. Low-altitude oblique aerial view of Mauna Ulu summit region in 1974. Most of the flows were fed by lava tubes and channels, reflecting prolonged eruption. As seen here, the summit region is riddled with a complex network of interconnected tubes and channels. (Photograph by R. Greeley, 1974.)

FIGURE 9–8. View of the summit of Mauna Ulu in 1974, showing numerous lava channels radiating from the summit pit. The channels developed by repeated overflow of lava; channel in the background feeds lava to a perched lava pond (arrow) in the saddle between Mauna Ulu and the prehistoric cinder and spatter cone Puu Huluhulu (top of photograph). Compare to next figure. (Photograph by R. Greeley, 1974.)

FIGURE 9–9. View of the "perched" lava pond (midground), taken from Puu Huluhulu (foreground), showing the pond surface (1) and the self-accreted levee (arrows) that held the lake; channel marked with (2) fed the "perched" lake from the summit vent at Mauna Ulu (background). (Photograph by R. Greeley, 1974.)

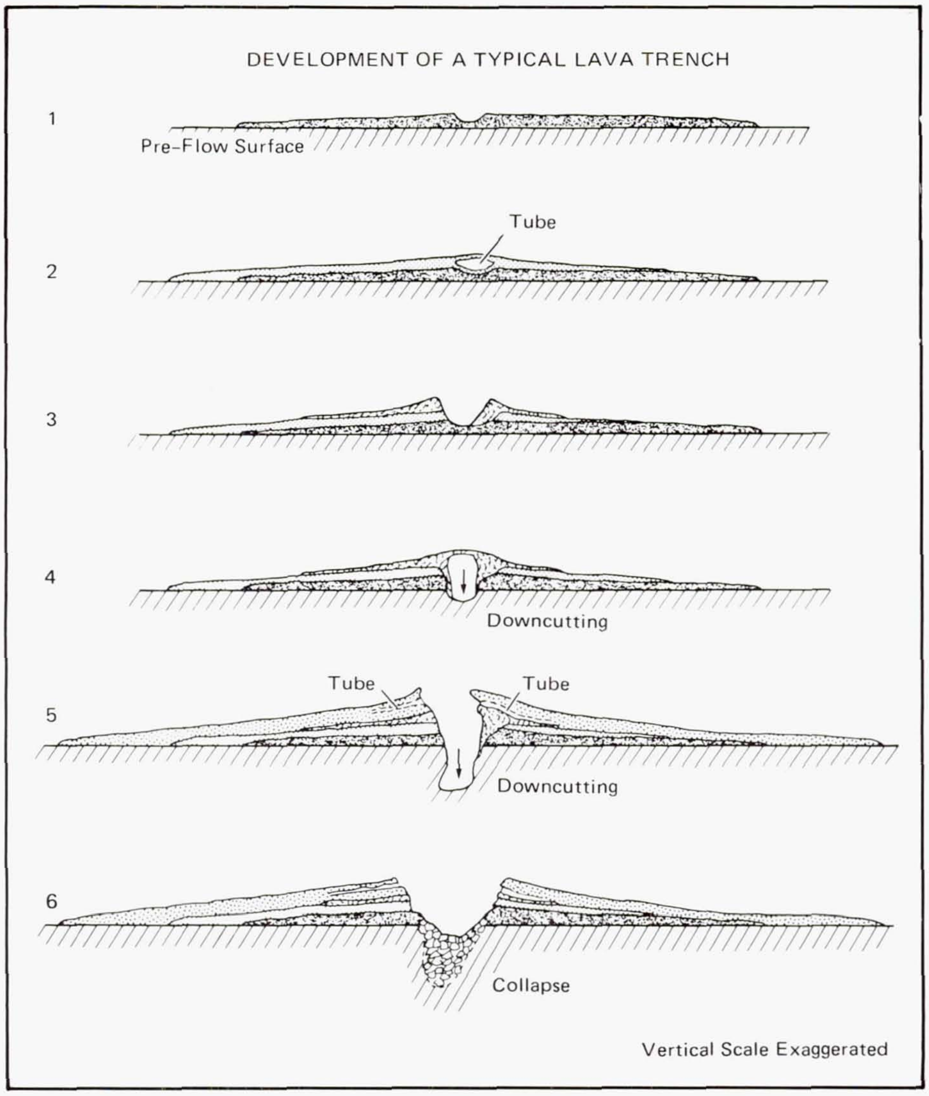

FIGURE 9–10. Sequence to show some of the stages in the development of a tube-fed lava flow. Stage 1 is a single flow emplaced by a shallow lava channel; Stage 2 involves a second flow, in which lava advanced down the previous channel and formed a roof. Stage 3 includes a third flow that formed a large channel; continued eruption of the same flow resulted in the formation of a roof (Stage 4), with downward erosion by melting and removal of some of the previous flow and preflow rocks. In Stage 5 a fourth flow was erupted at a high rate; it initially used the previous tube as the feeding conduit, but because the volume of lava was large, the roof was destroyed and an open-flow channel developed, segments of which may have become roofed; overflow from the channel formed distributary lava tubes and small channels. Stage 6 marks the end of eruption with collapse of roofed segments. Although this sequence is hypothetical, elements of each stage are based on observations of active lava tubes and channels and studies of cooled structures. (From Greeley, 1977.)

FIGURE 9–11. Vertical aerial photograph of complex flows (multiple flows from the same eruptive event) on the southwest flank of Mauna Loa, typical of the flows that constitute the Hawaiian shield volcanoes. Note the interbraided channel network of the flow of intermediate gray tone, and the lack of channels in the dark aa flow; the reasons for these differences are not well understood, but are at least partly due to differences in flow fluidity and rate of effusion. Photograph is about 4 km square. (U. S. Department of Agriculture, photograph EKL-14CC-36, March 1965.)

FIGURE 9–12. Low-altitude aerial photograph of lava channel formed in pahoehoe flows erupted from Mauna Ulu (compare with lava channel formed in aa, Figure 9–13). General flow direction is from left to right. Channel appears to have been roofed by a thin crust of cooled lava that collapsed during drainage of the channel, evidenced by the draped and cracked pahoehoe along the sides of the channel, as at "A"; surface of small flow lobe at "B" appears to have collapsed, possibly as a result of degassing of the flow; flow lobe at "C" appears to have advanced by budding of pahoehoe toes. (Photograph by R. Greeley, July 1974.)

FIGURE 9–13. Oblique aerial photograph of lava channel formed in aa flows on the flank of Mauna Loa, showing prominent channel levees. Levees appear to be compound (note parallel "ridges" of the levee), possibly resulting from several flows occupying the channel or from surges within a single flow. Dark areas are younger aa flows. (Photograph by R. Greeley, August 1969.)

FIGURE 9–14. Panoramic photographs of an aa channel developed in flows erupted from the southwest rift zone of Mauna Loa; photographed along Highway 11, near Kahuku. Note the slight channel banks and the pahoehoe both along the banks and within the channel. (Photographs by R. Greeley, July 1978.)

FIGURE 9–15. Panoramic mosaic of the July 1974 flow at Kilauea (see Figure 9–16); very fluid lava flowed down a gully from the right, banked high on the hill at "A" (note figure for scale), veneering the hill with a thin layer of glassy lava, and then flowed onto the floor of Kilauea Caldera. (Photographs by R. Greeley, July 1978.)


K

FIGURE 9–16. Panoramic mosaic of part of the July 1974 flow on the southwest rim of Kilauea Caldera (K). Flow erupted from a fissure (F) and flowed down gully toward the left, onto the floor of the caldera. The flow was extremely fluid, leaving "swash" marks high on the banks of the gully (note figure for scale). Judging from the shape of the channel cross section in comparison with adjacent gullies, it would appear that the lava flow widened the preflow gully slightly by erosion. Figure 9–15 is a view of the bank at "A." Profile of Mauna Loa is in the background. (Photographs by R. Greeley, July 1978.)

Page intentionally left blank

X. LAVA FLOW TEXTURES

Basaltic lava flows have a wide variety of surface textures, ranging from smooth and glassy to extremely rough with meter-size blocks. The Hawaiian terms *pahoehoe* and *aa* are used almost universally to characterize lava flows. Pahoehoe has a smooth, billowy or ropy surface, whereas aa has an extremely rough clinkery surface. A third type, *block lava*, is characterized by relatively smooth, large blocks but is rarely if ever found in Hawaii. Pahoehoe and aa grade into one another but rarely is it difficult to distinguish between the two. A pahoehoe flow may change downstream into an aa flow, especially if the flow goes down a steep slope (see Figure 8–3), but an aa never changes into a pahoehoe. The factors that determine whether a flow becomes pahoehoe or aa has long been a subject of debate. Fluidity is now believed to be the most important factor. Aa tends to form from more viscous flows than pahoehoe so that any factor that causes a decrease in fluidity, such as cooling, degassing, or a greater degree of crystallization, will tend to promote the formation of aa (Macdonald, 1953). In the case of the 1969-1971 Mauna Ulu eruptions, the degree of crystallinity appears to have been the controlling factor (Swanson, 1973).

Several types of pahoehoe have been recognized. *Shelly pahoehoe* is characterized by fragile gas cavities, small tubes, and a buckled or billowy surface. It generally forms when gas-charged lava erupts with little or no fountaining (Swanson, 1973). Surface textures vary greatly and may be bulbous, buckled, ropy, or imbricate. A second major type of pahoehoe is that which forms of lava erupted from high fountains. It differs from shelly pahoehoe in that it has a relatively smooth upper surface and contains very few large cavities. It is also much less vesicular. The differences are believed caused largely by degassing during fountaining and subsequent channel flow. A third major type of pahoehoe is a dense, hummocky type produced from lava tubes. The hummocky surface is caused partly by the presence of tumuli, which are very rare or absent in other types of pahoehoe. The texture of the surface is similar to shelly pahoehoe, commonly with numerous overlapping toes and lobes, but the toes are solid, not cavernous. Pahoehoe flows advance in two main ways. The more fluid flows advance with a rolling motion, with the upper part of the flow moving faster than the lower part, so that the flow front is rolled under and buried by the advancing front. Slower moving flows advance by successive formation of bulbous toes at the flow front.

Aa is characterized by an extremely rough, jagged surface which is almost completely covered with loose fragmental debris, or clinker. The clinkery surface covers a massive, relatively dense interior. As an aa flow advances, clinkery fragmental debris tumbles down the front of the flows so that clinkery layers occur both at the top and bottom of the flow.

Although surface textures cannot be seen in pictures of the martian surface, such differences in texture as described in this chapter could be inferred from the scattering properties of the surface and provide important clues as to the style of martian volcanism.

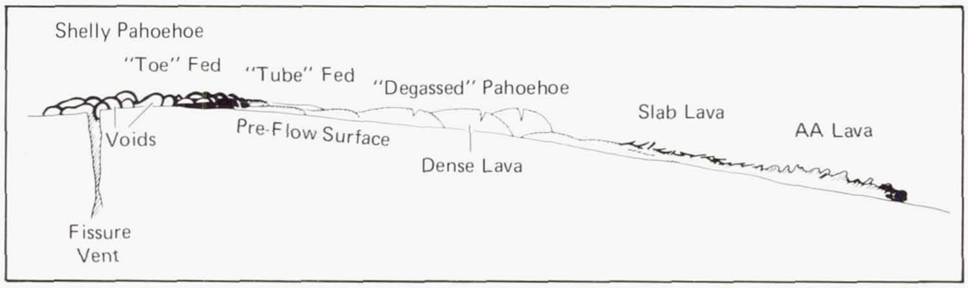

FIGURE 10–1. Diagram showing some types of basaltic lava flows related to the eruptive vent. The type of texture is dependent primarily on the interrelated parameters of lava viscosity, amount and state of volatiles, preflow topography, and others. In the simplest cases, with increasing distance from their vent, lavas cool, become less glassy, and degas, producing viscous textures, such as aa or block lavas (block lavas not shown here). Although a single lava flow could exhibit all the textures shown in this diagram, usually only a few are developed, depending upon the characteristics of the basaltic magma and the style of eruption.

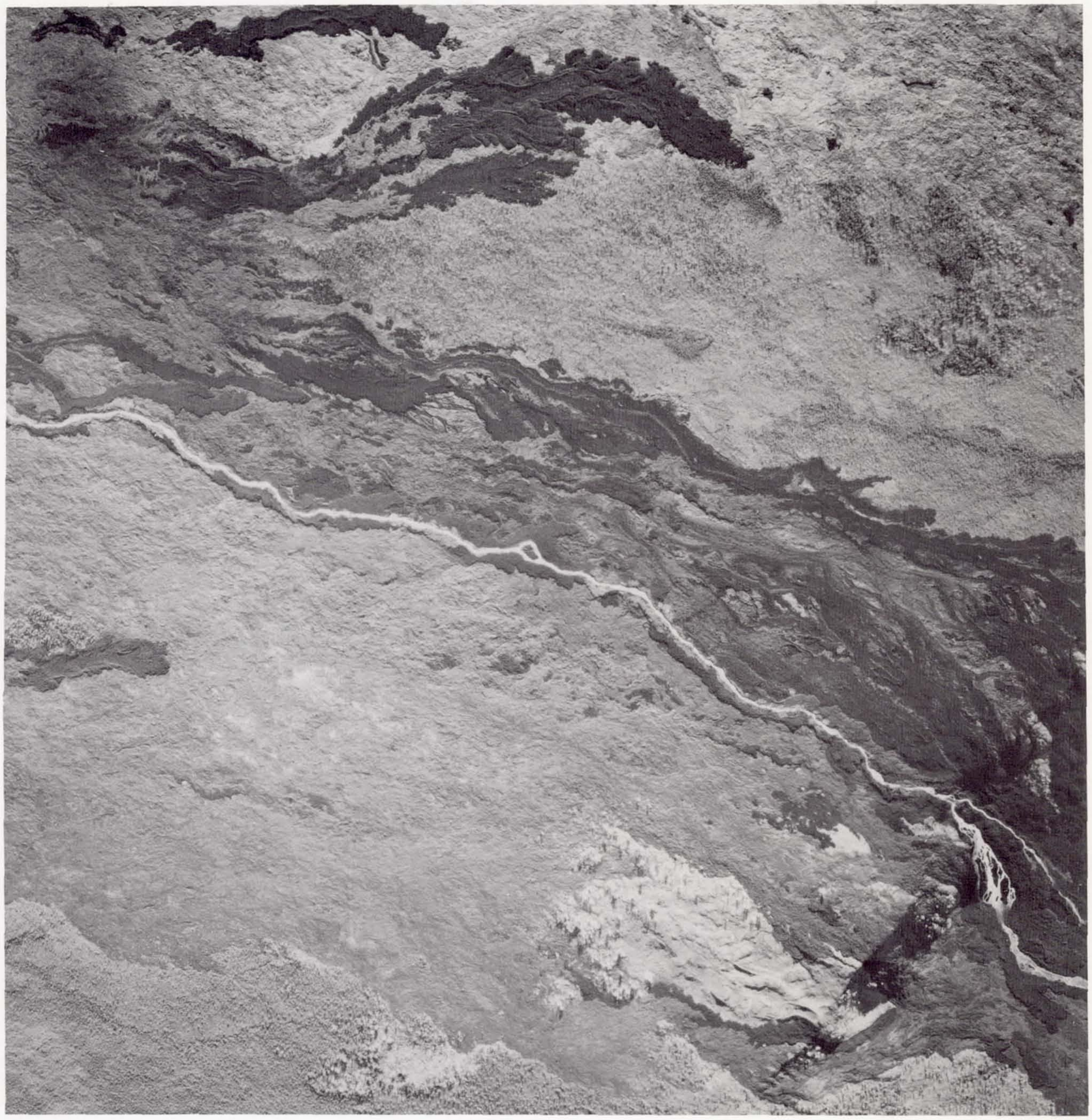

FIGURE 10–2. Vertical aerial photograph of recent flows from Mauna Ulu (active from 1969-1974), showing differences in graytone. Darkest areas are aa flows (clinkery surfaces), light areas are mostly gassy pahoehoe with glassy rinds; white area is actively flowing molten lava contained in a channel. All the flows are essentially the same chemical composition and were less than 5 years old when this photograph was taken. The differences in graytone are primarily a function of flow surface texture. (Photograph by Towill Corp., Honolulu, June 1, 1974.)

FIGURE 10–3. Typical corded surface texture on a "degassed," prehistoric pahoehoe lava flow in the Footprints Area, Kau Desert, Kilauea Volcano. Cords develop in the glassy rind of flows in response to continued flow of lava beneath the rind. Foreground is about 3 m wide. (Photograph by R. Greeley, July, 1978.)

FIGURE 10–4. Summit of Mauna Ulu crater in 1974 (compare with Figures 12–16 and 12–17), showing typical near-vent pahoehoe festoons and anastomosing channels. Molten lava shows as white lines on crater floor where the thin crust has cracked. (Photograph by R. Greeley, 1974.)

FIGURE 10–5. "Lava trees" in the November 1973 eruption near Pauahi Crater, east rift zone of Kilauea Volcano. This flow was active for about twelve hours and was very fluid as it passed through the Ohia tree forest. Lava accreted to the tree trunks and remained after the molten lava drained away. Lava trees stand about 2.5 m high and indicate the maximum height of the flow. (Photograph by R. Greeley, 1974.)

FIGURE 10–6. Lava tree in area shown in Figure 10–5. Note the thick accumulation of lava in relation to the small diameter of the tree trunks. Mauna Ulu is in the background. (Photograph by R. Greeley, 1974.)

FIGURE 10–7. Shelly pahoehoe in the July 1974 lava flow northwest of Lua Manu crater, Chain of Craters Road, Kilauea, showing cavernous "blisters" of glassy lava. Shelly pahoehoe forms in response to rapid outgassing of lava and is a good near-vent indicator. Shells may be as thin as a few millimeters; blisters may be more than a meter wide and caution must be exercised in traversing shelly pahoehoe. (Photograph by R. Greeley, July 1978.)

FIGURE 10–8. Vertical aerial photograph of flows from the 1969-1974 eruption of Mauna Ulu, showing typical transition from pahoehoe ("p," light toned areas) to aa ("A," dark toned areas) toward the distal end of flows, in response to increasing viscosity, probably resulting from cooling and loss of degassing. Note, however, that the lava in channel down the middle has remained pahoehoe; this may be partly accounted for because flow in the channel was smoother and more rapid than for non-channel flow. (Photograph R8-75HA-151 11-4, December 1975.)

FIGURE 10–9. Slab lava developed on the 1823 Keaiwa lava flow, southwest rift zone of Kilauea Volcano. Slab lava can form, following initial emplacement of the flow as pahoehoe, on which a smooth crust develops; subsequent movement of the still-molten lava beneath the crust breaks the surface into a jumble of plates. (Photograph by R. Greeley, March 1976.)

FIGURE 10–10. Aa lava flow margin, northern flank of Hualalai Volcano, showing typically clinkery surface and steep flow edge. (Photograph by R. Greeley, July 1978.)

FIGURE 10–11. Panoramic mosaic of the Keamoku flow, Mauna Loa, at a road cut on Highway 11, Kau District, showing typical cross section of an aa flow; note that the clinkery aa texture is found in the upper 2 m of the flow, above the massive interior. (Photograph by R. Greeley, July 1978.)

FIGURE 10–12. Aa flow surface, showing irregular, clinkery texture; 1887 lava flow from Mauna Loa erupted from the southwest rift zone; photograph taken near Highway 11, about 12 km west of Waiohinu. (Photograph by R. Greeley, July 1978.)

FIGURE 10–13. Accretionary lava ball in the prehistoric Keamoku lava flow from Mauna Loa, along the Footprints Trail, Kau Desert. Accretionary lava balls can form in aa lava flows in a manner similar to snowballs rolling downslope. (Photograph by R. Greeley, July 1978.)

XI. LAVA LAKES

Eruptions commonly result in the formation of lakes of molten lava in craters and other depressions. Such lakes are of two types. One type develops above a magma column and undergoes active circulation, periodic rises and falls, and constant replenishment in heat, volatiles, and possibly magma. Such an *active lake* is the type that Jagger described in Halemaumau and characterized the main vent at Mauna Ulu. The other type of lake is inactive, or stagnant, and results simply from lava collecting in a depression. This type undergoes little circulation and should be recognized simply as a ponded lava flow. Examples of such lakes include those in Kilauea Iki, Makaopuhi, Alae, and Pauhi Craters on Kilauea's east rift zone.

The general term *lava lake* refers to the solidified and partly solidified stages as well as to the molten lava. In lakes with active convection, the surface is continually being overturned. Newly exposed lava at areas of upwelling commonly forms a skin a few millimeters thick which is carried away by circulation. At varying distances from the source, the newly formed crust commonly turns downward and sinks into the main body of lava because of a density inversion set up by volatiles collecting beneath the solid or semi-solid crust. Alternatively, the skin may buckle and ride over the adjacent areas, particularly around those parts of the lake where there is upwelling. The repeated formation and ingestion of crust on active or circulating lava lakes has been compared to the formation and movement of lithospheric plates on the Earth (Duffield, 1972). New crust forms in upwelling regions and moves away from the spreading center. The crust is subducted where it meets other plates and transform faults form along the boundaries of plates where they move laterally with respect to one another. These motions are best observed at night when glow from the edges of the plates contrasts sharply with the dark crusted areas. In less actively convecting lakes, the crust may be fairly stable and is characterized by slow rafting and repeated breakup of congealed lava at the surface. Occasionally, the whole lake may overturn in one movement with all former crust rolling over and sinking into the molten lava beneath.

Within minutes of exposure of molten lava at the surface of a lava lake, a crust forms and cracks develop in the crust. If the lake is fairly stable (inactive or stagnant) and not being continually overturned, then within hours, cracks divide the crust into polygons averaging several meters in width. As volatiles are lost from the lava, gasses accumulate beneath the crust near the center of the polygons and escape through the cracks on the margins. This causes upbowing of the center of the polygons so that each develops a half meter or so of vertical relief. As the crust thickens, the cracks propagate downward and new cracks may form which cut across the pre-existing polygons. Thus, the surface of a cooled lava lake is seldom flat but rather crossed by numerous intersecting cracks with bowed-up plates between.

FIGURE 11–1. Perched lava pond within a natural levee inside Halemaumau pit crater in 1885. The levee enclosing the lake is built up by spatter from small, rootless fountains on the lake and by repeated overflows, as seen here. At its maximum this lake stood about 12 m above the crater floor and was approximately 400 m in diameter. (National Park Service files photograph.)

FIGURE 11–2. Active lava lake in the pit crater Aloi. The pit crater is being fed in part by eruption along a fissure on the left side of the picture. The crater is overflowing and supplying lava to a flow in the upper half of the picture. (Photograph by L. S. Kadooka, May 1970.)

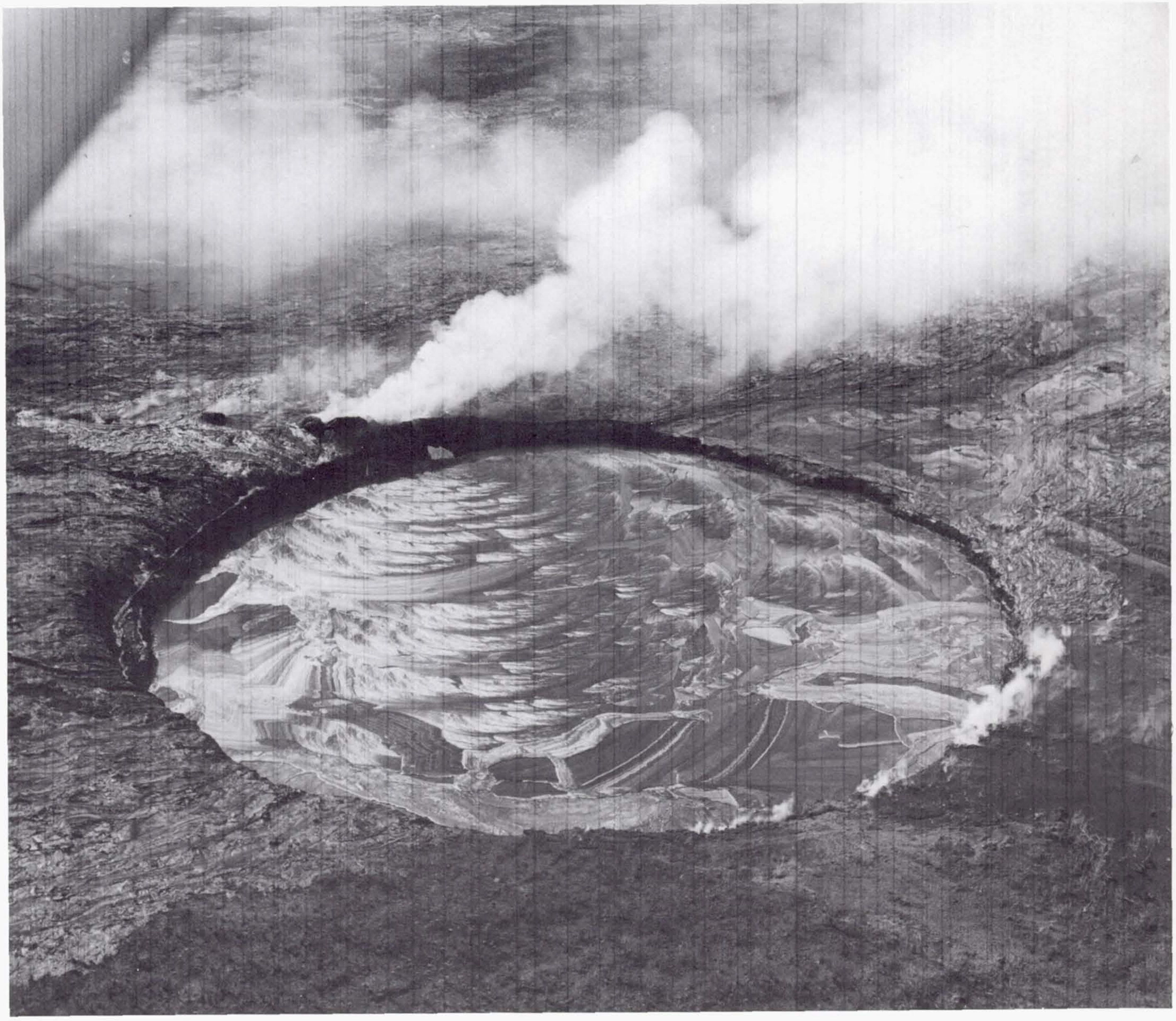

FIGURE 11–3. Lava lake in Aloi taken shortly after Figure 11–2. The level of lava in the lake has subsided. Spatter cones are clearly visible along the fissure which intersects the far side of the crater. Dark areas in the lake surface are where a crust has formed; light areas are newly exposed surfaces. The striation in the crusted areas mark the direction of flow of plates away from the zone of crust formation. The crust, where present, is probably only a few millimeters thick. (Photograph by R. T. Okamura, May 1970.)

FIGURE 11–4. An actively growing levee containing a lava lake at Mauna Ulu during eruption in 1974. Pahoehoe lava overflows the levee by accretion. The fountain feeding the lava lake is visible in the upper left. (Photograph by R. T. Holcomb, January 21, 1974.)

FIGURE 11–5. Floor of Kilauea Iki Crater. Cracks divide the central part of the floor into polygonal plates. The center of each polygon is bowed upward, partly as a result of accumulation of gases beneath the crust at the polygon centers. Many of the cracks are light colored because of fumarolic mineralization during outgassing. Along the margin of the lake, lava is plastered on the crater wall to form a lava subsidence terrace that marks the high level of lava within the lake. As the level in the lake fell, the thin crust was successively thrust outward over the adjacent crust at the lake edge to form the imbricate structure seen in the foreground. (Photograph by R. T. Holcomb, 1974.)

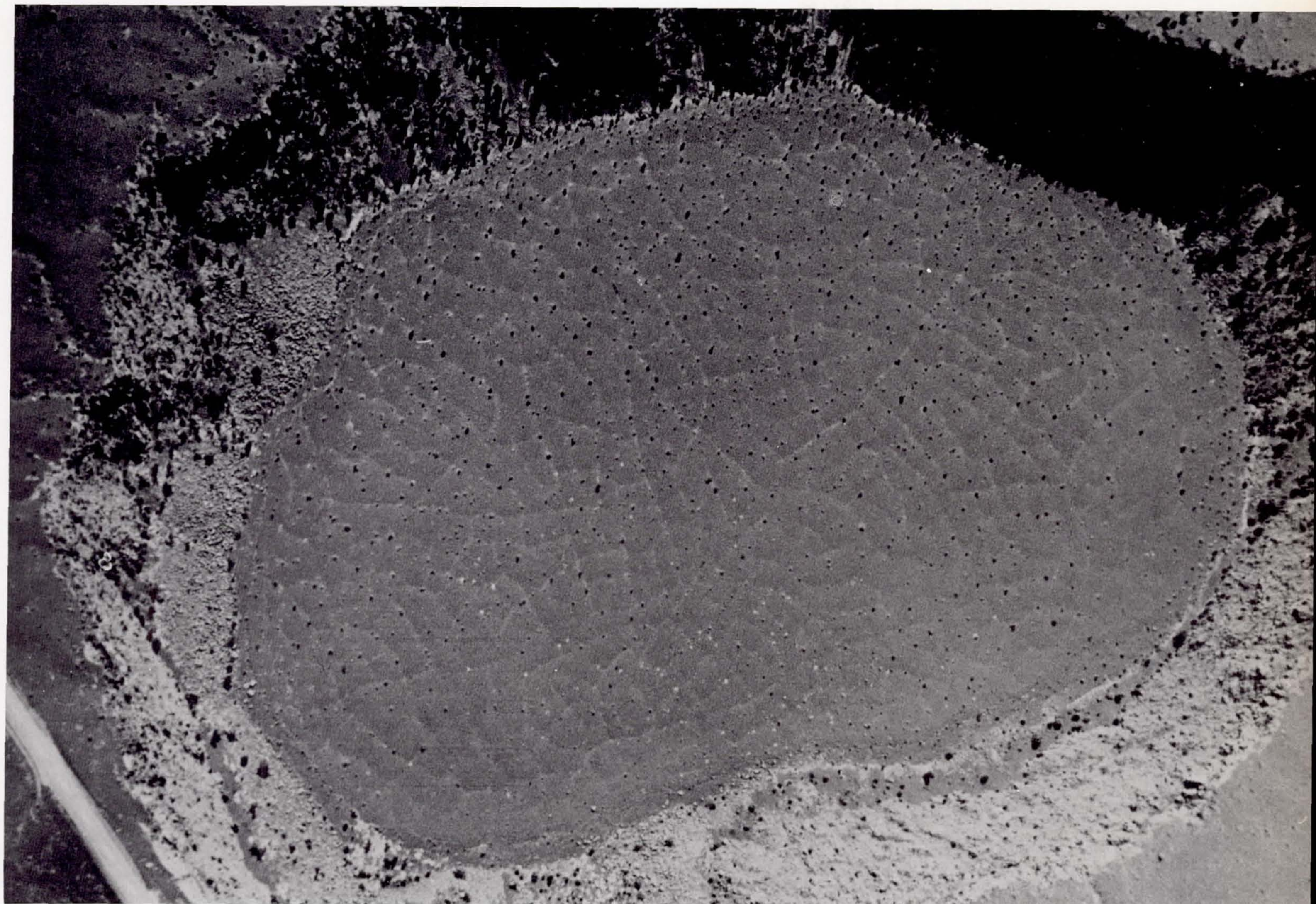

FIGURE 11–6. The 1877 lava lake in Keanakakoi Crater. As in the previous picture, the surface of the lake is divided into convex-upward polygons. The low intervening areas are here filled with light-colored pumice erupted in 1969. The lake is 250 m wide and 400 m long. (Hawaiian Volcano Observatory photograph.)

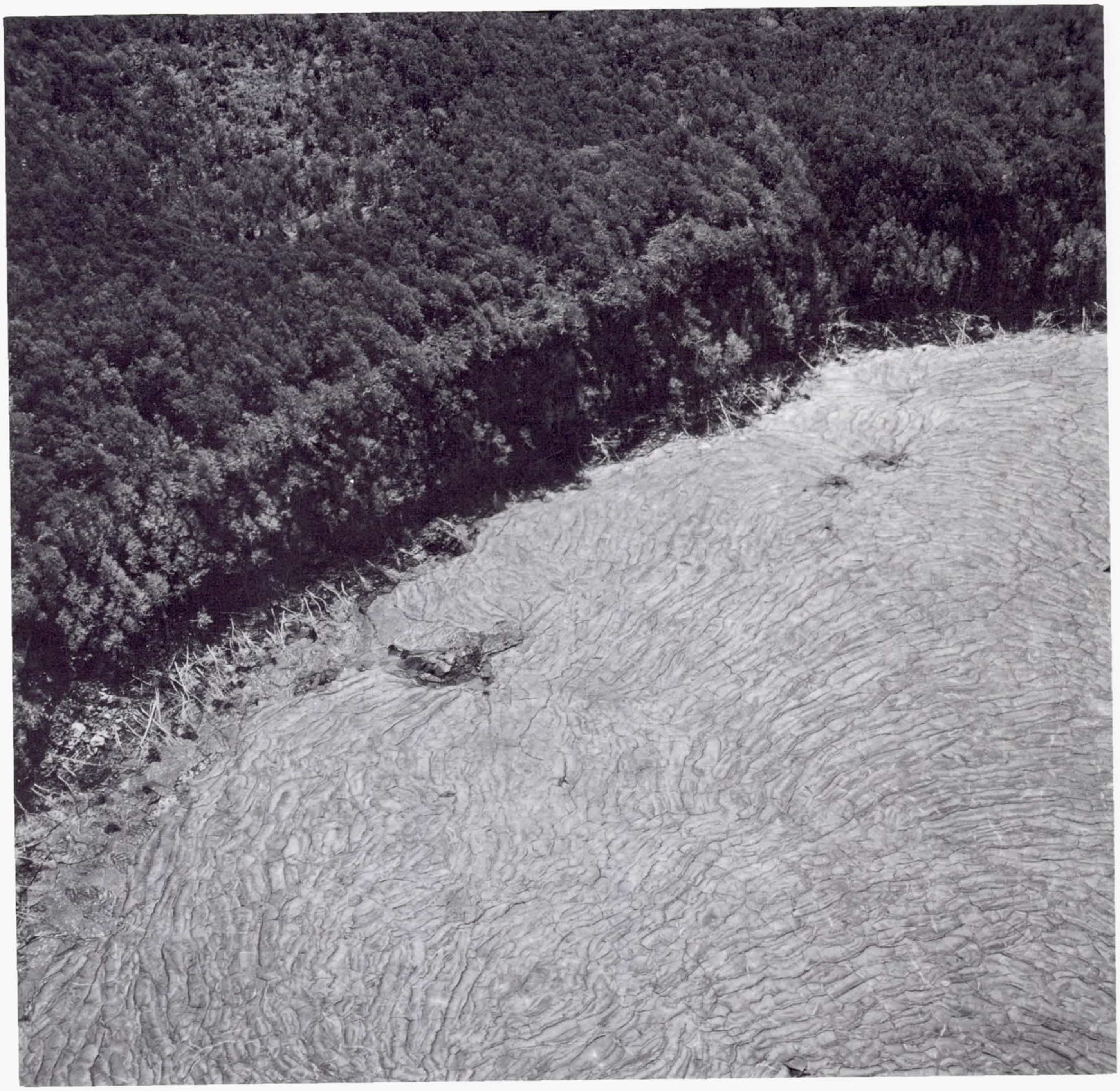

FIGURE 11–7. Surface of the 1965 lava lake in Napau. The picture was taken before later burial by flows in 1968. A ring around the lake, partly covered by fallen trees, marks the high lava level. (U. S. Air Force photograph, 1966.)

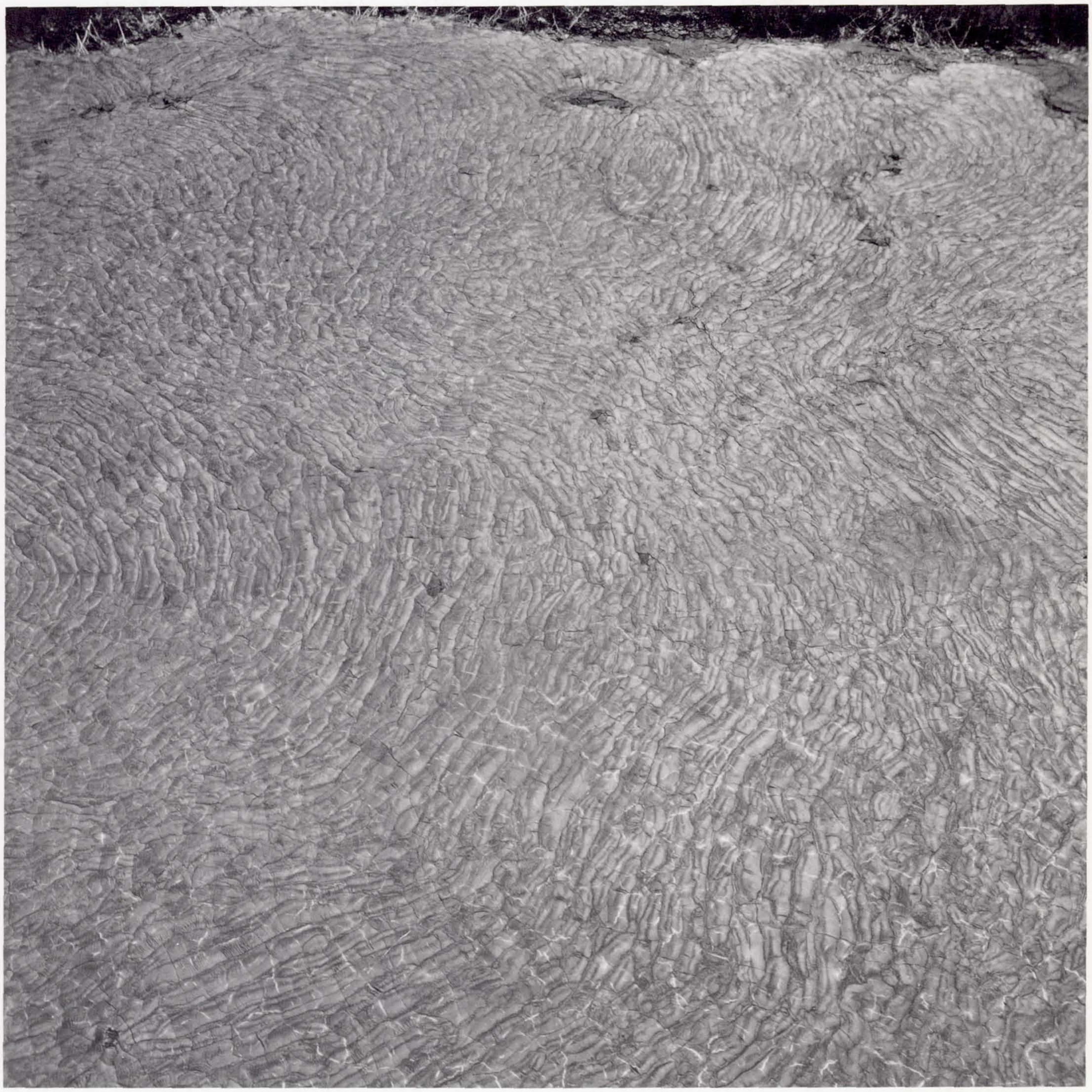

FIGURE 11–8. View of the 1965 Napau Lava lake, similar to previous figure. The surface texture is atypical and was probably caused by flow of lava from the left while the crust formed, plastically deforming it into subparallel wrinkles. (U. S. Air Force photograph, 1966.)

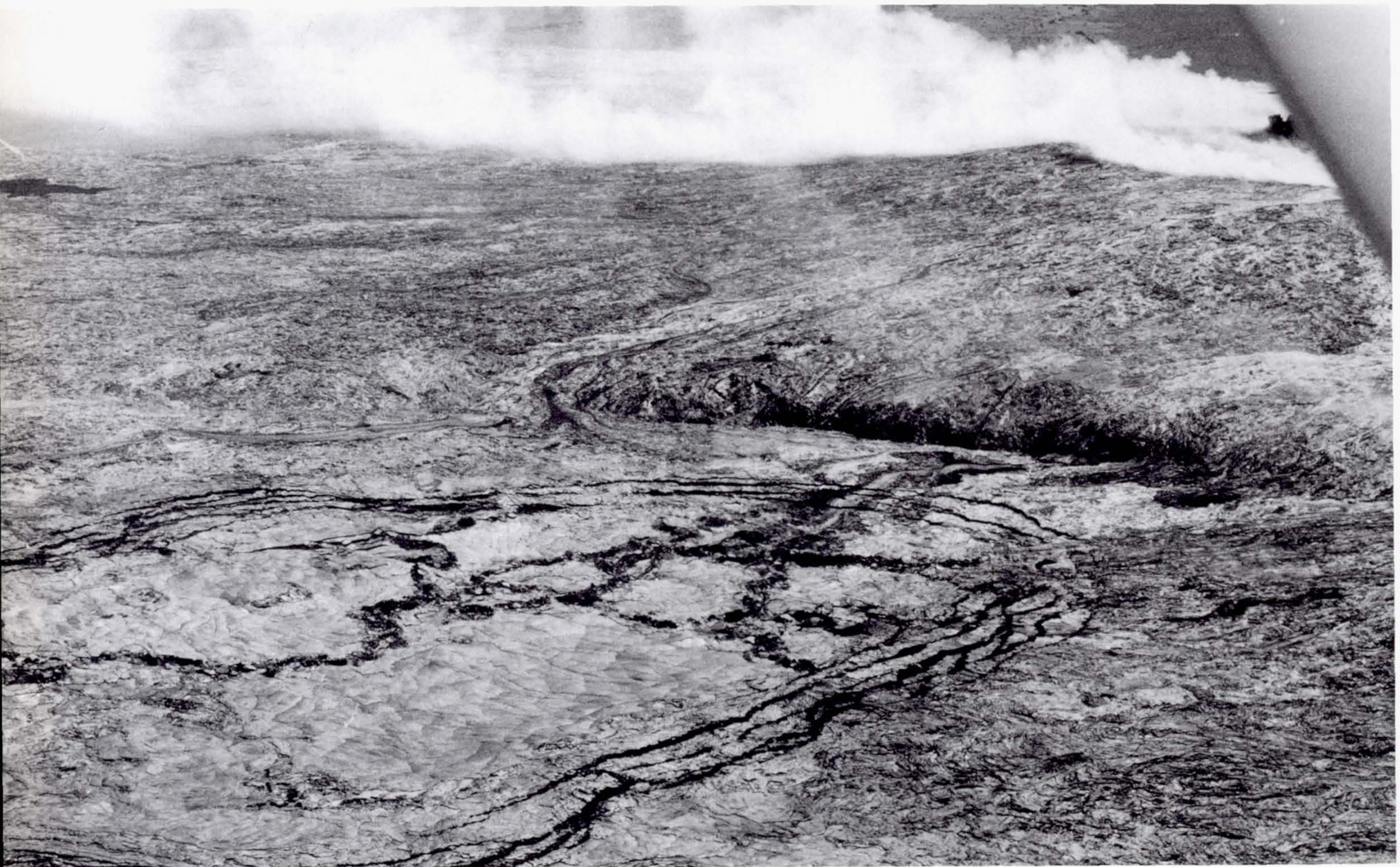

FIGURE 11–9. Oblique aerial view across Alae Crater toward Mauna Ulu (upper right, fume cloud), showing extensional fractures (outer concentric rings) and compressional ridges that formed on the lava lake crust as a result of drainage of the lake through lava tubes. (Photograph by R. Greeley, 1970.)

XII. MAUNA ULU ERUPTIONS

From May of 1969 to mid-1974, Kilauea was erupting almost continuously. Most of the activity was centered at Mauna Ulu, about 10 km from Kilauea Caldera on the east rift zone, but minor eruptions occurred within the summit caldera and along the southwest rift zone as well. The Mauna Ulu eruptions included lava fountaining, active, long-lived lava lakes, crater filling and draining, pahoehoe and aa flows, lava tube formation and construction of lava deltas as flows poured into the area. They illustrate vividly the variety of phenomena that can occur during a long-lived Hawaiian eruption and the complexity of the eruptive sequence. The illustrations are arranged in chronological order so that the sequence of events can be readily traced. The following account is a condensation of summaries written by the staff of the Hawaiian Volcano Observatory who continuously monitored the activity throughout the period.

The Mauna Ulu eruptions started on May 24, 1969, along an east-northeast trending fissure that passed through Aloi Crater and extended north of Alae Crater. Within an hour activity was localized along a segment of the fissure between the two craters and it was here that Mauna Ulu grew. Within days pools of molten lava formed within both Aloi Crater and Alae Crater. Activity subsided after several days but was renewed again in mid-June when one flow almost reached the sea after cascading over the Holei and Poliokeawe Palis. There followed several months of cyclic activity during which short periods of high fountaining were separated by days to weeks of relative quiet when activity was confined to the vent area itself. Typically, fountains built to peak heights within an hour or two, maintained their height — which in several cases was in excess of 400 m — for another hour or two, and then declined. Ponds around the former fountain would drain back into the vent to terminate this phase. The fountains fed new flows around the vent, one of which reached the sea 12 km to the south. Between fountaining episodes, lava would rise and fall somewhat like a piston within the vent and occasionally spill over and form small flows around the vent.

Most of the activity during the first half of 1970 was similar to the periods between fountaining in 1969. Overflows from the fissure vent were common and gradually a satellitic shield was built that was given the name *Mauna Ulu* (growing mountain). In April 1970 Aloi Crater was completely filled and by the end of June 1970 Mauna Ulu was 80 m high and 1 km across at its base.

In July 1970 a new east-northeast trending fissure opened on the eastern flank and overflows from the new vents built a broad ridge to the east of the Mauna Ulu summit. Meanwhile, tubes supplied lava to an underground reservoir in Alae Crater which in turn fed flows on the south flank of Kilauea via another system of lava tubes. In 1970 collapse pits began to form around vents on the east flank. By August the pits had coalesced to form an elongate trench which, in January 1971, finally merged with the summit vent. Tube-fed lava flows entered the ocean in the Fall of 1970 and Spring of 1971, creating lava deltas. Activity steadily declined after mid-1971; flow to the Alae reservoir was cut off and the lava level in the summit crater sank out of sight in mid-October, thus ending the first Ulu eruption (Swanson and others, 1979). Two small eruptions occurred in and to the southwest of Kilauea Caldera in August and September, respectively, but Mauna Ulu was little affected by either eruption.

Activity in Mauna Ulu resumed in February 1972, when lava reappeared in the central vent, flowed into the eastern trench, and re-entered the lava tube system that fed into the Alae reservoir. Growth of natural levees allowed the lava level within the trench to rise nearly to the height of the summit and extended the shield farther to the east-northeast. Frequent overflows fed flank flows, one of which reached Napau Crater, 6 km to the east. In mid-March 1972, the Mauna Ulu summit lake drained abruptly and two new vents opened to the east, one at the site of the former Alae Crater. The vent in Alae was probably fed by lava from Mauna Ulu via the tube system.

The rootless vent at Alae remained active for more than a year, sustaining a perched lava pond which fed flows throughout late 1972 and early 1973. Lava from Alae Crater gradually built a new shield that now abuts the southeast flank of Mauna Ulu. Some of the Alae flows partly filled the west pit of Makaopuhi Crater; others reached the sea between August and October 1972 and February and March 1973.

In June of 1973 lava drained from the summit crater and the Alae vent. Although lava slowly returned to Mauna Ulu, activity at the Alae vent ceased at this time. A quiescent period was followed by renewed fountaining and overflow at the summit in November 1973. After two days lava rapidly drained from the vent and eruptions occurred in Pauahi Crater. In mid-December lava returned to the Mauna Ulu vent and in mid-January fountaining occurred, quickly filling the vent and forming flows that travelled several kilometers. Episodic fountaining lasting several hours with intervening quiet periods of several days continued until June 1974, when vigorous activity ceased. Disappearance of lava from the central crater in July 1974 marked the end of the Mauna Ulu eruptive activity. A crater remains at the summit, approximately 115 m across and 135 m deep.

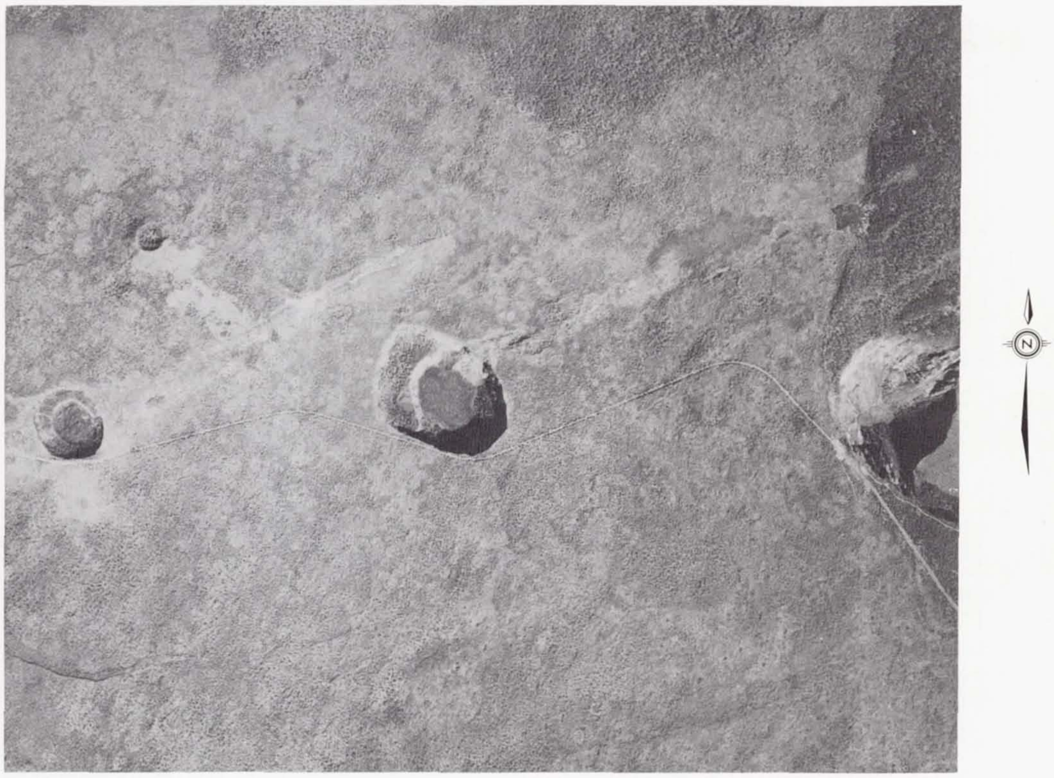

FIGURE 12–1. *Vertical aerial photograph of the site of the future Mauna Ulu in February 1965. The three pit craters along Chain of Craters are, from the left, Aloi, Alae, and Makaopuhi. The circular spatter cone, Puu Huluhulu, is to the northeast of Aloi. Eruptions started along a north-northeast trending fissure through Aloi. The center of the future Mauna Ulu shield is approximately midway between Aloi, Alae, and Puu Huluhulu. (U. S. Department of Agriculture, photograph EKL-12CC-174, 1965.)*

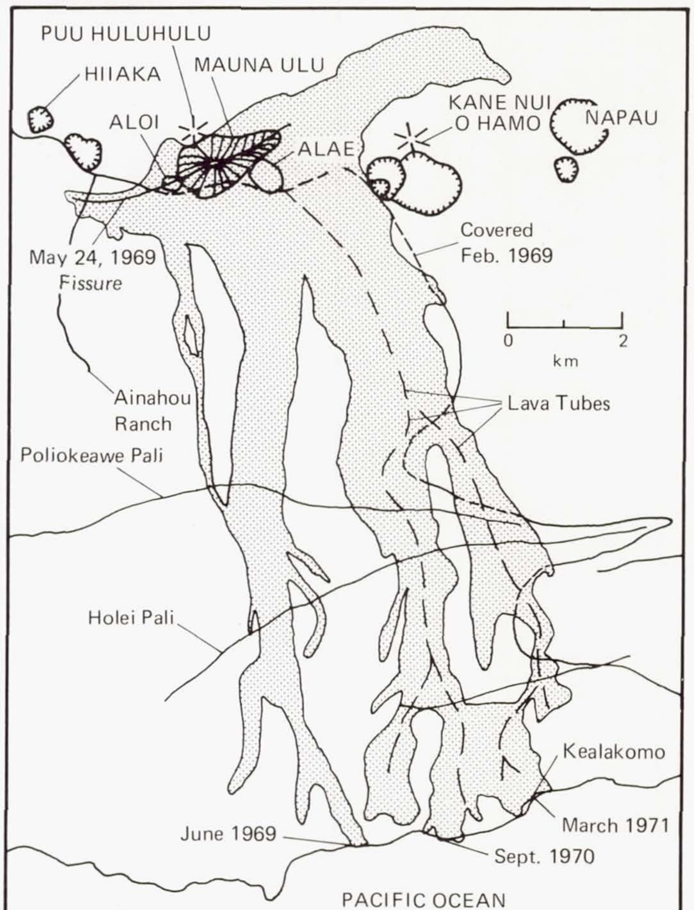

FIGURE 12–2. *Sketch map showing the distribution of lavas from the Mauna Ulu eruption through March 1971, and the location of present and former pit craters. The 1970 and 1971 flows to the east were formed largely by lavas fed through tubes from the Alae Crater reservoir. (From Swanson and others, 1971.)*

FIGURE 12–3. Oblique aerial view west along Holei Pali toward the ocean. Dark Mauna Ulu lava flows of 1969 through 1971 are draped over the pali. The shiny surface is caused by light reflected off older pahoehoe flows. (Hawaiian Volcano Observatory photograph, 1971.)

FIGURE 12–4. Same area as Figure 12–3, but looking east. The Holei Pali is a fault scarp. The area to the right has moved down and out toward the ocean during prehistoric slumping events. (Hawaiian Volcano Observatory photograph, 1971.)

FIGURE 12–5. Active lava lake in the vent at the Mauna Ulu summit. The top half of the picture shows the trench which formed on the east flank of the shield in 1970. The trench resulted from collapse around flank vents that first erupted in July 1970 and built a broad ridge to the east of the summit. The trench finally merged with the summit pit in January 1971. The pit at this time was 160 m long and 90 m across. (W. A. Duffield, February 1971.)

FIGURE 12–6. View southward across the eastern end of the trench in February 1972. After a relatively quiet second half of 1971, lava returned to the central vent and east trench. Levees, which repetitively formed around the trench, are clearly visible in this picture. Successive overflows, such as that in the foreground, built the east flank of the shield almost to the height of the summit. (Hawaiian Volcano Observatory photograph, February 1972.)

FIGURE 12–7. Vertical aerial photograph of the Mauna Ulu region in October 1972, similar to that shown in Figure 12–1. Puu Huluhulu is essentially unchanged but almost all the rest of the area is covered by Mauna Ulu lava flows. Irregular collapse pits have formed around rootless vents at the site of the former Alae Crater. Lava from these vents gradually built a new shield adjacent to the main Mauna Ulu shield whose summit retains its central pit and trench. Barely visible on the west edge of the picture is an area of collapse at the approximate site of Aloi Crater. The flow with a prominent lava channel at the top of the picture is from early 1972 and reached Napau Crater to the east. (Photograph by Towill Corp., Honolulu, frame 5815-9, October 19, 1972.)

FIGURE 12–8. Low-altitude aerial photograph of the satellitic shield that grew over the site of the Alae Crater in 1972. This photograph was taken same day as Figure 12–7. Perched lava ponds have temporarily subsided to form irregular depressions atop the shield. The upper pit is approximately 100 m across. (Photograph by Towill Corp., Honolulu, frame 5809-10, October 19, 1972.)

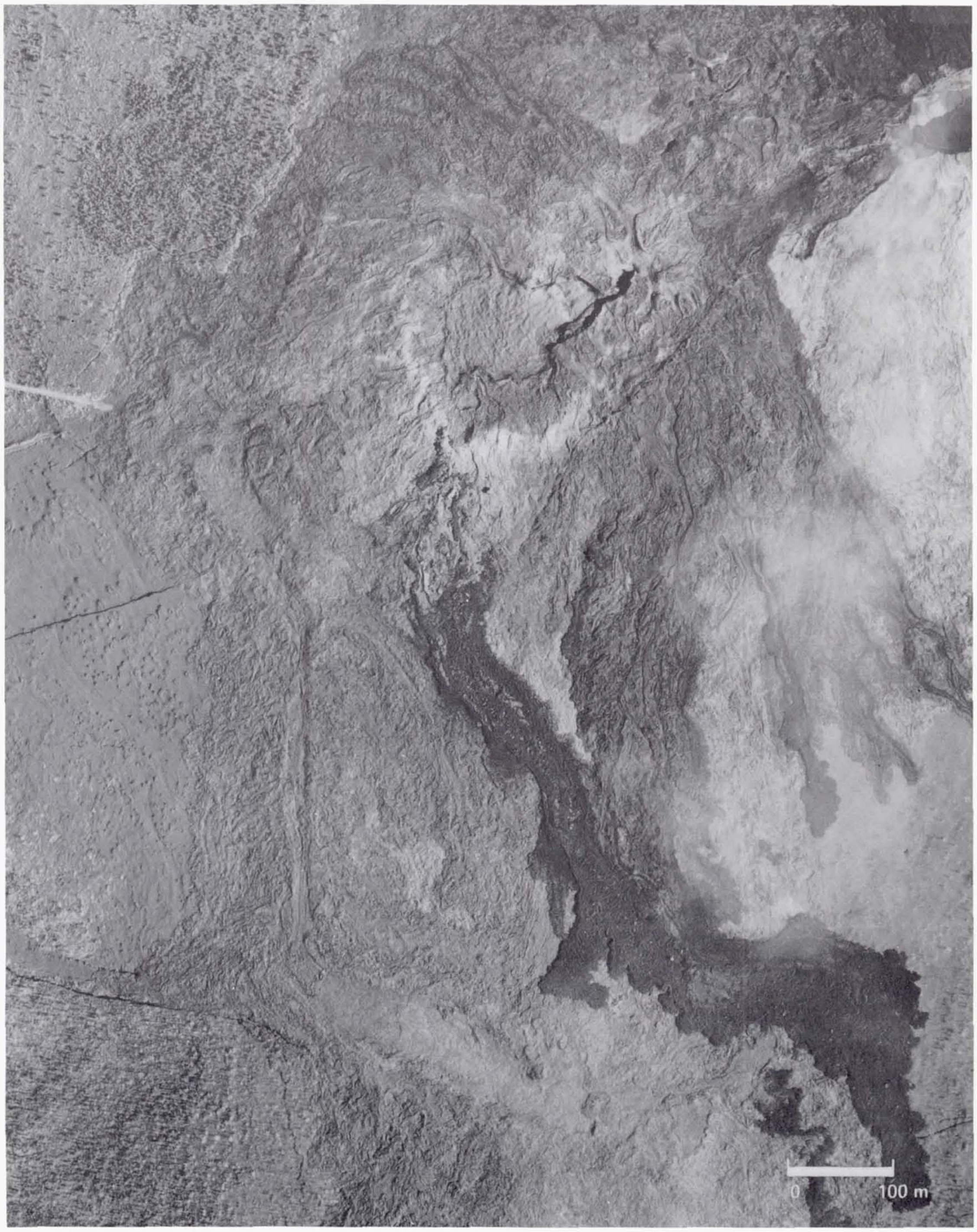

FIGURE 12–9. Irregular depression over the approximate site of the former Aloi Crater. Lava ponded above Aloi in February 1971. The viscous degassed lava overflowed to the south to form the blocky aa flow in the bottom half of the picture. The end of Chain of Craters Road is at the upper left. (Photograph by Towill Corp., Honolulu, frame 5812-10, October 19, 1972.)

FIGURE 12–10. Low-altitude oblique aerial view eastward across the summit of Mauna Ulu, May 1973. While the Alae vents were active, lava completely drained from the trench and stood very low within the summit pit. In the upper part of the picture, dark flows from Mauna Ulu summit, dating from early 1972, are overlain by younger flows from the Alae rootless vent. (Photograph by R. T. Holcomb, May 6, 1973.)

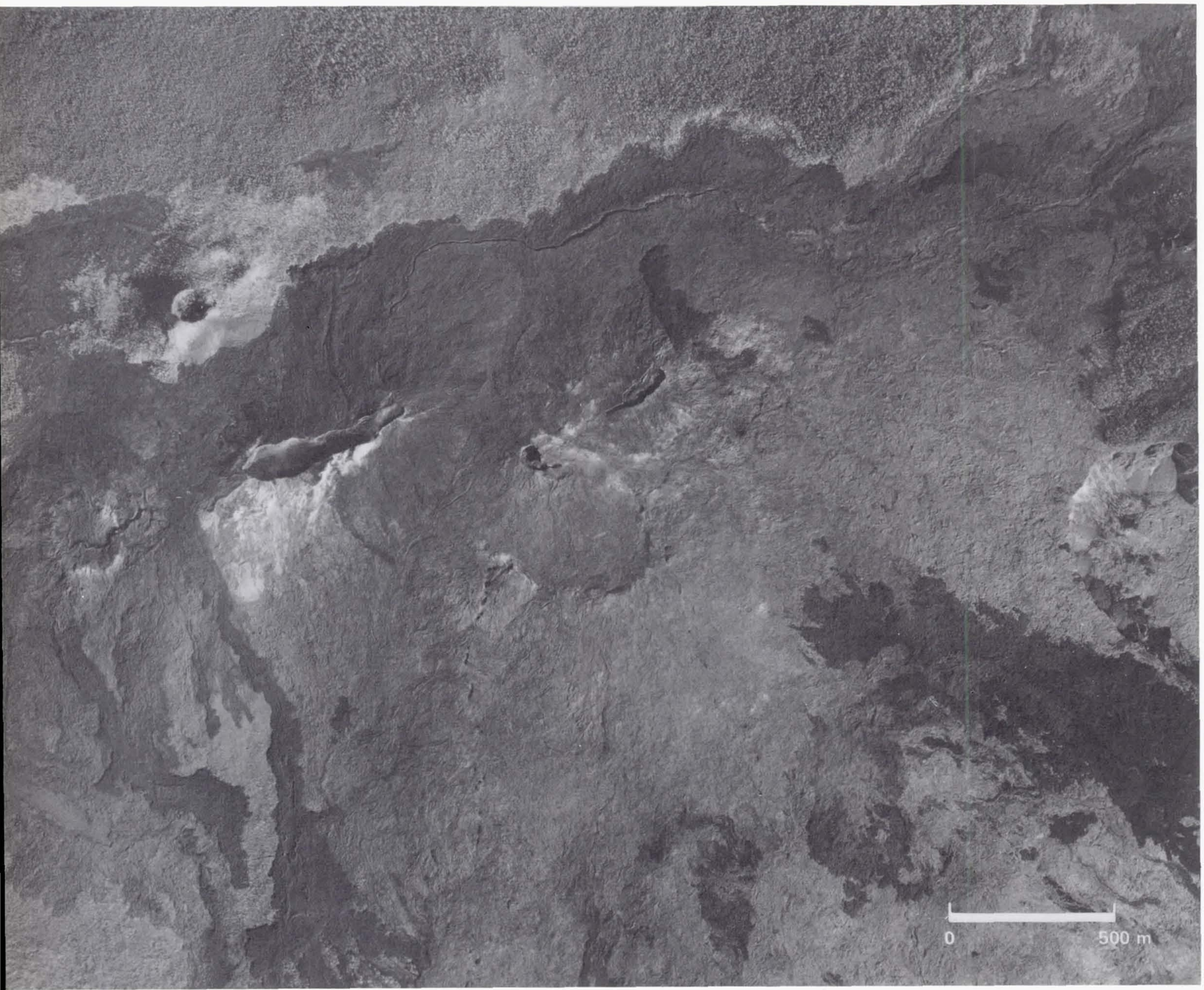

FIGURE 12–11. The Mauna Ulu area in July 1972; compare with Figures 12–1 and 12–7. Collapse has occurred at the site of the former Alae Crater to form a circular depression. A line of pits marks the trace of a large lava tube that distributed lava from the underground reservoir at Alae to flows to the south. The west pit of Makaopuhi Crater at the east edge of the picture has been partly filled by Mauna Ulu lavas. (Photograph by Towill Corp., Honolulu, frame 6111-7, December 13, 1973.)

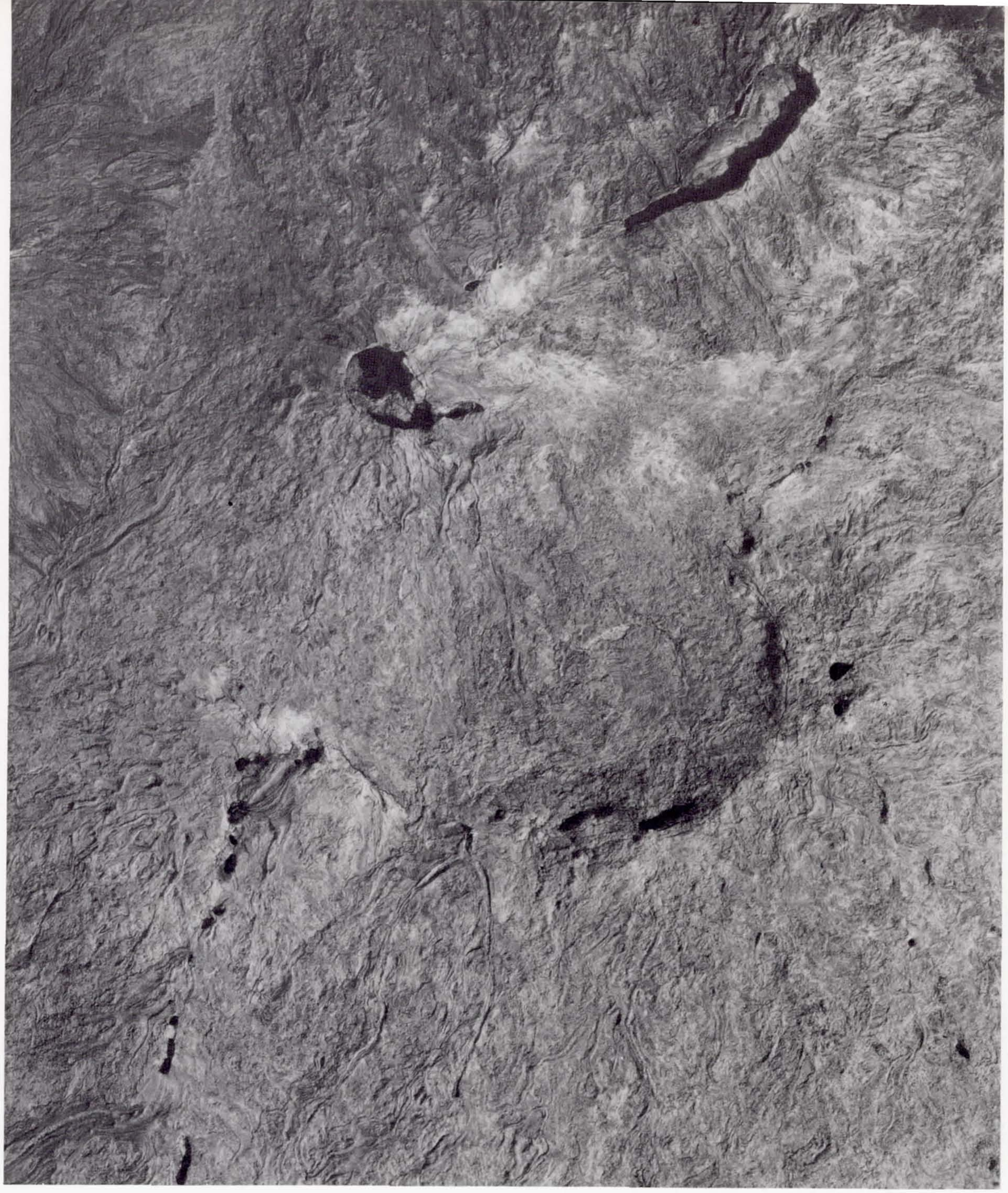

FIGURE 12–12. Detailed view of the 500-m-diameter depression at the site of the former Alae Crater. After eruptive activity ceased at Alae in the Spring of 1973, the summit of the new shield gradually subsided, leaving a shallow circular depression roughly outlining the former pit crater whose rim is buried beneath 60 m of lava. The vent in the upper left was fed by a lava tube from Mauna Ulu, and other vents at the site of Alae are similarly interpreted. Lines of small pits mark the course of lava tubes that distributed lava from the Aloe reservoir to surrounding flows. (Photograph by Towill Corp., Honolulu, frame 6113-5, December 3, 1973.)

FIGURE 12–13. During early 1974, activity at the Mauna Ulu summit was characterized by episodes of fountaining lasting a few hours and separated by quiet periods of several days. Here a flow has breached the levee of a perched lava lake around the Mauna Ulu vent. The lava stream is ponding in the saddle between Mauna Ulu and Puu Huluhulu and forming levees such as that in the foreground. (Photograph by R. T. Holcomb, January 25, 1974.)

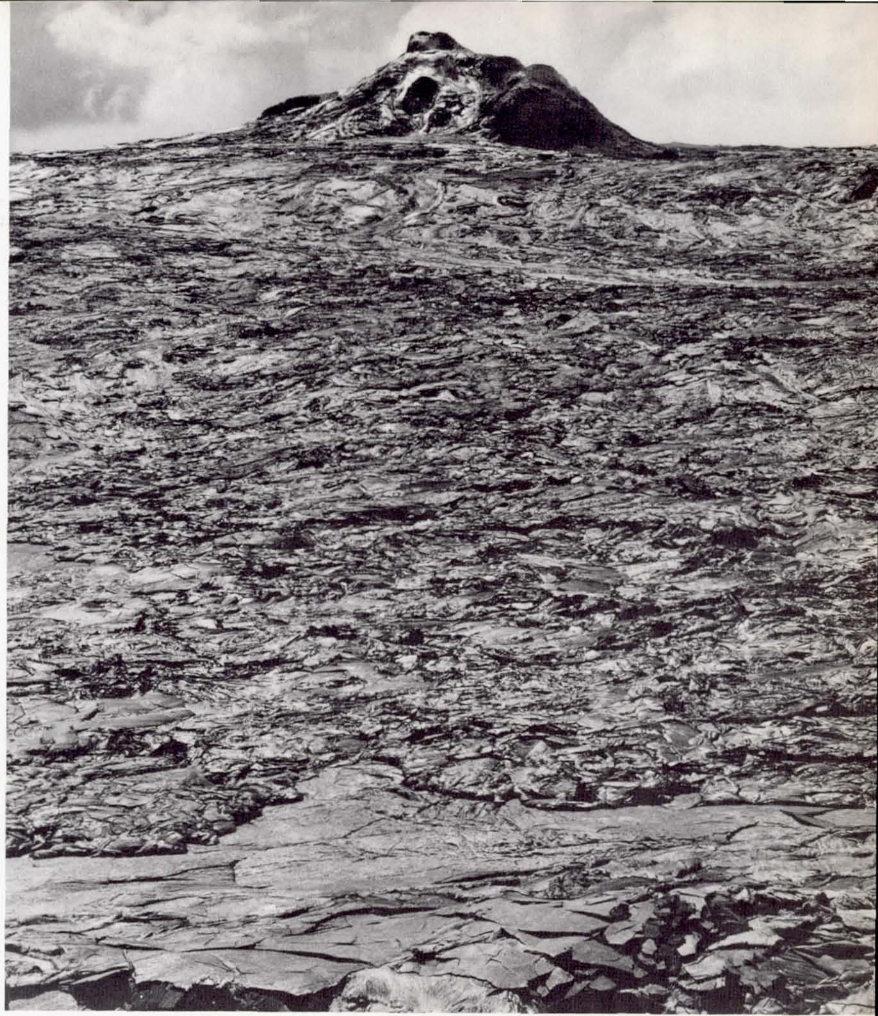

FIGURE 12–14. View of the Mauna Ulu shield in February 1974. A spatter cone has been built around the summit. The surface of the shield is covered with pahoehoe lava. In the foreground, pahoehoe flows cover the surface of the scene in the foreground of Figure 12–13. (Photograph by Hawaiian Volcano Observatory, February 1974.

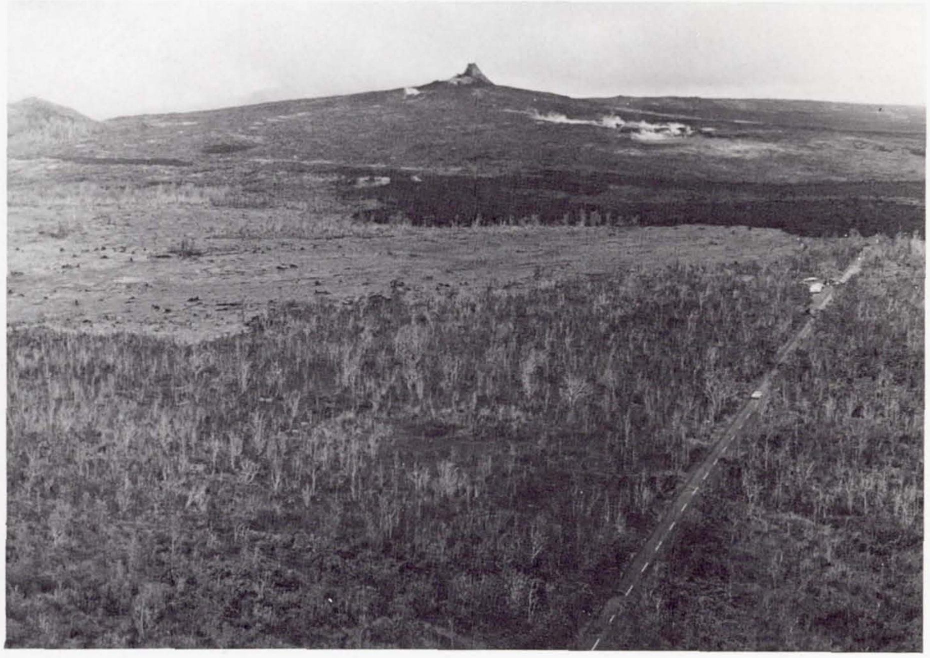

FIGURE 12–15. View of the Mauna Ulu shield from the west in March 1974. The steep-sided spatter cone at the summit grew over a period of a few weeks, then collapsed a short time later. The Alae shield is behind and to the right of Mauna Ulu. (Photograph by R. I. Tilling, March 27, 1974.)

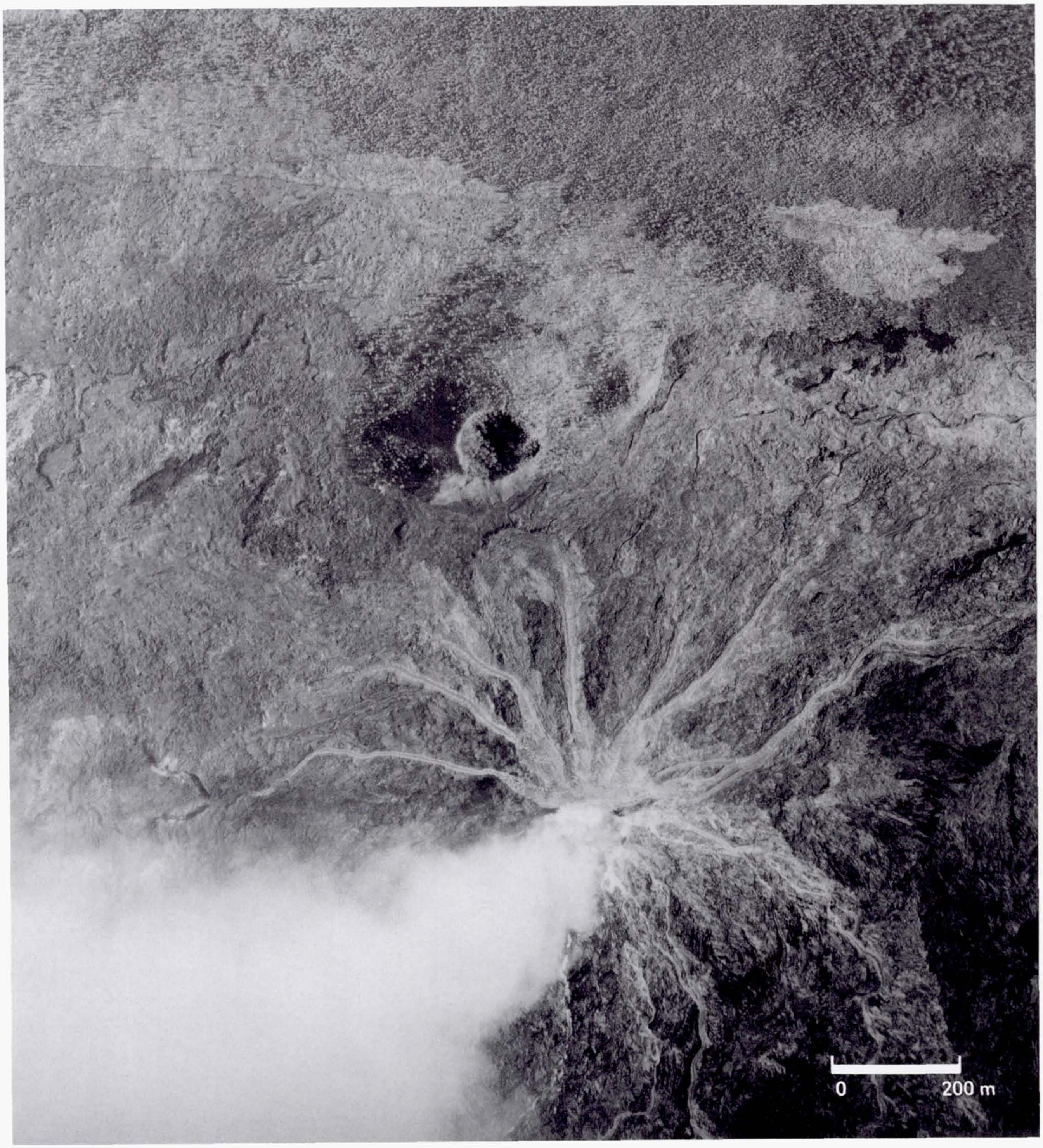

FIGURE 12–16. One of the final eruptive episodes of Mauna Ulu. Streams of flowing lava radiate in all directions from the summit. The lava pond in the saddle between Mauna Ulu and Puu Huluhulu has reformed, building a levee facing Puu Huluhulu. (Photograph by Towill Corp., Honolulu, frame 6246-1, June 1, 1974.)

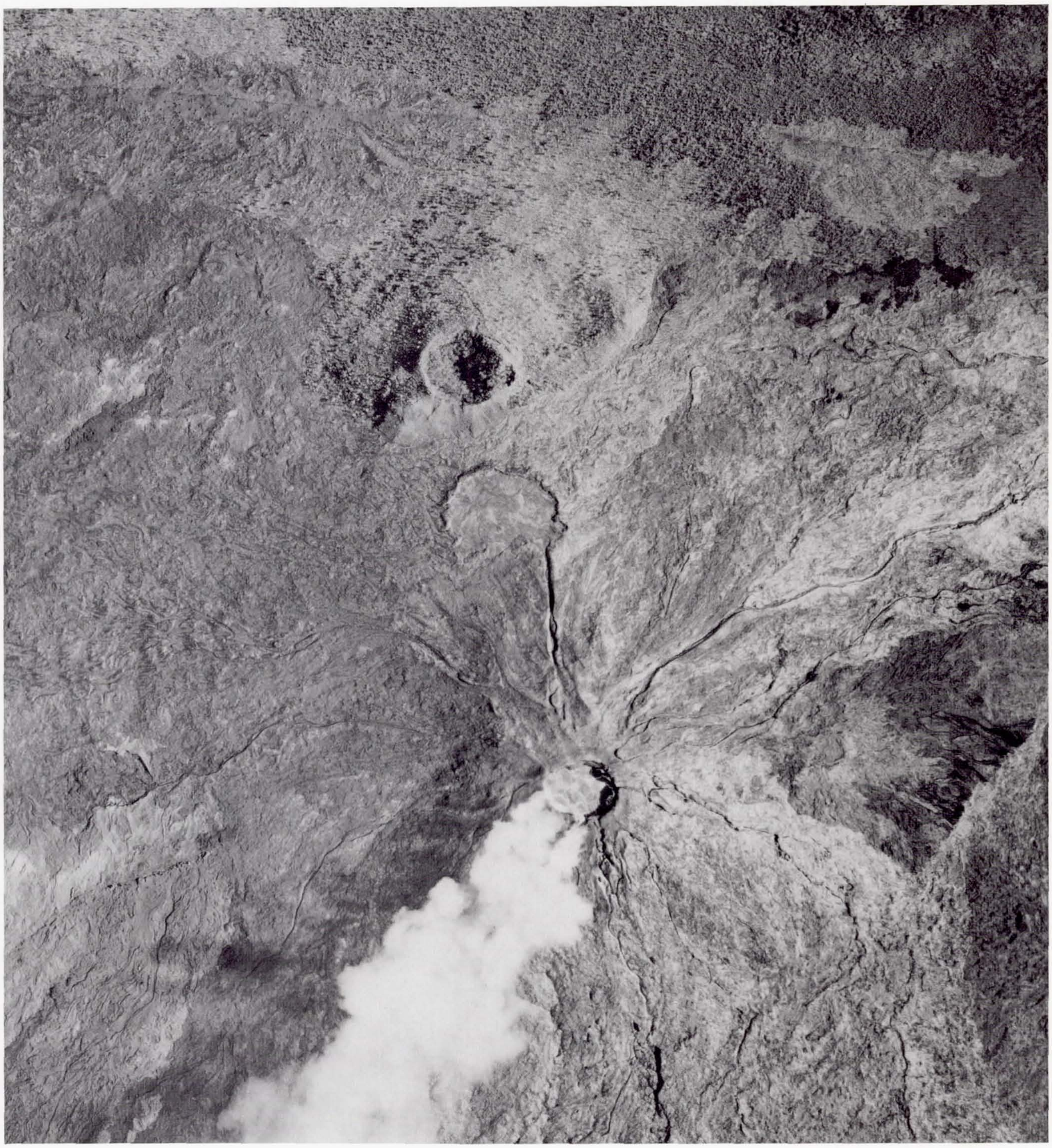

FIGURE 12–17. Mauna Ulu two days after the scene in Figure 12–16. Channels are now left at the positions of the former lava streams and the surface of the pond between Mauna Ulu and Puu Huluhulu has subsided. (Photograph by Towill Corp., Honolulu, frame 6270-5, June 3, 1974.)

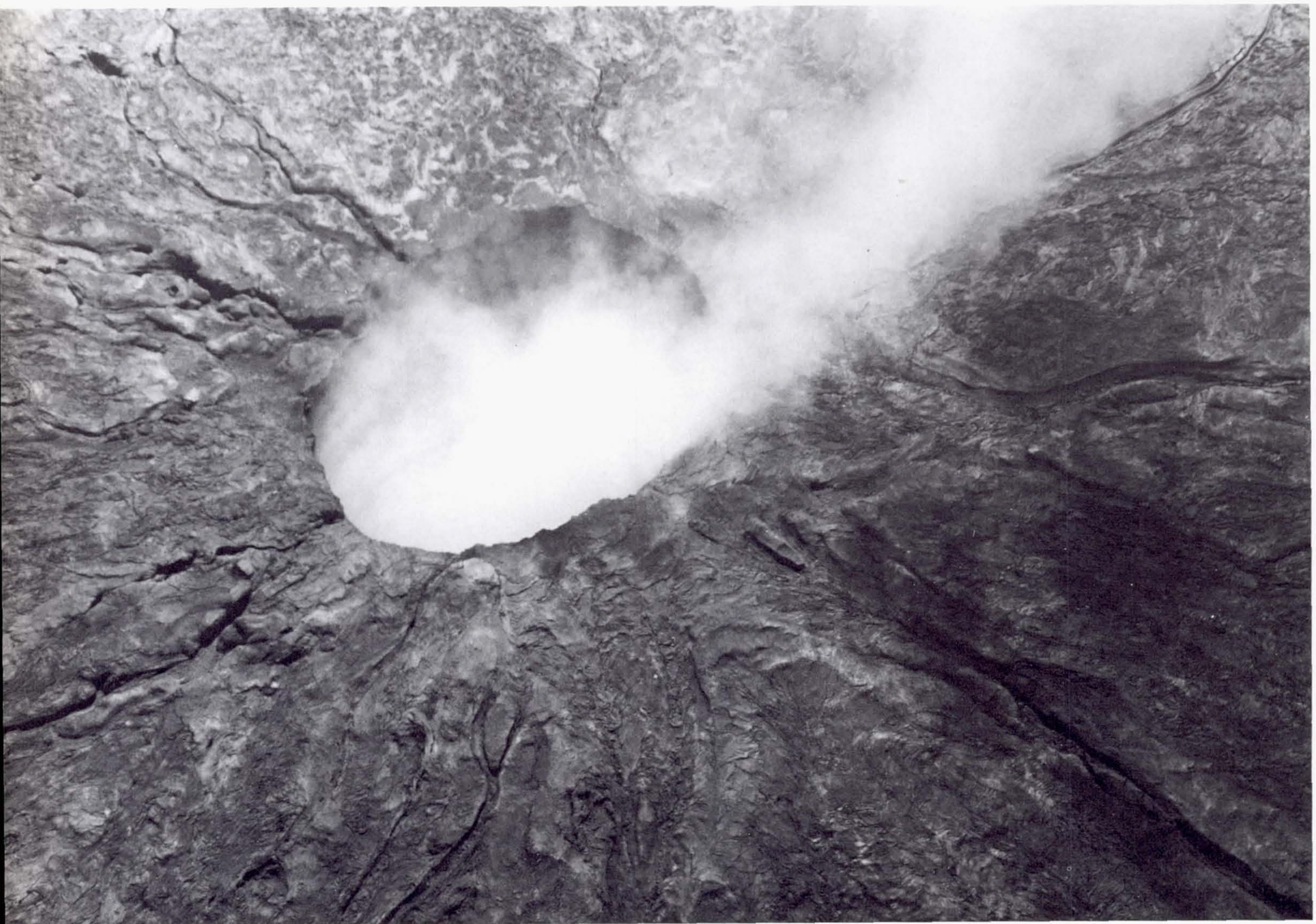

FIGURE 12–18. Summit pit of Mauna Ulu after the last eruption of June 1974. Fumes still emanate from an active lava lake deep within the pit. Lava finally disappeared from within the vent one month after this picture was taken. (Photograph by Hawaiian Volcano Observatory, June 1974.)

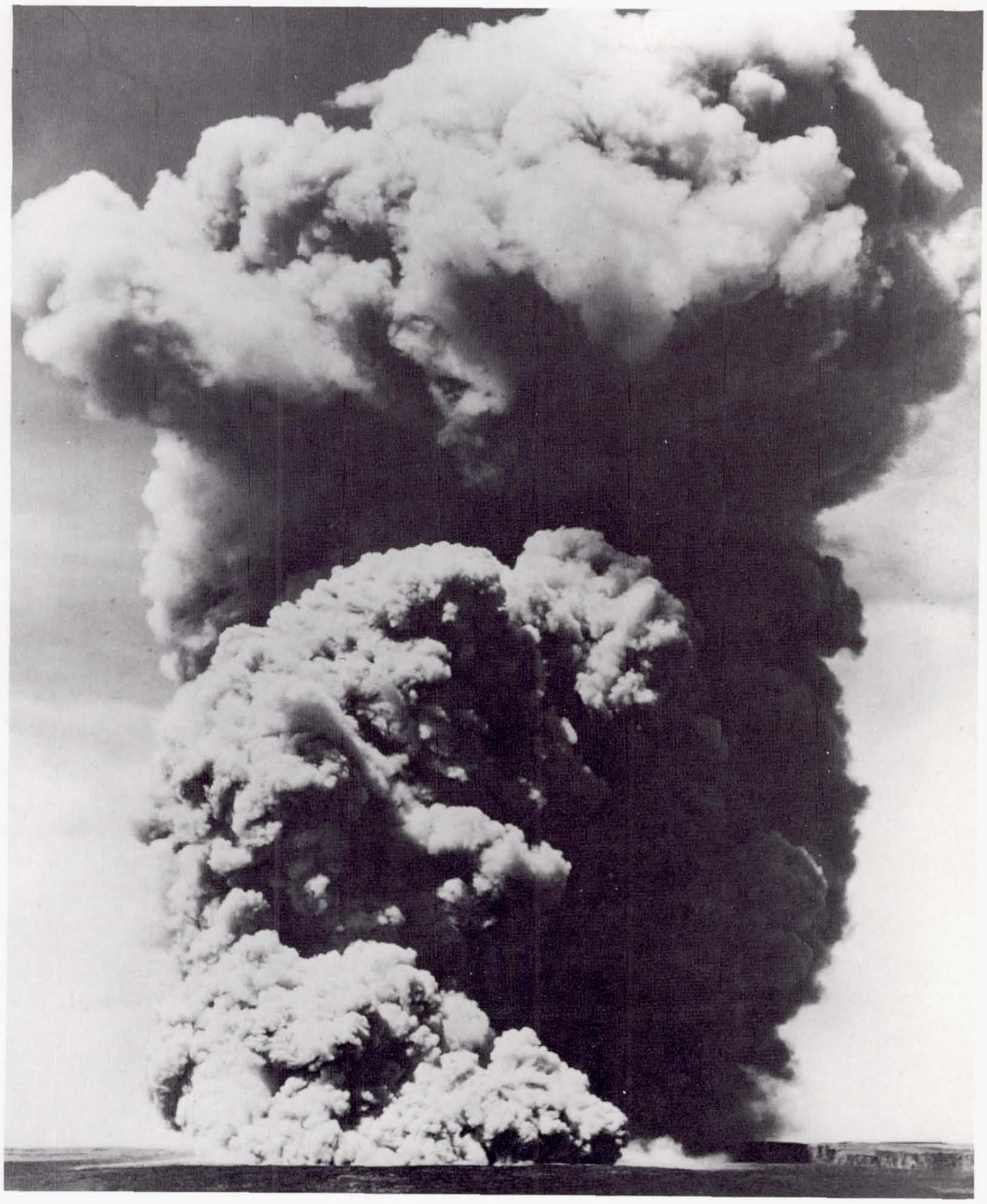

FIGURE 12–19. Phreatomagmatic explosion cloud of dust and steam arising from Halemaumau Crater within the Kilauea caldera during the 1924 eruption. This and the next figure are included to contrast with those of Mauna Ulu. They picture a style of eruption not represented by the Mauna Ulu sequence. Following withdrawal of lava from Halemaumau in 1924, the walls of the crater collapsed, widening it by 400 to 600 m. Gradually, water entered the vent, causing violent steam explosions and massive ejection of comminuted debris and small amounts of lava which formed dense clouds of dust and steam that towered several kilometers above the volcano. (Photograph by Tai Sing Loo, May 1924.)

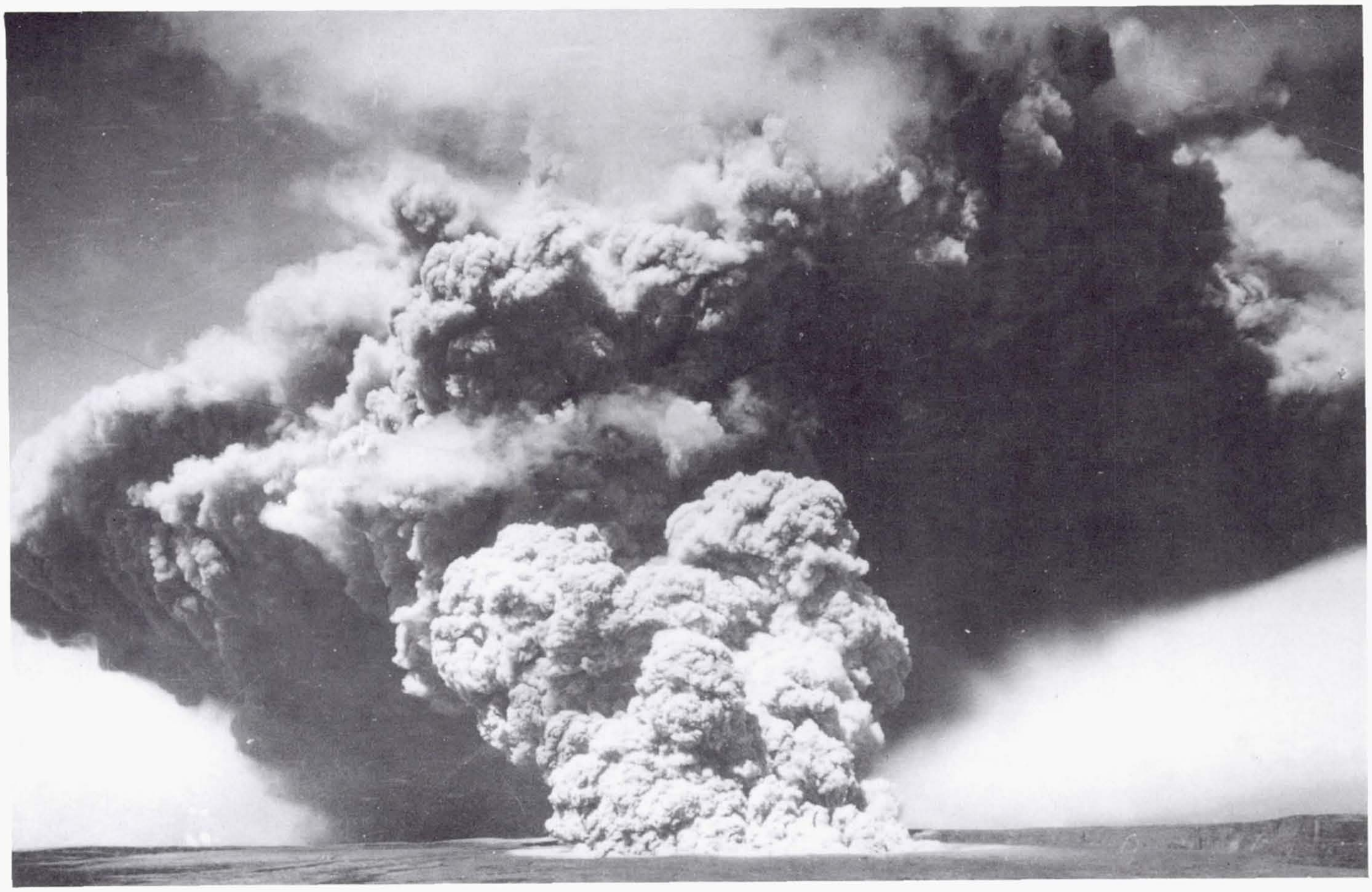

FIGURE 12–20. Another view of the phreatomagmatic eruption of 1924. Most of the material ejected during the eruption was pre-existing country rock, but some new lava was involved. (Photograph by Tai Sing Loo, May 1924.)

XIII. MARTIAN SHIELD VOLCANOES

Since the mid-1960's there has been an explosive growth in our knowledge of the surface of Mars. The planet had been observed through the telescope for decades, during which various surface markings were identified and changes on the surface and in the atmosphere were monitored. It was not, however, until 1964, when *Mariner 4* provided our first close-up look at the planet, that we obtained reliable information on surface topography (Leighton and others, 1965). The Mariner 4 pictures revealed a subdued cratered surface that superficially resembled the lunar highlands. Subsequent fly-bys reinforced this impression, although some distinctively non-lunar terrains were photographed and variously described as *chaotic terrain, etch-pitted terrain* and *featureless terrain* (Leighton and others, 1969). It was not until Mariner 9 started its systematic photographic coverage from orbit in 1971 that the extraordinarily diverse nature of the martian surface was revealed (Masursky, 1973). It was then realized that the planet has a far more complex and varied history than the Moon and that the history had left a distinctive imprint on the surface. Vast canyons cut across the surface close to the equator. Large areas of the surface have subsided to form arrays of jostled blocks termed chaotic terrain. Out of some of the chaotic regions arise large, dry river beds and elsewhere much of the older densely cratered terrain is dissected by numerous gullies and branching channels. Sparsely cratered plains cover more than half the surface and contrast sharply with the heavily cratered surfaces photographed by the early Mariner missions. At the poles a thick sequence of layered deposits overlies both the sparsely cratered plains and the densely cratered terrain.

Perhaps the most spectacular features on Mars are the huge shield volcanoes (Carr, 1973, 1975). The first shield volcanoes to be seen were those of the Tharsis region which appeared as dark spots on the early Mariner 9 pictures. When the Mariner 9 spacecraft arrived at Mars in November 1971, the entire planet was engulfed in a gigantic dust storm. Such dust storms had been observed at the telescope and one was predicted for the arrival time of Mariner 9. The spots were caused by the contrast between the dust-laden atmosphere and the dark summits of the volcanoes which stand above most of the atmosphere. It was not until the dust cleared that the enormous dimensions of these volcanoes were realized. The tallest volcano, *Olympus Mons*, towers 24 km (79,000 ft) above the surrounding plains and is more than 700 km across. *Alba Patera*, although lacking the vertical relief of Olympus Mons, is considerably larger in area extent, being at least 1500 km across. Before discussing the shield volcanoes further, it is appropriate to briefly review the photographic coverage available of Mars and also the general geology of the planet so that the limitations of the data are understood and the general geologic context of the volcanic features is appreciated.

Our present knowledge of the martian surface stems largely from photographs taken during the Mariner 9 and Viking missions. In 1971 and 1972 almost the entire surface of the planet was photographed by the Mariner 9 spacecraft at resolutions in the range of 1 to 3 km; about one percent of the planet was also imaged at resolutions of 100 to 300 m. In practice these nominal resolutions were rarely achieved, mostly because of variations in the clarity of the atmosphere which changes greatly according to time of day, season and location. The main difficulty was caused by the planet-wide dust storm of late 1971. Systematic mapping was started in January of 1972, but much dust still remained in the atmosphere. Local water and carbon dioxide clouds also hindered acquisition of good surface photography. In contrast, when the Viking spacecraft arrived at Mars in the Summer of 1976, the atmosphere was very clear. Early in the Viking missions, much of the orbiter photography was taken at ranges of 1500 to 3000 km which gave resolutions of 80 to 160 meters. In addition some lower resolution, regional coverage was acquired, mainly in the southern hemisphere (Carr and others, 1976). In the Spring of 1977, the planet was again engulfed in a vast dust storm and it was not until the Fall of 1977 that systematic photography of the surface could again be resumed. Since that time the entire planet has been photographed at resolutions of 300 to 500 meters and smaller fractions have been covered at a variety of resolutions ranging down to 10 meters. The resolution of the available photography is still coarse, compared with that available for the Earth, and this may be significantly biassing our impression of the surface; the characteristics of large features such as shield volcanoes are relatively well documented but the smaller features are relatively poorly understood. Resolution effects also interfere with comparison of the Hawaiian and martian shields in that small features such as spatter cones, cinder cones, and tumuli are close to or below the resolution of much of the available Mars photography, so are not readily identifiable on most photographs.

Comparison between the martian and Hawaiian shield volcanoes should also take into account the contrasting environmental conditions on the two planets. Mars has a very tenuous atmosphere compared to the Earth. The average atmospheric pressure on the surface ranges from 6 to 11 mb according to the season; winds mostly range from 8 to 40 km/h with gusts up to 100 km/h. Surface temperatures range from 150 K to 300 K (–190°F to 60°F), according to season, time of day, and location; the global mean is approximately 210 K (–81°F). Only small amounts of water are present in the atmosphere. There is, however, considerable circumstantial evidence of ground ice. A residual cap of water ice remains at the north pole in midsummer and it has been suggested that water ice may have been more extensive in the past.

General geology of Mars

Mars is extremely asymmetric in terms of both its geology and its topography (Mutch and others, 1976; Scott and Carr, 1978). The planet can be divided into two strikingly different hemispheres by a plane inclined about 40° to the equator. The more southerly hemisphere includes most of the ancient heavily cratered terrains while the more northerly hemisphere includes most of the sparsely cratered plains and young volcanic features. The figure of the planet is also markedly asymmetric. Much of the densely cratered terrain in the south stands 2–3 km higher than the northern plains. In addition there is a marked bulge in the planet's crust centered on the *Tharsis* region, the planet's most prominent volcanic area. The bulge is 7 to 10 km high and 7000 to 9000 km across, depending on how its boundaries are defined.

The southern hemisphere resembles somewhat the lunar highlands in that the surface is densely cratered with impact craters larger than 20 km in diameter. Several large impact basins such as Hellas, Argyre, and Isidis are also present, as in the case of the Moon. The number of large craters suggests that they date from very early in the planet's history, perhaps from over four billion years ago. However, the density of craters less than 20 km in diameter is considerably lower than in the lunar highlands, with much of the area between the large craters being only sparsely cratered. Most large craters tend to be shallower, have flatter floors, and more limited rim deposits than comparably sized lunar craters. The general impression is of an ancient surface much like the lunar highlands but partially buried by younger deposits. Many of the old crater rims and other remnants of ancient cratered terrain that protrude through the younger deposits are dissected by branching networks of small channels. These are puzzling because, although they resemble terrestrial river valleys, liquid water cannot exist on the martian surface under the present environmental conditions. The channels may indicate that conditions were sufficiently different early in the planet's history to allow liquid water to flow over the surface.

The northern plains are rather poorly understood, partly because of the poor quality of the available photography. The plains are generally thought to be volcanic with variable amounts of surficial aeolian debris. Only in Tharsis and Elysium, and some intercrater plains areas, however, can lava flows be unambiguously identified. Elsewhere the evidence for a volcanic origin is tenuous and based largely on the presence of ridges that resemble those on the lunar maria. The density of impact craters on the plains – a measure of the age of the units – range widely with the lowest being in the Tharsis region. The wide range in crater density suggests that the plains have accumulated over a very long period of time, perhaps over most of the history of the planet.

Most fresh martian impact craters are surrounded by layers of ejecta that appear to have been emplaced as debris flows, not ballistically as in the cases of the Moon and Mercury. This has been tentatively attributed to the presence of significant amounts of ground ice. The style of impact cratering appears to differ according to location. North of approximately 60°N, the so-called *pedestal craters* are more common than elsewhere. These are craters that occur within a low platform or pedestal with an irregular outline. It has been proposed that the platforms result from repeated deposition and stripping of aeolian debris and that the debris is preferentially retained around impact craters because of armoring by ejecta.

An extensive radial fracture system is associated with the bulge in the Tharsis region. So pervasive are the Tharsis radials that they are the dominant structural element of an entire hemisphere of the planet, extending as far as 4,000 km from the center of the bulge (Wise and others, 1979). The most intensely fractured regions are to the north and northeast of Tharsis where fractures wrap around the large volcano, Alba Patera, and extensive areas have closely spaced fractures that mask the characteristics of the pre-existing terrain. Intensely fractured zones also occur to the southeast and southwest of Tharsis. Even in the intervening sparsely fractured areas, erosion tends to be preferentially enhanced along directions radial to Tharsis.

In the equatorial region between longitudes 40° and 100° W is a vast system of interconnecting canyons (Blasius and others, 1977). Individual canyons may be up to 5 km deep and 200 km across, and the entire system is 4,000 to 5,000 km long. Most are aligned radial to Tharsis and it appears that their orientation has been controlled by the Tharsis fracture system. Layered rocks are exposed in the upper parts of the canyon walls; talus generally covers the lower parts. In some sections the walls are deeply gullied or dissected by branching valleys; in other places are enormous landslides. The origin of the canyons in unclear, although most workers regard faulting as the dominant relief-generating mechanism, with landsliding and fluvial processes as secondary.

At the eastern end of the canyon, large areas of the surface appear to have been disrupted and broken into numerous blocks that are at a lower elevation than the surrounding terrain. These areas have been termed chaotic terrain because of the seemingly random nature of the fracturing (Sharp, 1973). Large, dry river beds emerge full scale from many of the chaotic regions and can be traced for several hundred kilometers downslope to the north. The river beds contain numerous features such as teardrop-shaped islands, longitudinal grooves, and terraced walls – features that are common in large terrestrial flood features (Baker and Milton, 1974). Most observers consider the river beds evidence that water has periodically flowed across the surface of Mars in vast floods. Additional evidence for water erosion is provided by the previously mentioned small channels that dissect much of the densely cratered terrain. Most, but not all, of the large flood features occur in the Chryse region, east of the canyons. Others occur around the Hellas basin and along the boundary that separates the heavily cratered southern hemisphere from the more sparsely cratered northern hemisphere.

Distribution of shield volcanoes

Most martian shield volcanoes occur in the two provinces – Tharsis, centered at approximately 10° N, 110° W, and Elysium, centered at 25° N, 210° W. The Tharsis province is by far the larger and is generally assumed to include Olympus Mons and Alba Patera which, strictly speaking, lie outside Tharsis. Several large volcanoes occur in areas removed from these two provinces; prominent examples are the *Amphitrites* and *Hadriaca Paterae*, to the south and northeast of Hellas, *Tyrrhenna Patera* at 22° S, 254° W, and *Apollinaris Patera* at 8° S and 187° W. The freshest appearing volcanoes are those in the Tharsis region; consequently, most examples in the book are taken from this area.

In the center of Tharsis, three prominent shield volcanoes occur along a southwest-northeast trending line. They appear to be on a major fracture system that continues to the northeast as the *Tempe Fossae* and to the southwest as the *Memnonia Fossae*. The three shields are enormous by terrestrial standards, each being approximately 400 km across and standing 17 km above the surrounding plains. Olympus Mons, the tallest volcano on the planet, is situated 1,600 km northwest of the three Tharsis volcanoes. Its main shield is approximately 700 km across and its summit stands 25 km above the surrounding plains. It is also surrounded by an annulus of highly fractured terrain of obscure origin that extends as far as 1,200 km from the center of the volcano. Directly north of the most northerly of the three large Tharsis shields is another large volcano, Alba Patera. Although it has little vertical relief, probably less than 5 km, Alba Patera is by far the largest martian volcano in lateral extent, being at least 1,500 km across. Much of the volcano is intensely broken by Tharsis radial fractures which splay around the summit region to form an incomplete fracture ring. Elsewhere in Tharsis, particularly on the northeast extension of the volcano line, are numerous other smaller volcanoes which characteristically have a large central caldera.

The Elysium province is much smaller than the Tharsis province, including only three volcanoes – *Elysium Mons*, 170 km in diameter and approximately 14 km high, *Hecates Tholus*, 180 km in diameter and approximately 6 km high, and *Albor Tholus*, 130 km across and 3 km high. The Elysium volcanoes, like those of Tharsis, are situated on a broad dome which is approximately 2,000 km across and 5 km high. Although there are numerous northwest-southeast trending fractures to the west and southeast of Elysium, a well developed set of radial fractures is lacking.

General description of martian shield volcanoes

The term shield volcano is used here in a very general sense, referring to roughly circular mountains with central calderas and gently sloping ($<6^{o}$) flanks, built largely of fluid flows. In the martian case, evidence for the fluidity of the lavas is indirect but many features characteristic of Hawaiian flows, such as central channels, levees, collapse pits over lava tubes, and lobate flow margins, are also visible on martian flows, suggesting similar flow properties. Olympus Mons, the largest of the martian shields, has gently sloping flanks that are somewhat shallower at the summit and around the edge to give the volcano a sinusoidal profile. The summit caldera consists of several intersecting depressions, suggesting a complex history of subsidence around different centers. The upper flanks of the volcano are terraced with a roughly concentric pattern. The terraces are typically 15-50 km across, have a slightly convex surface, and are separated from one another by a sharp break in slope. The flanks everywhere have a radial texture caused by numerous narrow flows. A discontinuous, roughly circular, outward facing escarpment 550 km in diameter surrounds the main part of the shield. In many places flows are draped over the escarpment and extend several tens of kilometers beyond (Carr and others, 1977). Numerous landslides occur along the basal scarp where it is not covered by flows. Most of the features of the main edifice are similar to terrestrial shields and are consistent with the slow accumulation of fluid lava. One feature of Olympus Mons that has no terrestrial counterpart is the so-called *aureole*. This consists of numerous blocks of distinctively textured terrain that completely surrounds the main edifice and extends up to 1000 km from its center. The general impression is of blocks of intensively fractured terrain tilted slightly inward toward Olympus Mons and embayed by younger deposits. Its origin is unclear but suggestions include eroded ash flow tuffs, vast thrust sheets, subglacial eruptions and gigantic landslides.

The Tharsis shields resemble Olympus Mons in many respects but each has its distinctive characteristics. The southernmost Tharsis shield, Arsia Mons, has a simple 110-km-diameter summit depression surrounded by concentric grabens. There are also numerous graben on the flanks, some of which grade into simple breaks in slopes or strings of rimless depressions. A line of low mounds extends northeast-southwest across the floor of the central caldera which is otherwise featureless except for occasional impact craters and some small ($<$ 100 m across) elongate depressions. Several flows in the caldera originated at the walls. On the northeast and southwest flanks of the main shield are many rimless depressions, some of which coalesce to form large embayments in the edifice. These embayments are the source of numerous flows which fan out over the adjacent lava plains to the northeast and southwest and extend as far as several hundred kilometers from their sources. Those adjacent to the main shield cut across its radial and concentric fabric. It thus appears that after the main Arsia Mons edifice was built, subsidiary vents developed on the northeast and southwest flanks and these were the sources of large volumes of lava which extended far across the adjacent plains and buried part of the pre-existing shield (Crumpler and Aubele, 1978).

Pavonis Mons and Ascreus Mons have similar general characteristics to Arsia Mons. Each is topped by a caldera. Lines of pits, rilles or graben, concentric about the summit, occur on the terraced flanks and transect the radial fabric that is caused mostly by flow features. The main edifices are extensively modified and are embayed to the northeast and southwest by intersecting rilles, fractures, pits and spatulate depressions. The embayments have been the sources of flows that form the adjacent plains and cover the lower parts of the shields.

Each of the three Tharsis shields appears to have followed a similar evolutionary trend. The first recognizable event is the building of the main shield which was probably accompanied by repeated subsidence at the summit to form the central caldera. In the late stages of shield building, eruption was confined mainly to the northeast and southwest flanks where the shields became considerably modified as parasitic vents developed and merged together. These peripheral vents supplied vast quantities of lava that flowed over the surrounding plains and buried the lower flanks of the shields. The main part of the shield was also modified either by concentric fractures or by formation of numerous pit craters. A northeast-southwest asymmetry did not develop on Olympus Mons. The volcano retains a roughly radial symmetry with no prominent peripheral vents. The radial escarpment and surrounding aureole are unique to Olympus Mons and appear to have both formed relatively late in its history by processes as yet unknown.

Elysium Mons is the most prominent shield volcano of Elysium. The edifice is somewhat asymmetric, having two distinct ridges which extend to the west and southeast of the central caldera. The flanks have a vague, hummocky texture on a scale of about 10 km and a faint pattern caused partly by lines of craters and partly by very thin flows, just at the resolution limit of the available photographs. The flank slopes (10 to 12°) are significantly steeper than those of Olympus Mons and the Tharsis shields. The outer boundary of the volcano is indistinct and merges with the surrounding plains.

Although of broad areal extent – approximately 1,500 km across – Alba Patera is less than 5 km high at its summit, so that the edifice has an extremely low profile, with flanks sloping at only fractions of a degree. At the center is a caldera complex about 140 km in diameter. Numerous north-south graben cut across the edifice and wrap around the summit of the volcano to form a fracture ring approximately 500 km in diameter. On the flanks are numerous flows, the most conspicuous of which are referred to as *sheet flows*. These have well-developed lobate flow fronts and fairly level surfaces with a general lack of gross flow features such as channels or unroofed lava tubes. They are large, usually having lengths of several hundred kilometers and widths of tens of kilometers. Also present are tube and channel fed flows which commonly form radial ridges 5 to 10 km across with an axial channel or line of depressions indicating the presence of a lava tube. Alba Patera has no obvious terrestrial counterpart and is included here under shield volcanoes because it does have some of the characteristics of shield volcanoes, a central caldera, and numerous flow features on the flanks. The main differences from the other shields are an extremely low profile, a very large diameter, and the large-scale flow features on the flanks.

Numerous other smaller volcanoes are present on Mars, particularly in the Tharsis region. These generally have a summit caldera that is relatively large compared with the overall diameter of the edifice and a radial texture formed of long narrow flows, channels and lines of craters.

Origin of martian shield volcanoes

One of the main differences between the martian and Hawaiian shield volcanoes is scale. Not only are the martian shields both higher and wider than their Hawaiian counterparts but the individual components of the martian volcanoes are larger. The central calderas, individual flows, channels, levees, and so forth are all larger than for the Hawaiian shields, which are the largest volcanoes on Earth. The differences in overall size are partly explicable by the contrasting tectonic framework on each planet. In Chapter 2 the Hawaiian shields were explained as being relatively short lived because the motion of the Pacific plate, on which the volcanoes are built, carries the volcanoes northwestward from the deep magma source below the moving plate. As the volcanoes are carried away from the magma source, or 'hot spot,' old volcanoes become extinct and new volcanoes develop directly above the source. The magma source presently below Kilauea has provided magma not only for Kilauea but apparently for the entire Hawaiian Emperor chain during the last 70 million years. Mars, in contrast, appears to lack any significant plate tectonics, as there appears to be little, if any, motion of the martian crust with respect to the interior. Magma from a deep source within the planet will, therefore, likely accumulate in one large volcanic edifice rather than form a string of volcanoes as is the Hawaiian case.

This, however, is only a partial explanation of the large size. The height of a shield volcano is controlled by the pressure required to pump magma to the summit. During an eruption, the weight of a column of magma between its source and the vent must be balanced against the lithostatic pressure at the source caused by the overlying rocks. Magma is able to reach the volcano summit because of the contrast in densities between magma and the surrounding rocks. Accordant summits suggest that Mauna Loa and Mauna Kea in Hawaii are at their elevation limits. Plausible values for the density of tholeiitic magma and the crust and mantle rocks through which the magma must pass indicate that the magma source is at a depth of 50 to 60 km below Hawaii. The martian volcanoes achieve much higher elevations than the Hawaiian ones, at least in the Tharsis and Elysium regions. This implies either a larger density contrast between magma and lithospheric rocks on Mars, or a greater depth to the magma source. If terrestrial values are taken for the densities, then sources at depths of 100 to 200 km are implied, depending on how the lithosphere is layered. Another alternative is that martian magmas are more volatile-rich and start to vesiculate (outgas) at greater depths. The high gas pressure then forces the magma to higher elevations than in Hawaii. Crustal stability, the origin of magma at considerable depths, and high volatile content may then all contribute to the great size of the martian volcanoes.

Another point of contrast between the Hawaiian and martian volcanoes is the size of the flows visible on the volcano flanks. In the martian case, individual flows commonly can be traced for distances in excess of 200 km. Flows of this length are extremely uncommon anywhere on Earth, although they may occur during deposition of flood basalts, as in the case of the basalts of the Columbia Plateau in the Pacific northwest. A correlation exists between flow length and the volume and rate of eruption in the case of terrestrial flows. Presumably, the same relation holds on Mars. It appears likely, therefore, that eruptions on the martian shields generally involved large volumes of magma and higher eruption rates than is usual in the Hawaiian shields. This would also explain the anomalously long dimensions (by Earth standards) of lava channels.

Although each eruptive event involved very large volumes of magma, the edifices appear not to have been built rapidly. An estimate can be made of the age of features on a remote planet from the number of supposed impact craters. The method is very imprecise and not well calibrated. Nevertheless, wide differences in age can be detected. Numerous crater counts have been made of the martian shield volcanoes and of the flows on the surrounding lava plains that appear to originate at the shield. Counts on Arsia Mons and the surrounding flows, for example, range over an order of magnitude. By almost any calibration scheme, the counts imply that eruption from Arsia Mons has extended over a period of at least several hundred million years. This conclusion, combined with the large volumes of lava erupted during each volcanic event, suggests that the martian shield volcanoes have been built very slowly over a long period of time by extremely intermittent eruptions of large volume. They contrast, therefore, with the nearly continuous activity of the Hawaiian shields in their early shield building phase.

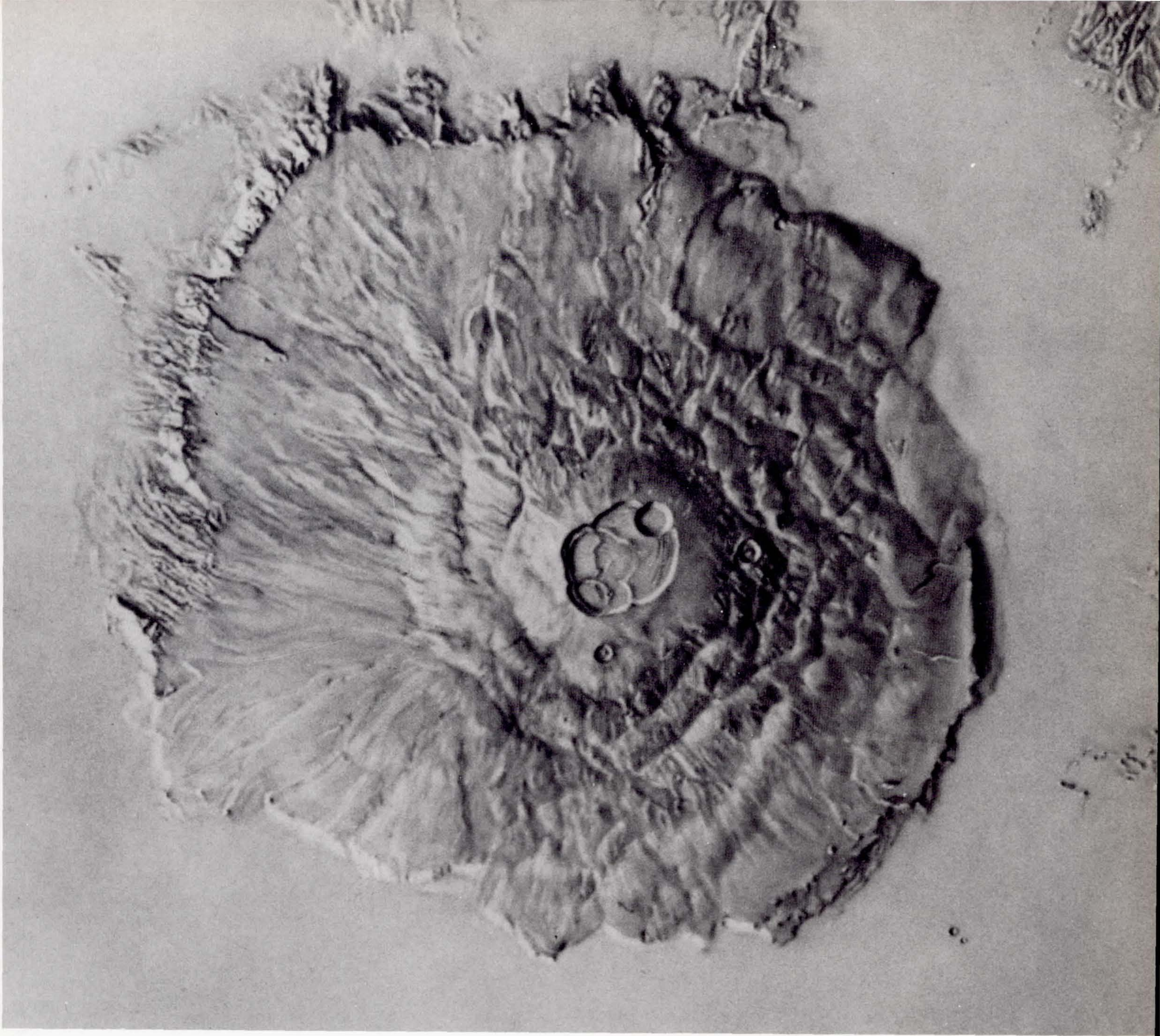

FIGURE 13–1. Shaded airbrush relief map of Olympus Mons prepared from Mariner 9 images by the U. S. Geological Survey. The volcano is about 600 km across and 27 km high; it is surrounded by a scarp that is up to 4 km high. Viking images show that flows drape across the scarp in many places and extend hundreds of kilometers onto the surrounding plains.

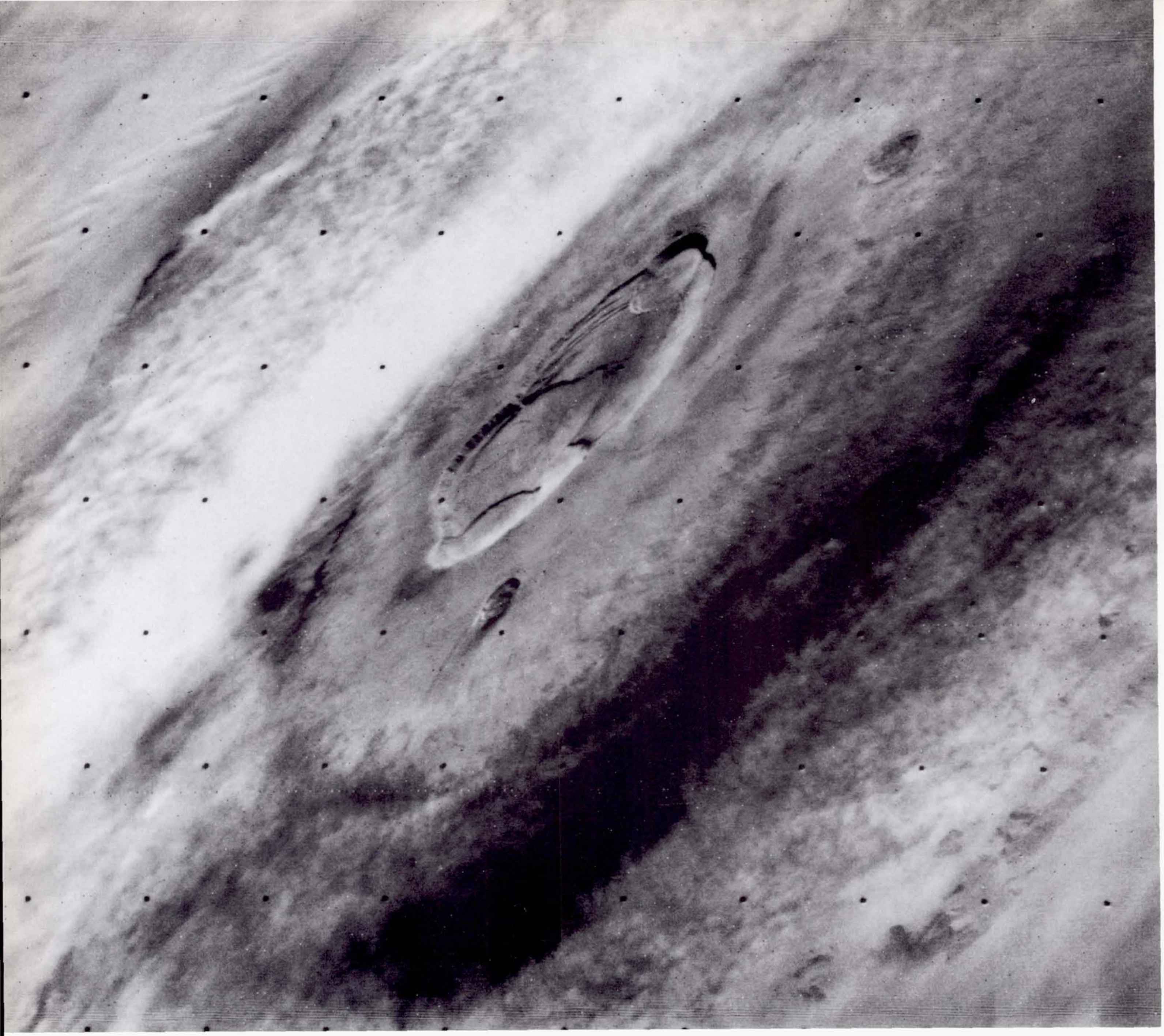

FIGURE 13–2. Oblique view of the summit of Olympus Mons, showing the multiple craters and slump-blocks typical of calderas associated with shield volcanoes; the Olympus Mons caldera is more than 80 km across.

FIGURE 13–3. Mosaic of high-resolution (~36 m) Viking Orbiter images, showing details in the summit caldera of Olympus Mons. The youngest feature seen here is the crater at the top of the picture; a substantial caldera in its own right, it measures more than 25 km across and is nearly 3 km deep. The oldest part of the caldera appears to be the area to the lower left, consisting of foundered segments of the floor; intermediate in age is the part of the caldera floor having numerous "wrinkle" ridges, similar in form to mare ridges found on lunar basalt flows. (Mosaic P-193818.)

FIGURE 13–4. High-resolution frame (~250 m) of part of the basal scarp of Olympus Mons, showing numerous flows that drape across the scarp; partly collapsed lava tubes and leveed channels seen here are indicative of relatively fluid lavas – probably basaltic in composition – erupted perhaps in a style analogous to Hawaiian volcanism as sporadic but prolonged activity. (Viking Orbiter, frame 47B43.)

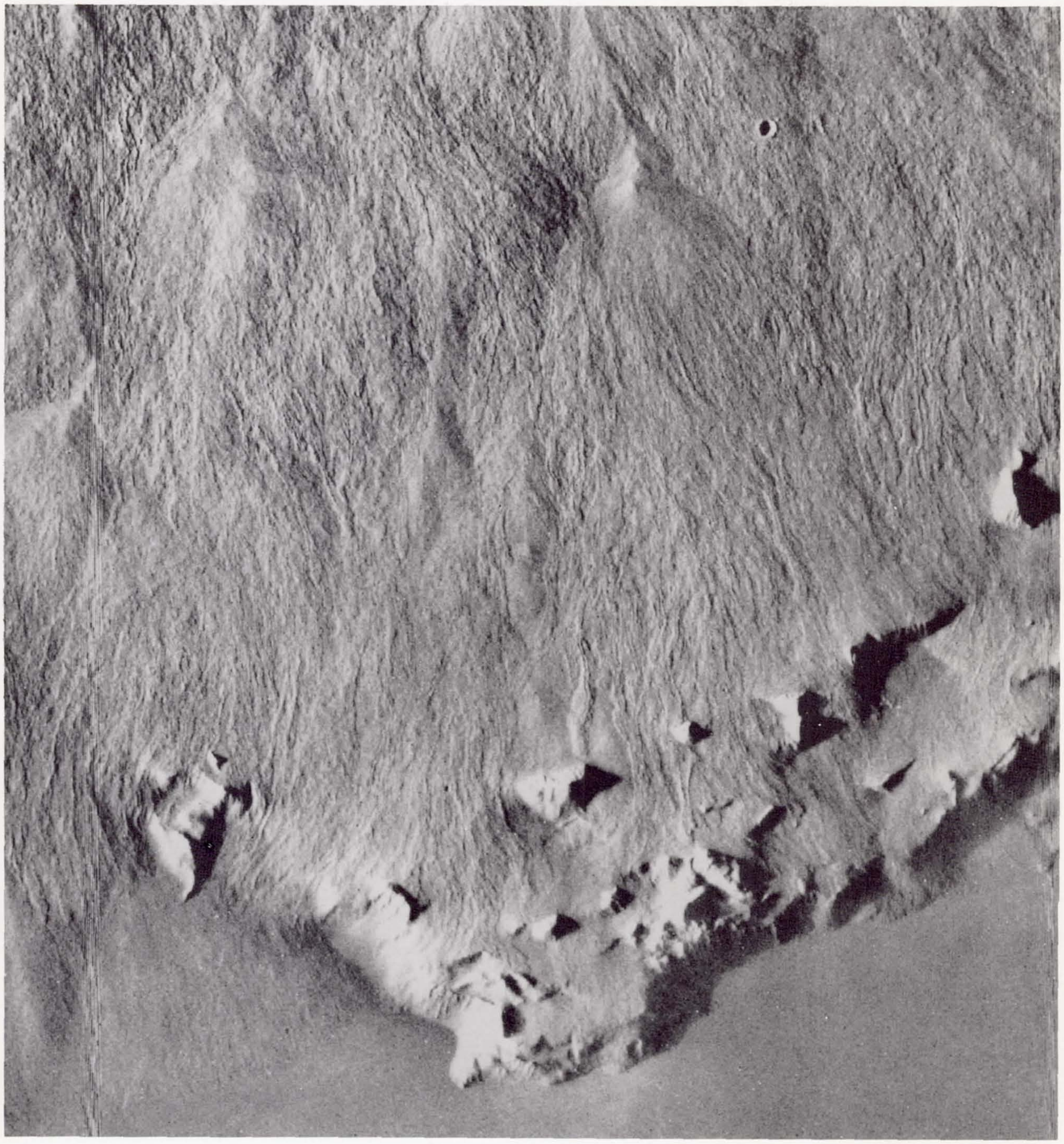

FIGURE 13–5. Another view of part of the Olympus Mons scarp and mantling lava flows; note that some parts of the scarp are not covered with lava. Although the mechansim of scarp formation is not clearly understood, the process appears to involve both faulting and mass wasting. Geometric relations indicate that scarp formation and lava flow emplacement were concurrent. Image area is about 80 km by 80 km. (Viking Orbiter frame 222A64.)

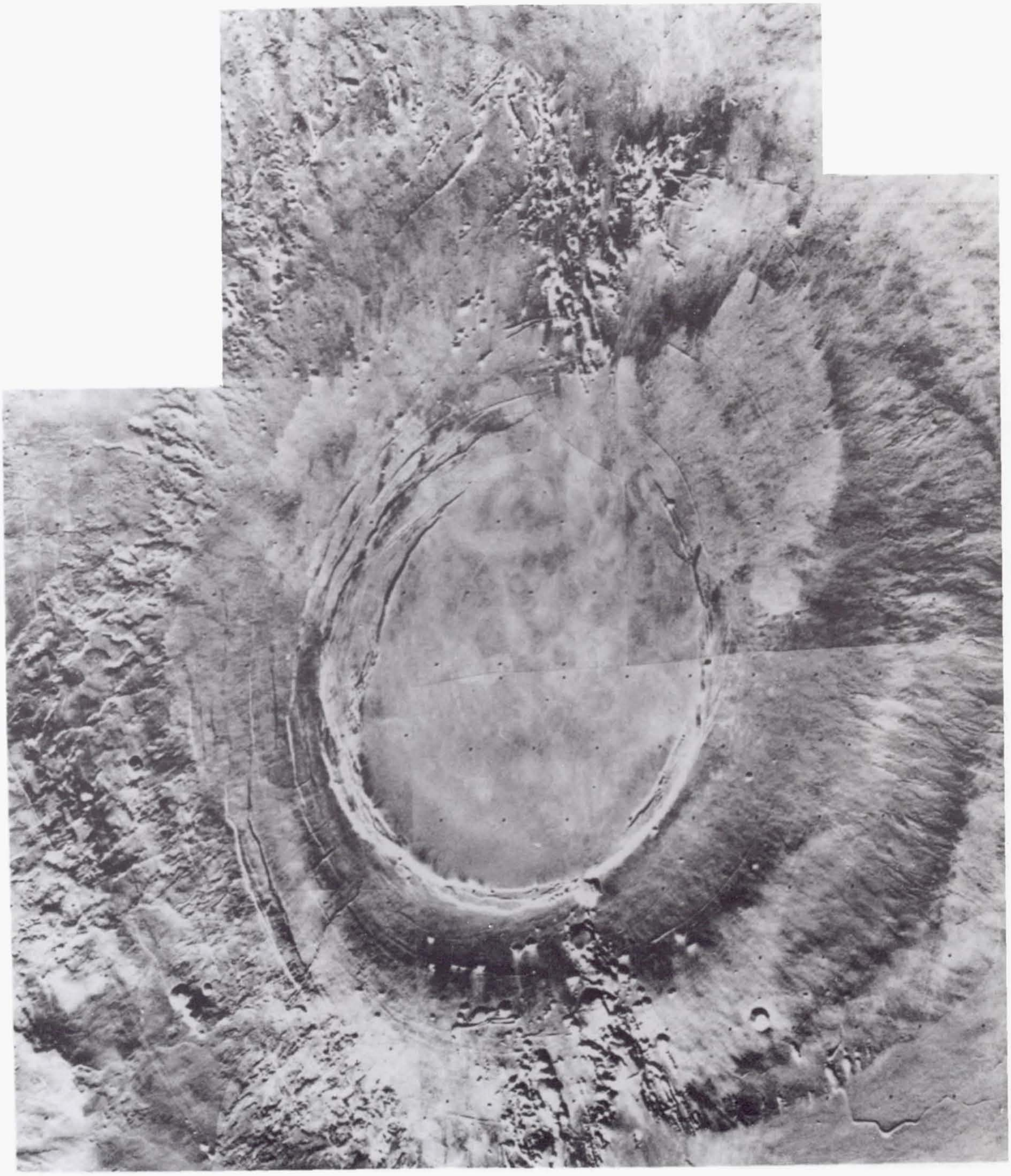

FIGURE 13–6. Mosaic showing summit region of Arsia Mons, southernmost of the giant shield volcanoes of Tharsis. This volcano stands about 19 km above the surrounding plains; its 120-km-diameter caldera is the largest of the Tharsis volcanoes. Numerous lava flows are visible as fine striations that radiate from the caldera. The irregular reentrants at the north and south ends of the caldera appear to be the source for vast lava flows that spread out from the main edifice. (Mosaic P-17863.)

FIGURE 13–7. High-resolution image of the northwestern part of the Arsia Mons caldera, showing extensive fault blocks and graben along the rim, indicating collapse that probably resulted from subsidence of the summit region of the caldera. At the bottom margin, several flows which originate at one of the concentric faults cover other, older faults, downslope. Area shown is about 40 km by 40 km. (Viking Orbiter frame 422A31.)

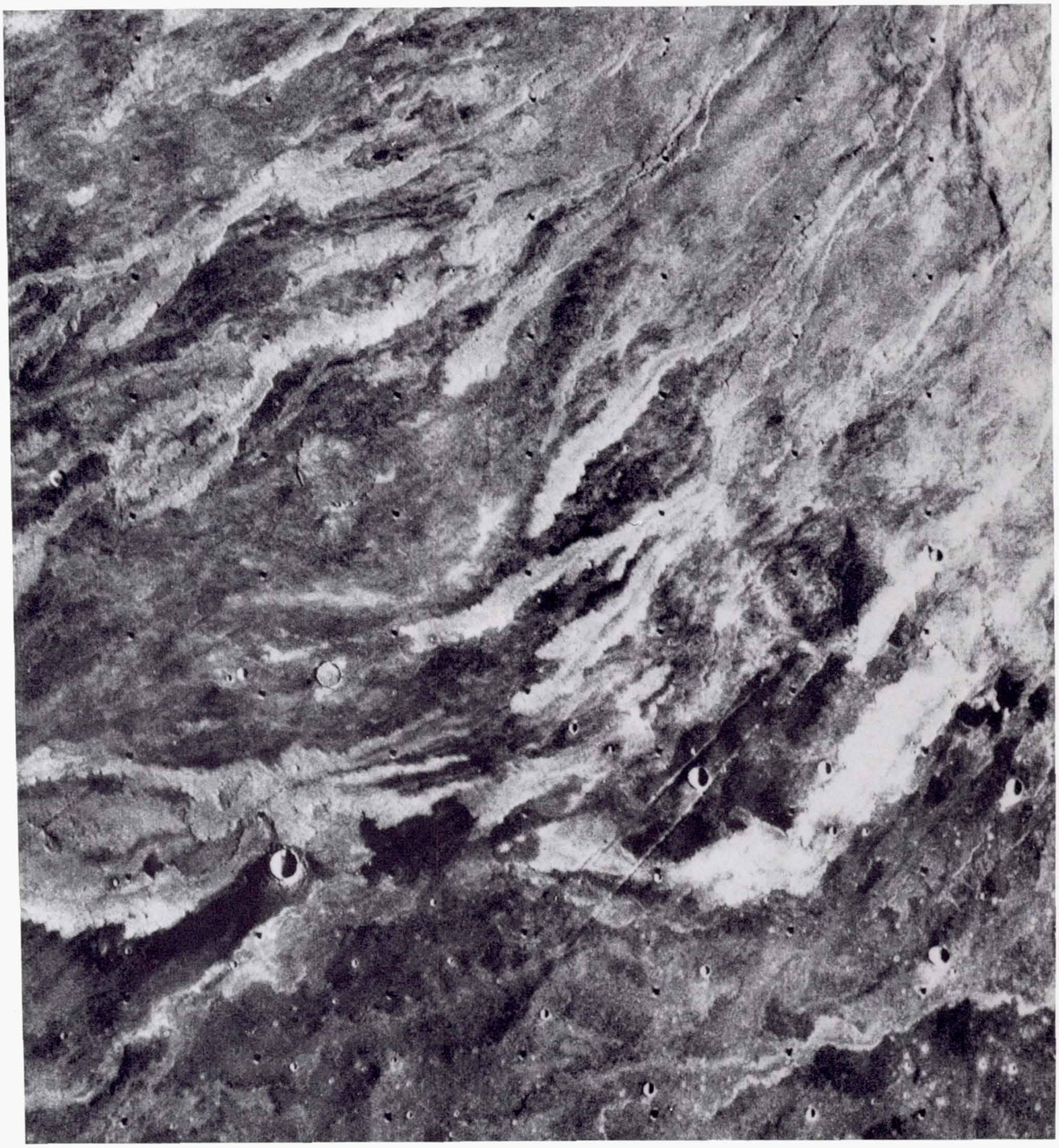

FIGURE 13–8. Image of the lava plains southeast of Arsia Mons at about 20°S, 117°W, showing numerous lava flows and leveed channels. Detailed mapping and analyses of crater frequencies show that these and similar flows intermittently erupted from vents on the northeast and southwest flanks of Arsia Mons over a very long period of time, probably hundreds of millions of years. (Viking Orbiter frame 56A26.)

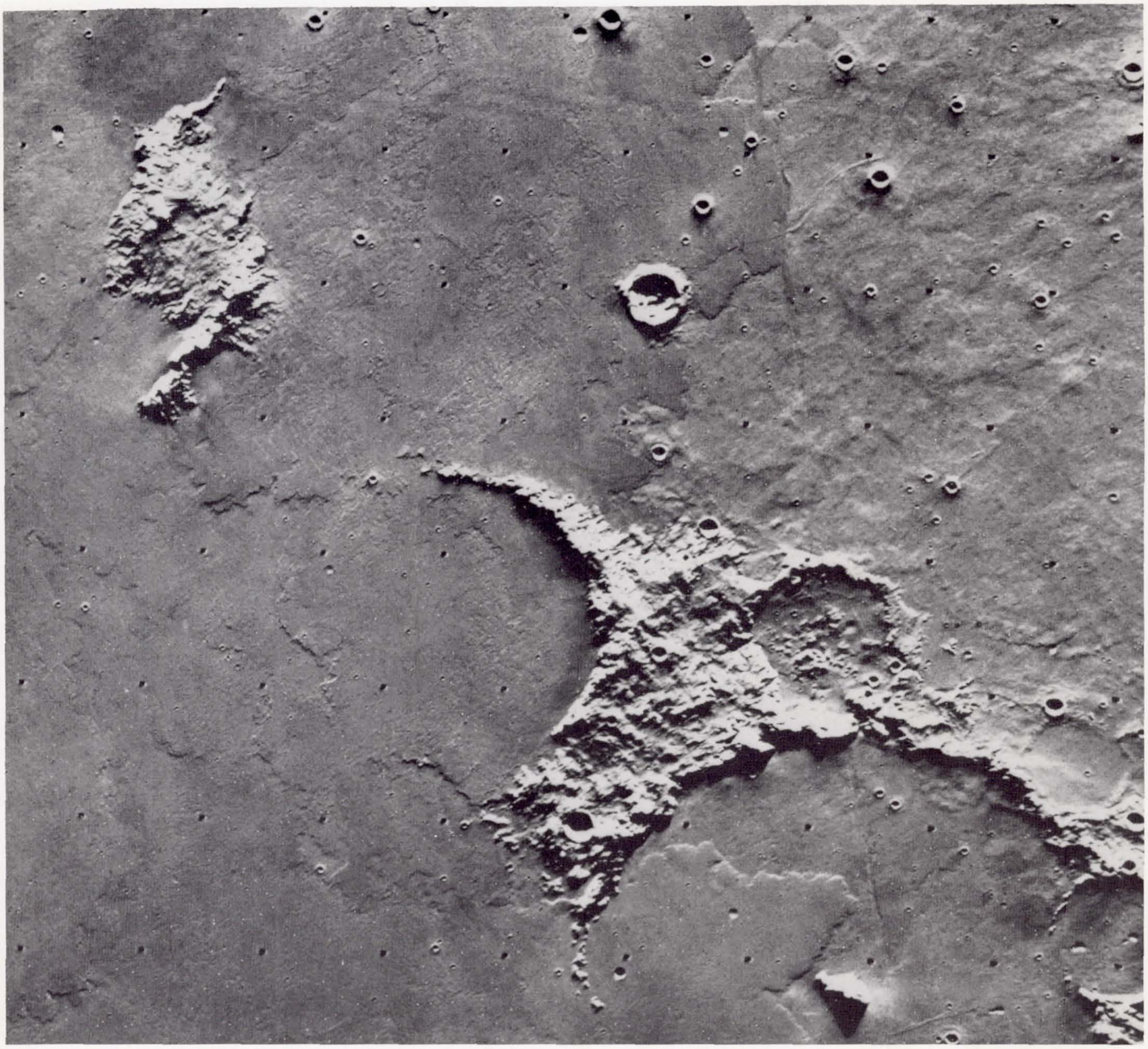

FIGURE 13–9. View of the lava plains south of the Tharsis volcanoes at about 32°S, 131°W, where the lava flows have flooded older cratered terrain (bottom of picture). Lack of flow features, such as lava tubes and channels, suggests that these are flood lavas erupted at high rates of effusion (higher than rates measured in Hawaii) from extensive fissure-vents. (Viking Orbiter frame 56A14.)

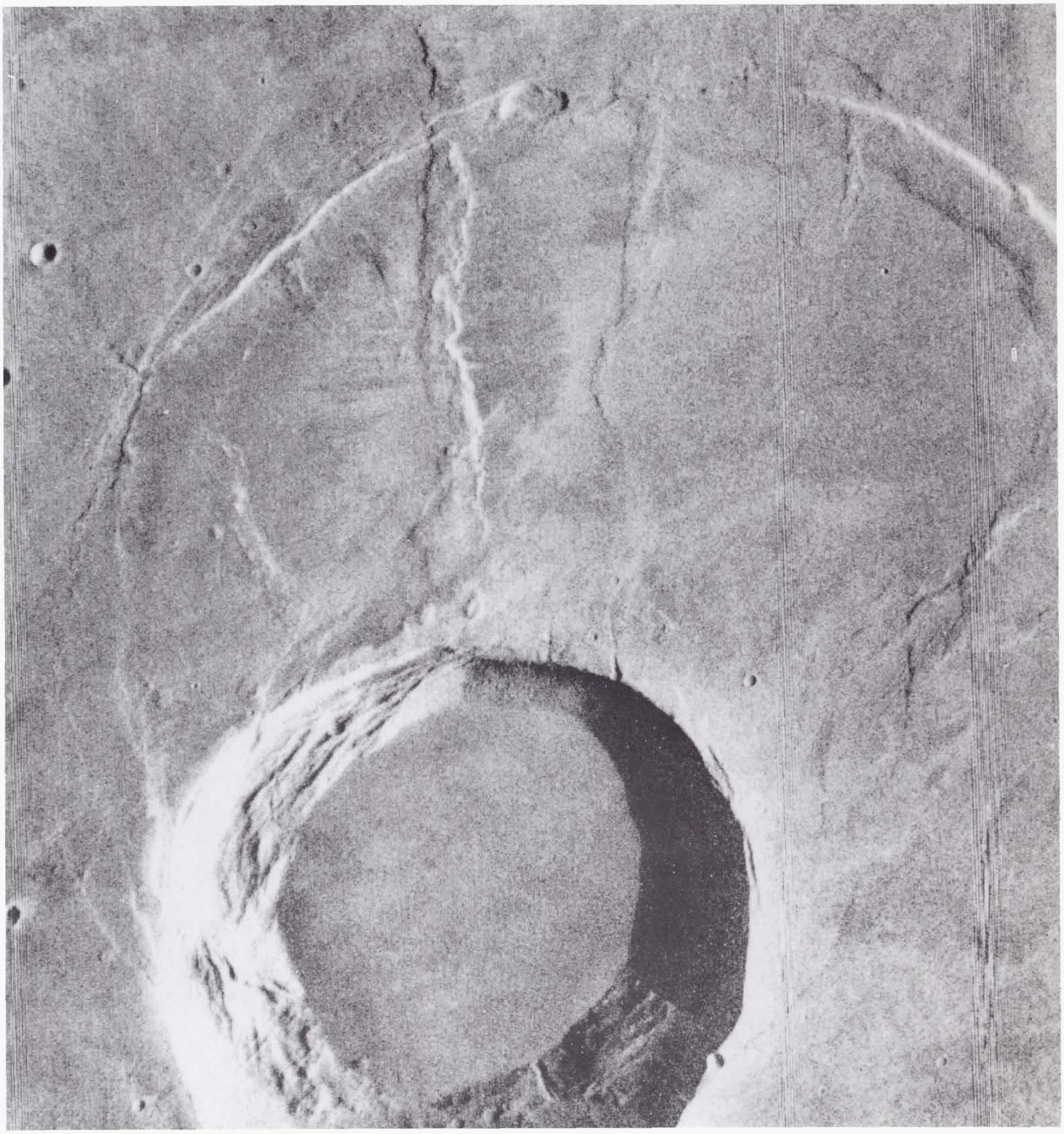

FIGURE 13–10. Medium-resolution image of the summit of Pavonis Mons, middle member of the three Tharsis shield volcanoes. The prominent caldera at the bottom of the picture is about 38 km across and appears to transect an older summit structure outlined by the circular and linear ridges. (Viking Orbiter frame 210A34.)

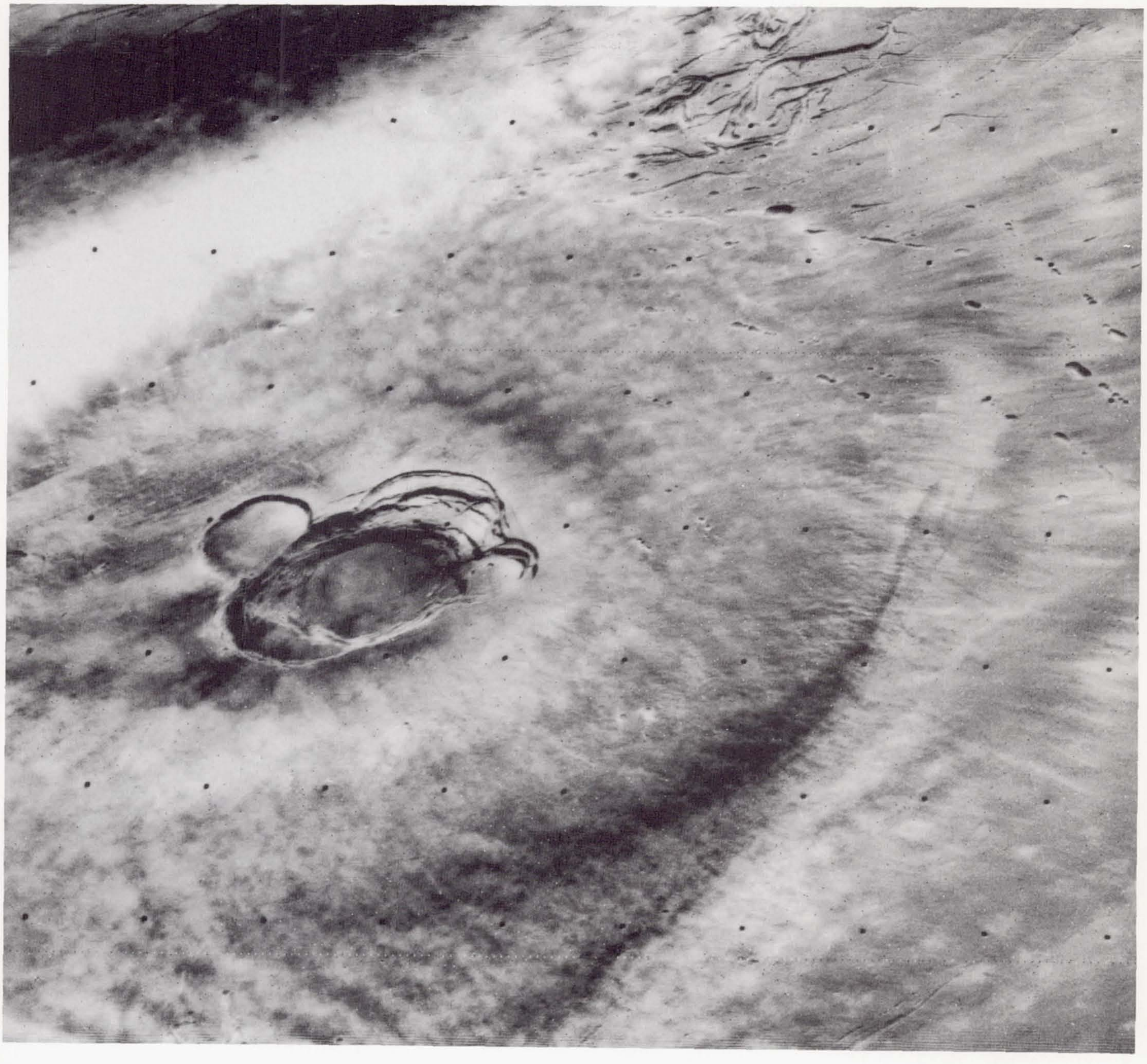

FIGURE 13–11. High-altitude oblique aerial view of Ascraeus Mons, northernmost member of the three large Tharsis shield volcanoes.

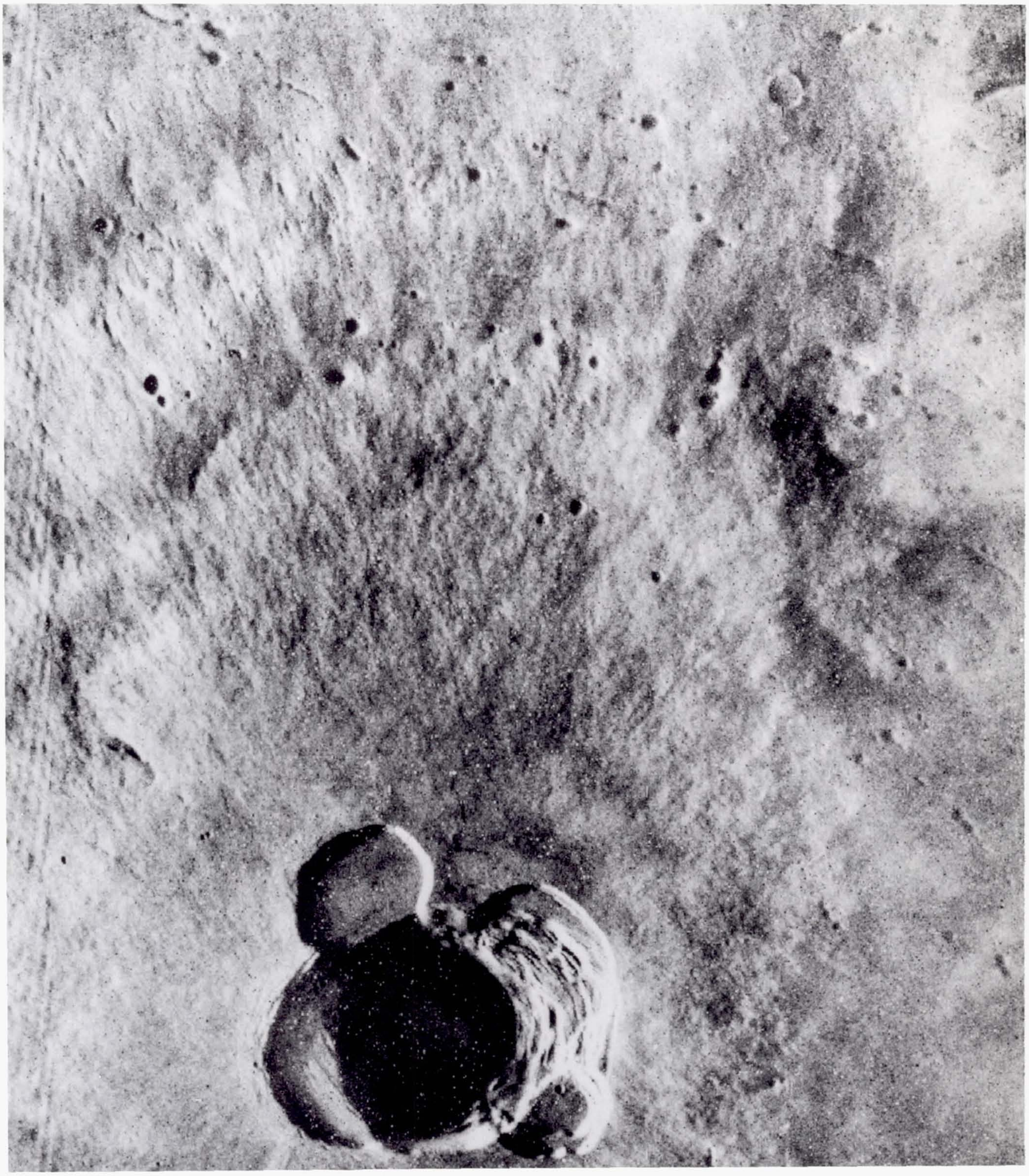

FIGURE 13–12. High-resolution image of the summit caldera of Ascraeus Mons, showing detail of the caldera walls and flow features on the volcano flanks. The main pit is 35 km across.

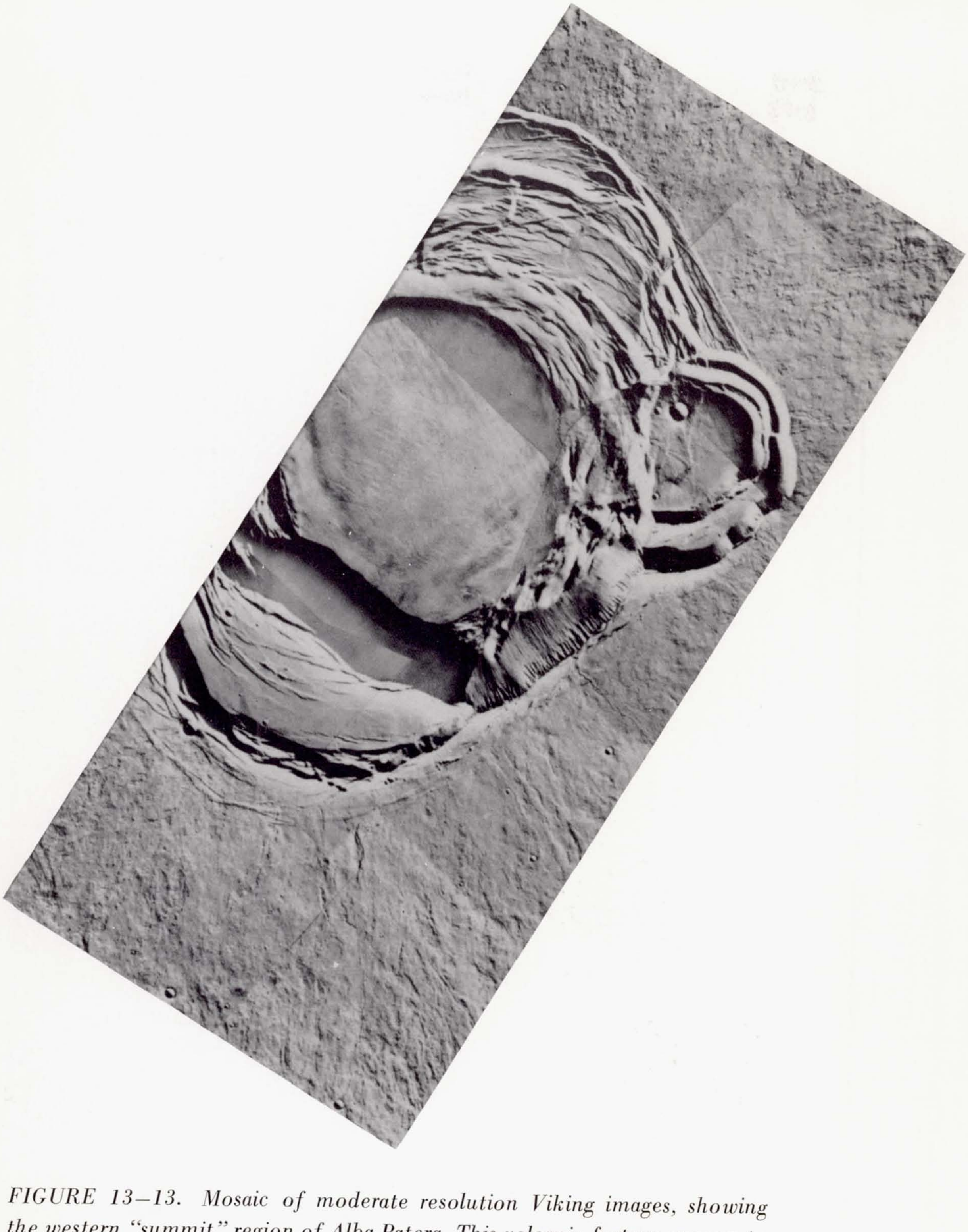

FIGURE 13–13. Mosaic of moderate resolution Viking images, showing the western "summit" region of Alba Patera. This volcanic feature appears to be unique not only on Mars but within the explored Solar System, having no counterpart on Moon, Earth, or the half of Mercury seen thus far. Alba Patera is nearly flat in profile, yet lava flows appear to originate from a central region (seen in the lower right-hand corner here) and extend outward for more than 1,600 km. The fracture ring is approximately 500 km in diameter. (Viking mosaic 211-5065.)

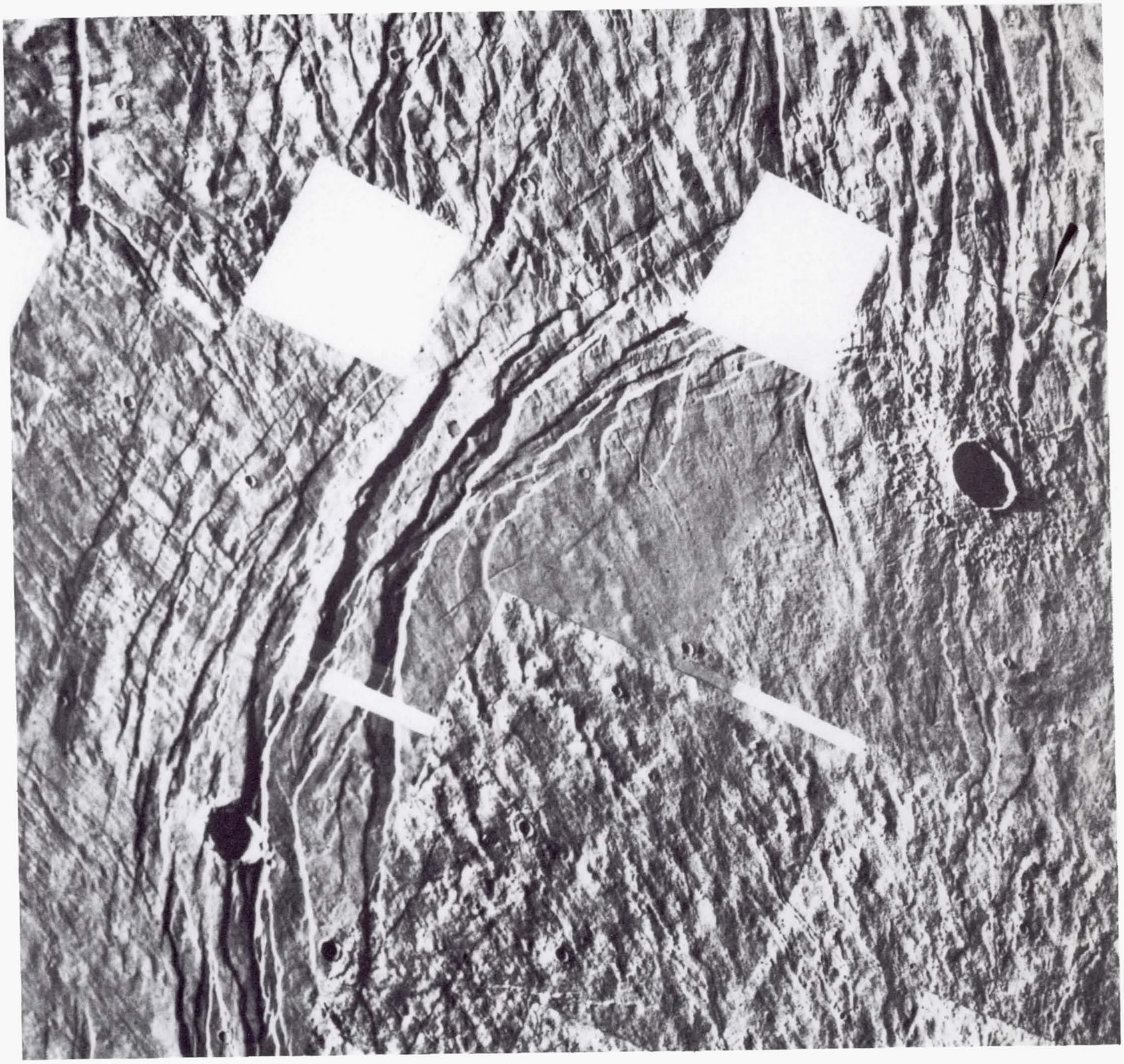

FIGURE 13–14. Lava flows associated with Alba Patera; numerous tube-fed and channel-fed flows cover the flanks of the volcano. Although some of the dendritic channel patterns seen here may be fluvial in origin, most appear to be volcanic. Impact crater at top of picture is approximately 20 km in diameter. (Viking mosaic 211-5065B.)

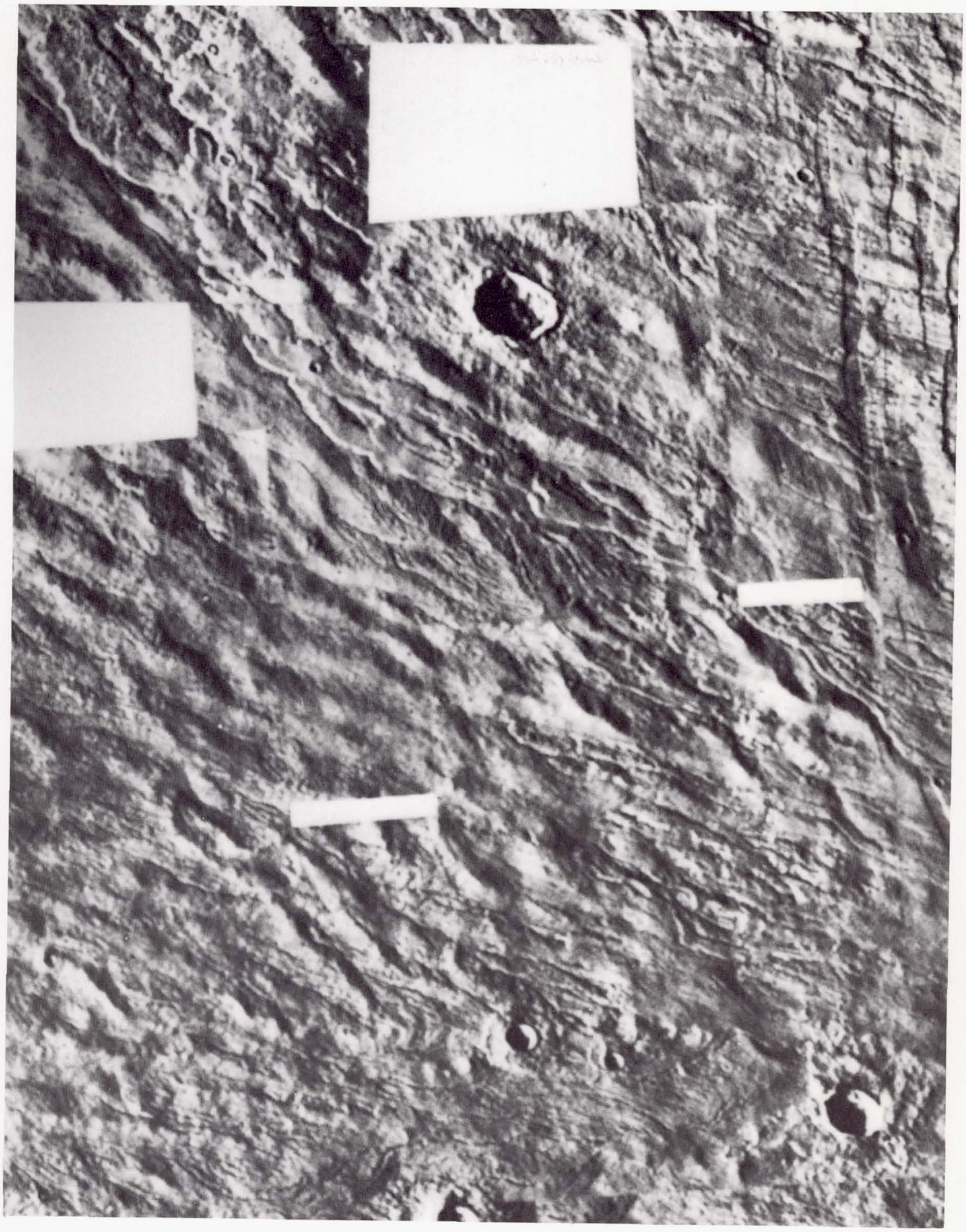

FIGURE 13–15. The prominent ridge seen here has a series of small holes along its crest. These are interpreted to be collapsed portions of a large lava tube that fed lavas on the flank of Alba Patera. Mosaic is 140 km x 110 km. (Viking mosaic 211-5063.)

FIGURE 13–16. High-resolution image of part of the fracture system associated with Alba Patera. The series of craters aligned with several of the fractures are of internal origin and may be analogous to pit craters. Image is about 50 km by 60 km. (Viking Orbiter frame 224A13.)

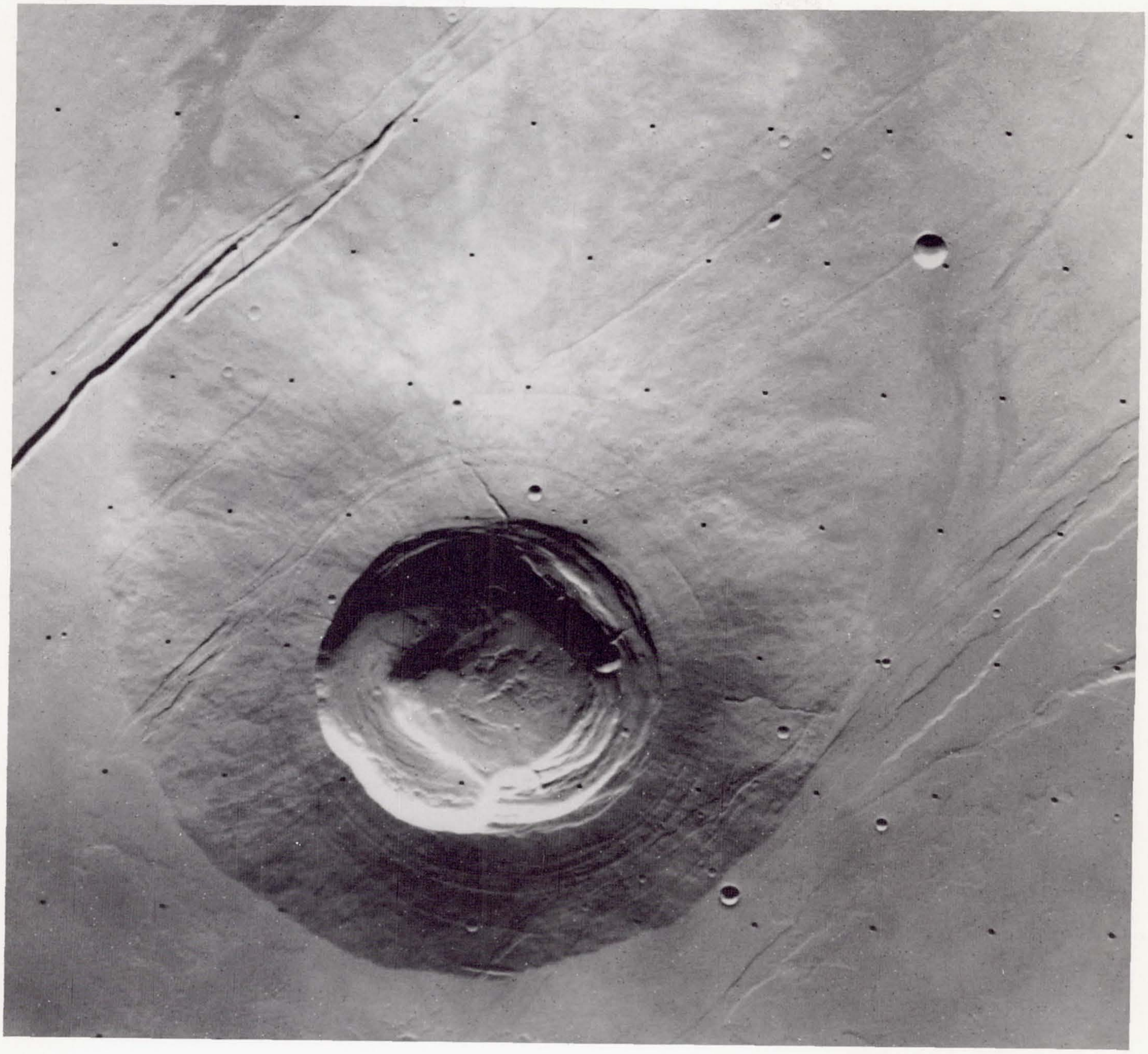

FIGURE 13–17. View of Biblis Patera in the northwest part of the Tharsis region. The exposed part of the volcano is about 100 km across; however, the summit caldera and features on its flanks suggest that it is similar to the younger shield volcanoes of Tharsis and that Biblis Patera is simply an older shield volcano that has been partly buried by younger lava flows. Cutting across the volcano are several graben that post-date the surrounding plains. (Viking Orbiter frame 44B50.)

FIGURE 13–18. View of Pavonis Patera, Tharsis region; similar to Biblis Patera, the volcano seems to be an older shield volcano that has been inundated by younger lava flows. The two smaller craters are probably impact structures, as indicated by the ejecta patterns and their central peaks. (Viking Orbiter frame 49B85.)

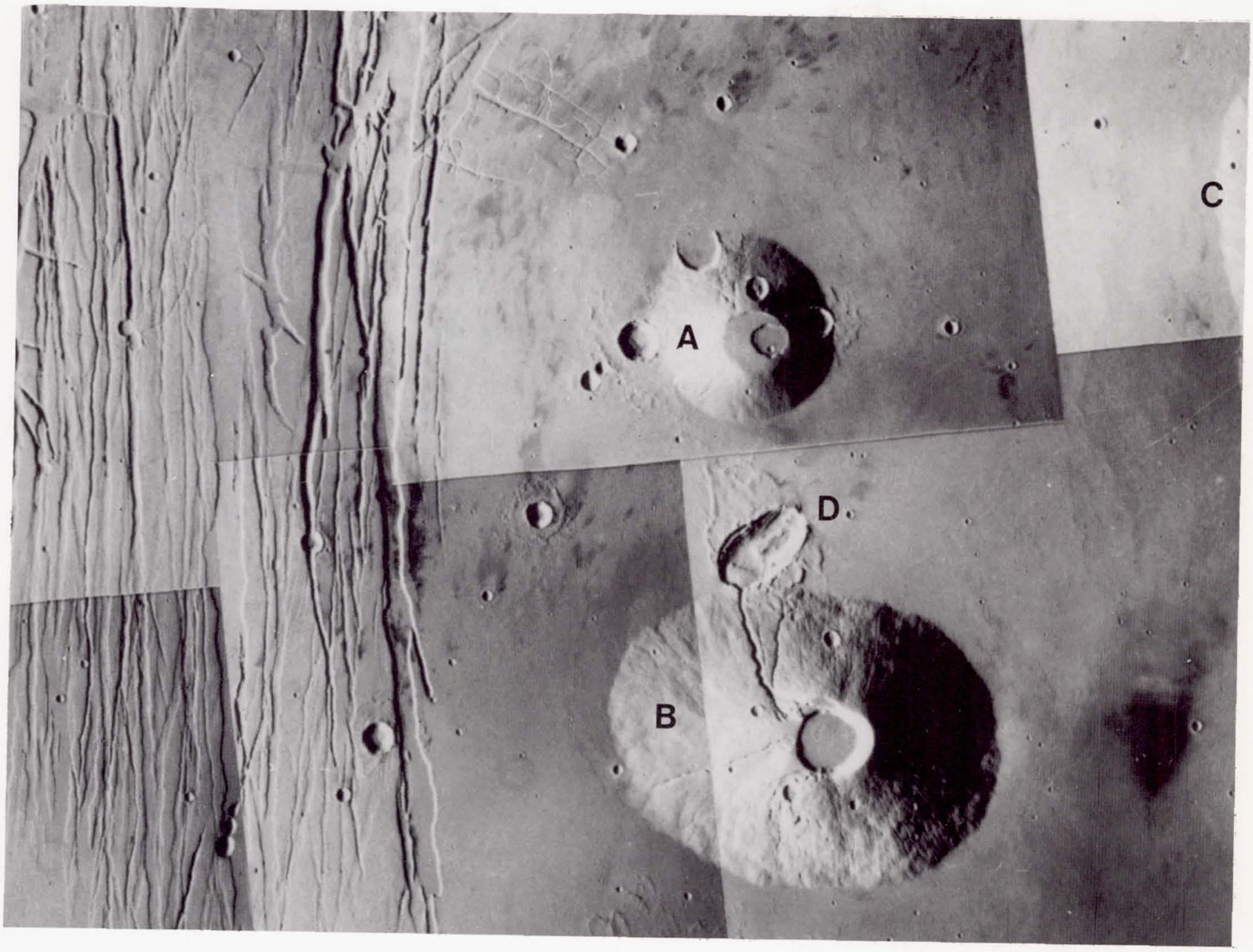

FIGURE 13–19. View of the northern Tharsis area, showing Uranius Tholus (A), Ceranius Tholus (B), part of Uranius Patera (C), and an impact crater at (D). Fractures to the west (left) are part of the tectonic pattern associated with Alba Patera, north of this area. Ceranius Tholus is about 110 km by 90 km. (Viking Orbiter mosaic 211-5639.)

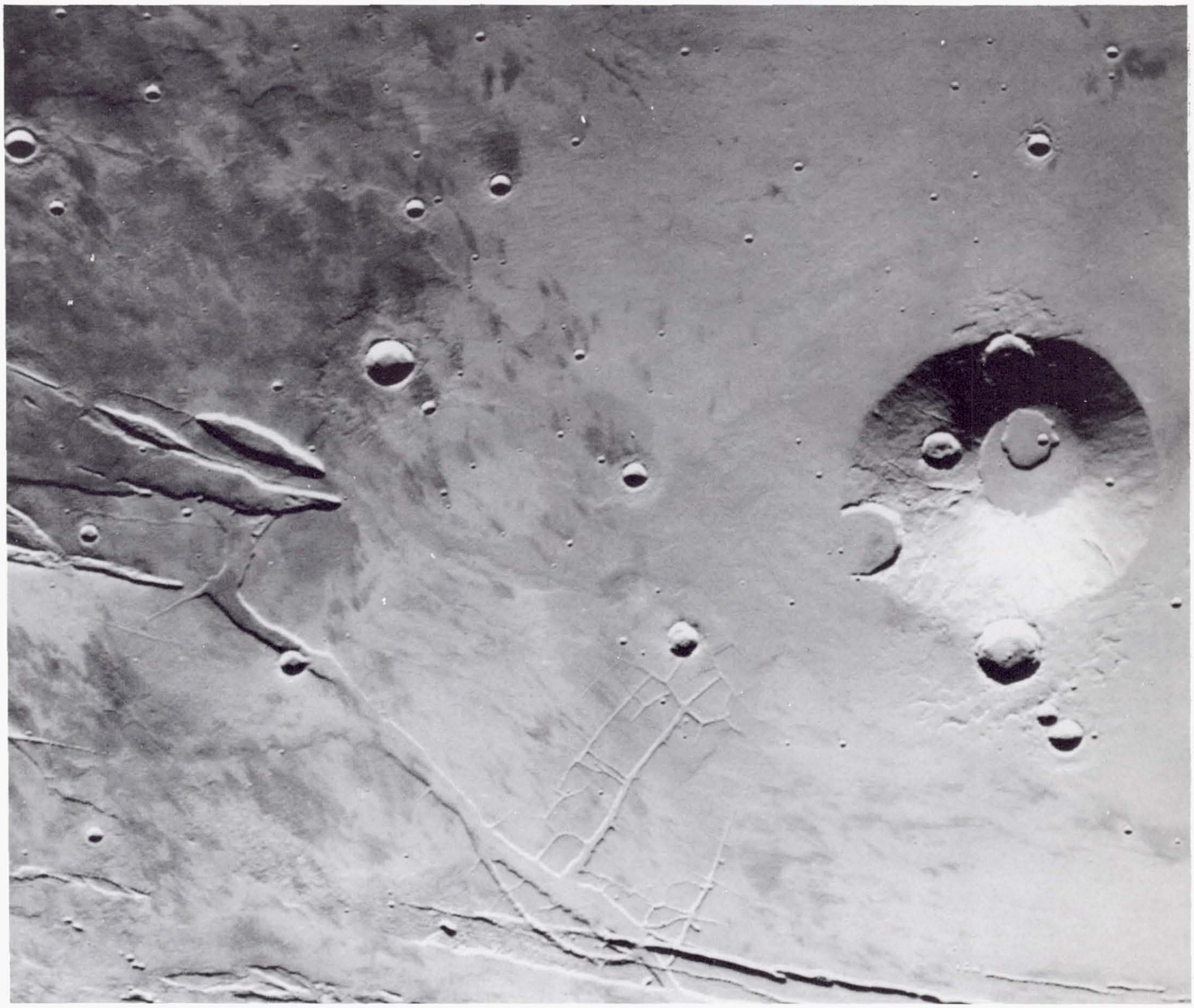

FIGURE 13–20. View of Uranius Tholus. The term Tholus – meaning dome – was applied to several volcanic features on Mars viewed on Mariner 9 images. The increased quality of Viking Orbiter images shows much more detail, and, as can be seen here, both Uranius Tholus and Ceranius Tholus (next figure) are volcanic constructs that have been partly buried by younger lavas, masking the true dimensions of the features. Frame dimensions are 223 km x 238 km. (Viking Orbiter frame 516A23.)

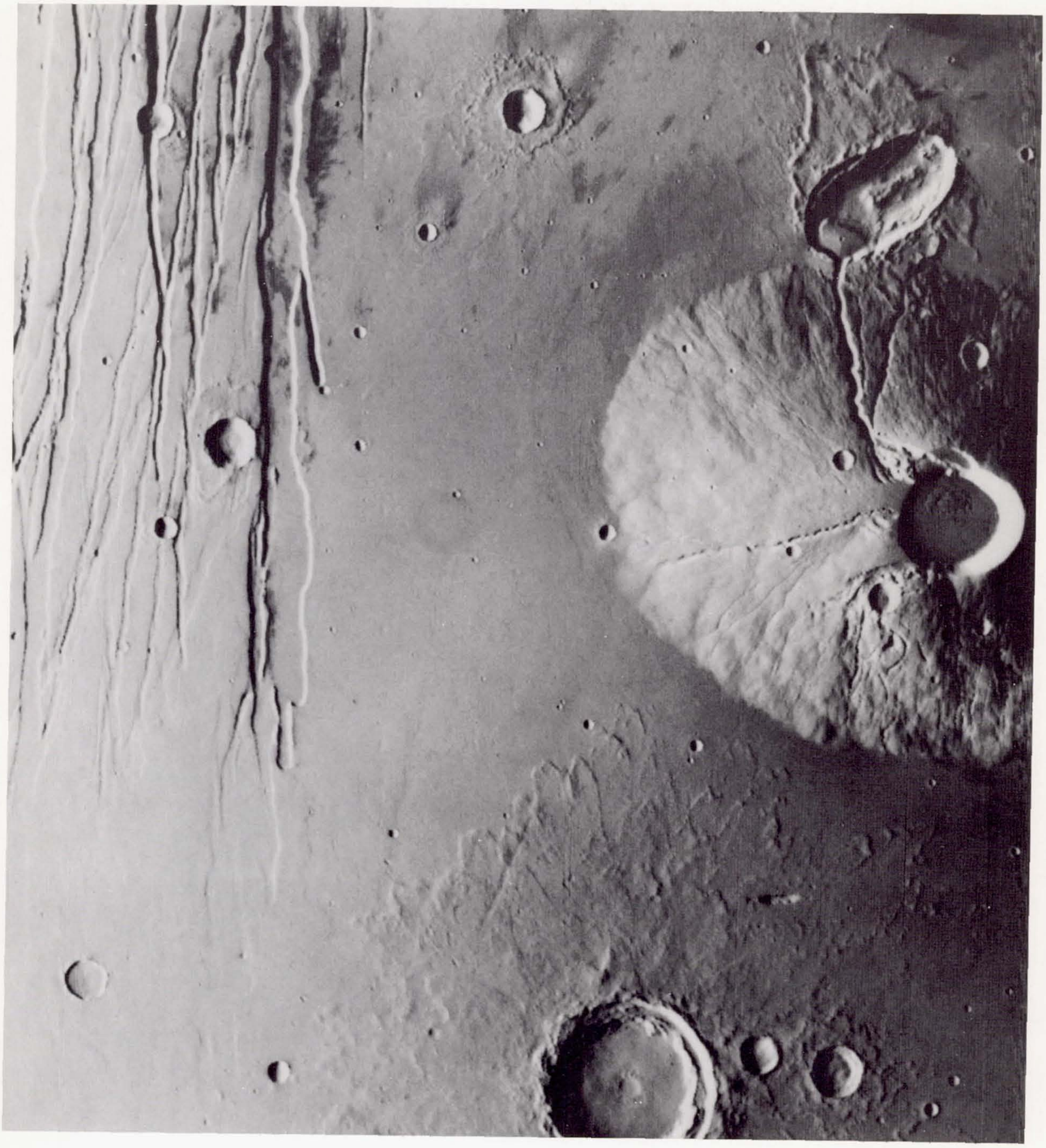

FIGURE 13–21. Moderate resolution view of Ceranius Tholus, showing radial lava flows, lava channels, and partly collapsed lava tubes on the flank of the construct. Several impact craters are visible on this view, one at the bottom of the image, several smaller ones scattered throughout the view, and one elongate crater on the north flank of Ceranius Tholus that has been breached by a lava channel. Frame dimensions are 220 km x 236 km. (Viking Orbiter frame 516A24.)

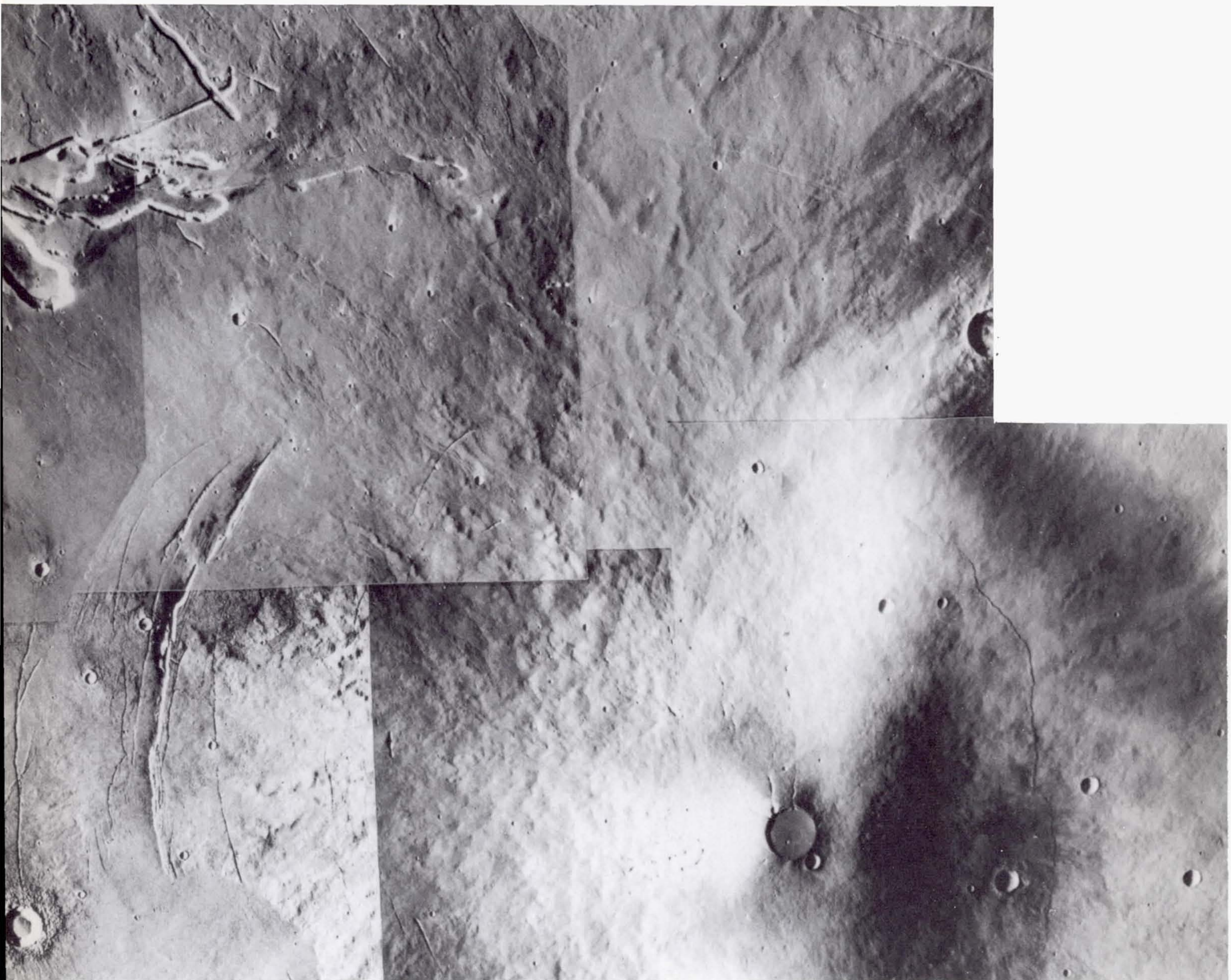

FIGURE 13–22. Vertical view of Elysium Mons. Slopes on the flanks of the volcano are steeper than those of the Tharsis shield volcanoes, suggesting either differences in lava rheology – perhaps being more viscous – or lower rates of effusion that would produce shorter flows. The summit caldera is about 15 km in diameter. (Viking Orbiter mosaic 211-5643.)

FIGURE 13–23. Two frame mosaic showing details of the summit Elysium Mons and the flanks of the volcano. (Viking Orbiter frames 541A44,46.)

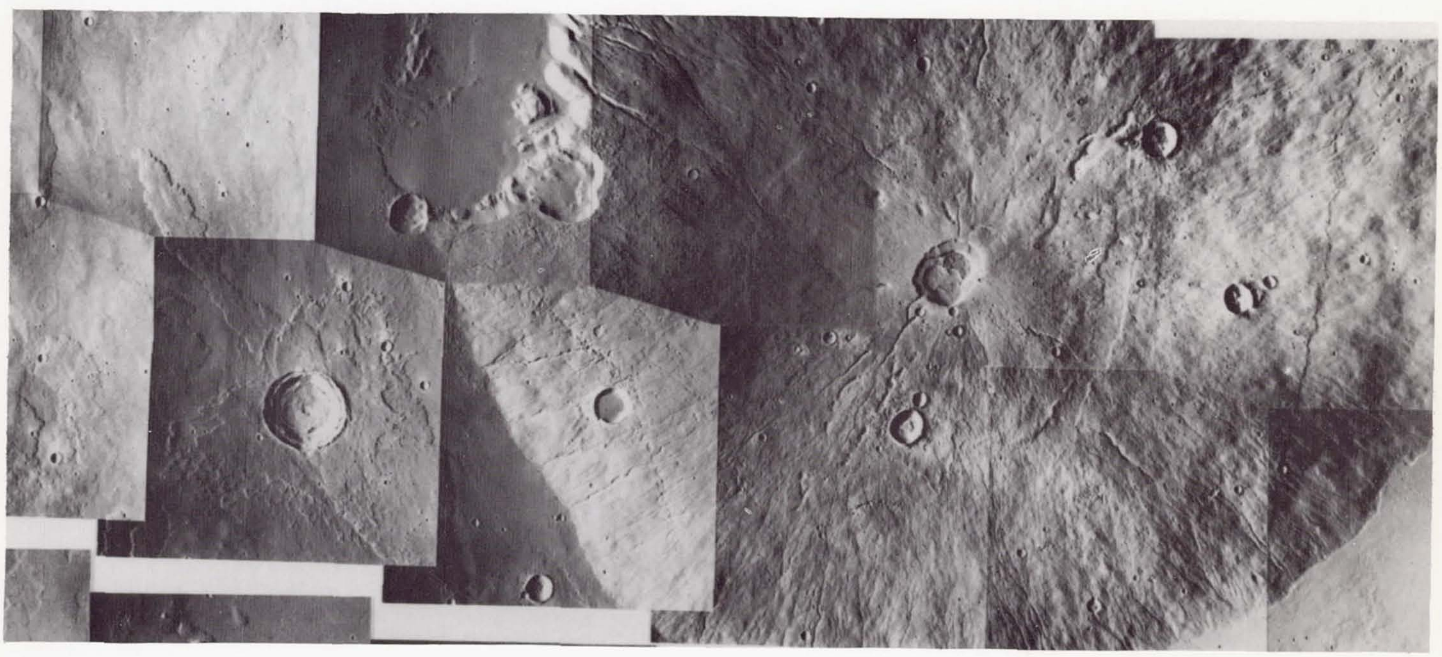

FIGURE 13–24. Mosaic showing part of Hecates Tholus, a volcano about 400 km northeast of Elysium Mons, showing a complex summit caldera, numerous radial lava flows, collapsed lava tubes, lava channels and younger lava flows that have partly buried the volcano. Hecates Tholus is about 150 km across. (Viking Orbiter mosaic 211-5787.)

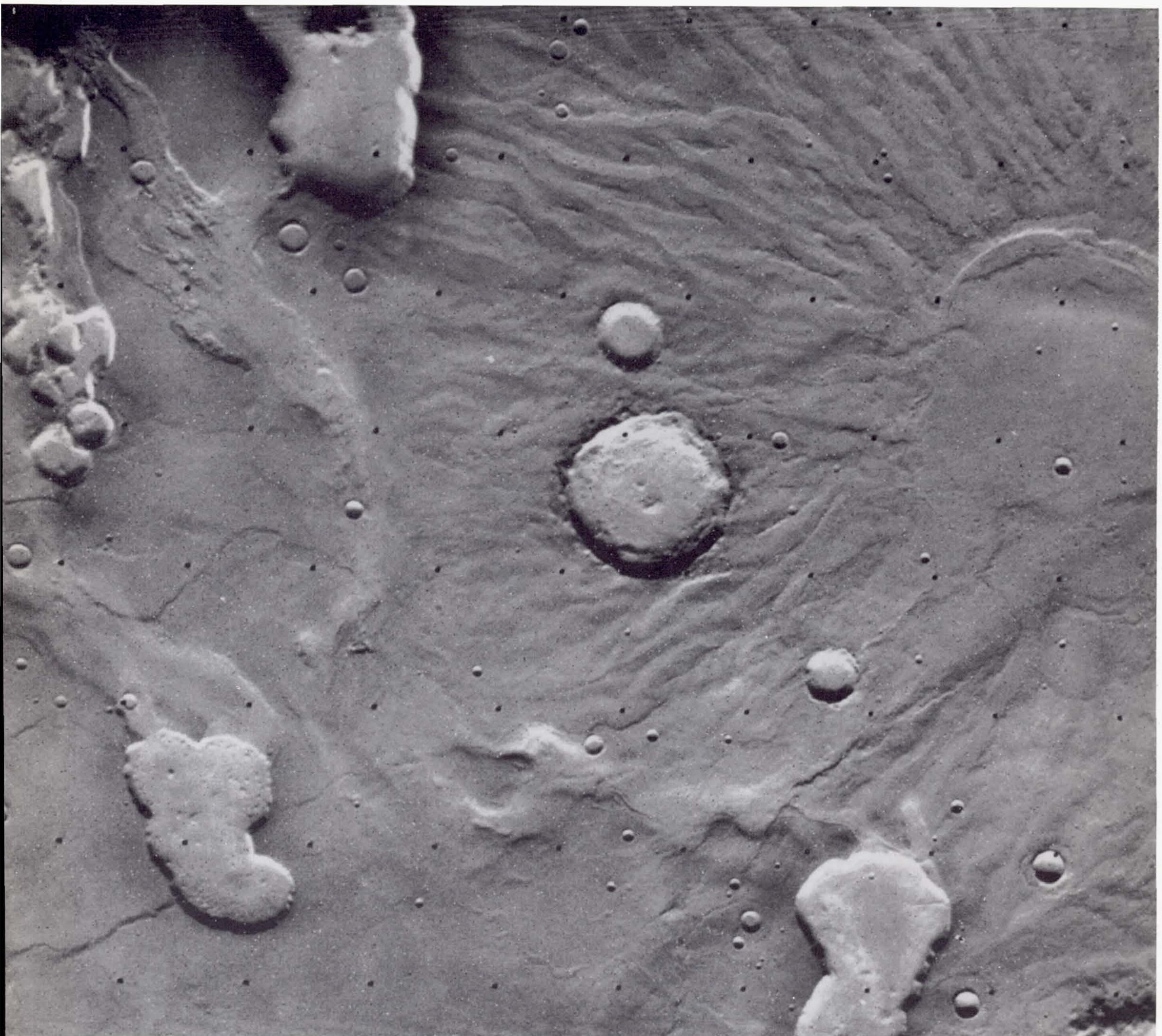

FIGURE 13–25. View of Hadriaca Patera at 31°S, 264°W. This volcano, typical of many patera, has a very low profile. The central caldera is about 60 km across. (Viking Orbiter frame 106A09.)

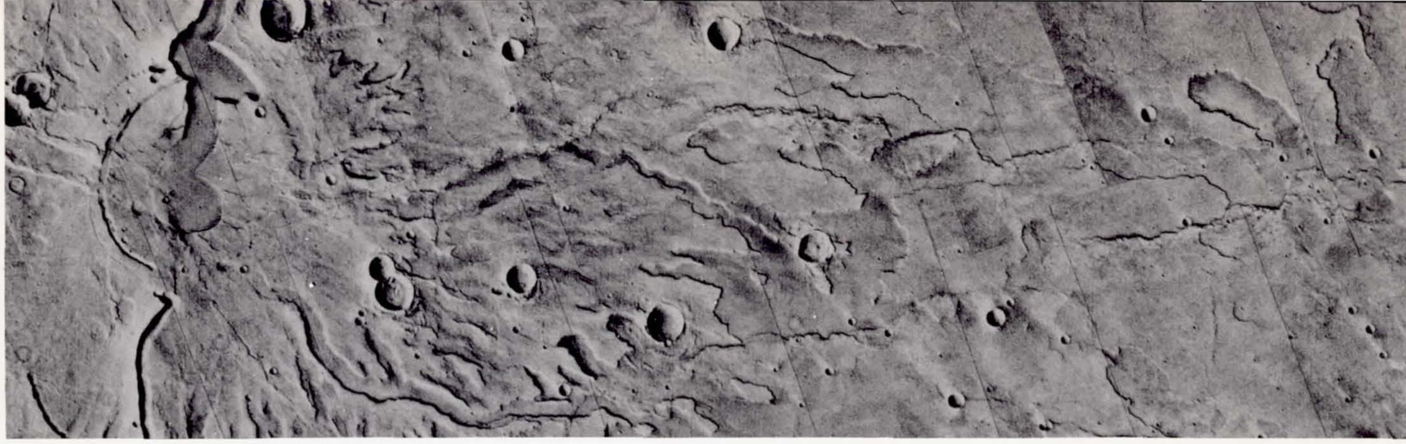

FIGURE 13–26. Mosaic of Tyrrhena Patera at 20°S, 252°W. A 12-km diameter caldera-like depression is surrounded by a partial fracture ring, 45 km in diameter. The crater margin of the patera is extensively dissected and several channels radiate from the center. (Viking mosaic 211-5730.)

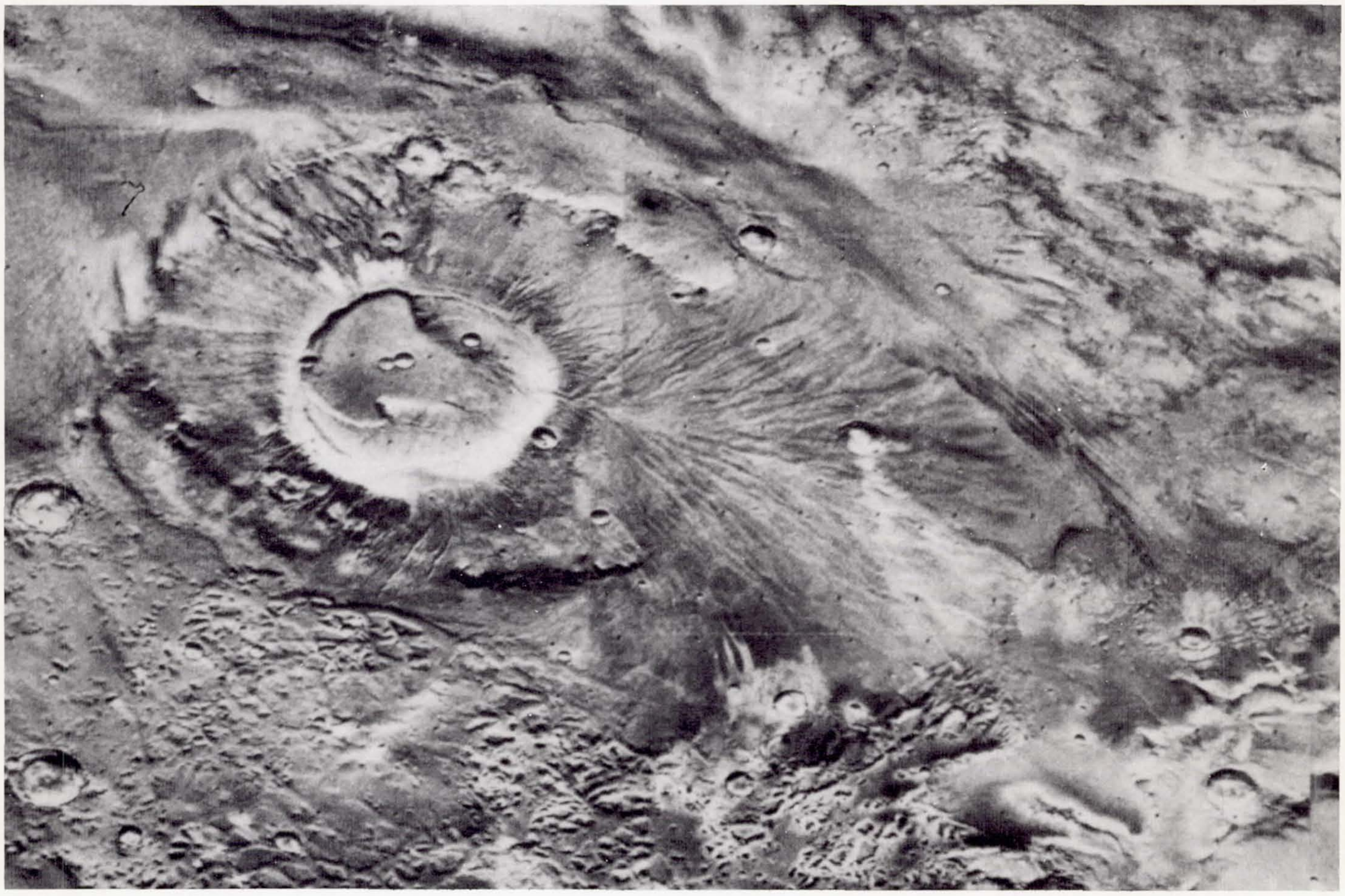

FIGURE 13–27. The volcano Apollinaris Patera at 8°S, 186°W. The volcano is probably relatively old, as is suggested by the number of superposed craters, some of which are probably impact. Flows appear to diverge from a rift zone on one flank. The central caldera is 75 km in diameter. (Mosaic P-18143.)

Page intentionally left blank

REFERENCES

Baker, V. R., and D. J. Milton, 1974. Erosion by catastrophic floods on Mars and Earth, *Icarus, 23,* 27 - 41.

Blasius, K. R., J. A. Cutts, J. E. Guest, and H. Masursky, 1977. Geology of the Valles Marineris: First analysis of imaging from the Viking Orbiter primary mission. *J. Geophys. Res., 82,* 4067 - 4091.

Carr, M. H., 1973. Volcanism on Mars, *J. Geophys. Res., 78,* 4049 - 4062.

Carr, M. H., 1975. The volcanoes of Mars., *Sci. Amer., 234,* 32 - 43.

Carr, M. H., K. R. Blasius, R. Greeley, J. E. Guest, and J. E. Murray, 1977. Observations on some martian volcanic features as viewed from the Viking Orbiters, *J. Geophys. Res., 82,* 3985 - 4015.

Carr, M. H., L. A. Crumpler, J. A. Cutts, R. Greeley, J. E. Guest, and H. Masursky, 1977. Martian craters and emplacement of ejecta by surface flow, *J. Geophys. Res., 82,* 4055 - 4065.

Carr, M. H., H. Masursky, W. A. Baum, K. R. Blasius, G. A. Briggs, J. A. Cutts, T. Duxbury, R. Greeley, J. E. Guest, B. A. Smith, L. A. Soderblom, J. Veverka, and J. B. Wellman, 1976. Preliminary results from the Viking Orbiter imaging experiment, *Science, 193,* 766 - 776.

Crumpler, L. S., and J. C. Aubele, 1978. Structural evolution of Arsia Mons, Pavonis Mons and Ascreus Mons, Tharsis region of Mars, *Icarus, 34,* 496 - 511.

Dalrymple, G. B., M. A. Lanphere, and D. A. Claque (in press). Conventional and $^{40}Ar/^{39}Ar$, K-Ar ages of volcanic rocks from Ogin (site 430), Nintoku (site 432), Suiko (site 433) seamounts and the chronology of volcanic propagation along the Hawaiian-Emperor chain: Initial reports of the Deep Sea Drilling Project, *55.*

Dalrymple, G. B., E. A. Silver, and E. D. Jackson, 1975. Origin of the Hawaiian Islands, *Amer. Scientist, 61,* 294 - 303.

Duffield, W. A., 1972. A naturally occurring model of global plate tectonics, *J. Geophys. Res., 77,* 2543 - 2555.

Eaton, J. P., 1962. Crustal structure and volcanism in Hawaii, in *Crust of the Pacific Basin* (G. A. Macdonald and H. Kuns, eds.), Geophys. Mono. 6, Amer. Geophys. Union, Washington, D.C., pp. 13 - 29.

Eaton, J. P., and K. J. Murata, 1960. How volcanoes grow, *Science, 132,* 925 - 938.

Fiske, R. S., and E. D. Jackson, 1972. Orientation and growth of Hawaiian volcanic rifts: the effect of regional structure and gravitational stresses, *Proc. R. Soc. London A., 329,* 299 - 326.

Greeley, R., 1977. Basaltic "plains" volcanism, in *NASA CR 154621,* 24 - 44.

Grommé, C. S., and F. J. Vine, 1972. Paleomagnetism of midway atoll lavas and northward movement of the Pacific plate, *Earth Planet. Sci. Letters, 17,* 159 - 168.

HVO Staff, 1974. Recent landforms at Kilauea Volcano, in *NASA CR 152416,* 50 - 86.

Jackson, E. D., E. A. Silvers, and G. B. Dalrymple, 1972. Hawaiian-Emperor Chain and its relation to Cenozoic circumpacific tectonics, *Geol. Soc. Amer. Bull., 83,* 601 - 618.

Jackson, E. D., and T. L. Wright, 1970. Xenoliths in the Honolulu Volcanic Series, Hawaii, *J. Petrol., 11,* 405 - 430.

Kinoshita, W. T., H. L. Krivoy, D. R. Mabey, and R. R. McDonald, 1963. Gravity survey of the island of Hawaii, *U. S. Geol. Survey Prof. Paper 475C,* 114 - 116.

Koyanagi, R. Y., E. T. Endo, and J. S. Ebisu, 1975. Reawakening of Mauna Loa Volcano, Hawaii: A preliminary evaluation of seismic evidence, *Geophys. Res. Letters, 2,* 405 - 408.

Koyanagi, R. Y., E. T. Endo, and P. L. Ward, 1976. Seismic activity on the island of Hawaii, 1970 - 1973, in *The Geophysics of the Pacific Ocean Basin and its Margin,* Amer. Geophys. Union Monograph 16, 169 - 172.

Leighton, R. B., N. H. Horowitz, B. C. Murray, R. P. Sharp, A. G. Herriman, A. T. Young, B. A. Smith, M. E. Davies, and C. G. Leovy, 1969. Mariner 6 and 7 television pictures: Preliminary analysis, *Science, 166,* 49 - 67.

Leighton, R. B., B. C. Murray, R. P. Sharp, J. D. Allen, and R. K. Sloan, 1965. Mariner IV photography of Mars: Initial results, *Science, 149,* 627 - 630.

Macdonald, G. A., 1953. Pahoehoe, aa, and block lava, *Amer. J. Sci., 251,* 169 - 191.

Macdonald, G. A., 1972. *Volcanoes,* Prentice-Hall, Englewood Cliffs, New Jersey, 510 pp.

Macdonald, G. A., and A. T. Abbott, 1970. *Volcanoes in the Sea: The Geology of Hawaii,* University of Hawaii Press.

Masursky, H., 1973. An overview of geologic results from Mariner 9, *J. Geophys. Res., 78,* 4037 - 4047.

McDougall, I., 1971. Volcanic island chains and sea-floor spreading, *Nature, 231,* 141 - 144.

McDougall, I., and D. A. Swanson, 1972. Potassium-argon ages of lavas from the Hawi and Pololu Volcanic Series, Kohala Volcano, Hawaii, *Geol. Soc. Amer. Bull, 83,* 3731 - 3738.

Morgan, W. J., 1971. Convection plumes in the lower mantle, *Nature, 230,* 42 - 43.

Morgan, W. J., 1972a. Deep mantle convection plumes and plate motion, *Amer. Assoc. Petrol. Geol. Bull., 56,* 203 - 213.

Morgan, W. J., 1972b. Plate motions and deep mantle convection. *Geol. Soc. Amer. Mem., 132.*

Mutch, T. A., R. E. Arvidson, J. W. Head, K. L. Jones, and R. S. Saunders, 1976. *The Geology of Mars,* Princeton University Press, Princeton, New Jersey.

Scott, D. H. and M. H. Carr, 1978. Geologic map of Mars, *Misc. Invest. Map I-1083,* U. S. Geological Survey, Reston, Va.

Sharp, R. P., 1973. Mars: Fretted and chaotic terrain, *J. Geophys. Res., 78,* 4073 - 4083.

Shaw, H. R., and E. D. Jackson, 1973. Linear island chains in the Pacific: Result of thermal plumes or gravitational anchors, *J. Geophys. Res., 78,* 8634 - 8652.

Shaw, H. R., D. L. Peck, T. L. Wright, and R. T. Okamura, 1968. The viscosity of basaltic magma: An analysis of field measurements in Makaopuhi lava lake, Hawaii, *Amer. J. Sci., 266,* 255 - 264.

Shaw, H. R., and D. A. Swanson, 1970. Eruption and flow rates of flood basalts, in *Proc. Second Columbia River Basalt Symposium* (E. H. Gilmour and D. Stradling, eds.), Eastern Washington State College Press, Cheney, Washington, pp. 271 - 299.

Stearns, H. T., and G. A. Macdonald, 1946. Geology and Groundwater Resources of the Island of Hawaii, *Hawaii Div. of Hydrography, Bull. 9,* 363 pp, colored geologic map.

Stearns, H. T., 1966. *Geology of the State of Hawaii,* Pacific Book, Palo Alto, 266 pp.

Swanson, D. A., 1972. Magma supply rate at Kilauea Volcano 1952-1971, *Science, 175,* 169 - 170.

Swanson, D. A., 1973. Pahoehoe flows from the 1969-1971 Mauna Ulu eruption, Kilauea Volcano, Hawaii, *Geol. Soc. Amer. Bull., 84,* 615 - 626.

Swanson, D. A., W. A. Duffield, and R. S. Fiske, 1976a. Displacement of the south flank of Kilauea Volcano: The result of forceful intrusion of magma into the rift zones. *U. S. Geol. Survey Prof. Paper 963,* 39 pp.

Swanson, D. A., W. A. Duffield, D. B. Jackson, and D. W. Peterson, 1979. Chronological narrative of the 1969-1971 Mauna Ulu eruption of Kilauea Volcano, Hawaii, *U. S. Geol. Survey Prof. Paper 1056,* 55 pp.

Swanson, D. A., D. B. Jackson, W. A. Duffield, and D. W. Peterson, 1971. Mauna Ulu eruption, Kilauea Volcano, *Geotimes, 16,* 12 - 16.

Swanson, D. A., D. B. Jackson, R. Y. Koyanagi, and T. L. Wright, 1976b. The February 1969 east rift eruption of Kilauea Volcano, Hawaii, *U. S. Geol. Survey Prof. Paper 891,* 30 pp.

Tilling, R. I., R. Y. Koyanagi, P. W. Lipman, J. P. Lockwood, J. G. Moore, and D. A. Swanson, 1976. Earthquakes and related catastrophic events, Island of Hawaii, Nov. 29, 1975: A preliminary report, *U. S. Geol. Survey Cir. 740,* 33 pp.

Walker, G. P. L., 1973. Lengths of lava flows, *Phil. Trans. R. Soc. London A., 274,* 107-118.

Wilkes, C., 1845. *Narrative of the United States Exploring Expedition during the Years 1838-1842, V. 4,* Philadelphia, pp. 87-231.

Wilson, J. T., 1963. A possible origin of the Hawaiian Islands, *Canad. J. Physics, 41,* 863-870.

Wise, D. U., M. P. Golombeck, and G. E. McGill, 1979. Tharsis province of Mars: Geologic sequence, geometry and a deformation mechanism, *Icarus, 38,* 456-472.

☆ U.S. GOVERNMENT PRINTING OFFICE : 1980—O-315-616